

Permian to Cenozoic structural evolution and salt tectonics in the Baltic sector of the North German Basin

Dissertation

with the aim of achieving a doctoral degree at the Faculty of
Mathematics, Informatics and Natural Sciences

Department of Earth Sciences

at Universität Hamburg

submitted by

Niklas Ahlrichs

Hamburg, 2022

Department of Earth Sciences

Date of Oral Defense: 15.09.2022

Reviewers: Prof. Dr. Christian Hübscher
Prof. Dr. Ulrich Riller

Members of the examination commission: Chair: Prof. Dr. Christian Hübscher
Prof. Dr. Ulrich Riller
Prof. Dr. Céline Hadziioannou
Prof. Dr. Dirk Gajewski
Dr. Sebastian Lindhorst

Chair of the Subject Doctoral Committee

Earth System Sciences: Prof. Dr. Hermann Held

Dean of Faculty MIN: Prof. Dr. Heinrich Graener

Abstract

The subsurface beneath the present southwestern Baltic Sea holds a unique geological archive of the tectonic evolution of an intracontinental sedimentary basin strongly influenced by salt tectonics. By means of seismic imaging, this thesis investigates the structural evolution of the Baltic sector of the North German Basin from Permian to recent times, thus, covering a timespan of approx. 300 million years. Main stages during the development of the North German Basin comprise initial Permo-Carboniferous wrench faulting and volcanism followed by Permian to Middle Triassic thermal subsidence, Late Triassic E-W extension, Middle Jurassic uplift, Late Cretaceous inversion and Cenozoic extension and glaciation. The analysis of the formation and overprinting of the North German Basin and its northern margin allowed a reassessment of salt tectonics within the regional tectonic framework. The results contribute to a better understanding of complex sedimentary basin evolution. This important aspect of geological research is relevant to socioeconomics due to the multitude of resources, potential hazards and subsurface use capabilities of such sedimentary basins (e.g. for carbon capture and storage, geothermal energy utilization or nuclear waste repositories).

Stratigraphic interpretation of the sedimentary subsurface is based on wells in combination with high-resolution 2D seismic data covering the marine area from the Bay of Kiel up to north of Rügen Island. The presented seismic images, in traveltimes and depth, continuously image the subsurface from the seafloor down to the base Zechstein. Regional maps, in a stratigraphic subdivision unprecedented for the study area, elucidate the Permian to recent structural development of the northeastern Glückstadt Graben, the salt structures within the Eastholstein-Mecklenburg Block and the fault systems of Western Pomeranian Fault System at the northeastern basin margin. Thereby, an update of the fault pattern including basement faults, is given. Mapping of the Zechstein succession allows a revision of the geometry of salt structures in the study area and reveals a novel salt pillow within the Little Belt.

In most parts of the Baltic sector of the North German Basin, mapping of the Buntsandstein and Muschelkalk units confirm the absence of salt movement during the Early to Middle Triassic. An exception might be the Kegnaes Diapir at the northern basin margin where seismic interpretation indicates salt movement and faulting already during deposition of the Buntsandstein. Furthermore, this work shows that major salt movement began in the northeastern Glückstadt Graben under regional E-W extension in Ladinian – Carnian times. Coeval thin-skinned faulting at the northeastern basin margin is associated with transtensional movements within the Trans-European Suture Zone. Thereby, a transtensional sub-basin formed at the northeastern basin margin with intensified accumulation of Keuper and Jurassic deposits. In between the fault systems of the northeastern basin margin and the northeastern Glückstadt Graben, the Eastholstein-Mecklenburg Block formed a more stable transition zone where salt movement had not started before latest Triassic – Early Jurassic times. This work proposes a thin-skinned extensional mechanism as the trigger of Late Triassic – Early Jurassic salt movement in the study area.

Uplift and erosion caused by the Mid Jurassic North Sea Doming event resulted in a regional stratigraphic gap encompassing the Middle Jurassic to Aptian. Sedimentation resumed in the Albian followed by a phase of relative tectonic quiescence lacking salt movement. This period ended with the Late Cretaceous inversion, whose onset in the study area is specified to the Coniacian – Santonian. Inversion was expressed by uplift of the Grimmen High, the reactivation of normal as reverse faults and the reactivation of minor salt flow at the northeastern Glückstadt Graben and in the Bay of Mecklenburg. Thin-skinned shortening is interpreted as the driving mechanism of Late Cretaceous salt movement. At the northeastern basin margin, salt flow driven by gravity gliding induced by basin margin tilt, seems unlikely based on a detailed discussion.

Following large-scale domal uplift in the beginning of the Paleocene, the late Paleocene to middle Eocene marked a renewed period of relative tectonic quiescence lacking salt movement. In the late Eocene to Oligocene, salt flow was reactivated in the northeastern Glückstadt Graben and local thickness variations of Cenozoic units suggests contemporaneous major growth of salt structures within the bays of Kiel and Mecklenburg. Cenozoic salt structure growth critically exceeded the growth during the Late Cretaceous. The different structural style of major Cenozoic reactivation of salt movement in the Glückstadt Graben compared to minor flow during Late Cretaceous inversion suggests a different driving mechanism for Cenozoic salt movement. This thesis proposes that extension triggered the Cenozoic reactivation of salt flow. The extensional event is possibly related to the coeval beginning development of the European Cenozoic Rift System.

Overall, salt structure evolution in the study area is strongly controlled by regional tectonics and phases of active salt movement correlate with periods of extension or shortening. Such times of active salt movement were replaced by periods of relative tectonic quiescence without salt movement, which were preceded by regional erosion events.

Zusammenfassung

Der Untergrund der heutigen südwestlichen Ostsee enthält ein einzigartiges geologisches Archiv der tektonischen Entwicklung eines intrakontinentalen Sedimentbeckens, welches stark durch Salztektonik geprägt wurde. In dieser Arbeit wird mit Hilfe von reflexionsseismischen Daten die strukturelle Entwicklung des Ostseeraums des Norddeutschen Beckens vom Perm bis zur Gegenwart untersucht. Dies entspricht einem Zeitraum von ca. 300 Millionen Jahren. Wichtige Ereignisse in der Entwicklung des Norddeutschen Beckens beinhalten: anfängliche permo-karbonische Blattverschiebungen und Vulkanismus gefolgt von thermischer Absenkung im Perm bis zur Mittleren Trias, Ost-West Extension in der Späten Trias, Hebung im Mittleren Jura, Inversion in der Späten Kreide und känozoische Extension und Vergletscherung. Die durchgeführte Analyse zur Entstehung und Überprägung des Ostseeraums des Norddeutschen Beckens und des Beckenrandes ermöglicht eine Neubewertung der Salztektonik im Kontext regionaler Tektonik. Die Ergebnisse tragen zu einem besseren Verständnis der Entwicklung komplexer Sedimentbecken bei. Dies ist aufgrund der Vielzahl von Ressourcen, Gefährdungspotenzialen und unterirdischen Nutzungsmöglichkeiten solcher Sedimentbecken ein wichtiger Aspekt der sozioökonomisch relevanten geologischen Forschung (z.B. für die Speicherung von Kohlendioxid, geothermische Energienutzung oder die Endlagerung von radioaktiven Abfällen).

Die stratigraphische Interpretation in dieser Arbeit basiert auf Bohrungen in Kombination mit hochauflösenden 2D seismischen Profilen. Der Datensatz deckt das Meeresgebiet von der Kieler Bucht bis nördlich der Insel Rügen ab. Die seismischen Abbilder (in Zwei-Wege Laufzeit und Tiefe) bilden den Untergrund vom Meeresboden bis zur Zechsteinbasis lückenlos ab. Regionale Karten in einer für das Untersuchungsgebiet bisher einmaligen stratigraphischen Untergliederung verdeutlichen die permische bis rezente Strukturentwicklung des nordöstlichen Glückstadt Grabens, der Salzstrukturen des Ostholstein-Mecklenburg Blocks und der Störungen des Vorpommerschen Störungssystems am nordöstlichen Beckenrand. Dadurch wird eine Aktualisierung des Störungsmusters, einschließlich der Grundgebirgsstörungen, ermöglicht. Die Kartierung des Zechsteins erlaubt eine Revision der Geometrie der Salzstrukturen im Arbeitsgebiet und offenbart ein bisher unbekanntes Salzkissen im Kleinen Belt.

In den meisten Teilen des Ostseeraums des Norddeutschen Beckens bestätigt die Kartierung des Buntsandsteins und des Muschelkalks das Fehlen von Salzbewegungen während der Frühen und Mittleren Trias. Eine Ausnahme könnte der Kegnaes Diapir am nördlichen Beckenrand bilden. Hier gibt die Seismik Hinweise auf Salzbewegungen und Störungsaktivität bereits während der Ablagerung des Buntsandsteins. Insgesamt zeigt sich, dass wesentliche Salzbewegungen im nordöstlichen Glückstadt Graben während des Ladiniums und Karniums einsetzten. In dieser Zeit war das Arbeitsgebiet regionaler Ost-West Dehnung ausgesetzt. Die zeitgleiche Aktivierung von Störungen am nordöstlichen Beckenrand, die teilweise durch das Zechsteinsalz vom Grundgebirge entkoppelt sind, wird mit transtensionalen Bewegungen innerhalb der Transeuropäischen Suturzone in Verbindung gebracht. Dadurch bildete sich ein transtensionales Subbecken mit erhöhter Akkumulation von Keuper- und Juraablagerungen. Zwischen den Störungssystemen des nordöstlichen Beckenrandes und dem

nordöstlichen Glückstadt Graben bildete der Ostholstein-Mecklenburg Block eine stabilere Übergangszone, in der Salzbewegungen erst in der Späten Trias - Frühen Jura einsetzten. Durch das Salz entkoppelte Extensionsbewegungen werden als Auslöser für die Anlegung der Salzstrukturen während der Späten Trias und im Frühen Jura interpretiert.

Aufwölbung und Erosion im Mittleren Jura führten zur Ausbildung einer regionalen stratigraphischen Lücke, die das Mitteljura bis Aptium umfasst. Mit der Wiederaufnahme der Sedimentation im Albium folgte eine Phase tektonischer Ruhe ohne Salzbewegungen. Diese Phase endete mit der Inversion in der Spätkreide, deren Beginn für das Arbeitsgebiet auf das Coniacium - Santonium präzisiert werden kann. Die Inversion äußerte sich in der Hebung des Grimmener Hochs, der Reaktivierung von Abschiebungen als Aufschiebungen und geringer Salzbewegung im Glückstadt Graben und der Mecklenburger Bucht. Krustenverkürzung wird als Auslöser der kretazischen Salzbewegung angesehen. Salzbewegung in der Mecklenburger Bucht und am nordöstlichen Beckenrand, die durch gravitatives Gleiten angetrieben wird, erscheint nach eingehender Diskussion unwahrscheinlich.

Nach regionaler Aufwölbung zu Beginn des Paläozäns folgte eine erneute Periode relativer tektonischer Ruhe ohne Salzbewegungen. Im späten Eozän bis Oligozän wurde der Salzfluss im nordöstlichen Glückstadt Graben reaktiviert. Lokale Mächtigkeitsunterschiede der känozoischen Einheiten implizieren gleichzeitiges Wiederaufleben der Akkumulation von Salz in den Strukturen der Kieler und Mecklenburger Bucht. Das Anwachsen der Salzstrukturen während des Känozoikums überstieg jenes in der Späten Kreide deutlich. Die strukturellen Unterschiede zwischen der intensiven känozoischen Reaktivierung im Glückstadt Graben im Vergleich zu dem geringen Ausmaß an Salzbewegung während der kretazischen Inversion, lassen auf einen anderen Antriebsmechanismus schließen. Diese Studie spricht sich für eine Reaktivierung der Salzbewegung im Känozoikum durch Extension aus. Dieses Extensionsereignis steht möglicherweise im Zusammenhang mit der gleichzeitig beginnenden Entwicklung des Europäischen Känozoischen Riftsystems.

Insgesamt wird die Entwicklung der Salzstrukturen im Untersuchungsgebiet stark von der regionalen Tektonik kontrolliert. Phasen aktiver Salzbewegung korrelieren mit Perioden von Extension oder Verkürzung. Solche Phasen aktiver Salzbewegungen wurden von Zeiten relativer tektonischer Ruhe ohne Salzbewegungen abgelöst, denen jeweils regionale Erosionsereignisse vorausgingen.

Table of contents

ABSTRACT	III
ZUSAMMENFASSUNG	V
TABLE OF CONTENTS	VII
LIST OF FIGURES AND TABLES	IX
LIST OF ABBREVIATIONS	XI
LIST OF DERIVED PUBLICATIONS	XIII
1. INTRODUCTION	1
1.1. STRUCTURE OF THE THESIS AND ASSOCIATED PUBLICATIONS	4
1.2. STUDY AREA: THE BALTIC SECTOR OF THE NORTH GERMAN BASIN	6
1.3. A BRIEF OVERVIEW OF THE BASIN EVOLUTION OF THE BALTIC SECTOR OF THE NORTH GERMAN BASIN	8
1.4. CONTRIBUTIONS FROM CO-AUTHORS.....	12
2. DATABASE AND METHODS	13
2.1. SEISMIC AND WELL DATA	13
2.2. SEISMIC IMAGING	16
2.3. DECIPHERING SALT FLOW: INTERPRETATION OF THE OVERBURDEN GEOMETRY	19
3. STRUCTURAL EVOLUTION AT THE NORTHEAST NORTH GERMAN BASIN MARGIN: FROM INITIAL TRIASSIC SALT MOVEMENT TO LATE CRETACEOUS- CENOZOIC REMOBILIZATION	21
ABSTRACT	21
3.1. INTRODUCTION.....	21
3.2. GEOLOGICAL SETTING.....	24
3.2.1. <i>Regional geological setting of the North German Basin</i>	24
3.2.2. <i>The northeast North German Basin margin</i>	24
3.2.3. <i>Salt tectonic framework of the northeastern North German Basin margin</i>	28
3.3. DATABASE AND METHODS	29
3.4. OBSERVATIONS	37
3.4.1. <i>Stratigraphic units and well correlation</i>	37
3.4.2. <i>Faults</i>	40
3.4.3. <i>Local depocenter analysis</i>	40
3.5. INTERPRETATION AND DISCUSSION.....	41
3.5.1. <i>Thick-skinned deformation</i>	41
3.5.2. <i>Salt tectonics and thin-skinned deformation</i>	45
3.6. SUMMARY	52
ACKNOWLEDGMENTS	53
4. TRIASSIC-JURASSIC SALT MOVEMENT IN THE BALTIC SECTOR OF THE NORTH GERMAN BASIN AND ITS RELATION TO POST-PERMIAN REGIONAL TECTONICS	55
ABSTRACT	55
4.1. INTRODUCTION.....	55
4.2. GEOLOGICAL SETTING.....	58
4.3. DATABASE & METHODS.....	61
4.3.1. <i>Seismic database</i>	61
4.3.2. <i>Stratigraphy</i>	62
4.3.3. <i>Mapping</i>	64
4.3.4. <i>Methodical uncertainties</i>	65

4.4.	OBSERVATIONS	67
4.4.1.	<i>Northwestern basin configuration</i>	67
4.4.2.	<i>Northern basin configuration and the Kegnaes Diapir</i>	68
4.4.3.	<i>Northeastern basin configuration</i>	69
4.4.4.	<i>Mapping</i>	71
4.5.	INTERPRETATION AND DISCUSSION	78
4.5.1.	<i>Timing of salt movement</i>	80
4.5.2.	<i>Faulting at the northeastern basin margin</i>	84
4.6.	CONCLUSIONS	86
	ACKNOWLEDGEMENTS	87
5.	IMPACT OF LATE CRETACEOUS INVERSION AND CENOZOIC EXTENSION ON SALT STRUCTURE GROWTH IN THE BALTIC SECTOR OF THE NORTH GERMAN BASIN	89
	ABSTRACT	89
5.1.	INTRODUCTION	89
5.2.	GEOLOGICAL SETTING	93
5.2.1.	<i>Late Permian to Early Cretaceous evolution</i>	93
5.2.2.	<i>Late Cretaceous to recent evolution</i>	95
5.3.	DATABASE AND METHODS	96
5.3.1.	<i>Seismic database</i>	96
5.3.2.	<i>Stratigraphy</i>	97
5.3.3.	<i>Depth imaging and refraction travelttime tomography</i>	98
5.3.4.	<i>Mapping</i>	100
5.4.	OBSERVATIONS	101
5.4.1.	<i>Key seismic profiles</i>	101
5.4.2.	<i>Thickness maps</i>	108
5.4.3.	<i>Faults</i>	112
5.5.	INTERPRETATION AND DISCUSSION	113
5.5.1.	<i>Late Cretaceous: from tectonic quiescence to inversion</i>	114
5.5.2.	<i>Late Paleocene: large-scale uplift</i>	116
5.5.3.	<i>Cenozoic salt movement</i>	117
5.5.4.	<i>Cause of Cenozoic reactivation of salt movement</i>	119
5.6.	CONCLUSIONS	121
	ACKNOWLEDGEMENTS	122
6.	DISCUSSION AND CONCLUSIONS	125
7.	OUTLOOK	129
	ACKNOWLEDGEMENTS	131
	REFERENCES	133
	EIDESSTÄTTLICHE VERSICHERUNG DECLARATION ON OATH	149

List of figures and tables

FIGURE 1.1: OVERVIEW OF THE STUDY AREA WITHIN THE CENTRAL EUROPEAN BASIN SYSTEM.....	5
FIGURE 1.2: CRUSTAL PROVINCES OF CENTRAL EUROPE INCLUDING MAIN TECTONIC STRUCTURES AND LINEAMENTS.....	7
FIGURE 1.3: STRUCTURAL OVERVIEW OF THE NORTHERN NORTH GERMAN BASIN (AHLRICH ET AL., 2022).....	8
FIGURE 1.4: LITHOSTRATIGRAPHIC CHART OF THE NORTH GERMAN BASIN SHOWING THE KEY SEISMIC REFLECTORS, DOMINANT LITHOLOGY, AVERAGED THICKNESS, MAIN TECTONIC EVENTS AND GLOBAL EUSTATIC SEA-LEVEL CURVES.....	11
FIGURE 2.1: SEISMIC AND WELL DATABASE USED IN THIS STUDY.	14
FIGURE 2.2: SCHEMATIC VISUALIZATION OF MARINE SEISMIC IMAGING.	17
FIGURE 2.3: VISUALIZATION OF THE PROCESSING WORKFLOW APPLIED TO THE BALTEC DATA INCLUDING KEY PARAMETERS OF THE APPLIED ROUTINES.	18
FIGURE 2.4: PRINCIPLES OF INTERPRETATION OF OVERBURDEN GEOMETRY AND THICKNESS RELATIONSHIPS ACROSS SALT STRUCTURES.	20
FIGURE 3.1: (A) TECTONIC MAP OF THE NORTH GERMAN BASIN INCLUDING MAJOR GEOLOGICAL STRUCTURES	23
FIGURE 3.2: LITHOSTRATIGRAPHIC CHART SHOWING THE DOMINANT LITHOLOGY AND AVERAGE THICKNESS WITHIN THE STUDY AREA.	27
FIGURE 3.3: CORRELATION OF ZECHSTEIN CYCLOTHEMS ALONG THE NORTHEAST NORTH GERMAN BASIN MARGIN.	28
FIGURE 3.4: SUBCROP MAP OF THE EARLY CIMMERIAN UNCONFORMITY (ECU) (BASE NORIAN; GERMAN: “ALTKIMMERISCHE HAUPTDISKORDANZ,” BEUTLER & SCHÜLER, 1978) INCLUDING ONSHORE WELLS USED FOR STRATIGRAPHIC CORRELATION.	30
FIGURE 3.5A: SEISMO-STRATIGRAPHIC CONCEPT FOR THIS STUDY.....	31
FIGURE 3.6: WELL-TO-SEISMIC TIE FOR WELLS (A) E Gv 1/78, (B) E PEW 1/65, AND (C) E DKE 1/68.....	33
FIGURE 3.7A: BGR16-254 TIME MIGRATED AND INTERPRETED SECTION.	35
FIGURE 3.8: INTERPRETED CENTRAL PART OF PROFILE BGR16-254; SEE FIGURE 3.1B FOR LOCATION.....	39
FIGURE 3.9: SKETCH ILLUSTRATING THE TECTONIC EVOLUTION AT THE NORTHEASTERN NORTH GERMAN BASIN MARGIN AS DERIVED FROM THE PRESENTED ANALYSIS OF PROFILE BGR16-254.....	44
FIGURE 3.10: SKETCH ILLUSTRATING SALT PILLOW GROWTH MECHANISMS. (A) INITIAL SITUATION WITH SALT LAYER AND PREKINEMATIC OVERBURDEN. (B) THICK-SKINNED EXTENSION AND SUBSEQUENT THICK-SKINNED SHORTENING. (C) THIN-SKINNED EXTENSION AND SUBSEQUENT THIN-SKINNED SHORTENING. (D) DIFFERENTIAL LOADING. (E) GRAVITY GLIDING.....	49
FIGURE 4.1: STRUCTURAL OVERVIEW OF THE NORTHERN NORTH GERMAN BASIN.....	57
FIGURE 4.2: LITHOSTRATIGRAPHIC CHART OF THE NORTH GERMAN BASIN SHOWING DOMINANT LITHOLOGY, MAIN TECTONIC EVENTS, AVERAGE THICKNESS AND LITHOSTRATIGRAPHIC SUBDIVISION OF THE TRIASSIC AND JURASSIC	61
FIGURE 4.3: SEISMIC AND WELL DATABASE USED IN THIS STUDY	62
FIGURE 4.4: WELL-TO-SEISMIC TIE FOR THE KEGNAEAS-1 WELL.....	63
FIGURE 4.5: PROFILE A AND PROFILE B, LOCATED AT THE NORTHWESTERN BASIN MARGIN (SEE FIG. 4.3). UNINTERPRETED SECTION IN TWO-WAY TRAVELTIME AND INTERPRETED SECTION.	66
FIGURE 4.6: PROFILE CROSSING THE NORTHERN BASIN MARGIN (SEE FIG. 4.3). A: UNINTERPRETED AND INTERPRETED SECTION IN TWO-WAY TRAVELTIME.	70
FIGURE 4.7: PROFILE A (BGR16-221) AND PROFILE B IMAGING THE NORTHEASTERN BASIN MARGIN.....	71
FIGURE 4.8: ZECHSTEIN. A: BASE ZECHSTEIN TIME-STRUCTURE MAP IN TWT. B: ZECHSTEIN ISOCHRON MAP IN TWT.	72

FIGURE 4.9: BUNTSANDSTEIN. A: BASE BUNTSANDSTEIN (TOP ZECHSTEIN) TIME-STRUCTURE MAP IN TWT. B: BUNTSANDSTEIN ISOCHRON MAP IN TWT.	74
FIGURE 4.10: MUSCHELKALK. A: BASE MUSCHELKALK TIME-STRUCTURE MAP IN TWT. B: MUSCHELKALK ISOCHRON MAP IN TWT.	75
FIGURE 4.11: KEUPER II (GRABFELD, STUTTGART AND WESER FORMATIONS). A: BASE KEUPER TIME-STRUCTURE MAP IN TWT. B: KEUPER II ISOCHRON MAP IN TWT.	76
FIGURE 4.12: KEUPER I (ARNSTADT AND EXETER FORMATIONS). A: EARLY CIMMERIAN UNCONFORMITY (ECU) TIME-STRUCTURE MAP IN TWT. B: KEUPER I ISOCHRON MAP IN TWT.	77
FIGURE 4.13: JURASSIC. A: BASE JURASSIC TIME-STRUCTURE MAP IN TWT. B: JURASSIC ISOCHRON MAP IN TWT.	78
FIGURE 4.14: CONCEPTUAL MODEL ASSUMING HIGH SEDIMENTATION RATE AND SYNDEPOSITIONAL SALT FLOW DURING DEPOSITION OF THE KEUPER I FOLLOWED BY POSTKINEMATIC DEPOSITION OF THE LOWER JURASSIC (A) AND WITH ONGOING SALT MOVEMENT IN THE EARLY JURASSIC (B).	81
FIGURE 5.1: STRUCTURAL ELEMENTS OF THE NORTHERN NORTH GERMAN BASIN (MODIFIED AFTER AHLRICHS ET AL., 2020).....	91
FIGURE 5.2: LITHOSTRATIGRAPHIC CHART SHOWING THE INTERPRETED KEY SEISMIC REFLECTORS, DOMINANT LITHOLOGY AND AVERAGE THICKNESS.....	94
FIGURE 5.3: MAPS SHOWING THE LOCATION OF SEISMIC PROFILES AND WELLS USED IN THIS STUDY.	97
FIGURE 5.4: PROFILE AL526-20, COVERING THE EASTHOLSTEIN TROUGH IN THE WESTERN BAY OF KIEL: TIME MIGRATED SECTION WITH WELL TIE TO UNDISCLOSED INDUSTRY WELL DATA.	101
FIGURE 5.5: PROFILE BGR16-232, LOCATED IN THE BAY OF KIEL: UNINTERPRETED PRESTACK DEPTH MIGRATED SECTION SHOWING VELOCITY RESULTS FROM THE TRAVELTIME TOMOGRAPHY (TOP) AND INTEPRETED SECTION (BOTTOM).	103
FIGURE 5.6: ZOOM OF PROFILE BGR16-232 (FIG. 5.5), LOCATED IN THE BAY OF KIEL.....	104
FIGURE 5.7: PROFILE BGR16-230, LOCATED IN THE BAY OF MECKLENBURG:.....	106
FIGURE 5.8: PROFILE BGR16-254, LOCATED IN THE BAY OF MECKLENBURG:.....	107
FIGURE 5.9: ZOOM OF PROFILE BGR16-254 (FIG. 5.8), LOCATED IN THE BAY OF MECKLENBURG.	108
FIGURE 5.10: ZECHSTEIN ISOCHORE MAP (ISOCHROME MAP CONVERTED USING A CONSTANT INTERVAL VELOCITY OF 4500 M/S.	109
FIGURE 5.11: ISOCHORE MAPS OF THE UPPER CRETACEOUS (ISOCHROME MAPS CONVERTED USING A CONSTANT INTERVAL VELOCITY).	111
FIGURE 5.12: ISOCHORE MAPS OF PALEOGENE AND NEOGENE UNITS (ISOCHROME MAPS CONVERTED USING A CONSTANT INTERVAL VELOCITY).	113
FIGURE 5.13: CONCEPTUAL MODEL VISUALIZING THE NECESSITY OF A CENOZOIC PHASE OF SALT MOVEMENT.	119
FIGURE 5.14: REGIONAL SKETCH MAP SHOWING LATE EOCENE TO OLIGOCENE STAGE OF STRUCTURAL EVOLUTION OF THE EUROPEAN CENOZOIC RIFT SYSTEM (ECRIS) IN RELATION TO THE GLÜCKSTADT GRABEN AND SALT STRUCTURES IN THE STUDY AREA.	121
 TABLE 2.1: SEISMIC ACQUISITION PARAMETERS OF SURVEYS USED IN THIS THESIS.	15
TABLE 5.1: INTERVAL VELOCITY INFORMATION FROM PUBLISHED LITERATURE	99

List of abbreviations

AF	Anklam Fault	NJF	Nord Jasmund Fault
AFS	Agricola Fault System	NMO	Normal moveout
AVF	Agricola Svedala Fault	NNE	North-northeast
Å/T	Ratio of aggradation rate and translation rate	NNW	North-northwest
BF	Bergen Fault	NW	Northwest
BG	Bresse Graben	PaF	Parchim Fault
BGR	Federal Institute for Geosciences and Natural Resources	PD	Prerow Depression
BN	Boltenhagen Nord (salt pillow)	PF	Plantagenet Fault
CCS	Carbon Capture and Storage	PFZ	Prerow Fault Zone
CDF	Caledonian Deformation Front	PR	Prerow salt pillow
CG	Central Graben	RG	Roer Graben
CMP	Common Midpoint	S	South
E	East	SASO	Strukturatlas südliche Ostsee
ECU	Early Cimmerian Unconformity	SE	Southeast
ECRIS	European Cenozoic Rift System	SF	Strelasund Fault
EEC	East European Craton	SKF	Skurup Fault
EG	Eger Graben	SRB	South Rügen Block
EHMB	Eastholstein-Mecklenburg Block	SRME	Surface related multiple attenuation
EHT	Eastholstein Trough	SSE	South-southeast
EL	Elbe Lineament	SSW	South-southwest
ESE	East-southeast	STZ	Sorgenfrei-Tornquist Zone
F	Fault	SVF	Svedala Fault
FF	Falster Fault	SW	Southwest
Fm	Formation	TESZ	Trans-European Suture Zone
GA	Gridding artefact	TN	Trollegrund Nord (salt pillow)
GG	Glückstadt Graben	TTZ	Teisseyre-Tornquist Zone
GTA	Geotektonischer Atlas von Nordwestdeutschland und dem deutschen Nordsee-Sektor	TWT	Two-way traveltime
HF	Hiddensee Fault	URG	Upper Rhine Graben
HG	Hessian grabens	USO	Untergrundmodell Südliche Ostsee
HoG	Horn Graben	VA	Velocity artefact
LG	Limagne Graben	VDF	Variscan Deformation Front
MPS	Mid-Polish Swell	VE	Vertical exaggeration
MPT	Mid-Polish Trough	W	West
MRB	Middle Rügen Block	WF	Wiek Fault
MVA	Migration velocity analysis	WeF	Werre Fault
N	North	WFZ	Werre Fault Zone
NE	Northeast	WPFS	Western Pomeranian Fault System
NGB	North German Basin	WNW	West-northwest

List of derived publications

Ahrlrichs, N., Hübscher, C., Noack, V., Schnabel, M., Damm, V., Krawczyk, C.M. (2020). Structural evolution at the northeast North German Basin margin: From initial Triassic salt movement to Late Cretaceous-Cenozoic remobilization. *Tectonics*, 39 (7), 1-26, <https://doi:10.1029/2019TC005927>.

Ahrlrichs, N., Noack, V., Hübscher, C., Seidel, E., Warwel, A., Kley, J. (2021). Impact of Late Cretaceous to Cenozoic inversion phases on salt structure growth in the Baltic sector of the North German Basin. *Basin Research*, 34 (1), 220-250, <https://doi.org/10.1111/bre.12617>.

Ahrlrichs, N., Noack, V., Seidel, E., Hübscher, C. (2022). Triassic-Jurassic salt movement in the Baltic sector of the North German Basin and its relation to post-Permian regional tectonics. Submitted to *Basin Research*.

1. Introduction

The North German Basin is a sedimentary intracontinental basin caused by prolonged subsidence driven by tectonic activity in the lithosphere and where sediments accumulate (e.g. Allen & Allen, 2005). The accumulation and preservation of sediments over long timespans make basins important geological archives of the Earth's evolution. The North German Basin is part of the superior Central European Basin System, which is known for its long and complex history of basin evolution since the Carboniferous. The basin system contains numerous salt structures composed of Permian Zechstein evaporites which have strongly overprinted the structural style of the post-Permian sedimentary basin fill by salt tectonics (e.g. Peryt et al., 2010). The understanding of the formation and subsequent overprinting of such complex intracontinental basins is highly relevant to both basic research and socioeconomics due to the multitude of resources, potential hazards and subsurface use capabilities of sedimentary basins. Therefore, a profound understanding of basin evolution and its deep-rooted fault systems is an important aspect of research, especially for the usage of the deeper subsurface for e.g. Carbon Capture and Storage (CCS), geothermal energy utilization, storage of renewable energy and the search for a nuclear waste repository. For decades, the Central European Basin System has been a prime area of geological research where numerous studies expanded the knowledge of the subsurface and its tectonic evolution and thereby, significantly contributed to the fundamental understanding of geological processes, especially in salt tectonics (Kockel, 1999; Maystrenko et al., 2008; Pharaoh et al., 2010; Kukla et al., 2019.).

The North German Basin (NGB) covers the Danish and German mainland as well as the North and Baltic Seas (Fig. 1.1). Important geological events throughout its basin evolution comprise (1) initial Permo-Carboniferous wrench faulting accompanied by volcanism and thermal subsidence, (2) late Permian deposition of the Zechstein evaporites, (3) continuous late Permian to Mid Triassic thermal subsidence, (4) Late Triassic E-W extension and basin differentiation, (5) Mid Jurassic uplift due to thermal doming, (6) Late Cretaceous inversion, (7) Cenozoic rifting and glaciation (Pharaoh et al., 2010). The Baltic sector of the North German Basin comprises the northern part of the basin and the transition from Paleozoic consolidated crust, the West European Platform, to the Precambrian East European Craton (Figs. 1.1 and 1.2). Main structural elements in this area include the northeastern part of the Glückstadt Graben, which experienced intensive extension and salt movement during the Triassic, and the Mesozoic Western Pomeranian Fault System, a series of Tornquist Zone related fault systems at the northeastern basin margin (Fig. 1.3) (Krauss & Mayer, 2004; Maystrenko et al., 2005a, 2005b; Seidel et al., 2018). Within the Baltic sector of the North German Basin, several marine geophysical studies conducted in the 1980s to early 2000s have investigated the crustal structure and its influence on the tectonic evolution of the area (EUGENO-S Working Group, 1988; BABEL Working Group, 1991, 1993; Schlüter et al., 1997; DEKORP-BASIN Research Group, 1999; Krawczyk et al., 1999; Scheck et al., 1999; Krawczyk et al., 2002). These studies focused on a better understanding of the deep-rooted structural framework and the investigation of Caledonian deformation. The Glückstadt Graben and adjacent areas were studied in the context of the development of the "Tectonic Atlas of Northwest Germany and the German North Sea

Sector (GTA)”, which investigated the structural setting of pre-Zechstein basement blocks and the Permian to Cenozoic structural evolution (Baldschuhn et al., 2001 and e.g. Frisch & Kockel, 1999; Kockel, 2002, 2003). Later on, the Mesozoic to recent structural evolution of the Glückstadt Graben was reassessed and the key role of salt tectonics during the post Permian evolution was emphasized (Maystrenko et al., 2005a, 2005b). Based on deep reflection seismic data, the development of Zechstein salt pillows has been investigated in the context of the structural evolution of the northeastern part of the NGB (Kossow et al., 2000; Kossow & Krawczyk, 2002). As part of the USO project, the fault systems and the structural setting of the offshore area around Rügen Island has been investigated based on reprocessed seismic data of the Petrobaltic database (Deutschmann et al., 2018; Seidel et al., 2018). Further marine reflection seismic studies carried out over the course of the BaltSeis and Neobaltic projects added insight into the post-Permian structural evolution of the southwestern Baltic Sea area. The corresponding studies used a dense network of shallow high-resolution reflection seismic data to investigate salt tectonic and neotectonic processes in the Baltic sector of the North German Basin (Hübscher et al., 2004; Hansen et al., 2005; Hansen et al., 2007; Hübscher et al., 2010; Al Hseinat & Hübscher, 2014; Al Hseinat et al., 2016; Kammann et al., 2016; Al Hseinat & Hübscher, 2017; Hübscher et al., 2019).

The studies mentioned above discussed the regional tectonic framework and its impact on salt structure evolution based on seismic imaging and mapping of post-Permian units with a seismo-stratigraphic subdivision in the order of geological series. Data gaps along the basin margin, incomplete seismic images, where either the shallow successions or the deeper part including the base Zechstein were not imaged, and partly limited spatial coverage of the available seismic data, have made a regional and comprehensive analysis of regional tectonics and salt movement challenging. Additionally, the relatively spacious distribution of well data and lack of offshore wells within the study area hampered a seismo-stratigraphic subdivision beyond the temporal scale of geological series. In the scope of the MSM52 research expedition in March 2016, the University of Hamburg in cooperation with the Federal Institute for Geosciences and Natural Resources (BGR), University of Greifswald, Polish Academy of Sciences, Uppsala University and the German Research Centre for Geosciences Potsdam acquired the BalTec data, a network of 2D high-resolution multichannel reflection seismic data spanning from the western Bay of Kiel up to Swedish and Polish territorial waters northeast of Bornholm. Due to its profile network and acquisition parameters, the BalTec data allow creating a continuous image from the base Zechstein up to the seafloor and a regional connection of previous more local surveys (Hübscher et al., 2016).

In this thesis, the BalTec dataset is used in combination with seismic profiles from other 2D marine seismic surveys in order to investigate the structural evolution of the Baltic sector of the North German Basin from Permian to recent times. The main objectives and questions to be answered are:

- Refinement of the seismo-stratigraphic framework of the Mesozoic and Cenozoic in the study area by using the regional network of high-resolution seismic data and all available well data.
- Identification and mapping of fault systems and key horizons from the base Zechstein to seafloor.
- Reassessing salt tectonics in the Baltic sector of the North German Basin under consideration of the following questions:
 - When did salt movement start and which active phases of salt movement since the deposition of the Zechstein can be differentiated?
 - Are there spatial differences in the timing of salt movement, especially between the Glückstadt Graben and adjacent areas?
 - What triggered salt movement? Is the trigger mechanism of salt movement basement-controlled or thin-skinned? Can gravity gliding explain salt deformation at the northern basin margin?
 - What is the impact of Late Cretaceous to Cenozoic inversion on salt structures in the Baltic sector of the North German Basin?
 - When exactly did inversion start?
 - Is it possible to differentiate individual inversion events in the sedimentary record?

The results of this thesis improve the understanding of the structural evolution of the Baltic sector of the North German Basin with a special focus on the development of salt structures in relation to regional tectonics. Besides the interest to geoscientific research and usage of the subsurface, the results contribute to national and European geological 3D modelling projects, such as the prospective offshore extension of the recently published German TUNB geological overview model (TUNB Working Group, 2021) or the 3D geomodelling for Europe (3DGEO-EU) (GeoERA Working Group, 2022).

1.1. Structure of the thesis and associated publications

This thesis is subdivided into six chapters, of which the chapters 3, 4 and 5 represent scientific articles published in international geoscience journals.

Chapter 1 provides an overview of the study area and its geological evolution and outlines the main research question, which are addressed in chapters 3-5.

Chapter 2 explains the basic concepts of the seismic imaging method and describes the database used in this thesis as well as the applied seismic processing workflow.

Chapter 3 is based on an article published in the journal *Tectonics*: Ahlrichs, N., Hübscher, C., Noack, V., Schnabel, M., Damm, V., Krawczyk, C. M. (2020). *Structural evolution at the northeast North German Basin margin: From initial Triassic salt movement to Late Cretaceous-Cenozoic remobilization*. *Tectonics*, 39 (7), 1-26, <https://doi.org/10.1029/2019TC005927>. This chapter analyses the Triassic to Cenozoic structural evolution of the northeastern NGB margin based on a 170 km long seismic transect running from the Bay of Mecklenburg to northeast Rügen Island. The seismo-stratigraphic framework developed for the study area is described in detail and the well-to-seismic tie is shown exemplary for three nearby onshore wells. Additionally, the chapter discussed the evolution of salt pillows in the Bay of Mecklenburg in the light of thick- and thin-skinned tectonics, gravity gliding and differential loading.

Chapter 4 is based on an article submitted to the journal *Basin Research*: Ahlrichs, N., Noack, V., Seidel, E., Hübscher, C. (2022). *Triassic-Jurassic salt movement in the Baltic sector of the North German Basin and its relation to post-Permian regional tectonics*. *Basin Research*, submitted for publication. This chapter focuses on the Triassic-Jurassic structural evolution and salt movement in the Baltic sector of the North German Basin and presents long seismic profiles across the northeastern, northern and northeastern basin margin of the study area. A present-day Zechstein map shows the structural setting of the unit and gives an update of basement fault in the bays of Kiel and Mecklenburg. By using regional maps with a refined stratigraphic subdivision, the onset of salt movement within the study area is shown and the Triassic-Jurassic development of salt pillows is elucidated. This chapter describes and discusses spatial differences in the evolution of salt structures in the study area and explains the development of salt diapirs at the northern basin margin by extension and erosional unroofing. Additionally, the tectonic evolution of the northeastern basin margin, including the faults systems of the Western Pomeranian Fault System, is discussed.

Chapter 5 is based on an article published in the journal *Basin Research*: Ahlrichs, N., Noack, V., Hübscher, C., Seidel, E., Warwel, A., Kley, J. (2021). *Impact of Late Cretaceous to Cenozoic inversion phases on salt structure growth in the Baltic sector of the North German Basin*. *Basin Research*, 34 (1), 220-250, <https://doi.org/10.1111/bre.12617>. This chapter focuses on the Cretaceous to Cenozoic structural evolution of the Baltic sector of the North German Basin based on seismic depth images and regional maps of Late Cretaceous and Cenozoic units with a refined stratigraphic subdivision. This allows investigating the nature and impact of individual Late Cretaceous to Cenozoic inversion events on salt movement. The onset of Late Cretaceous inversion is shown to have occurred in the Coniacian-Santonian

accompanied by uplift and minor salt movement. The Paleocene event is characterized by a large-scale domal uplift. The trigger mechanism of major Cenozoic salt movement is discussed and it is concluded that a thin-skinned extensional control related to opening of the European Cenozoic Rift System is likely. However, Cenozoic salt movement could have also been triggered by Alpine/Pyrenean-controlled thin-skinned compression.

Chapter 6 discusses the results of chapters 3-5, draws overall conclusions and provides an outlook to future work.

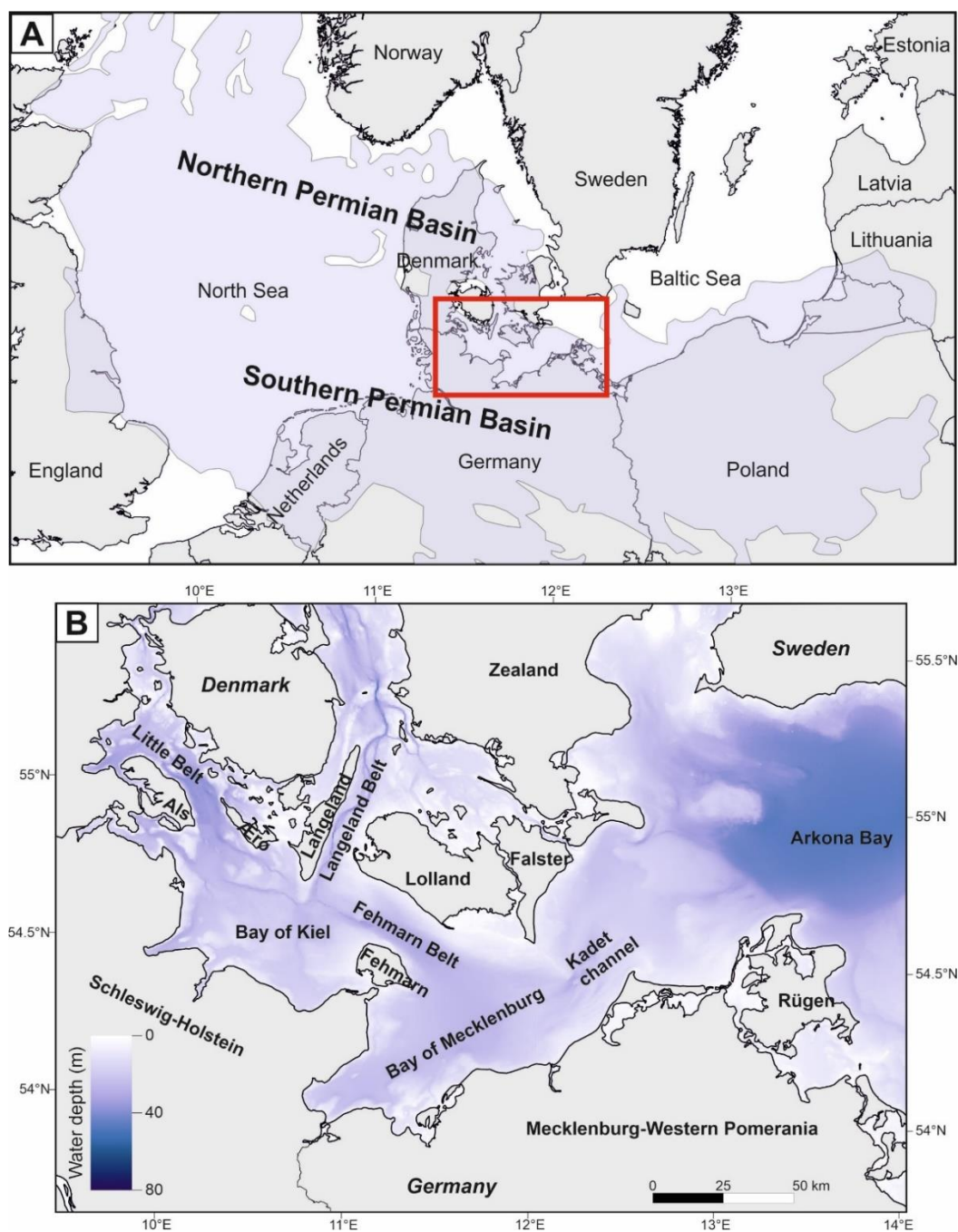


Figure 1.1: Overview of the study area within the Central European Basin System. A: Outline of the Central European Basin System as given by the present-day limit of the Permian deposits (modified after Maystrenko & Scheck-Wenderoth, 2013). Red box indicates the study area of this thesis. B: Bathymetry of the study area (Baltic Sea Hydrographic Commission, 2013).

1.2. Study area: The Baltic sector of the North German Basin

The Baltic sector of the North German Basin (NGB) comprises the Danish and German offshore area of the southwestern Baltic Sea, which includes the Little Belt, Bay of Kiel, Langeland Belt, Fehmarn Belt, Bay of Mecklenburg, Kadet channel and the Arkona Bay (Fig. 1.1). The crust below is made of a complex assemblage of terranes, namely the Paleozoic West European Platform (hereinafter just “Paleozoic Platform”) and its transition to the Precambrian East European Craton (Fig. 1.2) (e.g. Guterch et al., 2010). These terranes amalgamated during the Ordovician-Silurian Caledonian Orogeny and Devonian-Carboniferous Variscan orogeny. During the Caledonian Orogeny, the paleo-continent of East Avalonia, Baltica and Laurentia collided forming the continent of Laurussia (e.g. Guterch et al., 2010). During the Variscan Orogeny in Devonian-Carboniferous times, closure of the Rheic Ocean led to the collision of Gondwana and Laurussia which caused the amalgamation of the Armorican Terrane to Laurussia and the formation of the supercontinent of Pangaea (Fig. 1.2) (e.g. Maystrenko et al., 2008; Guterch et al., 2010 and references therein). The transition zone of the Paleozoic Platform to the East European Craton is termed the Trans-European Suture Zone, which spans from the Caledonian Deformation Front in the north to the Elbe Line in the south (Fig. 1.2) (Berthelsen, 1992; Guterch et al., 2010). Within this zone, Avalonia crust was thrust onto Baltica crust which progressively thins southwards and wedges out towards the Elbe Line (DEKORP-BASIN Research Group, 1999). Thereby, thrust Ordovician rocks form an accretionary wedge that developed in front of the advancing East Avalonia Terrane (DEKORP-BASIN Research Group, 1999). The Caledonian Deformation Front marks the present northernmost extent of the deformed Ordovician units, and thus, the northern limit of the accretionary wedge (Guterch et al., 2010). The northern part of the Trans-European Suture Zone spatially overlaps with the post-collisional Tornquist Fan, which is characterized by a northwestward widening zone of Paleozoic faults (Thybo, 1997). A prominent structural element in the northeastern part of the study area is the Tornquist Zone, an approx. 2000 km long NW striking tectonic lineament, which is subdivided into two branches, the southern Teisseyre-Tornquist Zone (TTZ) and the northern Sorgenfrei-Tornquist Zone (STZ). The latter represents an intracratonic border within the East European Craton separating the craton into a northeastern stable part and a southwestern intensively faulted zone, which was inverted during the Late Cretaceous (EUGENO-S Working Group, 1988; Erlström et al., 1997). In the past, the TTZ was considered as a lithospheric weakness zone separating the Precambrian crust of the East European Craton from the younger Paleozoic Platform, which was repeatedly reactivated since the Caledonian Orogeny (e.g. Guterch et al., 1986; Berthelsen, 1992; Thybo, 1997; Scheck-Wenderoth & Lamarche, 2005). Based on seismic, gravity and magnetic data, some studies observed the continuation of the East European Craton along the TTZ and correlated the TTZ with a crustal keel beneath undeformed lower Paleozoic units (Mazur et al., 2015; Mazur et al., 2018). Thus, these authors regard the TTZ as an intraplate feature of the East European Craton. However, a recent study could not reveal the existence of the keel and invoked the necessity of further research on the crustal structure of the TTZ (Janik et al., 2022).

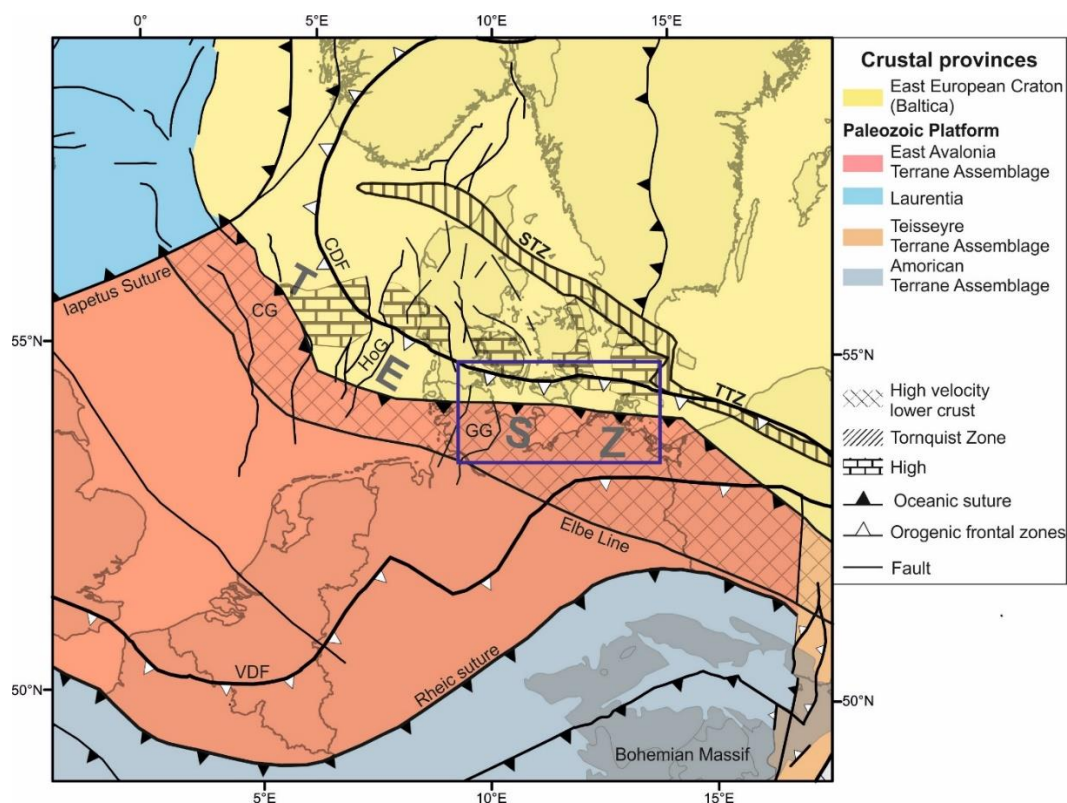


Figure 1.2: Crustal provinces of Central Europe including main tectonic structures and lineaments. The study area (blue rectangle) is located within the Trans-European Suture Zone (TESZ), the crustal transition zone between the Paleozoic Platform and the Precambrian East European Craton. CDF: Caledonian Deformation Front; CG: Central Graben; GG: Glückstadt Graben; HoG: Horn Graben; STZ: Sorgenfrei-Tornquist Zone; TTZ: Teisseyre-Tornquist Zone; VDF: Variscan Deformation Front. Compiled after Ziegler, 1990a; Vejbaek, 1997; Guterch et al., 2010; Mazur et al., 2018 and references therein.

Above this crustal association, the intracontinental Central European Basin System developed (Fig. 1.3). This system of sedimentary sub-basins covers the area from the North Sea to Poland and from Norway to the German mainland. It can be subdivided into the Northern Permian Basin and Southern Permian Basin, whereas the NGB is part of the latter. Main structural elements of the NGB are the Ringkøbing-Fyn High, Møn High and Arkona High. This series of WNW-ESE trending basement highs (sensu Peacock & Banks, 2020) mark the northern NGB margin and separate the NGB from the Norwegian-Danish Basin in the north. The highs are characterized by elevated Precambrian basement and a generally thin cover of Mesozoic and Cenozoic sediments (EUGENO-S Working Group, 1988). During late Carboniferous – early Permian WNW-ESE extension and transtension, the Ringkøbing-Fyn High experienced less stretching and thus, relatively less subsidence than the adjacent strongly subsiding North German and Norwegian Danish basins (Vejbaek, 1997). The western part of the Baltic sector of the NGB includes the Glückstadt Graben, one of the deepest post-Permian structures within the Central European Basin System (Fig. 1.3) (Maystrenko et al., 2005a). The Glückstadt Graben is a NNE-SSW trending Mesozoic-Cenozoic graben system with up to 11 km of post-Permian sediment thickness, which is strongly influenced by salt tectonics (Maystrenko et al., 2005b). The Eastholstein Trough forms the eastern part of the Glückstadt Graben and its northeastern part is located within the western Bay of Kiel (Fig. 1.3). Adjoining the Glückstadt Graben in

the east, the Eastholstein-Mecklenburg Block marks the peripheral region between the Glückstadt Graben and the faulted northeastern basin margin. The Eastholstein-Mecklenburg Block includes the central and eastern Bay of Kiel and Bay of Mecklenburg, where the post-Permian sedimentary thickness is decreased to 2 - 4 km and major Mesozoic-Cenozoic faults are absent (Fig. 1.3) (Maystrenko et al., 2005b; Hansen et al., 2007). The northeastern basin margin is characterized by a series of NW-SE to NNW-SSE striking Mesozoic fault systems, collectively referred to as the Western Pomeranian Fault System (Fig. 1.3, e.g. Werre Fault Zone, Prerow Fault Zone, Agricola Fault System, Wiek Fault System). These faults often border Y-shaped grabens or half-grabens, which formed during the Triassic by a reactivation of preexisting Paleozoic faults (Krauss & Mayer, 2004).

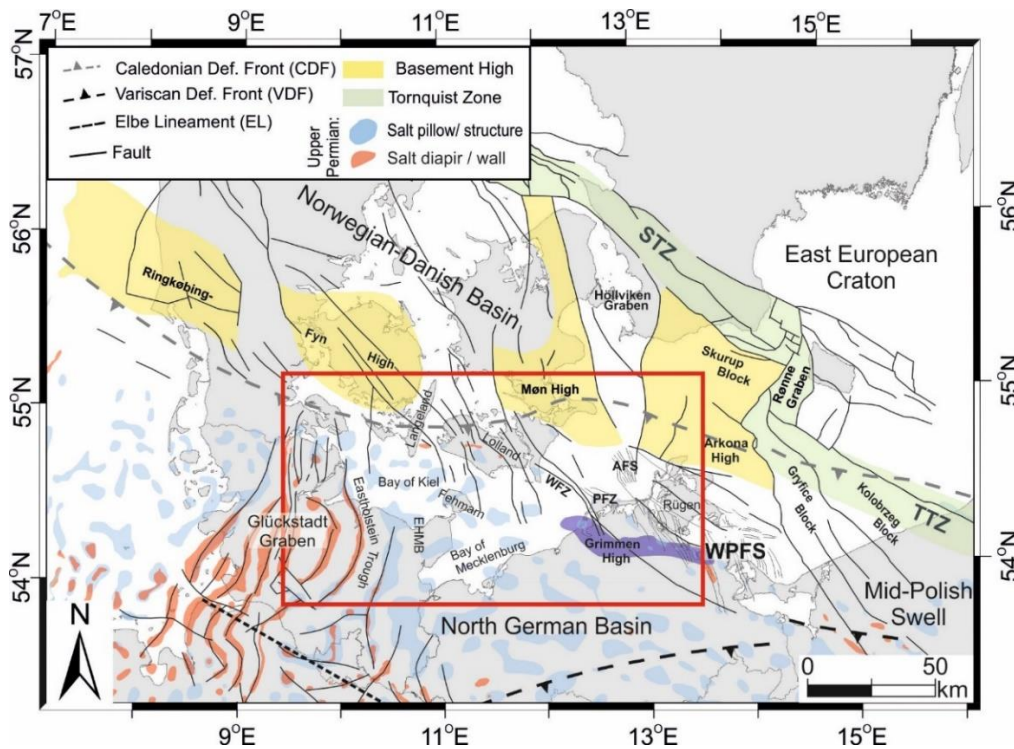


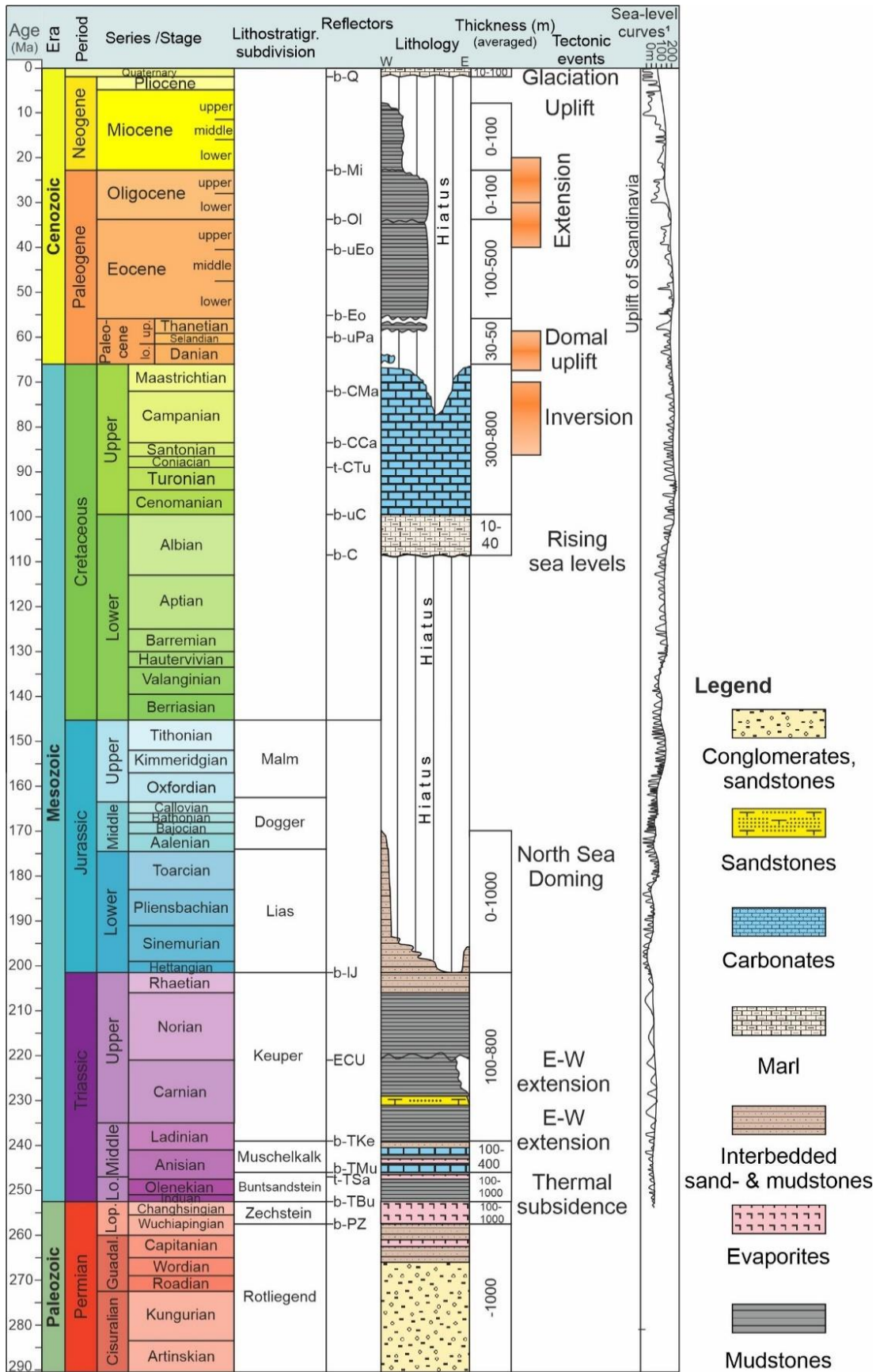
Figure 1.3: Structural overview of the northern North German Basin (Ahlrichs et al., 2022). AFS: Agricola Fault System; EHMB: Eastholstein-Mecklenburg Block; PFZ: Prerow Fault Zone; STZ: Sorgenfrei-Tornquist Zone; TTZ: Teisseyre-Tornquist Zone; WFZ: Werre Fault Zone; WPFS: Western Pomeranian Fault System.

1.3. A brief overview of the basin evolution of the Baltic sector of the North German Basin

At the end of the Variscan orogeny (late Carboniferous - early Permian), wrench faulting destabilized the crust of the Variscan foreland causing intensive magmatic activity and thermal thinning of the lithosphere (Ziegler, 1990a; Pharaoh et al., 2010). Following the decay of the thermal doming during the early Permian, the crust began to subside resulting in the formation of the Northern and Southern Permian basins (Inset of Fig. 1.3) (Ziegler, 1990a; Van Wees et al., 2000). In the late Permian, several marine transgressions flooded the basin, which was located at paleogeographic low latitudes. Repeated restricted seawater influx under arid conditions led to extensive evaporation and the deposition of the Zechstein evaporite succession which formed numerous salt

structures during the Mesozoic and Cenozoic (Fig. 1.4) (Tucker, 1991; Strohmenger et al., 1996; Pharaoh et al., 2010). The Zechstein succession is subdivided into seven units with repeating sequences, referred to as cyclothem, that each consist of varying amounts of clay/carbonates, anhydrite, halite and potash sequences (Z1: Werra; Z2: Stassfurt; Z3: Leine; Z4: Aller; Z5: Ohre; Z6: Friesland; Z7: Fulda) (Tucker, 1991; Strohmenger et al., 1996). However, the Friesland and Fulda cyclothem are only present in the southern part of the Baltic sector of the North German Basin (Best, 1989). The Werra cyclothem contains proportionally mostly anhydrite, which has a higher viscosity than pure halite and thus, is less mobile. The Stassfurt, Leine, Aller and Ohre cyclothem contain larger proportions of mobile halite with the largest proportion being found within the Stassfurt sequence, making the Stassfurt cyclothem the most important for salt tectonics in the study area (Kossow et al., 2000; Warren, 2010).

Thermal subsidence continued during Early and Middle Triassic times during deposition of the Buntsandstein and Muschelkalk units (Fig. 1.4) (Van Wees et al., 2000). Locally, approximately E-W extension interrupted the tectonic quiescence by forming a narrow graben in the central Glückstadt Graben caused by syndepositional faulting accompanied by salt movement (Brink et al., 1992). During the Late Triassic, tectonic activity increased throughout the study area. Late Triassic E-W extension widened the Glückstadt Graben causing intensive salt movement within the Glückstadt Graben and initiated salt structure growth in other parts of the study area (Fig. 1.4) (Brink et al., 1992; Hansen et al., 2005; Maystrenko et al., 2005b; Hansen et al., 2007; Hübscher et al., 2010; Al Hseinat et al., 2016). At the northeastern basin margin, Late Triassic extension and dextral transtensional movements within the Trans-European Suture Zone led to a reactivation of preexisting NW-SE oriented Paleozoic faults and the development of the Western Pomeranian Fault System (Krauss & Mayer, 2004; Seidel et al., 2018). Furthermore, the study area was affected by Late Triassic erosion causing a major unconformity, the Early Cimmerian Unconformity, within the Keuper succession (Fig. 1.4). At the northern and northeastern basin margin, Late Triassic erosion partially removed the entire lower Keuper deposits (Beutler & Schüler, 1978; Clausen & Pedersen, 1999).



*Global eustatic sea level curves (short and long term)

Figure 1.4: Lithostratigraphic chart of the North German Basin showing the key seismic reflectors, dominant lithology, averaged thickness, main tectonic events and global eustatic sea-level curves (compiled after Ahlrichs et al., 2020; Ahlrichs et al., 2021a; Ahlrichs et al., 2022 and references therein). Reflector abbreviations: b-Q: base Quaternary Unconformity; b-Mi: base Miocene; b-Ol: base Oligocene; b-uEo: base upper Eocene; b-Eo: base Eocene; b-uPa: base upper Paleocene; b-CMa: base Upper Cretaceous Maastrichtian; b-CCa: base Upper Cretaceous Campanian; t-CTu: top Upper Cretaceous Turonian; b-uC: base Upper Cretaceous; b-C: base Cretaceous; b-IJ: base Lower Jurassic; ECU: Early Cimmerian Unconformity; b-TKe: base Triassic Keuper; b-TMU: base Triassic Muschelkalk; b-TSa: top Triassic Salinarröt; b-TBu: base Triassic Buntsandstein; b-PZ: base Permian Zechstein. Other abbreviations: Guadal.: Guadalupian; Lo.: Lower; Lop.: Lopingian; Oligo.: Oligocene; Paleo.: Paleocene; Pl.: Pleistocene; Qu.: Quaternary.

From Middle Jurassic times until the Albian, basin subsidence was interrupted by a period of uplift and non-deposition related to the Mid North Sea Doming event (Fig. 1.4) (Ziegler, 1990a; Underhill & Partington, 1993). Corresponding widespread erosion removed much of the Jurassic and partly Upper Triassic deposits in the study area (Hansen et al., 2007; Japsen et al., 2007; Hübscher et al., 2010). Apart from the easternmost part of the study area, where Jurassic deposits are preserved to a higher degree, Jurassic remnants are almost exclusively preserved in rim-synclines, which was interpreted as an indication for ongoing salt movement at least during the Early Jurassic (Fig. 1.4) (Hansen et al., 2005). Rising sea-levels resumed sedimentation in the Albian followed by a period of relative tectonic quiescence during the Cenomanian to Turonian (Fig. 1.4) (Kossow & Krawczyk, 2002; Vejbaek et al., 2010). This period ended in the late Turonian to Santonian with the onset of the Africa-Iberia-Europe convergence, which subjected the study area to compression (Kley & Voigt, 2008). Resulting horizontal shortening induced during the Late Cretaceous caused uplift, erosion, the reactivation of normal as reverse faults and a rejuvenation of salt flow within the study area (Fig. 1.4) (Hansen et al., 2007; Hübscher et al., 2010; Al Hseinat & Hübscher, 2017). The Glückstadt Graben was only mildly inverted indicated by minor uplift of diapir roofs and minor salt movement in the outer Glückstadt Graben (Maystrenko et al., 2005b, 2006). A large-scale domal uplift followed in the late Paleocene, which removed lower Paleocene sediments (Fig. 1.4) (Vinken & International Geological Correlation Programme, 1988; Ziegler et al., 1995). During early to middle Eocene times, the study area underwent a period of relative tectonic quiescence which was interrupted by revived E-W extension and reactivated salt movement in the Glückstadt Graben with thickest accumulation of syntectonic deposits in the marginal parts (Fig. 1.4) (Hinsch, 1986; Katzung, 2004; Maystrenko et al., 2005b; Al Hseinat et al., 2016). Salt movement continued during the Oligocene in the eastern Glückstadt Graben and onshore eastern Germany (Hinsch, 1986; Katzung, 2004). Due to the temporal correlation, this late Eocene-Oligocene period of revived salt movement was related to approx. N-S directed intraplate compression induced by the Alpine and Pyrenean orogenies (Kley, 2018; Huster et al., 2020). In Miocene times, the North Sea Basin experienced strong subsidence while the basin margins were uplifted causing uplift of the Ringkøbing-Fyn High and adjacent areas (Fig. 1.4) (Rasmussen, 2009; Japsen et al., 2015). Corresponding erosion removed much of the Miocene, Oligocene and partly Eocene deposits in the study area while more complete stratigraphic sequences are only preserved in the Glückstadt Graben and onshore Germany (Hinsch, 1986, 1987; Katzung, 2004). During the Quaternary, the study area was affected by at least three extensive glaciations, which further eroded Neogene and Paleogene sedimentary units

(e.g. Sirocko et al., 2008). Glacial isostatic adjustments from the last (Weichselian) glaciation are still ongoing in the Baltic sector of the North German Basin (Lehné & Sirocko, 2010).

1.4. Contributions from co-authors

Chapters 3, 4 and 5 are based on articles either published or submitted to scientific journals. The articles were written in collaboration with co-authors mentioned at the beginning of each article. Their individual contribution to each article is stated in the following:

Chapter 3: Christian Hübscher, Vera Noack and Michael Schnabel contributed to the interpretation and discussion of the results. Michael Schnabel contributed to the development of the seismic data processing workflow applied to create the final images published in the article. Volkmar Damm and Charlotte M. Krawczyk contributed to data acquisition during the MSM52 cruise, which lay the foundation for this article. All co-authors reviewed the manuscript.

Chapter 4: All co-authors (Christian Hübscher, Vera Noack, Elisabeth Seidel) contributed to the interpretation and discussion of the results and reviewed the manuscript.

Chapter 5: Christian Hübscher, Vera Noack and Elisabeth Seidel contributed to the interpretation and discussion of the results. Arne Warwel applied the refraction traveltime tomography, extracted the velocity information and mainly wrote the paragraph describing the methodology of the tomography in chapter 5.3.3. Jonas Kley contributed to the discussion of the results and their association with inversion events in Central Europe. All co-authors reviewed the manuscript.

2. Database and Methods

2.1. Seismic and well data

The database used in this thesis consists of marine 2D reflection seismic profiles with a total profile length of more than 10,000 km acquired during multiple seismic surveys between 1976 and 2019 (Fig. 2.1). The database includes five industry 2D seismic profiles kindly provided by ExxonMobil Production Deutschland GmbH (Fig. 2.1). Furthermore, the database contains seismic data of the former consortium Petrobaltic, which acquired a dense profile network of 2D reflection seismic data offshore Rügen Island between 1978 and 1989 (Fig. 2.1). This data was partly reprocessed in the 1990s (Rempel, 1992; Scheidt et al., 1995; Arndt et al., 1996; Schlüter et al., 1997). Additionally, marine seismic reflection profiles of the DEKORP BASIN'96 campaign were used (Fig. 2.1) (DEKORP-BASIN Research Group, 1999). All these surveys image the deeper subsurface, however, the shallow part of the profile including the seafloor is not resolved. The database includes seismic data from surveys of the Universities of Aarhus and Hamburg, carried out between 1998 and 2004, which acquired high-resolution 2D seismic profiles in the Danish and German Baltic Sea over the course of the BaltSeis and NeoBaltic projects (Fig. 2.1) (Hübscher et al., 2004). Additional data was added during annual student expeditions of the University of Hamburg between 2005 and 2019 (Hansen et al., 2005; Hansen et al., 2007; Hübscher et al., 2010; Al Hseinat & Hübscher, 2014; Al Hseinat et al., 2016; Kammann et al., 2016; Al Hseinat & Hübscher, 2017; Hübscher et al., 2019). This data has high-resolution and resolves the shallow subsurface including the seafloor. However, the deeper subsurface is not imaged due to limited signal penetration. Furthermore, the database used in this thesis includes the BalTec data, a 2D reflection marine seismic dataset acquired in 2016 over the course of the MSM52 cruise by the University of Hamburg in cooperation with the Federal Institute for Geosciences and Natural Resources (BGR), University of Greifswald, Polish Academy of Sciences, Uppsala University and the German Research Centre for Geosciences Potsdam (Fig. 2.1) (Hübscher et al., 2016). The BalTec profiles span a network of high-resolution multichannel seismic data from the western Bay of Kiel up to Swedish and Polish territorial waters northeast of Bornholm Island. This data continuously images the Zechstein salt base up to the seafloor which allows a connection of the previously mentioned rather local surveys both spatially and in depth.

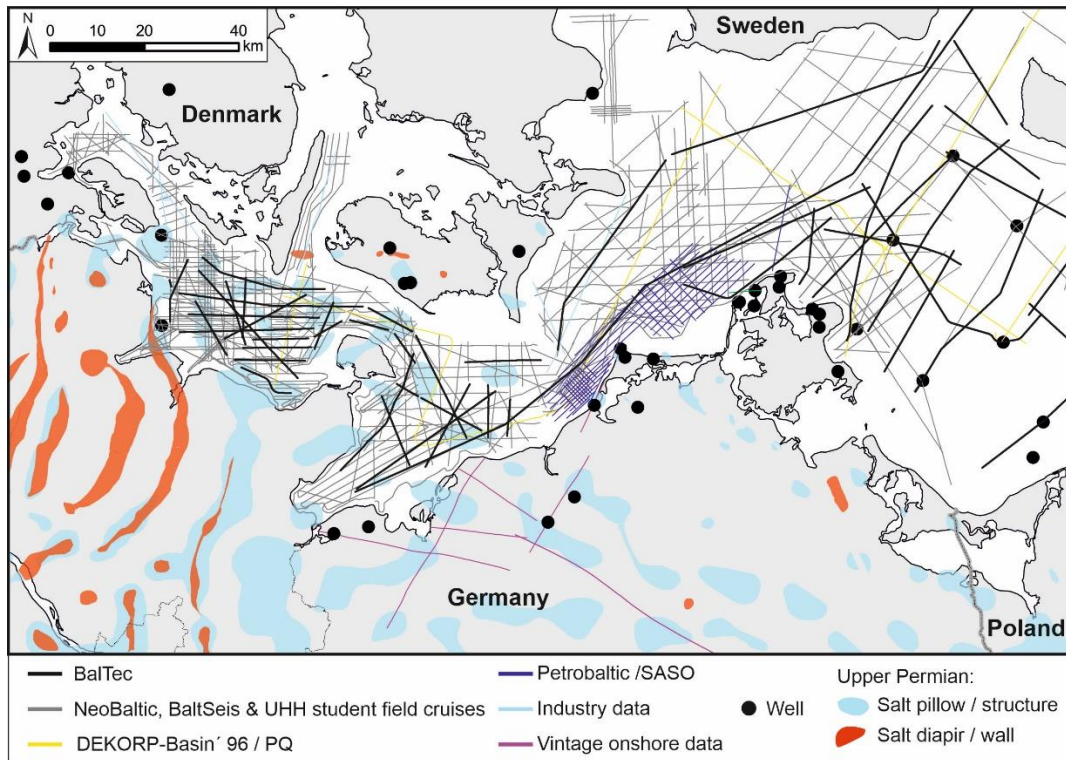


Figure 2.1: Seismic and well database used in this study. The seismic database consists of multiple surveys acquired between 1976 and 2016.

Each seismic survey had different acquisition parameters and setups, which are summarized in table 2.1. Additionally, table 2.1 provides an estimation of the vertical resolution of each survey using a quarter of the wavelength ($\lambda/4$) as an estimate for vertical resolution and an interval velocity of 2 km/s to 5 km/s.

Stratigraphic interpretation of seismic units in this thesis is based on well data from offshore and nearby onshore wells (Fig. 2.1). The well database consists of deep research and hydrocarbon exploration wells, which are located in Germany, Denmark and Poland (Nielsen & Japsen, 1991; Hoth et al., 1993; Schlüter et al., 1997). Additionally, undisclosed industry well data from the western Bay of Kiel was used. Well data includes stratigraphic markers, lithological records and well logs (gamma ray, resistivity, for some wells sonic and density logs). Stratigraphic markers were converted from depth to two-way traveltimes using check shot and vertical seismic profiling data.

Dataset	BalTec	Petrobaltic	Industry data	DEKORP/ PQ	BaltSeis	NeoBaltic	Student cruises
Sources	8 Airguns (GI-gun, G-gun)	Airgun / Vaporchoc	Airgun	10 Airguns	4 sleeve guns	4 sleeve guns	4 sleeve guns / 1 GI gun / Sparker
Shot interval (m)	25	25	50	75	12.5	12.5	12.5
No. Channels	216	24 / 48		84	48	96	48 / 64
Channel interval (m)	12.5	50	50	25	6.25	6.25	4 / 3.125
Sample rate (ms)	2	4	4	4	1	1	1 / 0.5
CMP Interval (m)	12.5	25	25	12.5	3.125	3.125	12.5 / 3.125
Assumed Dominant Frequency (Hz)	80	30	35	15	75	80	110 / 250
Vertical resolution (m)	6 - 16	17 - 42	14 - 36	33 - 83	7 - 17	6 - 16	2 - 11

Table 2.1: Seismic acquisition parameters of surveys used in this thesis.

2.2. Seismic imaging

The method of reflection seismic imaging allows investigating the Earth's subsurface by artificially generated seismic waves which travel through the subsurface and are reflected at geological layer boundaries due to contrasts of rock properties (Fig. 2.2) (e.g. Hübscher & Gohl, 2014). During marine seismic data acquisition, a vessel drags a source, such as an air-gun array, and receivers, usually several hydrophones built into a streamer (Fig. 2.2). The seismic signal generated by the source is a pressure wave travelling through the water column and within the subsurface. A small proportion of the down-going signal is reflected at layer boundaries, while the rest is transmitted into the deeper subsurface and thus, reflected at the subsequent layer boundaries. Hydrophones within the streamer record the reflected signal which can be processed to create an image of the subsurface with a good vertical and horizontal structural resolution. In a reflection seismic measurement, the distance between source and receiver is small compared to the target depth implying that the recorded reflections reach the surface at steep angles (Fig. 2.2) (Hübscher & Gohl, 2014). A seismic wave that has been reflected only once before its recording is called a primary reflection (black lines in Fig. 2.2). A wave reflected more than once, i.e., multiple times at the sea surface, is called a multiple (grey lines in Fig. 2.2). Multiples are commonly unwanted signals as they might mask primary reflections.

Seismic processing is necessary in order to create a high-quality image of the subsurface enabling geological interpretation. To achieve this, seismic data processing makes use of various available methods which generally aim to reduce or eliminate unwanted components (noise) in the data (i.e. multiples), while enhancing signal carrying the desired subsurface information (i.e. primary reflections from geological boundaries). In the scope of this thesis, seismic data processing was done for the BalTec data while seismic images of all other used profiles were provided as final processed sections. Their processing and the applied processing routine of the BalTec data are briefly described in the following. For a comprehensive theoretical and practical background of the used routines, the reader is referred e.g. to Yilmaz (2001).

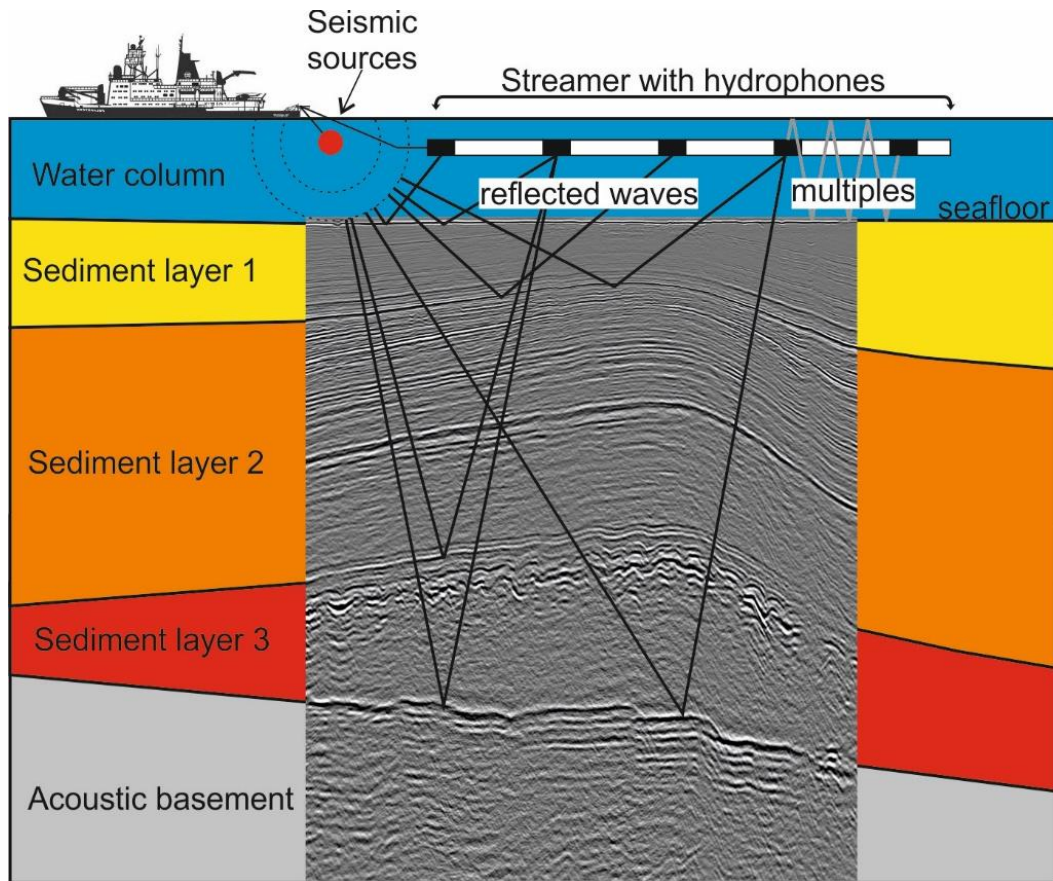


Figure 2.2: Schematic visualization of marine seismic imaging. Artificially generated seismic waves travel through the subsurface and are reflected at geological layer boundaries due to contrasts of rock properties. Black lines show exemplary ray paths of reflected waves, which are recorded by hydrophones built into a streamer. Grey lines show exemplary ray paths of multiple reflections, which reverberate within the water column. Modified after Hübscher & Gohl, 2014. Seismic data taken from Ahlrichs et al. (2021b).

The processing routine applied to the BalTec data is visualized in Figure 2.3. A major processing task was to remove surface multiples reverberating within the water column. Due to the shallow water of the Baltic Sea, these multiples have high amplitudes and mask signals from the deeper subsurface. Effective multiple attenuation was achieved using a combined approach including prestack predictive deconvolution in the slant-stack (τ - p) domain, surface-related multiple attenuation (SRME) (Verschuur, 2006) and poststack predictive deconvolution in the time domain. Time-variant frequency filtering, both prestack and poststack, amplitude recovery, F-X deconvolution, and muting of linear events enhanced the signal to noise ratio. An elaborate iterative velocity analysis was performed on every hundredth CMP position, which improved the results of the NMO correction and stacking. Furthermore, the data was migrated using a Kirchhoff Time Migration algorithm.

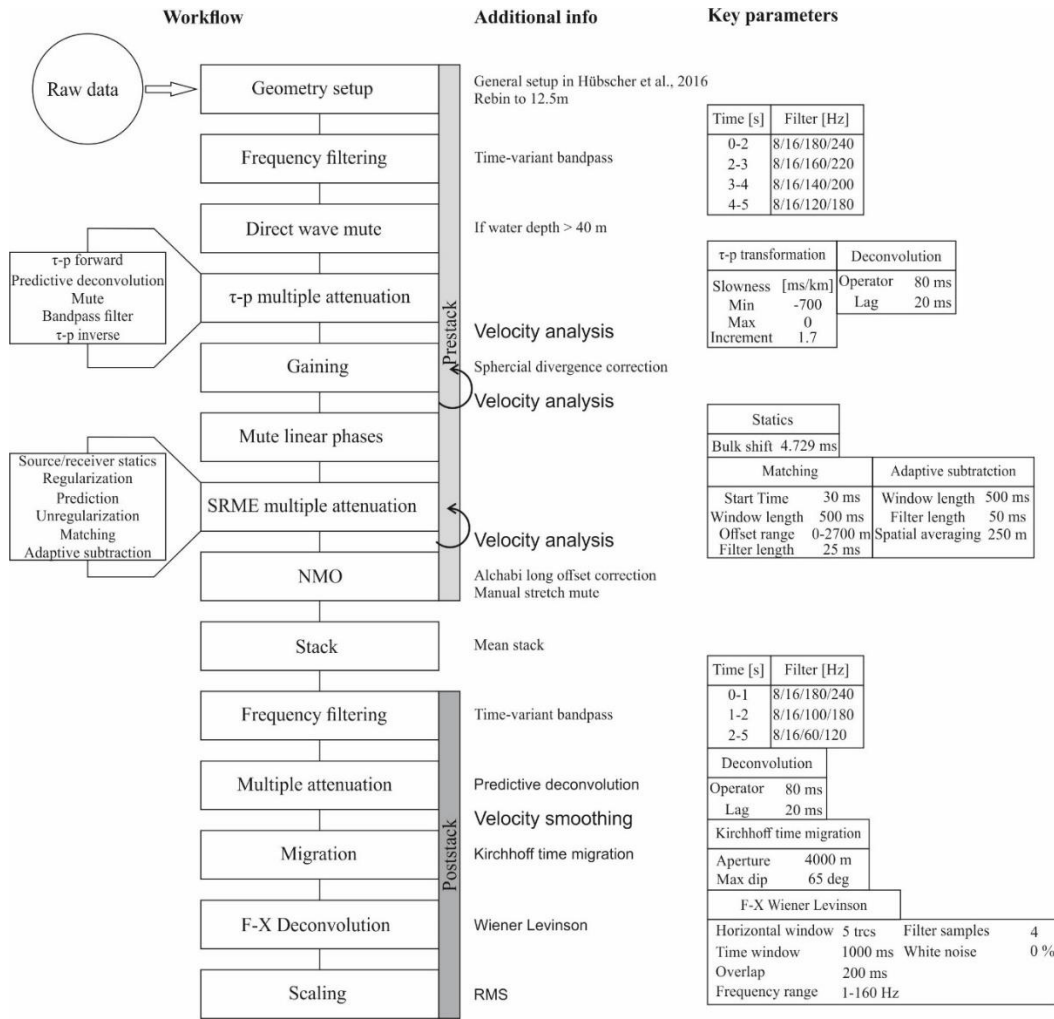


Figure 2.3: Visualization of the processing workflow applied to the BalTec data including key parameters of the applied routines.

The industry data, data of the Petrobaltic, DEKORP, BaltSeis, NeoBaltic and student cruise surveys all have been processed following standard processing procedures including frequency filtering, trace muting, amplitude recovery, statics, F-K filtering, NMO correction, stacking and migration. In order to attenuate multiples, a predictive deconvolution in the time domain has been applied (for further information, see BaltSeis, NeoBaltic, student cruises: Al Hseinat, 2016; DEKORP/PQ: Krawczyk et al., 2002; Petrobaltic: Scheidt et al., 1995; Arndt et al., 1996). The profiles of the Petrobaltic database have been partly reprocessed including enhanced multiple attenuation using radon filtering. A detailed report on the reprocessing is available at the Federal Institute for Geosciences and Natural Resources, Hannover (Scheidt et al., 1995; Arndt et al., 1996). In 2020, Tobias Häcker (University of Hamburg) has elaborately reprocessed seismic profiles of the NeoBaltic database located in the Bay of Mecklenburg and southeastern Bay of Kiel. Reprocessing included enhanced noise removal techniques and multiple attenuation by τ -p deconvolution and SRME.

2.3. Deciphering salt flow: interpretation of the overburden geometry

In this study, seismic imaging is used to improve the understanding of the structural evolution of sedimentary basins. Seismic data allows constructing a detailed image of the subsurface, which visualizes the depth of geological layer boundaries. In combination with well data, reflectors of key layer boundaries can be identified and incorporated into the chronostratigraphic framework. Mapping identified reflectors allows constructing structure maps (in two-way travelttime or depth) that visualize the depth structure of the subsurface. The difference between the depth locations of identified reflectors yields thickness information of stratigraphic units. In this study, seismic profiles, isochore maps (vertical thickness of a unit in meters) and isochrone maps (vertical thickness of a unit expressed in two-way travelttime) are used to identify local and regional thickness variations. To infer the geological history of a unit, spatial thickness variations of a unit can be interpreted as an expression for differential sedimentation or erosion caused by vertical tectonic movements, differential compaction and sedimentation processes (see e.g. Betram & Milton, 1989).

Rock salt is a sedimentary rock originating from evaporation. Strictly speaking, it consists purely of the mineral halite. However, pure halite sequences are rare in nature and therefore, in salt tectonics, (rock) salt refers to rock composed mostly of halite even though it incorporates other evaporites such as anhydrite or potash salts and even clastic sediments (Jackson & Hudec, 2017). In geology, salt is quite special as its mechanical properties differ from those of most clastic or carbonate rocks. Over geological time scales, salt can flow like viscous fluid if the salt body experiences deformational forces by differential loading. Major factors implying differential loading stem from gravity (gravitational loading) and tectonics (displacement loading) (Jackson & Hudec, 2017). A gravitational load is caused by differential sedimentation, thus lateral differences in sediment deposition above the salt body which causes differences in weight distribution and a corresponding downward force displacing the salt laterally. Displacement loading refers to lateral forces on the salt body originating from regional shortening or extension, which squeeze or stretch the salt body.

In the case of salt tectonics, the development of a salt structure can be inferred from the sediments overlying the salt body, the so-called overburden. The timing of salt movement can be determined by analyzing the geometric relationship between overburden and the salt body and the lateral thickness variations in the overburden across the salt structure (e.g. Jackson & Hudec, 2017). Salt flowing from the surrounding area into the salt structure causes the top of salt to subside which creates accommodation space for more sediments above the area of salt withdrawal (Fig. 2.4). This results in increased thickness of the unit deposited during salt flow (synkinematic unit) if compared to adjacent areas without salt movement. Likewise, salt flowing into the salt structure causes decreased accommodation space above the growing salt structure, which leads to a decreased thickness of the synkinematic unit (Fig. 2.4) (Jackson & Hudec, 2017). As a consequence, seismic reflectors within the synkinematic unit are divergent above the area of salt withdrawal and converge towards the salt structure (Fig. 2.4) (Sørensen, 1986). The reflection pattern and thickness variations can be identified on seismic images and thus, allow timing of active phases of salt movement.

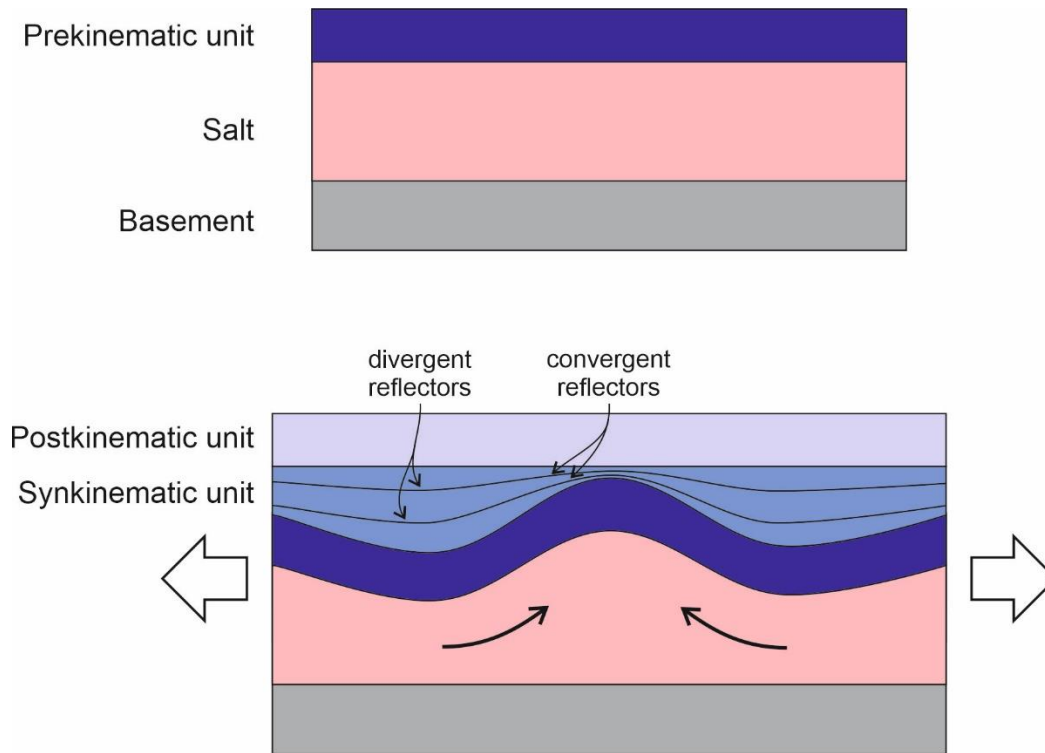


Figure 2.4: Principles of interpretation of overburden geometry and thickness relationships across salt structures. In this case, salt flow is triggered by extension, hence, displacement loading.

3. Structural evolution at the northeast North German Basin margin: From initial Triassic salt movement to Late Cretaceous-Cenozoic remobilization

Abstract

In this study, we investigate the regional tectonic impact on salt movement at the northeastern margin of the intracontinental North German Basin. We discuss the evolution of salt pillows in the Bay of Mecklenburg in the light of thick- and thin-skinned tectonics, including gravity gliding, and differential loading using seismic imaging. Stratigraphic and structural interpretation of a 170 km long, multichannel seismic line, extending from the Bay of Mecklenburg to northeast of Rügen Island, incorporates well information of nearby onshore wells. This new high-resolution seismic line completely images the stratigraphic and tectonic pattern of the subsurface, from the base of the Zechstein to the seafloor. Our analysis reveals that subsidence during Late Triassic to Early Cretaceous at the northeastern basin margin was associated with transtensional dextral strike slip movement within the Trans-European Suture Zone. We reinterpret the Werre and Prerow Fault Zones west of Rügen Island as an inverted, thin-skinned normal fault system associated with the formation of the Western Pomeranian Fault System. Salt movement in the Bay of Mecklenburg was initiated in the Late Triassic and lasted until the Early Jurassic. A second phase of salt pillow growth occurred during the Coniacian until Cenozoic and correlates with compression related regional basin inversion due to the onset of the Africa-Iberia-Europe convergence. Thin-skinned extensional initialization of salt pillow growth and compressional salt remobilization explains salt pillow evolution in the Bay of Mecklenburg. Additionally, we discuss an impact of gravity gliding on salt pillow evolution induced by basin margin tilt.

3.1. Introduction

Salt structures within continental basins frequently form as a result of plate and intraplate tectonic deformation, often in the vicinity of prominent basement faults due to extension or shortening (Vejbaek, 1997; Scheck-Wenderoth et al., 2008; Warren, 2008; Callot et al., 2012; Coleman et al., 2017; Krzywiec et al., 2019; Pichel et al., 2019; Warsitzka et al., 2019). In the presence of a salt layer that effectively decouples the overburden from the underlying basement faulting, thin-skinned deformation can alternatively initiate the development of salt structures. Differential sediment load is another important reason for the formation of salt structures (e.g. Trusheim, 1960; Jaritz, 1973; Davis & Engelder, 1985; Vendeville & Jackson, 1992; Kockel, 1999; Blanc et al., 2003; Hudec & Jackson, 2007; Stewart, 2007; Kukla et al., 2008; Callot et al., 2012; Jackson & Hudec, 2017; Warsitzka et al., 2019). Salt tectonics at continental margins has been intensively studied because of the availability of high-quality continuous seismic images from the basement up to the seafloor. Here along the passive margins, widely present gravity driven deformation by means of gravity gliding and gravity spreading, dominates the scientific discussion about the principle salt tectonic mechanisms. Gravity gliding refers to downdip gliding of the salt-sediment package caused by basin margin tilt, whereas gravity spreading is driven by differential

sediment load (Cobbold & Szatmari, 1991; Rowan et al., 2004; Jackson & Hudec, 2005; Brun & Fort, 2011, 2012; Rowan et al., 2012). The effect of gravity driven salt flow in the Southern Permian Basin has been rarely studied and often remained speculative (overview by Warsitzka et al., 2019. Allertal: Best, 1996; North Sea: Stewart & Coward, 1996; Thieme & Rockenbauch, 2001; Ems Trough: Mohr et al., 2005; Rheinsberg Trough: Scheck et al., 2003; Polish Basin: Krzywiec, 2012). Therefore, a detailed analysis of gravity driven deformation and its contribution to the salt tectonic evolution in intracontinental basins remains an open task. The Baltic Sea sector of the North German Basin (NGB) marks an excellent study area to further investigate the impact of regional tectonics on salt mobilization. The major structural element bounding the study area in the east is the Tornquist Zone. It consists of two segments, the southern Tornquist-Teisseyre Zone (TTZ) and the northern Sorgenfrei-Tornquist Zone (STZ). The latter represents the southwestern border between the stable Precambrian East European Craton (EEC) and its southwestern intensively faulted part (EUGENO-S Working Group, 1988; Erlström et al., 1997). The TTZ separates the EEC from the Paleozoic crust of Central Europe (Berthelsen, 1992). However, recent studies by Mazur et al. (2015) support the suggestion of Berthelsen (1998) that the TTZ represents a pseudo-suture and therefore can be regarded as an intraplate feature of the EEC. Adjacent to the TTZ, the Permian-Mesozoic Polish Basin developed contemporaneously to the NGB. Both are parts of the Southern Permian Basin, which is included in the Central European Basin System, a series of related intracontinental basins spreading from Britain to the Polish mainland (Maystrenko et al., 2008; Pharaoh et al., 2010). Within the central part of the NGB, the prominent Mesozoic-Cenozoic Glückstadt Graben marks the western border of the study area (Fig. 3.1).

The structural style of post-Permian deposits in the NGB is strongly influenced by salt tectonics resulting in many salt structures consisting of Upper Permian Zechstein evaporites. Several past marine geophysical studies, such as EUGENO-S Working Group (1988), BABEL Working Group (1991, 1993), Petrobaltic (e.g. Rempel, 1992), SASO (Schlüter et al., 1997) and DEKORP-BASIN Research Group (1999) documented major tectonic events in the Baltic Sea sector of the NGB. These projects focused mainly on a better understanding of deep-crustal structures. Studies carried out within the Neobaltic project (Hübscher et al., 2004; Hansen et al., 2005; Hansen et al., 2007; Hübscher et al., 2010; Al Hseinat et al., 2016; Al Hseinat & Hübscher, 2017) and studies by Kossow et al. (2000), Krawczyk et al. (2002), Kossow and Krawczyk (2002), Maystrenko et al. (2005b); Maystrenko et al. (2013), Seidel et al. (2018) and Deutschmann et al. (2018) provided further insight into Mesozoic and Cenozoic tectonics. These authors discussed the salt tectonic evolution in the context of its regional tectonic framework. However, they did not further elaborate on the causative processes due to data gaps along the basin margin and incomplete seismic imaging from the base of the Zechstein to the seafloor.

This study is part of the “StrucFlow” project, where we investigate the kinematic history of the northeast NGB margin from initial Triassic salt movement to Cretaceous-Cenozoic basin inversion and salt remobilization by means of new high-resolution reflection seismic data. This dataset closes the gap between former surveys and studies in terms of both seismic resolution and depth penetration in the study area. This allows

a first-time comprehensive analysis of emplacement and timing of salt movement from deposition to present day in the offshore sector of the NGB. We start our studies by stratigraphic interpretation, fault interpretation and analysis of local depocenters along a 170 km long seismic profile in order to identify and date salt movements. The profile images a significant part of the northeast NGB covering the deeper basin towards the basin margin. We discuss the impact of regional tectonics on salt movement at the northeast NGB margin in the light of thin- and thick-skinned tectonics, differential loading as well as an impact of gravity induced salt flow. This study provides new insight into the interaction between reactivated deep-seated fault zones and salt movement caused by regional tectonic stress. Our findings add to the understanding of the complex structural evolution of salt-floored intracontinental basins in their marginal domain.

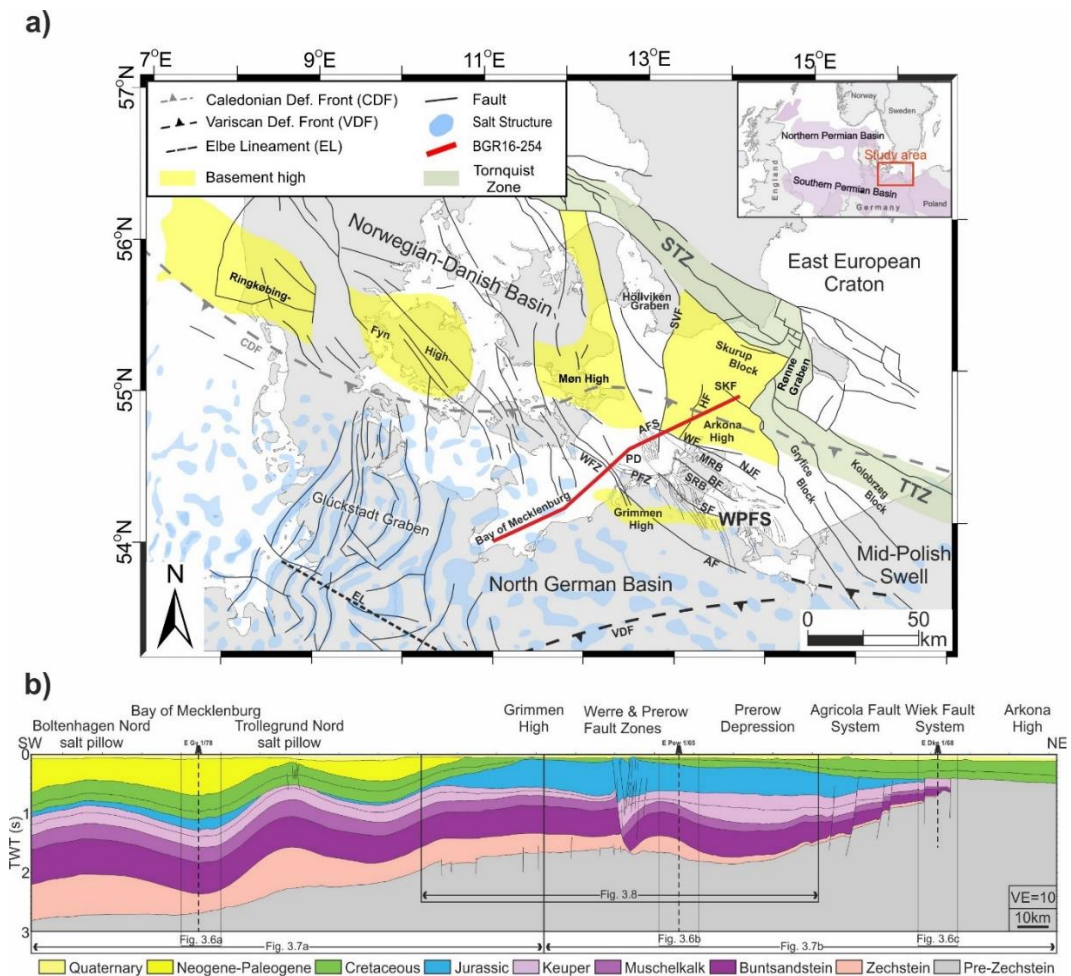


Figure 3.1: (a) Tectonic map of the North German Basin including major geological structures (based on Vejbaek & Britze, 1994; Schlüter et al., 1997; Baldschuhn et al., 2001; Pharaoh et al., 2010; Al Hseinat & Hübscher, 2017; Seidel et al., 2018; Mazur et al., 2020). Inset shows approximate outline of the northern and southern Permian Basin. Red line marks position of profile BGR16-254 analyzed in this study. AF = Anklam Fault; AFS = Agricola Fault System; BF = Bergen Fault; CDF = Caledonian Deformation Front; EL = Elbe Lineament; HF = Hiddensee Fault; MRB = Middle Rügen Block; NJF = Nord Jasmund Fault; PD = Prerow Depression; PFZ = Prerow Fault Zone; SF = Strelasund Fault; SKF = Skurup Fault; SRB = South Rügen Block; STZ = Sorgenfrei-Tornquist Zone; SVF = Svedala Fault; TTZ = Tornquist-Teisseyre Zone; VDF = Variscan Deformation Front; WFZ = Werre Fault Zone; WF = Wiek Fault; WPFS = Western Pomeranian Fault System. (b) Condensed geological cross section along profile BGR16-254 analyzed in this study, showing main structures and stratigraphic features. Seismic data acquired during cruise MSM52 (Hübscher et al., 2016).

3.2. Geological Setting

3.2.1. Regional geological setting of the North German Basin

The North German Basin (NGB) is part of the Southern Permian Basin, which extends from Britain over central Europe to Poland (e.g. Maystrenko et al., 2008) (Inset of Fig. 3.1). The basin is an intra-continental basin with a complex structural development from the Carboniferous to present. Its evolution began with WNW-ESE extension and transtension in the latest Carboniferous-Permian accompanied by the deposition of Carboniferous volcanics, coal and Lower Permian volcanics and clastics (Ziegler, 1990b; Bachmann et al., 2008; Maystrenko et al., 2008). Several marine transgressions at paleogeographic low latitudes led to extensive evaporation and the deposition of the Permian Zechstein (Wuchiapingian-Changshingian) evaporites. These evaporites formed numerous salt structures during the Mesozoic-Cenozoic (Tucker, 1991; Strohmenger et al., 1996; Maystrenko et al., 2008; Bachmann et al., 2010; Warsitzka et al., 2019). Thermal subsidence and phases of E-W extension characterize the Triassic basin evolution (Ziegler, 1990b; Van Wees et al., 2000; Maystrenko et al., 2008). From Middle Jurassic to Late Jurassic, thermal doming in the North Sea (centered in the Central Graben) caused large-scale uplift and erosion of Jurassic and partly Triassic deposits in the North German Basin (Underhill, 1998; Graversen, 2006). In Late Cretaceous times, NW-SE to N-S directed shortening changed the overall stress regime to compressive. Compressional stress caused inversion of normal faults, the initiation of reverse faults and folding. This compressive event marks the onset of the Africa-Iberia-Europe convergence. Additional pulses of uplift and inversion followed in the Early Paleocene and Late Eocene, accompanied by the development of E-W to NW-SE oriented extension (Kley & Voigt, 2008; Maystrenko et al., 2008; Bachmann et al., 2010; Kley, 2018).

3.2.2. The northeast North German Basin margin

Major structural elements bounding the North German Basin (NGB) are the Ringkøbing-Fyn, Møn and Arkona Highs in the north, and the Mid-Polish Swell (MPS) in the east (Fig. 3.1). The study area covers the region from the eastern Glückstadt Graben in the west towards the MPS (Fig. 3.1). This area includes deeper parts as well as the northeastern margin of the NGB. The northeastern basin margin developed partly above the transition of the Paleozoic lithosphere of central Europe to the Precambrian East European Craton. The crustal border marking this transition consists of a complex assemblage of terranes. This zone is termed the Trans-European Suture Zone, which spans between the Caledonian Deformation Front in the north and the Elbe Line in the south (Berthelsen, 1992; Pharaoh, 1999; Guterch et al., 2010 and references therein) (Fig. 3.1). The area around Rügen Island is characterized by the Western Pomeranian Fault System, a set of smaller fault zones (e.g. Werre Fault Zone, Prerow Fault Zone, Agricola Fault System, see Fig. 3.1 for location), whose development is associated with the Trans-European Suture Zone (Krauss & Mayer, 2004). The crust within this area consists of Caledonian and Variscan consolidated terranes (Brink et al., 1990; Ziegler, 1990b; Berthelsen, 1992; Krawczyk, McCann, et al., 2008; Krawczyk, Rabbell, et al., 2008; Maystrenko et al., 2008). Formation of the NGB began in the Late

Paleozoic and was associated with extensive volcanism, faulting, lithospheric thinning and following thermal relaxation of the thinned lithosphere (Ziegler, 1990b; Benek et al., 1996; Gast et al., 1998; Scheck & Bayer, 1999; Van Wees et al., 2000). The main phase of thermal subsidence started in the Early Permian and lasted until Middle Triassic times (Kossow et al., 2000; Van Wees et al., 2000). The lowermost basin fill at the northeast basin margin consists of upper Carboniferous to Permian volcanics overlain by lower Permian sediments (Scheck & Bayer, 1999; Geißler et al., 2008) (Fig. 3.2). Several marine transgressions of the epicontinental Zechstein Sea in combination with repeatedly restricted seawater influx under arid climate conditions led to the deposition of the Zechstein evaporites. The Zechstein succession involves seven cyclic units (cyclothems) each consisting of clay/carbonates, anhydrite and halite sequences (Tucker, 1991; Strohmenger et al., 1996). However, only five major cyclothems are present in the study area. The Werra (Z1) cyclothem consists mostly of anhydrite, which is less mobile than halite due to its higher viscosity. The Stassfurt (Z2), Leine (Z3), Aller (Z4) and Ohre (Z5) cyclothems contain thicker layers of mobile halite and less dominant anhydrite layers. A thicker anhydrite rich layer developed in the Leine cyclothem (e.g. Kossow et al., 2000; Katzung, 2004; Warren, 2008). The Stassfurt (Z2) sequence represents the most important cyclothem for salt tectonics in the study area due to its thick halite sequence (Kossow et al., 2000; Warren, 2008). Thickness of the Zechstein succession decreases towards the northeast NGB margin (Fig. 3.3). Mobile halite segments gradually reduce and pinch out northeast of the Prerow Fault Zone (Figs. 3.1 and 3.3). Near the west of Rügen Island, halite and anhydrite are absent within the Zechstein. Here, carbonates and siltstones, mostly of the Stassfurt cyclothem, dominate the marginal Zechstein succession (Fig. 3.3) (Zagora & Zagora, 1997; Kaiser, 2001).

The overlaying Triassic Buntsandstein succession consists mostly of intercalated claystone and siltstone deposited during accelerated basin subsidence (Hoth et al., 1993; Van Wees et al., 2000; Kossow & Krawczyk, 2002). A regional rise in sea level in the Middle Triassic led to the deposition of the Muschelkalk platform carbonates. Major faulting and indications for halokinesis are absent in the study area within the Buntsandstein and Muschelkalk units (Kossow & Krawczyk, 2002).

A eustatic sea level drop established terrestrial conditions in the Triassic Keuper (Nöldecke & Schwab, 1976; Scheck & Bayer, 1999). E-W directed extension occurred in the Glückstadt Graben resulting in salt movement in the surrounding area (Jaritz, 1987; Frisch & Kockel, 1999; Maystrenko et al., 2006). A major erosional event occurred within the Keuper. Beutler and Schüller (1978) described the event as the “Alt-kimmerische Hauptdiskordanz” (Early Cimmerian Unconformity in Bachmann et al., 2010). Erosion of the entire Lower Keuper down to Muschelkalk deposits occurred at the basin margin in the western Rügen area. Towards the basin center, Lower Keuper deposits are preserved (Fig. 3.4). This erosional event was contemporaneous to the development of the NE-SW trending Western Pomeranian Fault System between the Wiek and Anklam faults (Frisch & Kockel, 1999; Kossow et al., 2000; Beutler et al., 2012; Seidel et al., 2018) (Fig. 3.1). The fault system consists of several fault zones and smaller fault systems bordering Y-shaped graben structures such as the Werre and Prerow Fault Zones and Agricola Fault System. Their formation is associated with

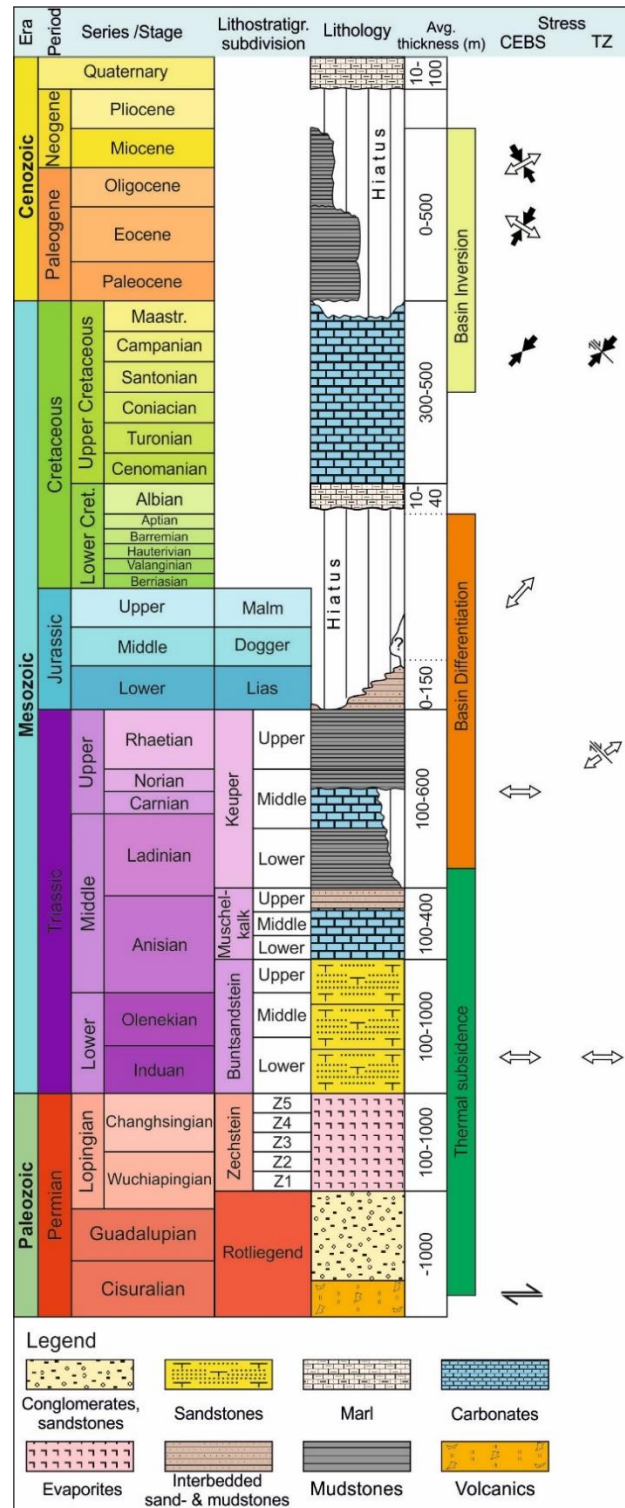
dextral transtensional movements above the Trans-European Suture Zone during the Late Triassic to Early Cretaceous (Krauss & Mayer, 2004; Deutschmann et al., 2018; Seidel et al., 2018). The authors attribute this Mesozoic dextral shear stress with NE-SW extension to the reactivation of existing NW-SE oriented Paleozoic faults, which were decoupled from the supra-salt succession by the partly overlying Zechstein salt.

A major transgression in the Rhaetian led to renewed sedimentation in shallow marine conditions lasting throughout the Jurassic (Kossow et al., 2000). From Late Jurassic times until the Albian, subsidence was interrupted by a period of uplift and non-deposition at the northeastern basin margin. Erosion of almost the entire Jurassic sequence and in some areas even Keuper units occurred. Lower Jurassic sediments preserved in rim-synclines indicate active salt movement during this time (Kossow et al., 2000; Maystrenko et al., 2005b). Due to an observed increasing amount of erosion from the Bay of Mecklenburg in westward direction, Hübscher et al. (2010) and Al Hseinat and Hübscher (2017) associate the uplift with the Central North Sea doming event (Ziegler, 1990b; Underhill & Partington, 1993; Graversen, 2006).

Rising sea levels during the Albian led to a major transgression and resumed sedimentation (Vejbaek et al., 2010). Shallow marine conditions and rising eustatic sea level prevailed until early Turonian times and mark a period of relative tectonic quiescence (Scheck & Bayer, 1999; Kossow & Krawczyk, 2002; Vejbaek et al., 2010). Sea level remained high until the Campanian. From the Santonian until the Cenozoic, the study area underwent several pulses of uplift and inversion associated with major plate reorganization and the onset of the Africa-Iberia-Europe convergence and Pyrenees and Alpine orogenies (Kley & Voigt, 2008; Kley, 2018). Horizontal shortening induced during the Late Cretaceous (late Turonian/Santonian to Maastrichtian) inversion pulse reactivated preexisting basement faults leading to uplift and erosion at the northeastern basin margin (Kossow & Krawczyk, 2002; Kley & Voigt, 2008; Kley, 2018). Uplift of the Grimmen High resulted in complete erosion of the Cretaceous deposits so that Cenozoic successions directly overlay Lower Jurassic sediments along this WNW striking basin edge structure. The pinch out of mobile Zechstein salt northeast of the Grimmen High is interpreted to have increased the basal friction between decoupled overburden and the basement. This caused increased resistance against the northward propagating overburden deformation, which resulted in uplift of the Grimmen High (Kossow et al., 2000; Kossow & Krawczyk, 2002).

Figure 3.2: Lithostratigraphic chart showing the dominant lithology and average thickness within the study area. Main phases of the development of the Central European Basin System are shown together with main stress direction. (based on Kossow & Krawczyk, 2002; Kley & Voigt, 2008; Al Hseinat & Hübscher, 2017; Seidel et al., 2018. Average thickness is based upon Hoth et al., 1993).

Further uplift events during the Cenozoic occurred during the Paleocene and late Eocene to late Oligocene. However, their exact timing and spatial extent is an aspect of recent discussion (Kley, 2018). Cenozoic sediments above salt pillows in the Bay of Mecklenburg reveal quite strong thickness reduction and increased salt pillow growth from Late Cretaceous to Cenozoic. A change of stress orientation from NE-SW to NW-SE directed extension during the Neogene caused another phase of intensified salt movement and fault reactivation (Hübscher et al., 2010; Kammann et al., 2016; Al Hseinat & Hübscher, 2017).



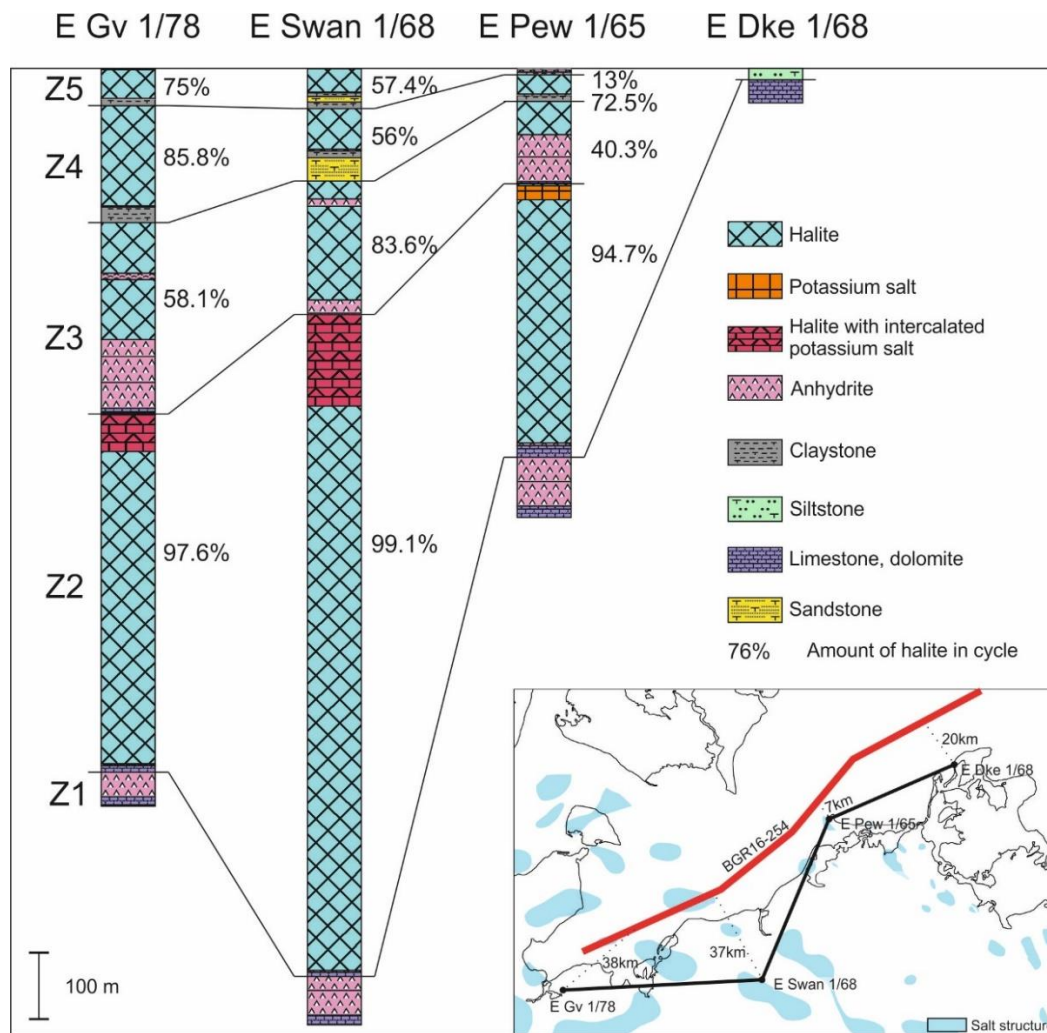


Figure 3.3: Correlation of Zechstein cyclothems along the northeast North German Basin margin. Z1 = Werra; Z2 = Stassfurt; Z3 = Leine; Z4 = Aller; Z5 = Ohre. Well information compiled after Hoth et al., 1993. Inset: salt structures after Reinhold et al. (2008). Numbers represent approximate distance from the well to similar position regarding salt distribution on the profile BGR16-254 (see also Figure 3.1 for location).

3.2.3. Salt tectonic framework of the northeastern North German Basin margin

According to several previous studies, many salt structures in the North German Basin were triggered and grew during multiple phases of extension. Salt structure growth is linked to normal faulting of the sub-salt basement (e.g. structures within the Glückstadt Graben) (Jaritz, 1973; Kockel, 1999, 2002; Maystrenko et al., 2005b; Mohr et al., 2005; Kukla et al., 2008; Warren, 2008). Salt structures in the northeastern part of the NGB have been widely studied with respect to their distribution, geometry and timing. Salt movement was analyzed as a function of the regional tectonic framework in the context of early stage salt movement within a continental basin (Kossow et al., 2000; Kossow & Krawczyk, 2002; Scheck et al., 2003; Zöllner et al., 2008; Hübscher et al., 2010; Warsitzka et al., 2019). However, a direct link between salt structure distribution and basement faults was not found.

The development of salt pillows in the Bay of Mecklenburg began after the deposition of the Triassic Muschelkalk (Zöllner et al., 2008). Hübscher et al. (2010) showed a Late Triassic initiation of salt pillow growth caused by E-W extension. This was

followed by a phase of (salt) tectonic quiescence from Early to latest Cretaceous times. A second phase of pronounced salt movements from the latest Cretaceous to Paleogene is related to basin inversion caused by compression (Kossow & Krawczyk, 2002). Crustal shortening induced basinwide tightening of pre-existing anticlinal structures, which amplified salt pillows. However, the amount of shortening significantly decreases from south to north. Hence, the effect of shortening on salt structures close to the northeastern basin margin remains quite unclear. Al Hseinat and Hübscher (2017) identified three major fault trends affecting salt movement in the study area. The authors relate NNE-SSW and N-S trending faults to the development of the Glückstadt Graben and the NW-SE trending faults to movement at the Tornquist Zone (Fig. 3.1).

3.3. Database and Methods

In March 2016, the University of Hamburg, in cooperation with the Federal Institute for Geosciences and Natural Resources (BGR), University of Greifswald, Polish Academy of Sciences, Uppsala University and the German Research Centre for Geosciences Potsdam, acquired 3500 km of high-resolution multichannel seismic data onboard RV Maria S. Merian, cruise MSM52, as part of the “BalTec” project (Hübscher et al., 2016). The seismic equipment consisted of an eight GI-Gun cluster (45/105 in³) allowing for deep signal penetration with a relatively wide frequency bandwidth with a dominant frequency of 80 Hz. The streamer had an active cable length of 2700 m with a minimum offset of 33 m. In this study, a major processing task was to remove strong, reverberating multiples caused by the shallow water of the Baltic Sea. We applied a combined strategy consisting of a τ -p domain prestack predictive deconvolution scheme, surface-related multiple attenuation (SRME) and poststack predictive deconvolution to effectively attenuate multiples (Verschuur, 2006). High amplitude refracted waves were muted. Further processing steps include frequency filtering, amplitude recovery, noise reduction and poststack time migration. Interval velocities in the study area range from 1600 m/s (Quaternary) to 5100 m/s (Zechstein) (Schlüter et al., 1997; Hansen et al., 2007; Noack et al., 2018). This results in a seismic vertical resolution in the order of 5-30 m. Horizontal resolution approximated by the width of the first Fresnel Zone after migration is 20-100 m.

This study focuses on structural and stratigraphic interpretation of a regional reflection seismic profile (BGR16-254) running from the Bay of Mecklenburg towards Rügen Island across the NGB margin into the Arkona Basin (Figs. 3.1 and 3.4). Stratigraphic interpretation of seismic units is based on information from nearby onshore wells (see table in Fig. 3.4). Additionally, we used marine seismic profiles from the Rerik-See area, kindly provided by Neptune Energy (Fig. 3.4), in order to validate our stratigraphic correlation. The well information used in this study comprises well reports of deep research wells and hydrocarbon exploration wells (Nielsen & Japsen, 1991; Hoth et al., 1993; Schlüter et al., 1997). For stratigraphic correlation, most important wells are E Gv 1/78, E WuoRD 6/77, E Pew 1/65, E Pew 2/66, E Dke 1/68, E Rn 2/67, E Rn 3/63, E Rn 5/66 (Fig. 3.4). Well reports include well markers and in some cases well logs (gamma ray, resistivity, sonic, density). Lithological information was taken from the detailed geological profiles presented in the well reports. We converted stratigraphic well markers to the time domain using check shot and vertical seismic

profiling data for the well-to-seismic tie. Thereby, we considered the position of the well in the structural basin setting to constrain the correlation. Due to the distance to the wells and their different structural positions, stratigraphic correlation is based on thickness, represented by traveltime difference, rather than directly upon depth. In addition, the stratigraphic interpretation was linked to results of previous studies (Katzung, 2004; Zöllner et al., 2008; Bachmann et al., 2010; Hübscher et al., 2010; Kammann et al., 2016; Al Hseinat & Hübscher, 2017; Deutschmann et al., 2018).

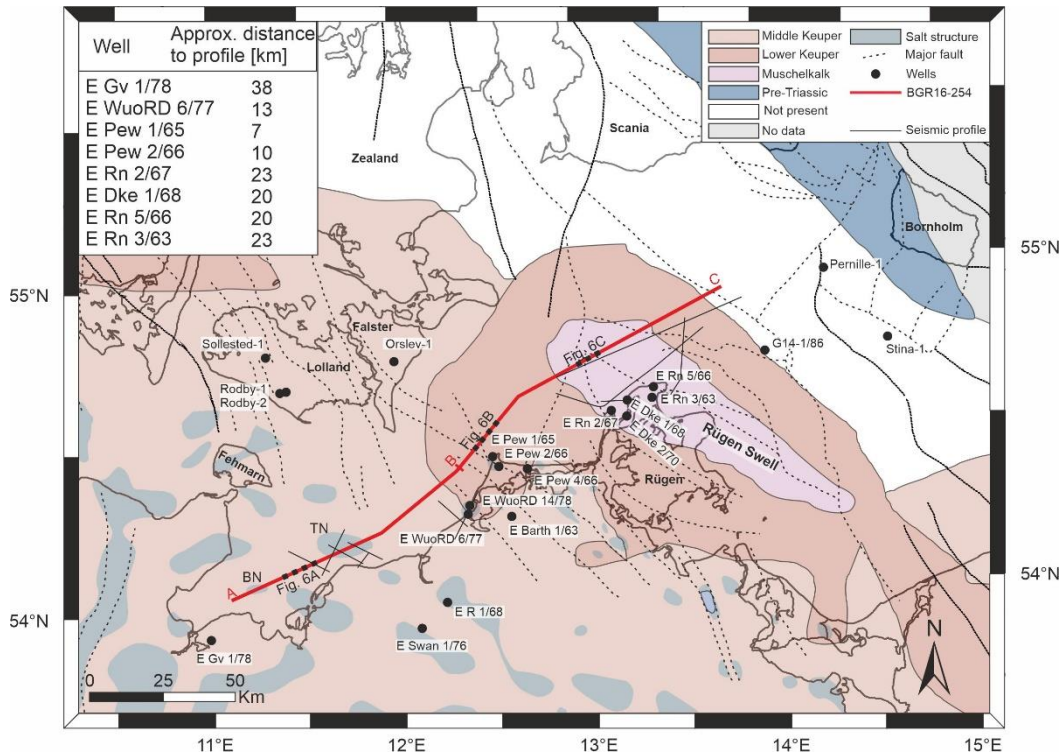


Figure 3.4: Subcrop map of the Early Cimmerian Unconformity (ECU) (Base Norian; German: “Altkimmerische Hauptdiskordanz,” Beutler & Schüler, 1978) including onshore wells used for stratigraphic correlation. Table marks the approximate distance of most important wells to the interpreted profile. Note the trend of the ECU resting on Muschelkalk deposits near northern Rügen Island to Lower and Middle Keuper sediments toward the Bay of Mecklenburg. Compiled after Schlüter et al., 1997; Reinhold et al., 2008; Bachmann et al., 2010; Al Hseinat & Hübscher, 2017. TN = Trollegrund Nord salt pillow; BN = Boltenhagen Nord salt pillow. Dashed black segments on the seismic profile BGR16-254 (red line) are shown in Figure 3.6. Positions A-B and B-C mark segments of the seismic profile shown in Figures 3.7a and 3.7b, respectively.

Epoch	Series	Stage	Reflectors	Polarity	Seismic Unit	Lithology	Amplitude / Frequency	Continuity	Bounding relationship	Characteristics	Seismic example
Cenozoic	Holocene	Pleistocene	T0	positive	Quaternary	Fine gravel Till	High amp. High freq.	Continuous	Discordant	Masked by multiples, subparallel, deformed, hummocky	
	Oligocene	A2	positive	Maastrichtian/Campanian	Chalk	Low amp. expect basal reflection Moderate freq.	Continuous	Discordant, convergent towards WFZ	Wavy in the SW, oblique to semiparallel at the basin margin		
											Eocene
	Palaeocene	T2'	positive	Turonian/Conomanian	Limestone Chalk Clay-marlstone	High amp. Low to moderate freq.	Semi-continuous	Discordant, convergent towards WFZ	Wavy in the SW, parallel in the NE, oblique at basin margin		
											Mesozoic
	Lower	B2	positive	Hiatus							
										Upper	T2
	Middle	T3	positive	Hiatus							
										Lower	T4
	Upper	E1	positive	Hiatus							
										Middle	E2
	Lower	L1	positive	Hiatus							
										Upper	L2
Middle	L3	positive	Hiatus								
										Lower	L4
Upper	L1	positive	Hiatus								
										Middle	L2
Lower	L3	positive	Hiatus								
										Upper	L4
Middle	L1	positive	Hiatus								
										Lower	L2
Upper	L3	positive	Hiatus								
										Middle	L4
Lower	L1	positive	Hiatus								
										Upper	L2
Middle	L3	positive	Hiatus								
										Lower	L4
Upper	L1	positive	Hiatus								
										Middle	L2
Lower	L3	positive	Hiatus								
										Upper	L4
Middle	L1	positive	Hiatus								
										Lower	L2
Upper	L3	positive	Hiatus								
										Middle	L4
Lower	L1	positive	Hiatus								
										Upper	L2
Middle	L3	positive	Hiatus								
										Lower	L4
Upper	L1	positive	Hiatus								
										Middle	L2
Lower	L3	positive	Hiatus								
										Upper	L4
Middle	L1	positive	Hiatus								
										Lower	L2
Upper	L3	positive	Hiatus								
										Middle	L4
Lower	L1	positive	Hiatus								
										Upper	L2
Middle	L3	positive	Hiatus								
										Lower	L4
Upper	L1	positive	Hiatus								
										Middle	L2
Lower	L3	positive	Hiatus								
										Upper	L4
Middle	L1	positive	Hiatus								
										Lower	L2
Upper	L3	positive	Hiatus								
										Middle	L4
Lower	L1	positive	Hiatus								
										Upper	L2
Middle	L3	positive	Hiatus								
										Lower	L4
Upper	L1	positive	Hiatus								
										Middle	L2
Lower	L3	positive	Hiatus								
										Upper	L4
Middle	L1	positive	Hiatus								
										Lower	L2
Upper	L3	positive	Hiatus								
										Middle	L4
Lower	L1	positive	Hiatus								
										Upper	L2
Middle	L3	positive	Hiatus								
										Lower	L4
Upper	L1	positive	Hiatus								
										Middle	L2
Lower	L3	positive	Hiatus								
										Upper	L4
Middle	L1	positive	Hiatus								
										Lower	L2
Upper	L3	positive	Hiatus								
										Middle	L4
Lower	L1	positive	Hiatus								
										Upper	L2
Middle	L3	positive	Hiatus								
										Lower	L4
Upper	L1	positive	Hiatus								
										Middle	L2
Lower	L3	positive	Hiatus								
										Upper	L4
Middle	L1	positive	Hiatus								
										Lower	L2
Upper	L3	positive	Hiatus								
										Middle	L4
Lower	L1	positive	Hiatus								
										Upper	L2
Middle	L3	positive	Hiatus								
										Lower	L4
Upper	L1	positive	Hiatus								
										Middle	L2
Lower	L3	positive	Hiatus								
										Upper	L4
Middle	L1	positive	Hiatus								
										Lower	L2
Upper	L3	positive	Hiatus								
										Middle	L4
Lower	L1	positive	Hiatus								
										Upper	L2
Middle	L3	positive	Hiatus								
										Lower	L4
Upper	L1	positive	Hiatus								
										Middle	L2
Lower	L3	positive	Hiatus								
										Upper	L4
Middle	L1	positive	Hiatus								
										Lower	L2
Upper	L3	positive	Hiatus								
										Middle	L4
Lower	L1	positive	Hiatus								
										Upper	L2

Era/Period	Series	Stage / Group	Formation	Reflectors	Polarity	Seismic Unit	Lithology	Amplitude / Frequency	Continuity	Bounding relationship	Characteristics	Seismic example		
Mesozoic	Triassic	Keuper	Upper	Triletes Contorta Röhltkeuper	K1		Rhaetian/ Norian	Claystone Sandstone	Continuous	Discordant, convergent towards SW anticline	Wavy in the SW, subparallel to even in the NE, oblique at basin margin, partly hummocky			
			Middle	Steinmergelkeuper	K2	positive			Moderate amp., high amp. basal reflection; Moderate freq.	Continuous				
			Lower	Lettenkeuper	M1	positive				Continuous to semi- continuous	Discordant in SW, draping, Convergent towards basin margin and NE anticline		Wavy in the SW, oblique in the NE, partly chaotic at SW anticlines	
		Muschel- kalk	Upper	Hauptmuschelkalk	M2			Muschelkalk	Limestone Marlstone	High amp., High freq.	Continuous		Discordant, draping, divergent towards SW	Wavy in the SW, oblique in the NE prominent reflection at units center
			Middle	Anhydrit										
			Lower	Wellenkalk	M3	negative				Low amp. expect basal reflection; Low freq.	Continuous basal reflection		Concordant, draping	Wavy in the SW, oblique in the NE relatively uniform thickness
		Buntsandstein	Upper	Myogorian					Buntsandstein I	Claystone	Continuous		Discordant, draping, divergent towards SW	Wavy in the SW, oblique in the NE transparent lower part
				Pellitrot	S1	positive								
				Salinarrot	S2									
				Soiling	S3									
Middle	Detfurth						Buntsandstein II	Claystone Siltstone	Continuous	Discordant, draping, divergent towards SW	Wavy in the SW, oblique in the NE transparent lower part			
	Volpriehausen	S4												
Palaeozoic	Permian	Lower	Bernburg											
			Calvörde	X1'	positive									
			A5r											
			Na5											
		Oltre (Z5)	A5											
			TS											
		Aller (Z4)	Na4											
			A4											
		Leine (Z3)	T4											
			Na3											
Stassfurt (Z2)	A3													
	Ca3 - T3													
Werra (Z1)	A2r													
	Na2-K2	Z1												
Rotl.	Ca2													
	A1	Z2												
	Ca1-T1	Z3												
	Elbe													
	Saxon													
	Wuchaping													

Figure 3.5b: Continuation of panel (3.5a). Seismo-stratigraphic concept. Reflectors in this study base upon Reinhardt (1993). Stratigraphic table after Menning (2016), size of individual series not scaled to true timespan. ECU = Early Cimmerian unconformity; b-TKe = base Triassic Keuper; b-TMu = base Triassic Muschelkalk; b-TSa = base Triassic Salinarrot; b-TBu = base Triassic Buntsandstein; t-PZAh = top Permian Zechstein anhydrite zone within Leine cyclothem; b-PZ = base Permian Zechstein.

Thickness in this study is expressed in two-way traveltime (TWT) difference between bounding reflectors of a seismic unit. Scaled by seismic velocity, increased traveltime difference locally represents increased thickness. Within the two southwestern rim-synclines adjacent to the salt pillows in the Bay of Mecklenburg, we examined local lateral thickness variations (see Fig. 3.4 for location). By the term “local depocenter”, we refer to the location of maximum thickness of a seismic unit within the rim-syncline (Sørensen, 1986; Jackson & Hudec, 2017). Over time, local lateral thickness variations occur due to salt movement. This causes an interpretable lateral migration in the local depocenter. However, we are aware that this does not necessarily represent the actual depocenter of that specific seismic unit as our analysis bases only on a single time seismic section. Horizon flattening and changing vertical exaggeration helped to identify small local depocenter migrations, although in many cases an exact location is not distinct. In this case, we picked a location vertically above the previous pick. Hence, the analysis of the local depocenter migration is only qualitative and should be treated with caution. Nevertheless, it was useful to get an idea of local lateral salt flow in the study area.

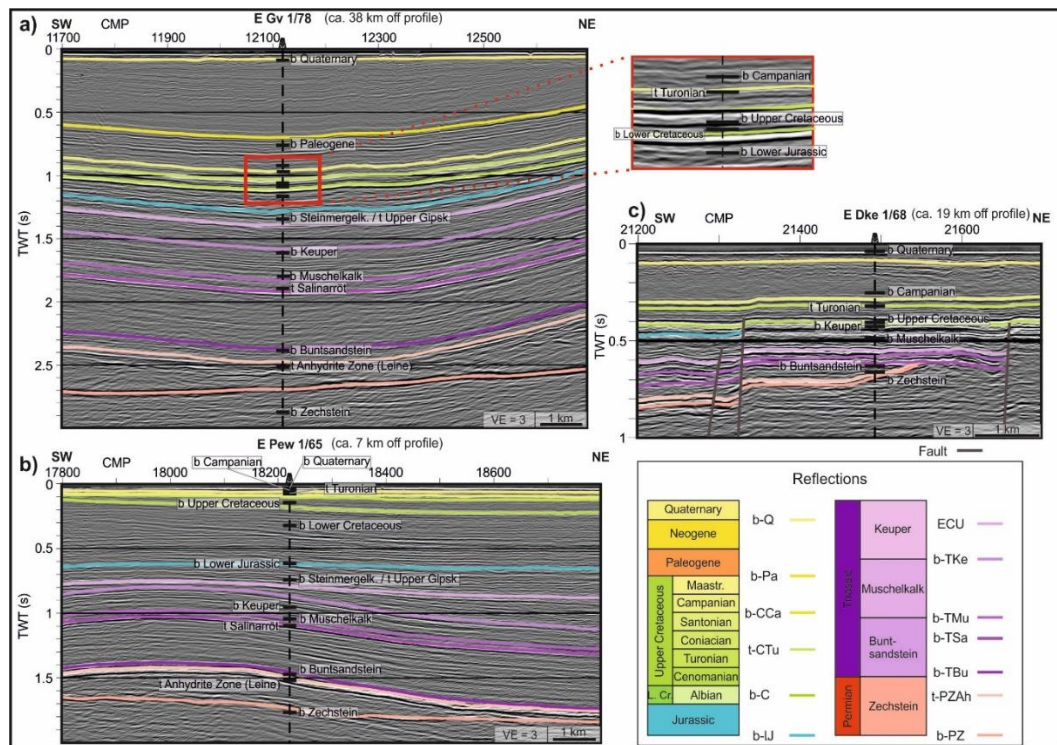


Figure 3.6: Well-to-seismic tie for wells (a) E Gv 1/78, (b) E Pew 1/65, and (c) E Dke 1/68. For abbreviations, see Figure 3.5. Well information from Hoth et al., 1993. Location of sections of profile BGR16-254 shown in Figures 3.1b and 3.4. “b” = base; “t” = top.

We developed a seismo-stratigraphic framework for the study area according to the stratigraphic table of Germany (Menning, 2016). The seismo-stratigraphic framework includes thirteen post-Carboniferous seismic units (Fig. 3.5). We use the term “seismic unit” for a mappable interval of seismic reflectors, expressed by seismic reflections, whose characteristics differ from those of adjacent seismic units. A seismic unit is bounded by marker reflections, unconformities or correlative conformities. The interpreted seismic units correspond to Quaternary, Paleogene-Neogene, Maastrichtian-

Campanian, Santonian-Coniacian, Turonian to Lower Cretaceous, Jurassic, Rhaetian-Norian, Carnian-Ladinian, Muschelkalk, Buntsandstein I (Myiogorian to Pelitröt), Buntsandstein II (Salinarröt to Calvörde), Zechstein I (Werra to Leine anhydrite) and Zechstein II (Leine anhydrite to Ohre) (Menning, 2016). Fig. 3.5 summarizes the seismo-stratigraphy in this study and provides lithological information based upon the well E Gv 1/78 (Hoth et al., 1993), seismic facies, terminations, key characteristic features of each unit and a seismic example. Identified bounding reflectors are based upon the seismo-stratigraphic framework in Reinhardt (1993). These are b-Q: base Quaternary; b-Pa: base Paleogene; b-CCA: base Upper Cretaceous Campanian; t-CTu: top Upper Cretaceous Turonian; b-C: base Cretaceous; b-IJ: base Lower Jurassic; ECU: Early Cimmerian Unconformity; b-TKe: base Triassic Keuper; b-TMU: base Triassic Muschelkalk; b-TSa: base Triassic Salinarröt; b-TBu: base Triassic Buntsandstein; t-PZAh: top Permian Zechstein Anhydrite Zone within Leine cyclothem; b-PZ: base Permian Zechstein.

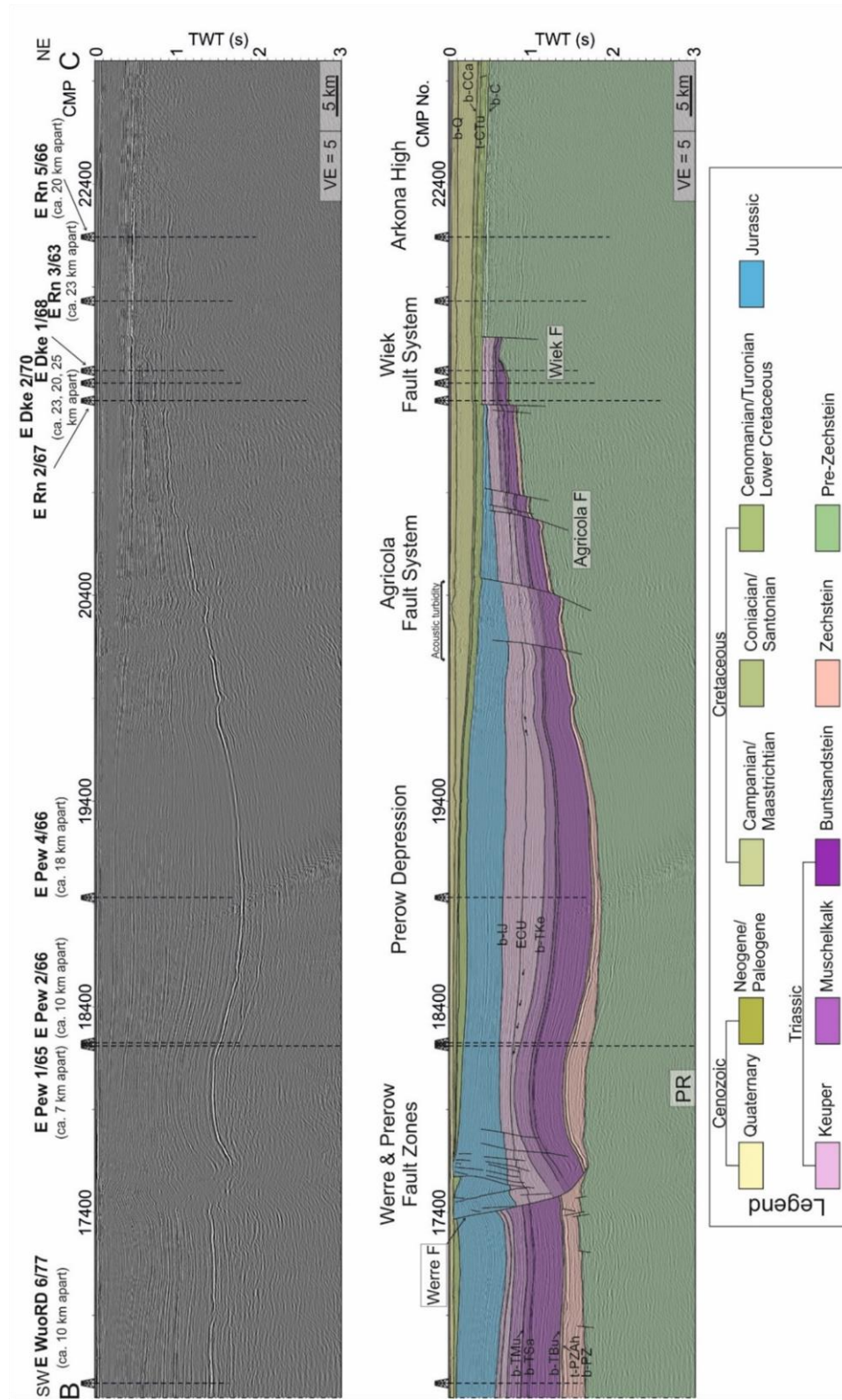


Figure 3.7b: Continuation of Figure 3.7a. BGR16-254 time migrated and interpreted section. CMP 16600–23000. F = fault; PR = Prerow salt pillow (Reinhold et al., 2008). Location of seismic profile BGR16-254 between B and C shown in Figures 3.1b and 3.4.

3.4. Observations

3.4.1. Stratigraphic units and well correlation

Figure 3.6 shows examples of the well-to-seismic tie for the wells E Gv 1/78, E Pew 1/65 and E Dke 1/68. The Zechstein seismic unit is the deepest unit imaged in this profile (Figs. 3.6 and 3.1b). The base Zechstein well marker of E Gv 1/78 does not match the seismic reflector since the well is situated in the deeper part of the basin (Figs. 3.6 and 3.4). For the wells E Pew 1/65 and E Dke 1/68, the well markers and base Zechstein reflector (b-PZ) coincide (Figs. 6 b and c). The base Zechstein is overlain by a reflection free area, which represents the Stassfurt (Z2) cyclothem. It is bound at the top by hummocky to chaotic high amplitude reflections (Figs. 3.6a and 3.7). They correlate with the main anhydrite sequence in the Leine (Z3) cyclothem. The top of this unit is marked by the Leine anhydrite zone reflector (t-PZAh). Towards the basin margin, thickness of the Zechstein II (Werra to Leine anhydrite) unit decreases (Fig. 3.7). This results in a thin Zechstein unit with high amplitude bounding reflectors. Towards the basin margin, the Ohre and Aller cyclothem pinch out (Figs. 3.3 and 3.7). The Zechstein terminates against the base Buntsandstein reflector (b-TBu) closely to the Wiek Fault in this profile (Fig. 3.7b).

The basal reflector (b-TBu) of the Buntsandstein II (Salinarröt to Calvörde) unit is in agreement with the depth of all three well markers (Fig. 3.6). Reflection amplitude in the southwest profile part is low due to the small seismic velocity contrast between compacted Triassic claystone and underlying halite of the Zechstein Ohre cyclothem (Fig. 3.7a). The Buntsandstein II unit shows maximum thickness in the southwest. Thickness of the unit decreases towards the basin margin, where it terminates close to the Wiek Fault in an onlap against the Zechstein. The Buntsandstein I unit (Myogorian to Pelitröt) shows a high amplitude basal reflector (t-TSa), which corresponds with the top of anhydrite deposits in the Salinarröt succession marked in the wells (Fig. 3.6). Well markers correspond with the low amplitude base Muschelkalk (b-TMu) reflector (Fig. 3.6). Intercalated limestone and anhydrite within the Middle Muschelkalk create a set of prominent reflectors (Fig. 3.7). We subdivide the overlying Triassic Keuper into an upper Rhaetian-Norian seismic unit overlying the lower Carnian-Ladinian unit. The Early Cimmerian Unconformity (ECU), marking the top Upper Gipskeuper at the base Norian, separates these units (Figs. 3.5 and 3.7). Towards the basin margin, the Carnian-Ladinian seismic unit pinches out (Fig. 3.7b). Here, Muschelkalk lime-marls form the ECU subcrop and create a high impedance contrast. Well markers and the ECU and base Keuper reflectors match in the Bay of Mecklenburg (Fig. 3.6).

Likewise, well markers are in agreement with the base Lower Jurassic (b-IJ) reflector. The Jurassic terminates as a toplap northeast of the Agricola Fault System (Fig. 3.7b).

The base Cretaceous reflector (b-C) is in agreement with the base Upper and Lower Cretaceous markers in the wells (Fig. 3.6). Thickness of the Lower Cretaceous Albian at the basin margin is 9 m (E Dke 1/68) and therefore below seismic resolution. A distinct base Lower Cretaceous reflector is not observed (Figs. 3.6 and 3.7). The well E Pew 1/65 shows a Lower Cretaceous thickness of 125 m with 110 m of pre-Albian sediments. In the nearby E Pew 4/66 well, the Lower Cretaceous consists of only 8 m of Albian sediments. Hence, the locally increased thickness in the E Pew 1/65 well is

very isolated as no pre-Albian Lower Cretaceous sediments were drilled in the surrounding wells. Deutschmann et al. (2018) interpreted a base Lower Cretaceous reflection, however with noting that it is mainly transparent. The increased thickness in the E Pew 1/65 well could be either fault related, since it was drilled between the Werre and Prerow fault zones (Deutschmann et al., 2018), or more likely the result of incorrect dating as also concluded by Hübscher et al. (2010) (Fig. 3.4).

The top Turonian reflector (t-CTu) corresponds closely with the marker in all three wells (Fig. 3.6). The overlying Santonian-Coniacian seismic unit is bound by the base Campanian reflector (b-CCA) and is truncated by the Quaternary at the flanks of the Grimmen High (Fig. 3.8). The base Campanian reflector (b-CCA) separates a less to higher stratified reflection pattern, which correlates to the base Campanian marker in the wells E Gv 1/8 and E Dke 1/68. In the well E Pew 1/65, thickness of the Campanian is decreased. At the Grimmen High, the reflector terminates in an onlap against the top Turonian (Fig. 3.8). From the Grimmen High towards the SW, thickness of the Maastrichtian-Campanian unit increases and reflectors are divergent.

The overlying Neogene-Paleogene seismic unit terminates as a toplap against the Quaternary in the Grimmen High area (Fig. 3.8). The base-Paleogene (b-Pa) reflector corresponds with the well marker of the well E Gv 1/78 (Fig. 3.6a). The angular unconformity of the base Quaternary correlates with the base of glacial deposits, which overlie Cenozoic clay in the E Gv 1/78 and Cretaceous chalk in the wells E Pew 1/65 and E Dke 1/68.

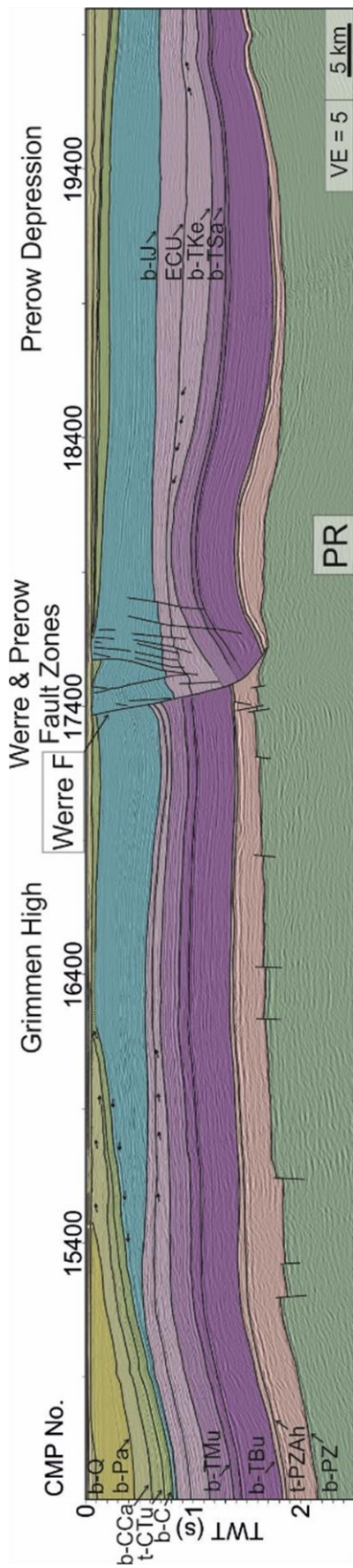


Figure 3.8: Interpreted central part of profile BGR 16-254; see Figure 3.1b for location.

3.4.2. Faults

In the southwest part of the analyzed seismic profile, above the Trollegrund Nord salt pillow, a set of crestal faults dipping towards the anticline center pierce the Upper Cretaceous and eventually die-out within the Keuper (Fig. 3.7a).

In the central part of the profile (Fig. 3.7b, Werre Fault Zone), a prominent NE dipping listric fault dissects almost the entire sedimentary cover from the Zechstein to the Quaternary. It was identified as the Werre Fault in the literature (e.g. Deutschmann et al., 2018). Normal faults pierce the base of the Zechstein in this area. In the overburden, additional synthetic normal faults as well as a set of antithetic normal faults characterize the Werre Fault Zone. Normal faults in the SW part of the hanging wall form Y-shaped grabens, while towards the northeast, normal faults dip SW. A precise analysis of fault displacement is difficult for the Werre Fault Zone as reflectors are difficult to trace. The Buntsandstein and Muschelkalk units show constant fault displacement at the Werre Fault and constant thickness in the hanging wall. Thickness is increased in the Keuper and Jurassic. Reflectors in these units show a divergent pattern towards the Werre Fault, which indicates the extensional phase of activity of this fault zone. The base Cretaceous in the hanging wall of the Werre Fault is located above the corresponding reflector in the footwall (Fig. 3.8).

A set of listric faults in the northeast part of the profile correspond geographically with the Agricola Fault System (e.g. Deutschmann et al., 2018) (Figs. 3.7b). One of them could be identified as the Agricola Fault. All faults dip SW and pierce the pre-Zechstein to Jurassic successions. These faults show quite constant throw in the Zechstein, Buntsandstein and Muschelkalk units. Fault displacement decreases in the Keuper and Jurassic and vanishes in the Cretaceous units. Further northeast, we identified the Wiek Fault (Krauss & Mayer, 2004; Seidel et al., 2018). Beyond this fault, Triassic deposits are either absent, too thin to be resolved or masked by multiples.

3.4.3. Local depocenter analysis

The two rim-synclines in the Bay of Mecklenburg reveal a local, lateral migration when comparing the local depocenter trace (Figs. 3.7a, red dotted lines). For the Buntsandstein and Muschelkalk successions in the RM1 rim-syncline, the local depocenter trace is nearly vertical. Within the Carnian-Ladinian successions, a NE migration of the local depocenter becomes visible. This NE migration continued with less displacement within the Norian-Rhaetian until the base Jurassic. The Jurassic is only preserved as a thin erosional remnant, which hampers the depocenter analysis. The Cretaceous Santonian-Coniacian local depocenter was relocated further SW. It gradually migrated NE during the Santonian-Coniacian. Within the Maastrichtian-Campanian, the local depocenter migrated further NE with enhanced displacement. In the lower Cenozoic successions, the migration of the local depocenter trace decreases slightly. In the upper part, it is no longer traceable. In total, we observe a migration of approx. 880 m from Keuper to Jurassic times and 1.5 km from the Cretaceous to Cenozoic within the RM1 rim-syncline.

We observe similar variations at the RM2 rim-syncline (Figs. 3.7a). The location of the local depocenter remained fixed in the Buntsandstein and Muschelkalk. In the Keuper Carnian-Ladinian unit, the local depocenter began migrating NE. Migration persisted with a relatively large displacement within the Norian-Rhaetian. However, the overall thickness variations in this area are minor, which limits accuracy. The Cretaceous local depocenter was relocated further SW and there is no observable lateral migration from Cenomanian to Santonian times. Within the Maastrichtian-Campanian, the depocenter trace shows a continuous NE migration within the unit until the lower Cenozoic. In total, we interpret a lateral migration of roughly 2 km from Keuper to Jurassic times and ca. 875 m within the Late Cretaceous within the RM2 rim-syncline. However, the observed 2 km of lateral migration in the Keuper seem rather large. Thickness variations within the RM2 rim-syncline Keuper succession are small, which hampers a precise identification of the local depocenter. Therefore, the real lateral migration is especially uncertain in this area.

3.5. Interpretation and discussion

In this chapter, we discuss the interpretation of regional tectonic structures in terms of their thick-skinned or thin-skinned character. Thick-skinned deformation involves the subsalt successions and/or basement in an extensional (Vendeville & Jackson, 1992) or compressional setting (Coward, 1983). In the presence of a detachment layer, e.g. caused by salt, deformation is decoupled in the underlying and overlying successions. Thin-skinned deformation refers to deformation within the detachment layer and its overburden either in an extensional or compressional tectonic regime (Coward, 1983; Vendeville & Jackson, 1992). In the following, we analyze the timing and activity of faults and salt structures imaged on our seismic profile, describe their thick- or thin-skinned characteristics, and discuss potential salt pillow growth mechanisms within the regional geological context. In this study, by thick-skinned faults, we refer to faults rooted in the pre-Zechstein successions.

3.5.1. Thick-skinned deformation

Major faults intersect the Zechstein succession in the northeast part of the profile (Fig. 3.7). Faults of the Wiek Fault System and Agricola Fault System (AFS) are thick-skinned as they dissect the entire Jurassic, Triassic and Zechstein successions and are rooted within the sub-Zechstein. In the Werre Fault Zone (WFZ), we interpret the main Werre Fault as NE dipping listric fault, which dissects the Jurassic and Triassic. However, it is detached near the base Zechstein. Faults piercing the base Zechstein could indicate that the fault zone is affected by thick-skinned deformation; however, its main components are thin-skinned.

Thicknesses of the Zechstein, Buntsandstein and Muschelkalk units shown in the profile gradually increase in southwest, basinward direction. This implies increased subsidence towards the basin center, most pronounced in the Buntsandstein (Fig. 3.7). These observations are in accordance with previous studies and the concept of thermal subsidence from Permian to Middle Triassic times. Subsidence was highest in the

basin center, which led to thicker sedimentary infill with Zechstein, Buntsandstein and Muschelkalk deposits (Ziegler, 1990b; Scheck & Bayer, 1999; Van Wees et al., 2000) (Fig. 3.9a).

Lower and, partly, Middle Keuper units are absent at the northeast basin margin in this profile (Figs. 3.7b). Falling sea-levels during the Carnian and resulting falling sedimentation base levels affected the sedimentation during this time (Ziegler, 1990b; Katzung, 2004). This explains the observed lack of Lower to Middle Keuper sediments caused by non-deposition and erosion along the relatively higher area of the Rügen Swell and Arkona High (Figs. 3.7b). Here, the Early Cimmerian Unconformity (ECU) directly overlies the Muschelkalk unit. In southwest direction, towards the Bay of Mecklenburg, Lower Keuper and Middle Keuper units build the ECU subcrop. This trend coincides with the Early Cimmerian Unconformity subcrop map (Fig. 3.4) and allows the correlation of the ECU reflector. Therefore, its deposition marks the end of a stratigraphic gap from the top Upper Gipskeuper (Weser Formation, close to the base Norian) to base Steinmergelkeuper (Arnstadt Formation, in the Norian) (Beutler et al., 2005). The ECU erosionally truncates Carnian-Ladinian reflectors in a toplap at the Grimmen High and NE flank of the Prerow salt pillow (Fig. 3.8, CMP 15400-16400). We associate this with the falling sea level during the Carnian (Katzung, 2004). However, the stronger erosion between the Grimmen High and Prerow salt pillow suggests that this area experienced less subsidence.

The Agricola Fault System is characterized by a set of SW dipping normal faults on this seismic transect (Fig. 3.7b). Thickness of the Buntsandstein and Muschelkalk are uniform within the hanging wall and footwall of the Agricola Fault. The Carnian-Ladinian seismic unit within the hanging wall appears increased and fault throw along the Agricola Fault decreased from ca. 40 ms at the base Keuper to ca. 11 ms at the ECU. However, as the seismic data is in time, true fault throw is scaled by velocity and might be larger than visible in the data. The Rhaetian-Norian seismic unit shows increased thickness in the hanging wall with slightly divergent reflections. This indicates syndepositional faulting in the Late Triassic (Figs. 3.7b). Within the Prerow Depression, deposits of the Carnian-Ladinian as well as Rhaetian-Norian units show increased thickness and reach a local maximum (Fig. 3.7b). Comparing this to Keuper thickness further southwest, maximum Keuper thickness almost doubled in the Prerow Depression and reaches ca. 650 m (480 ms TWT; ca. 2700 m/s; Schlüter et al., 1997). This indicates that the Prerow Depression experienced subsidence during the Late Triassic and formed a local basin bound to the northeast by the contemporaneous active AFS, which was also stated by Deutschmann et al. (2018) (Fig. 3.9b). Active faulting and subsidence in the Carnian was coeval with E-W to ENE-WSW extension, related to accelerated activity in the North Sea rift system and Glückstadt Graben (Ziegler, 1990b). At the Carnian – Norian transition, rifting activity decreased (Schröder, 1982; Ziegler, 1990b) and further subsidence within the Rhaetian-Norian is difficult to relate to normal faulting caused by E-W extension. However, increased Rhaetian-Norian thickness suggests ongoing faulting and subsidence in the Prerow Depression. We interpret this in accordance to the results of Krauss and Mayer (2004) and Deutschmann et al. (2018), who associated faulting within the AFS with the reactivation of Middle Devonian-Early Carboniferous faults during Late Triassic and the contemporaneous

formation of other fault zones included in the Western Pomeranian Fault System. These faults were induced by NW-SE dextral strike slip movements within the Trans-European Suture Zone, which were accompanied by approximately NE-SW directed transtension (Erlström et al., 1997; Seidel et al., 2018). Faults of the AFS strike ca. NNW-SSE, which is almost perpendicular to the main extensional stress. Therefore, a reactivation of these faults is likely and could explain subsidence in the adjacent Prerow Depression (Fig. 3.9b). Indications of a general uplift of the Baltic Shield and corresponding influx of clastics during the Rhaetian (Erlström et al., 1997) fit this structural evolution by providing sufficient local basin fill.

Around Rügen, the Jurassic gradually thickens along the AFS and Prerow Depression towards the WFZ and Grimmen High (Fig. 3.7b). Fault throw in the AFS further decreased suggesting syntectonic deposition and ongoing subsidence of the Prerow Depression. In the Bay of Mecklenburg, the Jurassic unit is strongly reduced and preserved strata concentrates in the rim-synclines. Uplift related to the Middle-Late Jurassic North Sea doming event (Ziegler, 1990b; Underhill, 1998; Graversen, 2006) caused erosion of most of the Jurassic, in some extent even Upper Triassic strata, from westward direction in the Bays of Kiel and Mecklenburg (Hansen et al., 2005; Hansen et al., 2007; Hübscher et al., 2010; Al Hseinat & Hübscher, 2017). The thinned Jurassic unit in the Bay of Mecklenburg corresponds with this interpretation. However, the preservation of thicker Jurassic deposits in the Prerow Depression suggests ongoing subsidence and thereby a different origin. Due to its closer position to the basin margin, the Zechstein successions in the Prerow Depression lacks large amounts of mobile halite (Figs. 3.3 and 3.7b). Therefore, we expect the effect of salt movement on lateral thickness variations in this area to be minor. However, modelling results by Hansen et al. (2007) show a locally increased tectonic subsidence in this area. Similar to Deutschmann et al. (2018), we explain the increased subsidence and subsequent deposition of the Jurassic in the Prerow Depression by ongoing normal faulting in the AFS related to transtensional movements at the Trans-European Suture Zone (Fig. 3.9c). The listric SW dip of the Agricola Fault suggests rotational block faulting possibly caused by increased basement tilt. This is in accordance to basement subsidence rates calculated by Kossow and Krawczyk (2002), which show relatively higher subsidence rates towards the basin center from the Late Permian to Late Triassic. This suggests a deepening of the basin resulting in increased basement tilt in the Late Triassic and Jurassic. This could explain locally increased subsidence at the basin margin above the rotated hanging walls of deep-seated basin margin faults, which could be detached near the Paleozoic basement (Krawczyk et al., 2002).

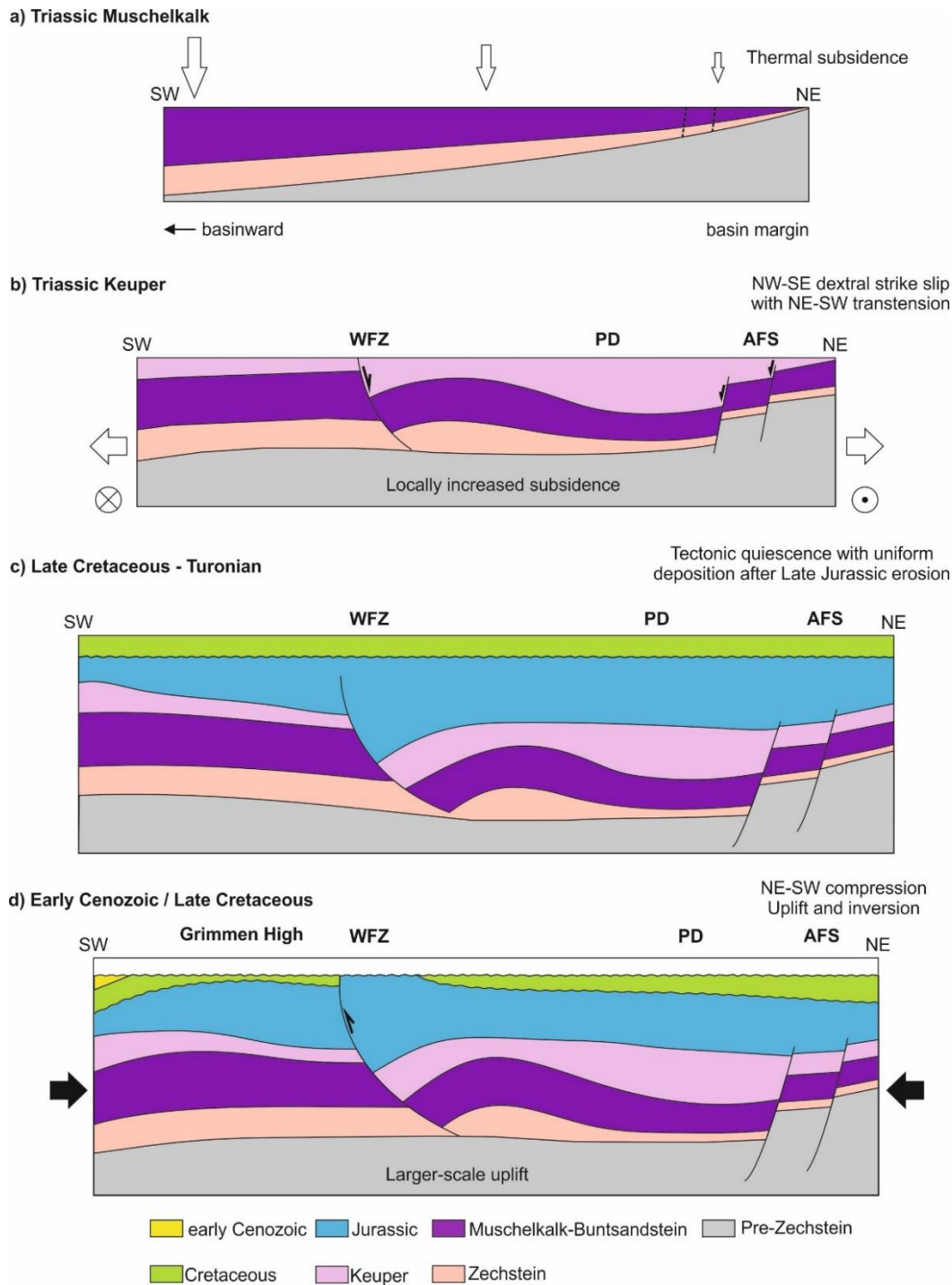


Figure 3.9: Sketch illustrating the tectonic evolution at the northeastern North German Basin margin as derived from the presented analysis of profile BGR16-254.

Apart from the area of the WFZ, the Turonian-Cenomanian-Lower Cretaceous unit has uniform thickness along the profile (Fig. 3.7). Major faulting is absent. We interpret this in accordance to Kossow and Krawczyk (2002); Kley and Voigt (2008); Hübscher et al. (2010); Al Hseinat and Hübscher (2017) as a period of tectonic quiescence and rising sea levels lasting from the Albian transgression until the Campanian (Fig. 3.9c). Thickness of the Santonian-Coniacian unit slightly decreases from the northeast towards the Werre Fault Zone (WFZ) (Figs. 3.7b and 3.8). From the southwest towards the Grimmen High, thickness of the Santonian-Coniacian unit decreases

and the base Campanian (b-CCA) onlaps to the Turonian-Lower Cretaceous. This indicates synkinematic deposition and the onset of uplift of the Grimmen High (Fig. 3.8). The Maastrichtian-Campanian unit is convergent with thinned deposits at both the NE as well as the SW flank of the Grimmen High. At its center, the Maastrichtian-Campanian is completely eroded, which suggests intensified uplift (Fig. 3.9d). It is a clear indication for the onset of the basinwide inversion phase in the Late Cretaceous and coeval uplift of the Grimmen High (Kley & Voigt, 2008; Kley, 2018) (Fig. 3.9a). In contrast to Kossow and Krawczyk (2002) and Deutschmann et al. (2018), we observe a thin Late Cretaceous remnant above the Grimmen High due to the improved imaging of shallow successions. This suggests that the seismic profile images the western boundary of the Grimmen High. Taking the Cretaceous succession at the northeast end of the profile as a reference and assuming it did not experience erosion, thickness at the Grimmen High prior to inversion was ca. 460 m (430 ms TWT, 2150 m/s, Schlüter et al., 1997). This represents a relative uplift of approx. 460 m. Kossow and Krawczyk (2002) calculated the amount of erosion and relative uplift to approx. 500 m. The authors however stated higher internal velocities for the Cretaceous ranging from 2000 m/s to about 3300 m/s. Assuming an average velocity of 2650 m/s yields a relative uplift of 570 m for our data. Accordingly, the observed amount of uplift in this study is in agreement with results of Kossow and Krawczyk (2002).

Kossow et al. (2000) and Kossow and Krawczyk (2002) interpreted the Grimmen High as a drag-related anticline forming a fault-bend-fold geometry due to northward increasing resistance against overburden deformation. As a cause, the authors mention the pinch out of the decoupling Zechstein units, which caused increasing basal friction and resulted in up-thrusting of the overburden onto the basin edge. The authors suggested a possible strike slip and transpressive component based upon the similarity with a positive flower structure. In principle, this study confirms the uplift of the Grimmen High starting within the Coniacian-Santonian and intensifying in the Campanian-Maastrichtian. However, we propose that the tilted basin margin configuration with the Prerow Depression and AFS affected the uplift in the Baltic sector of the NGB. NE-SW directed shortening possibly inverted southwest dipping older extensional faults at the northeastern basin margin. This induced reverse faulting partially decoupled by the Zechstein salt. Compressional deformation caused uplift of rotated basement blocks and was distributed within the overburden causing uplift and erosion of the Cretaceous in the area of the Grimmen High and Prerow Depression (Fig. 3.9d).

3.5.2. Salt tectonics and thin-skinned deformation

In this study, the analysis of thin-skinned deformation deals with the detaching salt layer and its supra-salt cover. Our analysis mainly focuses on thickness variations and faulting of the overburden due to local lateral salt flow. The location of maximum thickness of an individual unit corresponds with the local depocenter during this time and we interpret a lateral migration as a consequence of lateral salt movement.

The observed internal seismic layering of the Zechstein unit with a lower rather reflection free part, which indicate halite rich formations, and a high amplitude upper part corresponding with anhydrite rich successions at the top, is in good accordance with

the Zechstein stratigraphic framework (Fig. 3.7) (Tucker, 1991; Strohmenger et al., 1996; Katzung, 2004; Warren, 2008). The t-PZAh reflector marks the transition from intercalated anhydrite within the Leine (Z3) salt to the main anhydrite formation of the Leine cyclothem (Figs. 3.5 and 3.7). The high amplitude but disrupted reflections within the anhydrite zone indicate internal deformation including boudinage and folding of the anhydrite layers similar to the Z3 stringer observed in the Netherlands (van Gent et al., 2010; Strozyk et al., 2012). The underlying thick, almost reflection free area of the Lower Zechstein unit accordingly corresponds with the Stassfurt and Werra cyclothem. Well information suggests that its major portion is Stassfurt halite (Figs. 3.3 and 3.7a). Northeast of the Werre Fault Zone, thickness of the Zechstein decreases accompanied by a facies change due to decreasing amounts of halite and anhydrite towards the basin margin (Katzung, 2004). In the Rügen area, the high amplitude reflection characterizing the Zechstein seismic unit corresponds with increasing amount of carbonates, especially of the Stassfurt cyclothem (Zagora & Zagora, 1997; Kaiser, 2001; Katzung, 2004).

3.5.2.1. *Thin-skinned deformation in the Werre Fault Zone*

The Werre Fault has a listric NE dipping shape with thinned Zechstein salt in the hanging wall and a folded overburden. We interpret this as a rollover structure. Both the Carnian-Ladinian and Rhaetian-Norian seismic units show increased thickness northeast of the fault. This marks the infill of the syndepositional half-graben (Fig. 3.9b). Many normal faults dip towards the center of the halfgraben. They were created in response to the subsiding hanging wall of the Werre Fault. This evidences the initiation of normal faulting at the Werre Fault during the Late Triassic. The development of the half-graben continued during the Early Jurassic indicated by the increased thickness of the Early Jurassic seismic unit (Figs. 3.7b and 3.9c).

To the northeast, this area is connected to an anticline associated with the Prerow salt pillow (Reinhold et al., 2008; Pr in Fig. 3.7b and salt structure adjacent to E Pew 1/65 well in Fig. 3.4). Deutschmann et al. (2018) made similar observations based upon seismic profiles closer to the coast. Here, the Prerow salt pillow is more pronounced. However, the anticline on our profile is mainly caused by the absence of salt within the Werre Fault Zone (WFZ) than actual salt accumulation as Zechstein thickness southwest of the WFZ and within the anticline are nearly equal. Though, the anticline on our profile could represent the edge of the Prerow salt pillow. Further, the absence of salt in the WFZ could be caused by out of plane salt flow possibly accumulating in the SE located central part of the salt pillow. Modeling results of Hansen et al. (2007) show a SE increase in Zechstein thickness towards Rügen along the Werre Fault, which is in accordance with our interpretation. The general increase of Zechstein thickness southwest of Rügen Island shown by Hansen et al. (2007) can be explained by increased primary thickness due to proximity to the basin center (Kossow et al., 2000) as the basin margin bends northeast along southern Rügen Island (Katzung, 2004). Therefore, we interpret only a local, minor fault-controlled salt flow between the WFZ and Prerow Fault Zone.

The exact timing of the initialization of the WFZ is an aspect of recent discussion. Krauss and Mayer (2004) referred to the Werre and Prerow fault zones as a system of NNW-SSE trending pull-apart graben structures due to Early Cimmerian (Late Triassic) reactivation of basement faults of Caledonian and Variscan origin. Al Hseinat and Hübscher (2017) mention that the E-W directed extensional tectonic regime affecting the NGB reactivated deep-rooted basement faults in this area. Deutschmann et al. (2018) proposed transtensional movements due to Cimmerian tectonics during the Late Triassic to Early Jurassic and the formation of a rollover structure. Observations by Seidel et al. (2018) northeast of Rügen agree with Krauss and Mayer (2004). They associate the WFZ with en echelon structures of the Western Pomeranian Fault System, which developed during Mesozoic extensional tectonics. In principal our observations agree with recent studies, however, allow a more precise timing and complete image of the fault zone. Our observations of active normal faulting in the Carnian-Ladinian, Rhaetian-Norian and Jurassic seismic unit suggest that the initialization of the WFZ was coeval with extension in the Late Triassic - Early Jurassic and corresponding active faulting in the AFS and subsidence in the Prerow Depression (Fig. 3.9b and c). Decoupled by the mobile Zechstein salt, thin-skinned normal faulting at the approx. NW-SE striking Werre Fault was caused by NW-SE dextral strike slip movements and associated NE-SW directed transtension within the Trans-European Suture Zone (Krauss & Mayer, 2004; Deutschmann et al., 2018; Seidel et al., 2018). During Late Cretaceous basin inversion, the NE-SW compressional stress orientation was perpendicular to the NW-SE trending Werre Fault, which made the fault especially prone to reactivation (Al Hseinat & Hübscher, 2017; Seidel et al., 2018). The associated compression reactivated the Werre Fault resulting in the displacement of the base Cretaceous reflector in the hanging wall above its counterpart in the footwall (Fig. 3.9d). The related uplift caused erosion of almost the entire Cretaceous successions over an approx. 3 km wide area northeast of the Werre Fault. Accordingly, this study provides a reinterpretation of the WFZ as an inverted thin-skinned normal fault system.

The Prerow Fault Zone as mapped by Deutschmann et al. (2018) further southeast, is not visible in our seismic data, which was acquired further to the northwest. Probably, the Prerow Fault Zone merges with the WFZ to a combined fault system in this area.

3.5.2.2. *Timing of salt movement in the Bay of Mecklenburg*

In the Bay of Mecklenburg, two salt pillows are imaged by our profile, namely the Trollegrund Nord (TN) and Boltenhagen Nord (BN) pillows (Fig. 3.4) (Reinhold et al., 2008). Both analyzed depocenter traces within the adjacent rim-synclines (RM1 and RM2, Figs. 3.7b) nearly vertically transect the Buntsandstein and Muschelkalk successions and no local thickness variations are observable. Hence, salt movement was not yet triggered which is in accordance to previous studies (Kossow et al., 2000; Zöllner et al., 2008; Hübscher et al., 2010; Al Hseinat & Hübscher, 2017).

The NE migration in the depocenters and thinning of the Keuper towards the pillow crest evidence the initiation of salt movement and pillow growth during deposition of the Keuper. The starting of the NE migration of the local depocenter traces suggest a

Carnian-Ladinian triggering. However, larger Norian-Rhaetian thickness variations within the RM1 rim-syncline beneath the overlaying thin Jurassic unit indicate that the main phase of salt flow was during the Norian-Rhaetian (Figs. 3.7a). Therefore, this study allows a more precise timing than the previously stated Late Triassic initiation (Kossow et al., 2000; Zöllner et al., 2008; Hübscher et al., 2010; Al Hseinat & Hübscher, 2017). This timing correlates with the initiation of many other salt structures in the southern part of the NGB (Meinhold & Reinhardt, 1967; Jaritz, 1973; Rühberg, 1976) and within the Polish Basin (e.g. Krzywiec et al., 2017).

The Jurassic sequence is strongly eroded in the Bay of Mecklenburg. This hampers interpretation of salt movement during this time and requires consideration of additional adjacent seismic profiles. However, thicker remnants of Jurassic strata are preserved in both rim-synclines (Fig. 3.7a). Uplift in the Jurassic and resulting erosion occurred on a larger scale as discussed in chapter 3.5.1. Therefore, assuming a local similar degree of erosion above the pillow crest and rim-synclines during the Jurassic, we suggest that thickness of the Jurassic was increased within the rim-synclines prior to erosion. This indicates ongoing salt pillow growth at least in Early Jurassic times. Thickness is uniform within the Lower Cretaceous to Turonian. Therefore, we interpret a cessation of local salt flow during this time.

Changed depositional regimes possibly affected by basement tilt, as described in chapter 3.5.1, relocated the local depocenter traces in the Late Cretaceous (Figs. 3.7a). The observed NE depocenter migration in both rim-synclines marks a phase of renewed salt flow and pillow growth beginning in the Santonian-Coniacian and lasting until the Cenozoic. Local thinning of the Upper Cretaceous successions towards the TN pillow center is overprinted by the general SW thickness increase caused by uplift of the Grimmen High (Fig. 3.8). A set of normal faults piercing the Cretaceous above the pillow crest remind of a crestal collapse graben structure. We associate this with overburden extension and bending as a result of rising salt. The Cenozoic is clearly thinned above the TN pillow while thick successions within both rim-synclines express ongoing salt movement. When exactly salt movement ceased is an aspect of future work and requires a detailed stratigraphic subdivision of the Cenozoic.

In summary, we observed two phases of salt movement, which are coeval with phases of increased regional tectonic stress. Initiation of salt pillow growth was in the Late Triassic (mostly Rhaetian-Norian) with movement lasting at least throughout the Early Jurassic. During this time, the study area was affected by extension. The second phase took place from the Santonian-Coniacian until the Cenozoic. It correlates to the onset of the Africa-Iberia-Europe convergence and resulting phase of basinwide inversion, the change of the regional stress field from extensional to compressional and associated uplift of the Grimmen High.

3.5.2.3. *Pillow growth mechanisms*

In a literature-based compilation, Warsitzka et al. (2019) summarized the salt tectonic evolution of the Southern Permian Basin and mapped potential trigger mechanisms that caused salt structure initiation. For the northeastern North German Basin margin,

their compilation suggests a triggering either by gravity gliding or by thin-skinned or minor basement involved extension. However, the referenced studies were rather speculative and partly far away from the actual basin margin in the Baltic Sea sector. In the following, we revise potential trigger and salt pillow growth mechanisms for our study area and discuss their compatibility with the regional tectonic interpretation described above (Fig. 3.10). Besides the mechanisms mentioned by Warsitzka et al. (2019), we further consider for completeness salt pillow growth driven by differential loading or basement-involving faulting.

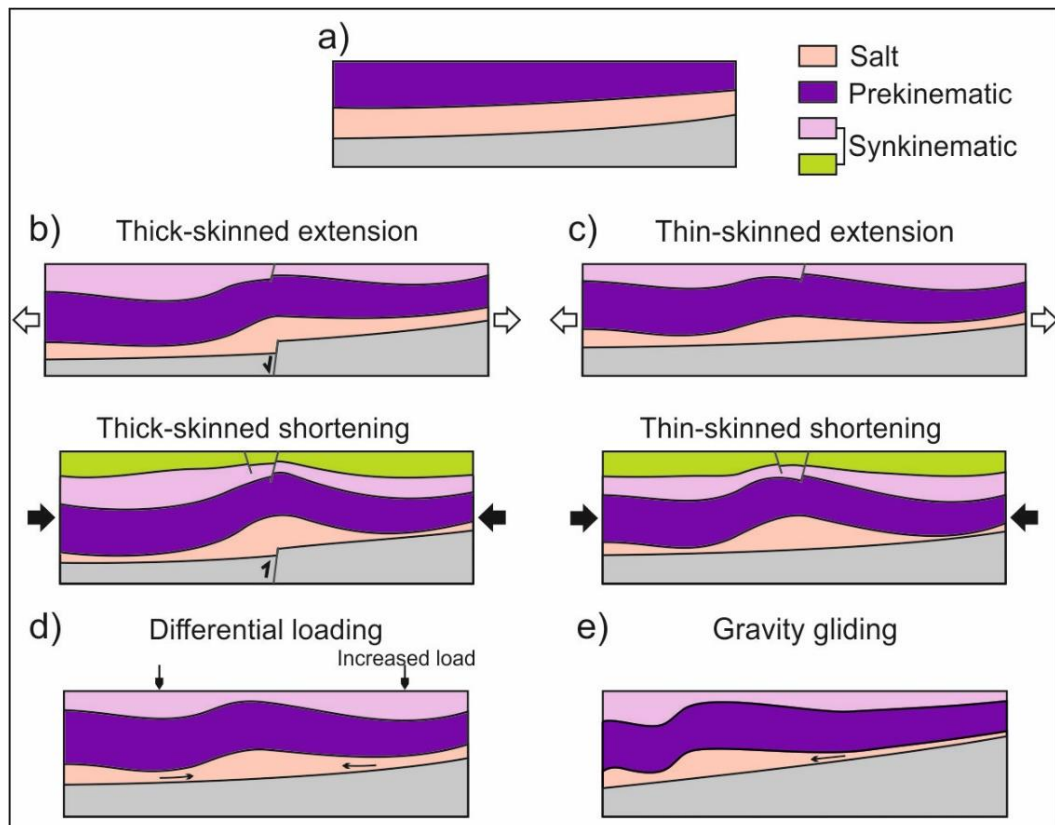


Figure 3.10: Sketch illustrating salt pillow growth mechanisms. (a) Initial situation with salt layer and prekinematic overburden. (b) Thick-skinned extension and subsequent thick-skinned shortening. (c) Thin-skinned extension and subsequent thin-skinned shortening. (d) Differential loading. (e) Gravity gliding. Based upon terminologies introduced by Stewart (2007); Warren (2008); Brun and Fort (2011) and Jackson and Hudec (2017).

A basement involving fault-controlled salt structure evolution (as in Jackson et al., 1994; Stewart & Coward, 1996; Withjack & Callaway, 2000; Warren, 2008) (Fig. 3.10b) is well-known to have created salt anticlines above basement faults in the Southern Permian Basin, e.g. in the Glückstadt Graben, and in other basins such as the Levant Basin (e.g. Kockel, 1999; Warren, 2008; Reiche et al., 2014; Warsitzka et al., 2019). However, our seismic profile does not show basement faults underneath both salt pillows.

A thin-skinned salt pillow evolution (Fig. 3.10c) requires effective decoupling of the overburden from the basement. Numerous authors stated this for the northeast NGB margin (Kossow et al., 2000; Kossow & Krawczyk, 2002; Krauss & Mayer, 2004; Zöllner et al., 2008; Hübscher et al., 2010; Al Hseinat & Hübscher, 2017). Triggering

of the salt flow in the Bay of Mecklenburg occurred during E-W directed extension. Major faults underneath the salt pillows are not visible. As discussed in chapter 3.4.1, Norian-Rhaetian to Jurassic transtensional dextral strike slip movements within the Trans-European Suture Zone affected the Werre Fault Zone ca. 50 km northeast of the salt pillows. This correlates directly with the initiation of salt pillow growth in the Bay of Mecklenburg. The Zechstein succession in the Bay of Mecklenburg contains relatively thick Stassfurt halite units (Figs. 3.6a and 3.3). This allows effective decoupling of sub-Zechstein induced deformation within the Trans-European Suture Zone and the distribution of deformation within a relatively wide zone in the overburden (Richard et al., 1991). Therefore, a thin-skinned reactive pillow growth is a possible mechanism. During reactive growth, regional extensional stress, as evidenced in the Werre Fault Zone, creates a tectonic differential load by thinning the overburden and forming grabens or half grabens. Then, pressurized salt can flow into these structurally thinned zones (as in Vendeville & Jackson, 1992; Hudec & Jackson, 2007) (Fig. 3.10c). Initial normal crestal faults are not prominent in the Keuper successions imaged in our profile. However, the base Cretaceous unconformity directly overlies the Norian-Rhaetian deposits, which, therefore, were affected by Late Jurassic erosion that possibly removed the records of initial normal faulting. The observed salt structures never reached a diapiric stage and thick burial by undeformed Early to Middle Triassic successions precludes an active stage. NW-SE transtensional strike slip movements within the Trans-European Suture Zone were parallel to the present day dominant trend of salt structures within the eastern part of the NGB (Scheck-Wenderoth et al., 2008) (Fig. 3.1). This is in agreement with a thin-skinned pillow formation.

The second phase of salt pillow growth occurred from the Coniacian-Santonian to early Cenozoic and eventually continued throughout the Cenozoic. Timing of salt pillow growth correlates with the phase of basinwide inversion and uplift of the Grimmen High related to the onset of the Africa-Iberia-Europe convergence. Associated NE-SW directed compression induced horizontal shortening (Kley & Voigt, 2008). Due to the decoupling, thin-skinned shortening inducing salt movement is a possible growth mechanism during the second phase (as in Hudec & Jackson, 2007; Callot et al., 2012) (Fig. 3.10c). As a result of compression, the salt's overburden may buckle allowing the salt to flow into the low-pressure cores of overburden anticlines. Preexisting structures are especially prone to be amplified by later shortening (Vendeville & Nilsen, 1995; Hudec & Jackson, 2007). Kossow and Krawczyk (2002) mention 8.5 km of shortening of the supra-salt in the NGB, of which 70 % accumulated in thrust structures at the southern NGB margin. The remaining amount of shortening distributes over the northern basin area with decreasing deformation towards the northeastern basin margin. Uplift of the Grimmen High and inversion of the Werre Fault as a reverse fault evidence compressional forces, which possibly induced overburden buckling above the southwestern pillows. However, we do not observe any signs of thrust faulting of the salt pillow overburden. This suggests that the mobile salt effectively provided the infill of detachment folds rather than creating thrust faults (Stewart, 1996). Whether shortening in the Bay of Mecklenburg was sufficient to induce salt pillow growth requires further analysis. However, thin-skinned extension triggering salt pillow growth in the Late Triassic and subsequent remobilization by thin-skinned

shortening in the Late Cretaceous is a possible scenario explaining salt pillow formation in the Bay of Mecklenburg (Fig. 3.10c). The two observed phases of pillow growth correlate with regional tectonic deformation and the thick halite units within the Zechstein sequence allows effective decoupling.

Differential loading causing downbuilding of the salt pillows is another possible mechanism for pillow growth (e.g Jackson & Hudec, 2017) (Fig. 3.10d). The Buntsandstein, Muschelkalk and lower Keuper show a locally relatively uniform deposition in the Bay of Mecklenburg. Accordingly, the gravitational load prior to the deposition of the Rhaetian-Norian seismic unit was rather equally distributed as evidenced by the locally uniform thickness of underlying pre-Norian sediments. This contradicts a Late Triassic triggering of salt movement by differential loading, as there is a lack of varying gravitational load between rim-synclines and pillow crest. However, after an initiation by thin-skinned extension as described above, differential loading is a possible component driving ongoing salt movement during the Late Triassic and Early Jurassic due to the thicker deposits within the rim-synclines. This could have resulted in increased pressure on the salt underneath the rim-synclines leading to salt expulsion and pillow growth. The subsequent remobilization of salt movement in the Late Cretaceous does not fit to the concept of differential loading, as the gravitational load after the sedimentation during the Cretaceous tectonic quiescence was again rather uniform.

Gravity driven salt movements have been intensively studied at passive margins, however, its applicability to intracontinental basins is questionable. Gravity gliding (as in Cobbold & Szatmari, 1991; Duval et al., 1992; Brun & Nalpas, 1996; Brun & Fort, 2011, 2012; Rowan et al., 2012) was discussed for some areas of the Southern Permian Basin (e.g. Warsitzka et al., 2019) and in the following we discuss a possible effect on the salt pillow evolution at the northeastern North German Basin (NGB) margin (Fig. 3.10e). The second phase of observed salt flow from the Santonian to Cenozoic correlates with the phase of basinwide inversion and uplift of the basin margin including the Grimmen High. This caused increased basin margin tilt at the northeastern margin. The continuous NE migration of the local depocenter within both rim-synclines suggest a SW directed down-dip salt flow (Fig. 3.7a). The base Zechstein reflector (b-PZ, Fig. 3.7a) dips SW with approx. 1° in a length of ca. 90 km. Gravity gliding in the Kwanza Basin, offshore Angola, occurred with slope dips below 1° over distances of more than 150 km. Locally, gliding occurred at slopes of ca. 50 km length and angles of roughly 2.5° (Jackson & Hudec, 2005). Brun and Fort (2011) used analog models to calculate that margin tilt angles lower than 1° for wide basins (200-600 km), covered by initial sedimentary cover thickness of up to 1 km, allow dominant gliding. Shorter basins require steeper angles and less sedimentary cover. Based upon these estimations, the basin configuration of the northeastern NGB margin with approx. 1° slope angle over 90 km might allow gravity gliding in principle. However, the comparable short slope length and thick sedimentary overburden contradict substantial gliding and therefore might, if at all, allow only minor translation. Additionally, we need to consider some major differences in the geological setting between the two basins. The Kwanza basin is located at a passive continental margin. Sediment load concentrates updip on the slope. Gravity gliding and gravity spreading induced forces both add up in downdip direction. The NGB on the other hand is an intracontinental basin with

maximum sediment load at the center. This load concentration induces counteracting, updip forces which possibly further limit downdip salt translation. For the northeastern basin margin, salt flow by gravity gliding would be downdip in southward direction. The Bay of Mecklenburg would represent the contractional domain where shortening causes salt pillow growth, whereas the Grimmen High and WFZ correspond with the extensional domain of updip salt depletion. Zechstein thickness at the Grimmen High is not entirely reduced compared to the salt pillows in the Bay of Mecklenburg (ca. factor of 2-3). Additionally, there is a general SW thickness increase due to the closer proximity to the basin center (e.g. Kossow et al., 2000). Hence, the overall small amount of lateral thinning indicates minor actual salt flow. The total depocenter migration in this study is less than 2 km. This also fits to an interpretation of only minor salt translation comparing to the relatively huge depocenter migrations of more than 5 km observed by Jackson and Hudec (2005) in the Kwanza basin. Their modeling results showed that a high ratio of aggradation rate to translation rate down the ramp (\dot{A}/\dot{T}) results in steeply dipping depocenter traces while a low \dot{A}/\dot{T} ratio creates gently dipping depocenter traces. The steeply dipping depocenter traces observed in the Bay of Mecklenburg suggest a high \dot{A}/\dot{T} ratio. This is either caused by a high amount of sedimentation or minor actual salt flow down the slope. Both are consistent with our observations. A thick overburden overlies the Zechstein sequence and actual salt flow seems minor due to considerations above. Based upon this discussion, gravity gliding might not have played a dominant role at the northeastern NGB margin. Salt flow is more likely controlled by thin-skinned extensional and compressional deformation. However, gravity gliding could have temporally contributed and caused minor downdip salt flow. We propose a scenario of gravity gliding induced slow creeping down the tilted basin slope during the Late Cretaceous to Cenozoic. This resulted in updip salt depletion at the Grimmen High and accumulation within the investigated salt pillows. Consequently, only minor updip thin-skinned extension without significant faulting occurred.

We analyzed lateral salt flow based on a NE-SW directed seismic profile. Our results provide valuable findings and mark a first step for further studies, where we strive for a comprehensive reconstruction and timing of salt movements in the whole area of the Baltic Sea sector by means of further available multichannel seismic data. This will allow addressing lateral salt movement in all directions and their influence on the structural development of the area. Depth conversion and section restoration of the seismic profile analyzed in this paper will be part of future work.

3.6. Summary

- For the first time, we present a complete image from the base of the Zechstein to the seafloor ranging from the Bay of Mecklenburg to the northeast of Rügen Island. The seismic section images Late Permian to recent Cenozoic deposits.
- The basin margin faults of the Agricola Fault System and associated Werre Fault Zone initiated during ENE-WSW extension in the Late Triassic. In between, subsidence in the Prerow Depression formed a marginal sub-basin. The main phase of

subsidence attributes to the Rhaetian-Norian until Early Jurassic times, where transtensional dextral strike slip movements within the Trans-European Suture Zone dominated.

- The Werre Fault Zone is reinterpreted as an inverted thin-skinned normal fault zone forming a rollover structure detached close to the base Zechstein. Antithetic normal faults are associated with the Prerow Fault Zone and suggest thin-skinned deformation related to the subsiding hanging wall of the Werre Fault. Faulting began in the Late Triassic and is associated with the formation of the Western Pomeranian Fault System.
- Major plate reorganization related to the Africa-Iberia-Europe collision led to basin scale inversion and uplift of the Grimmen High at the northeastern North German Basin margin. Uplift started in the Santonian-Coniacian with increased activity during the Maastrichtian-Campanian and amounts to values ranging from 460 m to 570 m. This led to erosion of much of the Cretaceous succession of the Grimmen High and within the Werre Fault Zone. The Werre Fault was inverted as a reverse fault causing uplift and erosion of the hanging wall.
- Salt pillow growth in the Bay of Mecklenburg initiated in the Late Triassic in an extensional tectonic regime. Continuous growth until the Jurassic preserved thicker Late Triassic and Early Jurassic deposits in the rim-synclines while thinning and partly erosion occurred above the pillow crests. A second phase of salt pillow growth was in the Late Cretaceous to Cenozoic correlating with the onset of basin inversion and reverse faulting in the Werre Fault Zone.
- We discussed salt pillow evolution in the Bay of Mecklenburg and invoked two possible driving mechanisms. In the first scenario, a thin-skinned extensional initialisation in the Late Triassic and Jurassic was followed by Late Cretaceous-Cenozoic thin-skinned shortening which led to further salt pillow growth. The second scenario discusses an effect of gravity gliding induced by basin margin tilt during the Late Cretaceous to Cenozoic. This could add to local salt flow by slow downdip creeping resulting in updip depletion, downdip salt accumulation and pillow formation.

Acknowledgments

We would like to thank the reviewers Piotr Krzywiec and Heijn W. van Gent for their critical reading and great suggestions, which significantly improved the manuscript. Further, we are thankful to Heidrun Stück, Fabian Jähne-Klingberg and Elisabeth Seidel for their helpful remarks on the interpretation as well as their help on improving the manuscript. We would like to thank Mark Rowan for fruitful discussions at the EGU General Assembly 2018.

Data is available from the Federal Institute for Geosciences and Natural Resources (BGR) (<https://www.geo-seas.eu/report/2633203>). The authors thank Neptune Energy for providing additional seismic lines for stratigraphic correlation. We thank Emerson for providing licenses of their software under the Paradigm University Research Program.

This project is funded by the Deutsche Forschungsgemeinschaft (DFG, German Research Foundation) - grant no. NO 1375/1-1.

The authors declare that they have no conflict of interest.

4. Triassic-Jurassic salt movement in the Baltic sector of the North German Basin and its relation to post-Permian regional tectonics

Abstract

The formation and overprinting of complex intracontinental basin, like the North German Basin, is a fundamental earth process, its understanding is not only of basic research but also of socioeconomic importance because of its multitude of resources, potential hazards and subsurface use capability. Major subsidence and structural differentiation of the Central European Basin System occurred during the Triassic-Jurassic. A dense network of high-resolution 2D seismic data together with nearby wells allow creating regional maps with refined stratigraphic subdivision of yet unprecedented spatial resolution, including an update of basement faults in the bays of Kiel and Mecklenburg. Cross sections covering the NW, N and NE basin margin allow reconstructing the structural evolution of the Zechstein salt and its overburden. At the northern basin margin, near the Kegnaes Diapir, thinning of the Buntsandstein and divergent reflectors indicate an Early Triassic stage of faulting and salt movement, which suggests that the common concept of relatively quiet tectonic conditions during Early Triassic thermal subsidence would have to be expanded. In the Late Triassic, tectonic activity increased expressed by the onset of salt movement in the northeastern Glückstadt Graben, major growth of the Kegnaes Diapir and faulting at the northeastern basin margin during deposition of the Keuper (Grabfeld, Stuttgart and Weser formations). We explain the pillow to diapir transition of the Kegnaes Diapir by extension and erosional unroofing during the Late Triassic. At the northeastern basin margin, we interpret the accumulation of Keuper and Jurassic deposits as a transtensional sub-basin, bordered by the Werre Fault Zone and Agricola Fault System. This area forms the northwestern prolongation of the Western Pomeranian Fault System, where Late Triassic transtension reactivated deep-seated Paleozoic structures. Between the Glückstadt Graben and the northeastern basin margin, the Eastholstein-Mecklenburg Block formed a more stable area, where salt movement first began the latest Triassic.

4.1. Introduction

The North German Basin forms part of the intracontinental Southern Permian Basin and has a complex and long history of basin evolution from the Carboniferous to Quaternary (see e.g. overviews: Ziegler, 1990a; Maystrenko et al., 2008; Pharaoh et al., 2010). Important stages of the basin evolution can be summarized to the (1) initial Permo-Carboniferous phase of wrench faulting, intense volcanism and thermal subsidence, (2) late Permian deposition of the Zechstein evaporites, (3) continuous late Permian to Mid Triassic thermal subsidence, (4) Late Triassic E-W extension and basin differentiation, (5) Mid Jurassic uplift due to thermal doming, (6) Late Cretaceous inversion and (7) Cenozoic rifting and glaciation (Pharaoh et al., 2010). Even though the overall basin evolution is well understood, the link between regional tectonics, salt movement and inherited deep-rooted structures at a regional scale and the temporal resolution of geological stages remains partly elusive. In times of growing interest in

the usage of the deeper subsurface, e.g. for geoengineering projects like Carbon Capture and Storage (CCS), geothermal energy utilization, storage of renewable energy or the search for a nuclear repository, a profound understanding of the evolution of the basin and its deep-rooted fault systems is very important (Gill, 2017).

The Baltic sector of the North German Basin (NGB) covers the northern basin margin at the transition from Variscan consolidated crust to the Precambrian East European Craton (Guterch et al., 2010). This part of the basin includes a part of the northeastern Glückstadt Graben, which experienced intensive extension and salt movement during the Triassic, and the Western Pomeranian Fault System at the northeastern basin margin, which developed due to Triassic transtensional tectonics (Fig. 4.1) (Krauss & Mayer, 2004; Maystrenko et al., 2005a, 2005b). Many salt structures spread across the entire area making the Baltic sector of the NGB an ideal study area to investigate the impact of regional tectonics on salt movement. Among the salt structures in the Baltic sector of the NGB are a set of four approx. WNW-ESE striking salt diapirs at the northern basin margin, spreading across the island of Lolland towards Langeland (Fig. 4.1). Their isolated location at the basin margin, surrounded by salt pillows, is unique within the NGB. The causative relation of salt tectonics, basin configuration and regional tectonics, which led to the formation of these diapirs at the northern basin margin, remains unclear.

In the past, much research analyzing the post Permian sedimentary record has been done in the Baltic sector of the NGB (Hübscher et al., 2004; Hansen et al., 2005; Maystrenko et al., 2005a, 2005b; Hansen et al., 2007; Zöllner et al., 2008; Hübscher et al., 2010; Al Hseinat & Hübscher, 2014; Al Hseinat et al., 2016; Kammann et al., 2016; Al Hseinat & Hübscher, 2017; Deutschmann et al., 2018; Hübscher et al., 2019; Frahm et al., 2020; Huster et al., 2020; Schnabel et al., 2021). These studies used seismic imaging and mapping of post-Permian units with a lithostratigraphic subdivision representing a vertical resolution in the order of geological series to analyze the regional tectonic and salt tectonic structural evolution. From this, four major post Permian tectonic phases important for salt structure evolution were identified: (1) Late Triassic – Early Jurassic extension triggering initial salt movement; (2) The Mid Jurassic North Sea Doming event causing large-scale uplift and erosion; (3) Late Cretaceous inversion; (4) Paleogene-Neogene reactivation of salt movement. In a recent study, Ahlrichs et al. (2021a) presented regional maps of the Baltic sector of the NGB with a refined stratigraphic subdivision of Late Cretaceous and Cenozoic units to show that the onset of Late Cretaceous inversion began alongside minor salt movement in the Coniacian-Santonian. Furthermore, the authors stated that major salt flow restarted in the late Eocene to Oligocene and that this phase of revived salt movement can be attributed to extension. For the Triassic, such regional maps resolving the stratigraphic subdivision beyond the level of the main lithostratigraphic units of the Germanic Triassic (in German: “Germanische Trias”, comprising the Buntsandstein, Muschelkalk, Keuper) are lacking in the Baltic sector of the North German Basin. Studies carried out in the adjacent onshore areas (Denmark: Clausen & Pedersen, 1999; Glückstadt Graben and Lower Saxony: Frisch & Kockel, 1999; Baldschuhn et al., 2001; Kockel, 2002; Warsitzka et al., 2016; Mecklenburg-Western Pomerania: Beutler et al., 2012) have a refined stratigraphic subdivision of the Triassic units and specified that

the onset of extensional tectonics and initial salt movement in the Late Triassic occurred during deposition of the Grabfeld and Weser formations.

In this study, we focus on the Triassic-Jurassic phase of basin evolution to deepen both the understanding of regional tectonics and the initial development of salt structures prior to Late Cretaceous inversion. We use a dense network of high-resolution 2D seismic data in combination with onshore and offshore wells to refine the stratigraphic subdivision of the Triassic and create regional maps of the Triassic - Jurassic units, which close the gap to adjacent onshore areas. We present key seismic profiles and regional time-structure and isochron maps of the Zechstein, Buntsandstein, Muschelkalk, Keuper II (Grabfeld, Stuttgart, Weser formations), Keuper I (Arnstadt, Exter formations) and Jurassic units to analyze the Triassic to Jurassic structural evolution of the region. Thereby, we strive for a detailed structural analysis of the basin margin and its fault systems and propose an explanation for the development of salt diapirs at the northern basin margin. Together with previous studies setting up the stratigraphic framework (Ahlrichs et al., 2020) and investigating the Late Cretaceous and Cenozoic development (Ahlrichs et al., 2021a), this study focuses on the Triassic and Jurassic, which completes the analysis of the impact of regional post-Permian tectonics on salt structure evolution in the Baltic sector of the NGB. Additionally, our results contribute to a prospective offshore extension of the recently published 3D geological overview model of the onshore part of the NGB, which was developed to meet the increasing demands on subsurface use in Germany (TUNB Working Group, 2021).

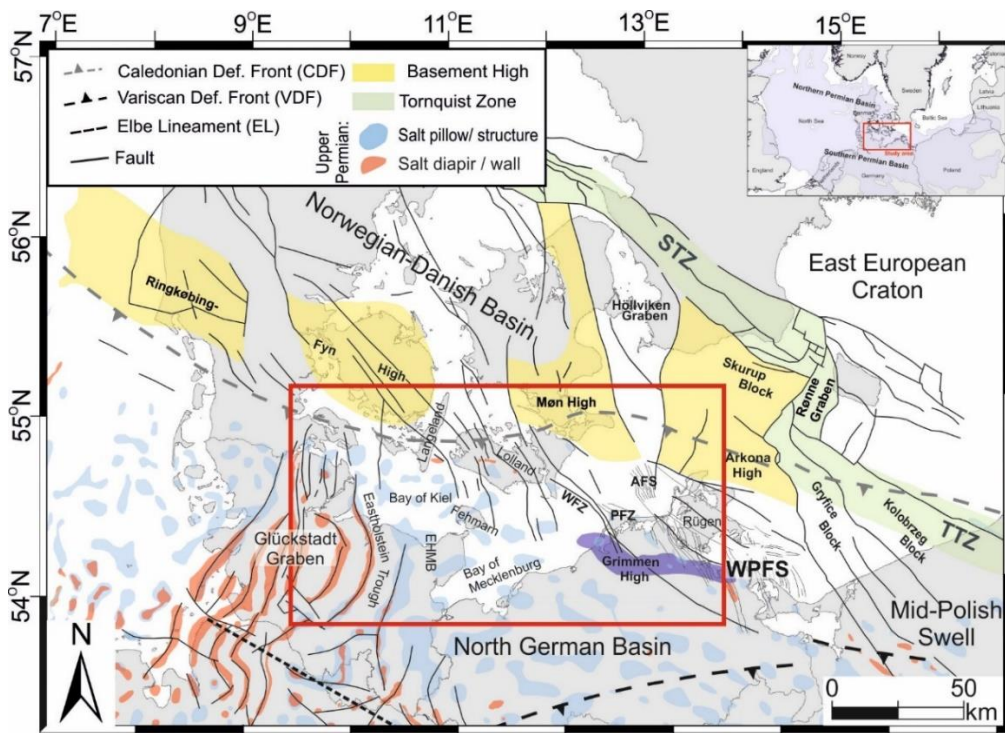


Figure 4.1: Structural overview of the northern North German Basin (modified after Ahlrichs et al., 2020; Ahlrichs et al., 2021a). Inset shows approximate outline of the northern and southern Permian Basin (present day limit of Permian deposits after Maystrenko & Scheck-Wenderoth, 2013). Red box shows study area. Salt structures were compiled after Vejbaek (1997); Dadlez and Marek (1998); Reinhold et al. (2008); Warsitzka et al. (2019); Ahlrichs et al., 2021a. AFS: Agricola Fault System; EHMB: Eastholstein-Mecklenburg Block; PFZ: Prerow Fault Zone; STZ: Sorgenfrei-Tornquist Zone; TTZ: Teisseyre-Tornquist Zone; WFZ: Werre Fault Zone; WPFS: Western Pomeranian Fault System.

4.2. Geological Setting

The study area is located at the northern margin of the North German Basin (NGB) and spans from the Bay of Kiel in the west to the Bay of Mecklenburg and Rügen Island in the east (Fig. 4.1). The crust below the Baltic sector of the North German Basin consist of a complex assemblage of terranes, the Paleozoic Platform, which comprise the Caledonian and Variscan consolidated crust of Central Europe, and its transition to the Precambrian East European Craton (Fig. 4.1) (e.g. Guterch et al., 2010). The transition from the Paleozoic Platform to the East European Craton is termed the Trans-European Suture Zone and spans from the Caledonian Deformation Front in the north to the Elbe Line in the south (Fig. 4.1) (Berthelsen, 1992; Guterch et al., 2010). The northern part of the Trans-European Suture Zone overlaps with the Tornquist Fan, a northwestward widening zone of dominantly Paleozoic faults south of the Tornquist Zone (Fig. 4.1) (Berthelsen, 1992; Thybo, 1997). The Ringkøbing-Fyn High, Møn High and Arkona High are a WNW-ESE trending series of basement highs (*sensu* Peacock & Banks, 2020), which separate the NGB and the Norwegian-Danish Basin (Fig. 4.1). The highs are characterized by generally thin cover of Mesozoic and Cenozoic sediments and elevated Precambrian basement (EUGENO-S Working Group, 1988). The Ringkøbing-Fyn High formed during late Carboniferous – early Permian WNW-ESE extension and transtension where the Ringkøbing-Fyn High experienced less stretching than the adjacent subsiding North German and Norwegian Danish basins (Fig. 4.1) (Vejbaek, 1997). The Ringkøbing-Fyn High remained a high until the Late Cretaceous (EUGENO-S Working Group, 1988; Cartwright, 1990). In the western part of the study area, the NNE-SSW trending Mesozoic-Cenozoic Glückstadt Graben formed a NGB depocenter with up to 11 km of post-Permian sediment thickness strongly influenced by salt tectonics (e.g. Maystrenko et al., 2005a) (Fig. 4.1). The Eastholstein Trough marks the eastern part of the Glückstadt Graben and partly extends into the western Bay of Kiel. The central and eastern Bay of Kiel together with the Bay of Mecklenburg cover the peripheral region between the Glückstadt Graben and the northeastern basin margin (Eastholstein-Mecklenburg Block), where the sedimentary cover is decreased to 2 – 4 km thickness (Fig. 4.1) (Maystrenko et al., 2005b). The eastern part of the study area is characterized by the Western Pomeranian Fault System, a series of NW-SE to NNW-SSE striking fault systems within the Mesozoic succession, often bordering Y-shaped grabens or half-grabens (e.g. Werre Fault Zone, Prerow Fault Zone, Agricola Fault System, see Fig. 4.1) (Krauss & Mayer, 2004).

Figure 4.2 briefly summarizes the development of the NGB showing the main tectonic events together with the dominant lithology. In the late Carboniferous-early Permian, basin formation began with wrench faulting, volcanism, lithospheric thinning and thermal subsidence (Ziegler, 1990b). During the late Permian, repeated restricted seawater influx under arid conditions led to extensive evaporation and the deposition of the layered Zechstein evaporite succession within the basin (Fig. 4.2). In the study area, it consists of seven cyclothems (Z1: Werra; Z2: Stassfurt; Z3: Leine; Z4: Aller; Z5: Ohre; Z6: Friesland; Z7: Fulda) with varying amounts of clay, carbonates, anhydrite, halite and potash sequences (Peryt et al., 2010; Strohmenger et al., 1996). However, the Friesland and Fulda cyclothems are only present in the southern part of our study

area (Best, 1989). Due to the highest amount of mobile halite and less relatively immobile anhydrite, the Stassfurt cyclothem is the most important for salt tectonics in our study area (e.g. Kossow et al., 2000). Thermal subsidence lasted until the Middle Triassic throughout the deposition of the Buntsandstein and Muschelkalk successions (Fig. 4.2) (Van Wees et al., 2000). Locally, subsidence was interrupted by extension forming a narrow graben in the central Glückstadt Graben during the Early and Middle Triassic (Brink et al., 1992).

An eustatic sea-level drop established terrestrial conditions in the Late Triassic during deposition of the Keuper units (Nöldecke & Schwab, 1976). During the Late Triassic, E-W directed extension widened the Glückstadt Graben and caused intensive salt movement (Brink et al., 1992; Maystrenko et al., 2005b). Contemporaneously, the Zechstein salt started moving in the other parts of the study area and initiated salt structure growth (Hansen et al., 2005; Hansen et al., 2007; Hübscher et al., 2010). Covering the Glückstadt Graben and much of northwest Germany, Frisch and Kockel (1999) refined the stratigraphic subdivision of the Keuper and observed discrete pulses of E-W extension during deposition of the Grabfeld and Weser formations (Lower and Upper Gipskeuper) (Fig. 4.2). With the deposition of the overlying Arnstadt Formation (Steinmergelkeuper), tectonic activity abated (Frisch & Kockel, 1999). In the eastern part of the study area, Late Triassic extensional and dextral transtensional movements caused the development of the Western Pomeranian Fault System (WPFS) by reactivation of preexisting NW-SE oriented Paleozoic faults, which were partly decoupled from the supra-salt by the overlying Zechstein salt (Krauss & Mayer, 2004; Seidel et al., 2018). Contemporaneously to the faulting in the WPFS, salt movement started in the Bay of Mecklenburg (Ahlrichs et al., 2020). In the WPFS, first signs of active faulting are indicated by increased thickness of the Grabfeld Formation within the graben structures (Beutler et al., 2012). A major erosional unconformity, termed the Early Cimmerian Unconformity (“Altkimmerische Hauptdiskordanz” by Beutler & Schüler, 1978), characterizes the Keuper succession in the study area. The unconformity forms the base of the Arnstadt Formation (base Norian, Fig. 4.2) and is especially prominent around Rügen Island, where in some areas the entire lower Keuper deposits are missing (Beutler & Schüler, 1978). The Rhaetian transgression reestablished shallow marine conditions lasting throughout the Early Jurassic (Kossow et al., 2000). From Middle Jurassic times until the Albian, the North Sea Doming event caused uplift and a phase of non-deposition during which widespread erosion removed much of the Jurassic and partly Upper Triassic deposits in the study area (Fig. 4.2) (Ziegler, 1990b; Underhill & Partington, 1993; Japsen et al., 2007; Hübscher et al., 2010). Jurassic deposits are almost exclusively preserved in rim-synclines of salt structures and mostly of Early Jurassic age (Hoth et al., 1993; Baldschuhn et al., 2001; Hansen et al., 2005; Zöllner et al., 2008; Hübscher et al., 2010). Assuming a locally similar degree of erosion, the correlation of thicker remnants of Jurassic deposits with the rim-synclines could suggest ongoing salt movement during the Early Jurassic (Hansen et al., 2005; Ahlrichs et al., 2020). Rising sea-levels led to resumed sedimentation in the Albian (Fig. 4.2). The Cenomanian to Turonian succession was deposited in a period of relative tectonic quiescence (Vejbæk et al., 2010). In the late Turonian to Santonian, a major plate reorganization and the onset of the Africa-Iberia-Europe convergence

subjected the study area to compressional stress leading to inversion at the northern NGB margin (Fig. 4.2) (Kley & Voigt, 2008). Resulting horizontal shortening caused uplift, erosion and fault reactivation (Hübscher et al., 2010; Al Hseinat & Hübscher, 2017; Ahlrichs et al., 2020). In the Bay of Mecklenburg, minor salt movement started contemporaneous with inversion of the Werre Fault Zone and uplift of the Grimmen High (Ahlrichs et al., 2021a). During the Paleocene, large-scale uplift caused a regional unconformity, which was followed by a period of tectonic quiescence in the Eocene (Ahlrichs et al., 2021a). In the late Eocene to Oligocene, intensified salt movement restarted in the Glückstadt Graben and likely also in the rest of the study area, whose underlying cause was interpreted to originate from revived E-W directed extension (Ahlrichs et al., 2021a). In Miocene times, regional uplift of the Ringkøbing-Fyn High and adjacent areas led to erosion of the Miocene, Oligocene and partly upper Eocene deposits in the study area outside the Glückstadt Graben (Hinsch, 1987; Rasmussen, 2009; Japsen et al., 2015). Quaternary glaciation eroded further Neogene and Paleogene sediments (e.g. Sirocko et al., 2008).

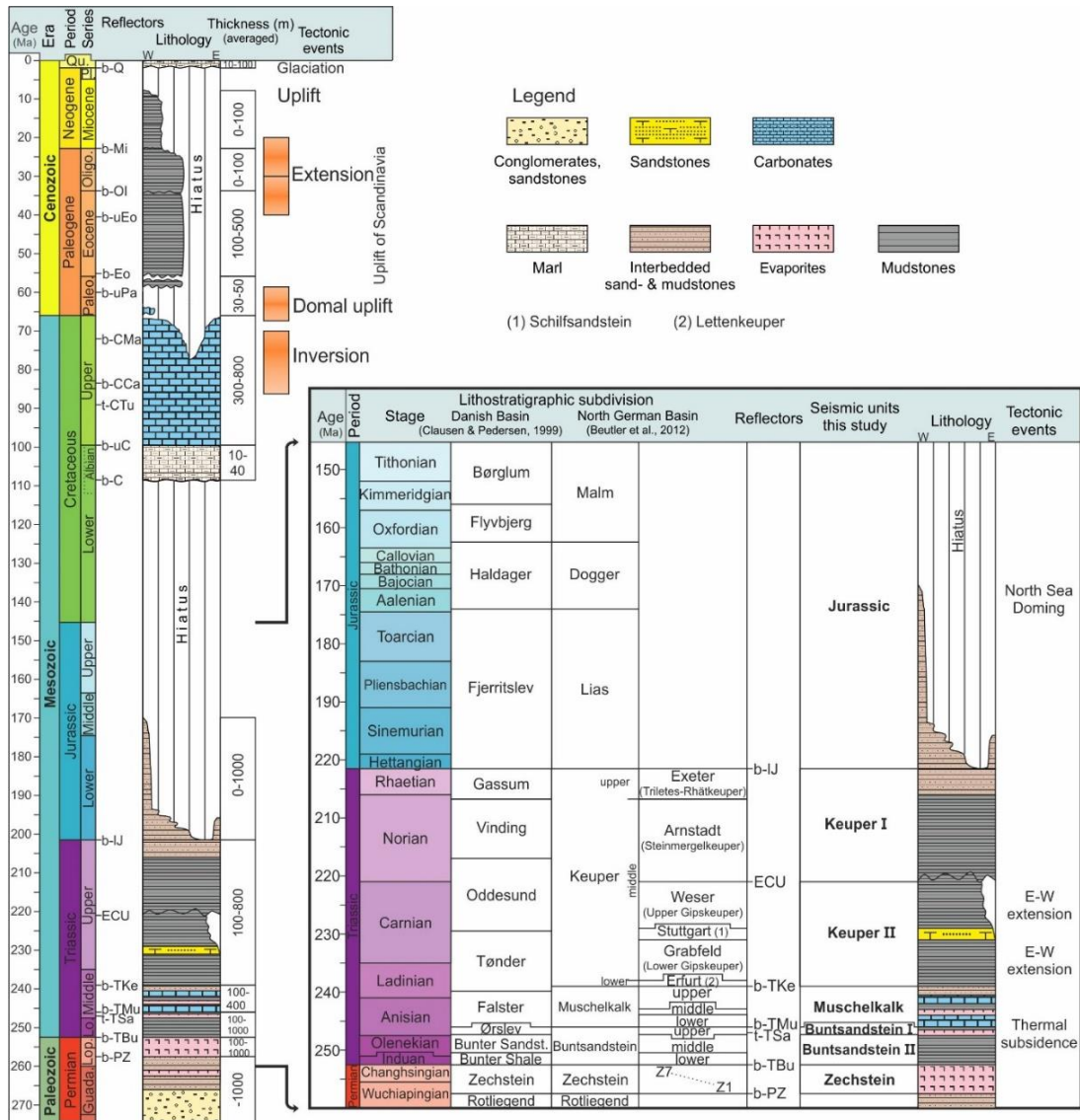


Figure 4.2: Lithostratigraphic chart of the North German Basin showing dominant lithology, main tectonic events, average thickness and lithostratigraphic subdivision of the Triassic and Jurassic (Compiled from Clausen & Pedersen, 1999; Kossow & Krawczyk, 2002; Bachmann et al., 2008; Beutler et al., 2012; STD 2016; Ahlrichs et al., 2021a). Reflectors modified after Ahlrichs et al. (2020). Seismic units mapped in this study are also shown. Reflectors: b-Q: base Quaternary Unconformity; b-Mi: base Miocene; b-OL: base Oligocene; b-uEo: base upper Eocene; b-Eo: base Eocene; b-uPa: base upper Paleocene; b-CMa: base Upper Cretaceous Maastrichtian; b-CCa: base Upper Cretaceous Campanian; t-CTu: top Upper Cretaceous Turonian; b-uC: base Upper Cretaceous; b-C: base Cretaceous; b-IJ: base Lower Jurassic; ECU: Early Cimmerian Unconformity; b-TKe: base Triassic Keuper; b-TMu: base Triassic Muschelkalk; t-TSa: top Triassic Salinarrot; b-TBu: base Triassic Buntsandstein; b-PZ: base Permian Zechstein. Other abbreviations: Bunter Sandst.: Bunter Sandstone; Guada.: Guadalupian; Lo.: Lower; Lop.: Lopingian; Oligo.: Oligocene; Paleo.: Paleocene; Pl.: Pleistocene; Qu.: Quaternary.

4.3. Database & Methods

4.3.1. Seismic database

The seismic database used in this study consists of high-resolution 2D seismic reflection data with a total profile length of more than 10,000 km acquired during multiple surveys (Fig. 4.3). The database consist of seismic profiles of the BaltSeis and Neo-Baltic projects (Hübscher et al., 2004, see Al Hseinat & Hübscher, 2017 for a detailed description), reprocessed profiles of the Petrobaltic database (Rempel, 1992; Schlüter

et al., 1997), profiles of the DEKORP-BASIN'96 survey (DEKORP-BASIN Research Group, 1999) and industry profiles (kindly provided by ExxonMobil Production Deutschland GmbH). These more local surveys were connected by the BalTec data (Hübscher et al., 2016), a regional network of high-resolution 2D seismic data imaging the subsurface continuously from the Zechstein salt base up to the seafloor (see Ahlrichs et al., 2020 for a more detailed description).

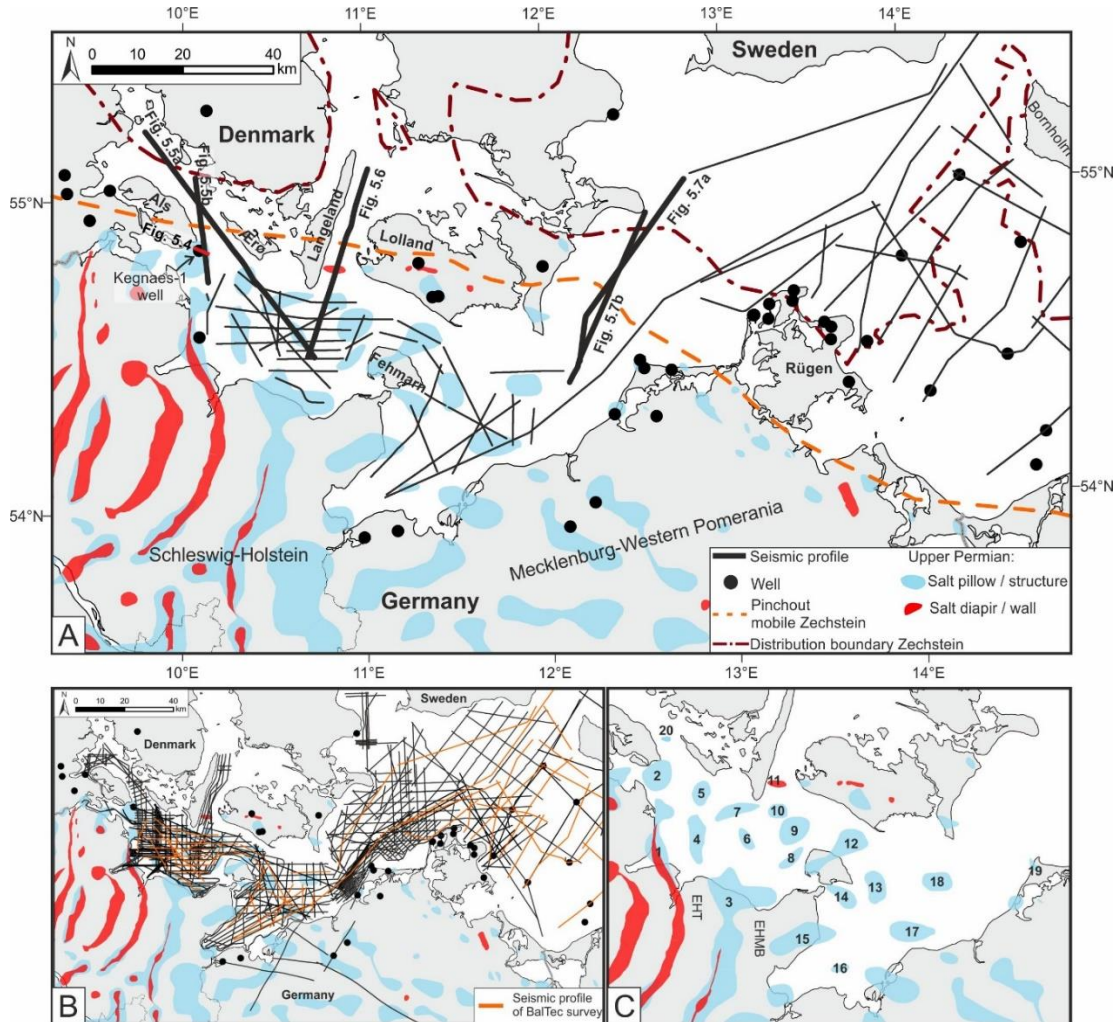


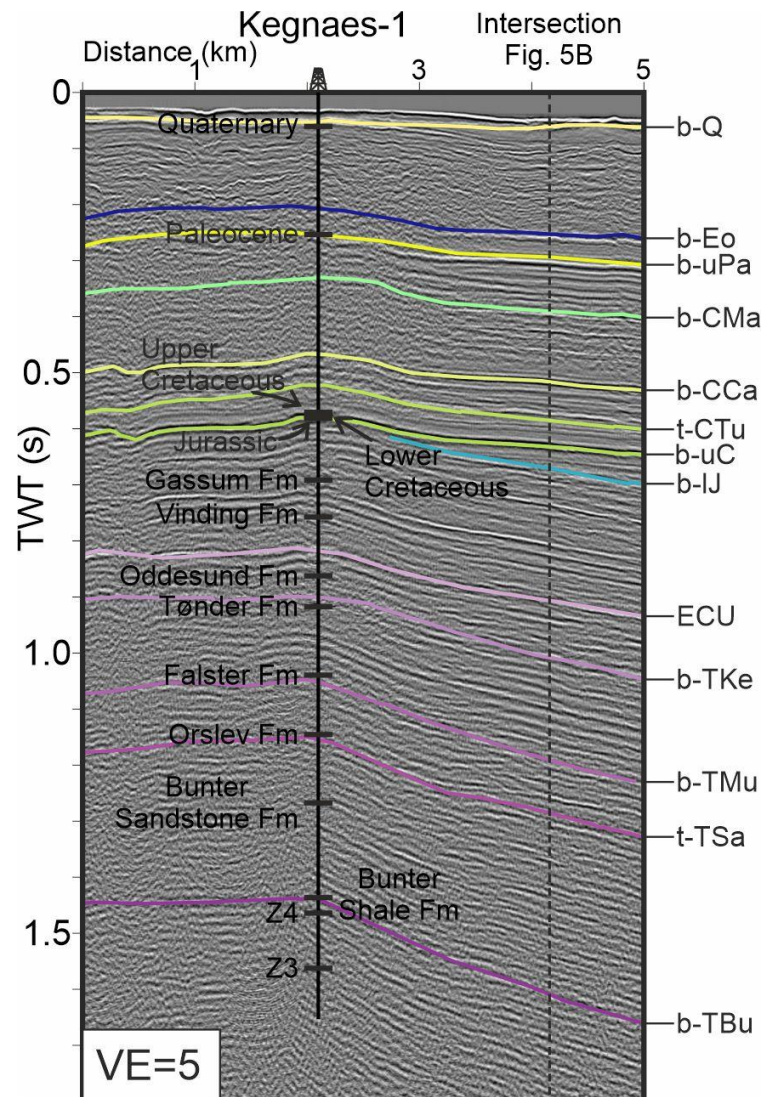
Figure 4.3: Seismic and well database used in this study (modified after Ahlrichs et al., 2021a). A: Seismic profiles of the BalTec survey and locations of shown profiles in this study together with wells in the study area. Distribution boundary of the Zechstein unit and pinch-out of mobile Zechstein units simplified after Katzung, 2004; Peryt et al., 2010; Seidel, 2019 B: Complete database with all available seismic profiles and wells used for mapping. Orange lines: seismic profiles of the BalTec survey. C: Names of salt structures. 1: Waabs; 2: Bredgrund; 3: Plön; 4: Kieler Bucht; 5: Schleimünde; 6: Langeland Süd; 7: Langeland; 8: Flüggesand; 9: Vinsgrav; 10: Langeland Ost; 11: Kegnaes; 12: Fehmarn; 13: Staberhuk Ost; 14: Fehmarnsund Ost; 15: Cismar; 16: Boltenhagen Nord; 17: Trollegrund Nord; 18: Neobaltic; 19: Prerow; 20: Als Ost (discovered in this study).

4.3.2. Stratigraphy

Stratigraphic interpretation in this study is based upon the stratigraphic framework described by previous publications, which were already carried out within the *StrucFlow* project and used the same database (Ahlrichs et al., 2020; Ahlrichs et al., 2021a). Within this framework, 18 seismic horizons were identified: *base Quaternary Unconformity*, *base Miocene*, *base Oligocene*, *base upper Eocene*, *base Eocene*, *base upper*

Paleocene, base Maastrichtian, base Campanian, top Turonian, base Upper Cretaceous, base Cretaceous, base lower Jurassic, Early Cimmerian Unconformity, base Keuper, base Muschelkalk, top Salinarröt, base Buntsandstein, base Zechstein (Fig. 4.2). However, the base Cretaceous and base Upper Cretaceous reflectors cannot be resolved as the thickness of the Albian unit between both reflectors is below seismic resolution in the study area. The calibration of the seismic data with well information from deep research and hydrocarbon exploration wells was set up for the Bay of Mecklenburg and the area west of Rügen Island (Nielsen & Japsen, 1991; Hoth et al., 1993; Schlüter et al., 1997, see Ahlrichs et al., 2020 for a detailed description). From there, we traced the horizons across the study area using all available seismic data (Fig. 4.3). Additional control on the well-to-seismic tie was provided by the Kegnaes-1 well in the Bay of Kiel (Fig. 4.4) and further Danish wells northwest of the Island of Als (Fig. 4.3) (Nielsen & Japsen, 1991). Furthermore, we linked the stratigraphic interpretation to previous onshore and offshore studies in the area (Michelsen, 1978; Clausen & Pedersen, 1999; Baldschuhn et al., 2001; Hansen et al., 2005; Maystrenko et al., 2005a, 2005b; Hansen et al., 2007; Zöllner et al., 2008; Hübscher et al., 2010; Al Hseinat et al., 2016; Deutschmann et al., 2018).

Figure 4.4: Well-to-seismic tie for the Kegnaes-1 well. Markers show the base of the units and are based on Nielsen and Japsen (1991). For location, see Fig. 4.3. See Fig. 4.2 for reflector abbreviations and juxtaposition of German and Danish lithostratigraphic units. Fm: Formation; VE: vertical exaggeration.



4.3.3. Mapping

In this study, we focus on mapping of the Zechstein, Triassic and Jurassic units to identify episodes of increased tectonic activity and salt movement in the Baltic sector of the North German Basin in the context of the regional Triassic-Jurassic basin evolution. Using the same database, the Zechstein unit was already mapped by Ahlrichs et al. (2021a). There, the BalTec, Petrobaltic, DEKORP-BASIN'96 and industry profiles contributed to the mapping of the Zechstein unit as these surveys have a deep signal penetration and clearly image both the base and top Zechstein horizons. In this study, we revisited all other profiles in the database, which image the shallow and medium depth range, and refined the Zechstein maps by adding further horizon picks, especially towards the basin margin, where the Zechstein unit is at shallower depth. For the Triassic and Jurassic units, we used all available seismic profiles in the database (Fig. 4.3b). The mapping procedure includes gridding using all available horizon picks for each horizon to create two-way traveltime (TWT) structure maps by minimum curvature spline interpolation with a grid cell size of 300 x 300 m. For the Cretaceous, we used the base Upper Cretaceous time-structure map of Ahlrichs et al. (2021a). Only faults, which could be traced across multiple seismic profiles have been included in the maps. For time-depth conversion, a precise velocity model covering the entire study area is necessary. This is a challenging aspect of future work as velocity information is sparsely distributed due to the lack of offshore wells and seismic depth data. Velocity information derived from migration velocity analysis has been published for the Bay of Mecklenburg (Schnabel et al., 2021), however, for other parts of the study area this is an open task. To give an idea of the depth range imaged by the presented seismic profiles in this study, we labeled the right profile axis with depth calculated using a constant velocity of 3 km/s. This velocity represents an average velocity of the subsurface in the study area based on published velocity information (Schnabel et al., 2021, see their table 1). We estimated the thickness of each mapped unit by calculating isochron maps (vertical thickness in TWT) for the Zechstein, Buntsandstein, Muschelkalk, Keuper II, Keuper I and Jurassic seismic units (see Fig. 4.2 for age constrains). We converted the thickness in TWT to thickness in meter by using a constant velocity selected for each unit based on previous studies (Schlüter et al., 1997; Hansen et al., 2007; Schnabel et al., 2021). The chosen velocity is mentioned in the respective figure legend.

In this study, we analyze seismic profiles and isochron maps to identify local and regional thickness variations in the Triassic and Jurassic units. We interpret regional and local thickness variations as an expression of differential sedimentation and erosion caused by vertical tectonic movements, differential compaction and sedimentation processes (Betram & Milton, 1989). During synkinematic sedimentation, the timing of the growth of a salt structure can be read from the surrounding sediments by analyzing the geometric relationship between overburden strata and the salt structure (e.g. Jackson & Hudec, 2017). Over geological time scales, salt can flow like a viscous fluid if the salt body experiences differential loading by e.g. a varying gravitational load (e.g. by differential sedimentation) or displacement loading (e.g. by extension or shortening) (Jackson & Hudec, 2017). When salt flows from the surrounding area into the salt structure, the top of salt subsides in the area of withdrawal, which creates

additional accommodation space for more sediments. These processes lead to increased thickness of the synkinematic unit if compared to adjacent areas without salt movement (e.g. Jackson & Hudec, 2017). Likewise, the accumulation of salt decreases accommodation space resulting in a thinner synkinematic unit above the salt structure. When the regional sedimentation rate exceeds the rise rate of the salt structure, the locally thickened synkinematic strata in the rim-syncline (peripheral sink, sensu Jackson & Hudec, 2017) is characterized by converging and diverging layering (Sørensen, 1986). In the case of a regional sedimentation rate smaller than the rise rate of the salt, angular unconformities between the layering of the peripheral sink and the pre-kinematic overburden develop (Sørensen, 1986).

4.3.4. Methodical uncertainties

Each step in the seismic imaging, mapping and interpretation procedure has inherited uncertainty, which needs to be integrated to evaluate the uncertainty of the results. The most important steps include acquisition, seismic processing, well-to-seismic-tie, horizon picking, fault detection, gridding, and geological interpretation. Even though all these steps are crucial for the results, they all contribute differently to the final degree of uncertainty and are in some cases difficult to quantify and subjective (e.g. Thore et al., 2002; Bond, 2015). In the following, we strive for a qualitative evaluation of uncertainty in this study, without claim to completeness.

In this study, solely 2D seismic data is available, which requires for accurate imaging that the incident and reflected signals are in the same plane. However, in the presence of complex geological structures, signal from a structure out of the plane of the seismic section can be apparent. Our seismic database consists of several seismic surveys with different acquisition parameters, however, all of them are offshore acquisitions with modern positioning systems and thus, positioning errors in the range of a few meters only. Survey mis-ties were corrected and residual mis-ties are negligible. During seismic processing, the most important sources for uncertainty stem from residual multiples and from migration by inaccurate migration velocity. The latter is especially sensitive to lateral velocity variations, which are known for the study area (Schnabel et al., 2021). The vertical resolution of the BalTec data is in the range of ca. 5 – 30 m, while horizontal resolution after migration approximated by the width of the first Fresnel Zone is approx. 20 – 100 m ((dominant frequency of ca. 80Hz, see Hübscher et al., 2016; Ahlrichs et al., 2020). Uncertainty in the stratigraphic interpretation increases with distance from the well locations and in this study, almost all available wells are located onshore (Fig. 4.3). However, our dense seismic network allows tracing of the main reflectors throughout the study area, which reduces uncertainty from the well-to-seismic tie. Uncertainty from horizon picking and fault detection strongly depend on structural complexity. For most parts of the study area, the used seismic data has very good quality allowing an interpretation with a high degree of certainty. The level of uncertainty increases in areas of high complexity, e.g. within fault zones. During the mapping procedure, uncertainty mostly stems from the profile network. The final resolution of the gridded maps depends on the distance between profiles, the location of the profile related to the imaged structures and the spatial extend of data gaps. Hence,

4.4. Observations

We use key seismic profiles, time-structure and isochron maps of the Zechstein, Triassic and Jurassic units to analyze the basin configuration, regional depositional patterns and local thickness variations in order to identify phases of active tectonics during the Triassic-Jurassic extensional stage of basin evolution. Thereby, we interpret local thickness variations across salt structures, characterized by thinning of the overburden towards the crest and thickening of the overburden above the rim-syncline of a salt structure as evidence for syndepositional salt movement and salt structure growth. This includes a converging and diverging reflector pattern, respectively. Accordingly, locally uniform thickness across salt structures indicate the absence of salt movement.

4.4.1. Northwestern basin configuration

In the northwestern part of the study area, two profiles, which run from the basin margin southwards into the Bay of Kiel, image numerous salt pillows (Fig. 4.5). The base Zechstein dips gently towards the south. Faults pierce the base Zechstein at the basin margin (Fig. 4.5a, profile km 13). South of the island of Ærø (Fig. 4.3), a prominent fault offsetting the base Zechstein by ca. 300 ms TWT is visible (Fig. 4.5a, profile km 50). Between the islands of Als and Ærø, the profiles show an unknown salt pillow, here named “Als Ost”, which is characterized by numerous faults in the Triassic-Jurassic overburden (Fig. 4.5a and b). Thickness of the Buntsandstein and Muschelkalk units gradually increases towards the south, and basin center, without any distinct local thickness variations and thus, no signs for active salt movement (Fig. 4.5a and b).

Shown by the NW-SE running profile (Fig. 4.5a), the Keuper II unit is thin but uniform in thickness close to the basin margin in the northwestern part of the profile. At the SW flank of the salt pillow “Als Ost”, the Keuper II unit has increased thickness, which indicates the onset of salt movement. Towards the southwest-located salt pillow “Schleimünde”, the ECU reflector erosionally truncates the Keuper II unit (Fig. 4.5a, profile km 50-55). Across the salt pillows “Schleimünde”, “Langeland” and “Langeland Süd”, the Keuper II unit shows varying thickness by thinning towards the crest of the structures indicating the syndepositional initiation of salt structure growth (Fig. 4.5a). Throughout most of the profile, the Keuper I unit is bound at the top by the Mid Jurassic Unconformity, here expressed by the b-uC reflector. Thus, the unit is strongly affected by postdepositional erosion and the imaged unit only represents the preserved remnants (Fig. 4.5a). In the northwest, almost the entire Keuper I unit is missing while thicker remnants are preserved towards the south (Fig. 4.5a). At the salt pillows “Langeland” and “Langeland Süd”, residual thickness is increased above the rim-synclines while the unit is thinner in the crestal part of the salt structures. Jurassic deposits are only preserved in the rim-syncline at the southwestern flank of the salt pillow “Als Ost” (Fig. 4.5a).

On the N-S profile (Fig. 4.5b), the Keuper II unit is thin and uniform in thickness in the northern part of the profile. In the hangingwall of the listric fault north of the salt pillow “Als Ost” (F1 in Fig. 4.5b), the Keuper II unit shows increased thickness.

Additionally, the Keuper II unit has increased thickness at the southern flank of the structure and slightly thins towards the crest, which would suggest salt movement. As observed in Fig. 4.5a, the Keuper I unit imaged by the profile is bound at the top by the Mid Jurassic Unconformity throughout most of the profile and thus, only represents remnants preserved from erosion (Fig. 4.5b). Residual thickness is especially reduced above the salt pillow “Als Ost” and to a lesser extent above the salt pillow “Bredgrund” (Fig. 4.5b). At the northern flank of the salt structure “Als Ost”, the reflection pattern of the Keuper I unit is divergent towards the listric fault labelled with F1 in Fig. 4.5b (close up in Fig. 4.5c, note divergence between dashed lines). This suggests syndepositional faulting and salt movement during the deposition of the Keuper I unit. In between the salt structures imaged by Fig. 4.5, a thin Jurassic unit is preserved.

4.4.2. Northern basin configuration and the Kegnaes Diapir

In the central part of the study area, a N-S striking profile runs from the basin margin into the Bay of Kiel imaging the salt diapir “Kegnaes” (Fig. 4.6). The width of the diapir is ca. 1 km at its top and 2.5 km at its stem. The narrow waist suggests that the diapir was mildly squeezed during its development. The base Zechstein dips towards the south. In the northern part of the profile, a normal fault pierces from the pre-Zechstein up into the Cretaceous overburden. Further south, there is an approx. 1.5 km wide zone with highly disturbed reflection pattern and unsure stratigraphy (Fig. 4.6a, profile km 8). North of the Kegnaes Diapir, the Zechstein unit is strongly reduced forming a distinct rim-syncline (Fig. 4.6a and b). In this area, the Triassic-Jurassic overburden is intensely faulted. Beneath, two basement step faults pierce the base Zechstein without reaching further into the suprasalt overburden. The Buntsandstein unit shows a general trend of gradually increasing thickness towards the south-directed basin center. The exception to this trend is a zone, where the Buntsandstein locally thins towards the south until reaching the northward dipping fault F2 (Fig. 4.6a and b, profile km 23 - 28). This local trend of thinning could suggest syndepositional uplift. Noteworthy, this zone is located above the footwall of the basement step faults (Fig. 4.6a and b). Above the northern rim-syncline of the diapir, the Buntsandstein unit within the hangingwall of the F3 labelled fault shows divergent reflectors towards the fault, which indicate an early phase of faulting and salt movement (Fig. 4.6c). The Muschelkalk concordantly overlies the Buntsandstein and shows relatively constant thickness across the profile (Fig. 4.6a). The Keuper II unit has a relative uniform thickness in the northern part of the profile. Between profile km 23 – 28, the Keuper II unit dips towards the south and gradually thins. In this area, multiple conflicting dips cross the Keuper unit. These conflicting dips are probably caused by out of plane reflections originating from the adjacent lateral subsurface of the 2D profile (see e.g. Drummon et al., 2004). In the fault zone north of the diapir, the Keuper II unit has increased thickness (Fig. 4.6b). This zone represents the primary peripheral sink and indicates salt movement and normal faulting (Fig. 4.6b). Thus, the Keuper II unit marks the initial pillow stage of the Kegnaes Diapir, whose crestal overburden was likely weakened by extension. At both flanks of the diapir, the Keuper II terminates in a toplap against the ECU reflector, which suggests that the ECU forms the unroofing unconformity (*sensu* Sørensen, 1998) and the erosion marked by the ECU together with the prior extension allowed

the diapir to pierce the overburden (Fig. 4.6b). Salt movement and faulting continued during deposition of the Keuper I indicated by the increased thickness within the faulted zone and at the southern flank of the diapir (Fig. 4.6b). Right there, Jurassic deposits were preserved from erosion. The Cenomanian – Turonian and Coniacian – Santonian units overly the Triassic-Jurassic deposits without visible thickness variations. (Fig. 4.6a, b).

4.4.3. Northeastern basin configuration

In the northeastern part of the study area, two profiles image the basin margin and the pinch-out of the Zechstein unit (Fig. 4.7a, b). In the center of both profiles, there is a southward dipping reflector terminating in a toplap against the Zechstein, which could represent the base Upper Carboniferous. Thickness of the Zechstein unit increases towards the south. In the northeastern part of the profiles, multiple basement faults pierce the southward dipping base Zechstein (Agricola Fault System, Fig. 4.7). The Falster Fault imaged by the profile in Fig. 4.7a only pierces the Mesozoic overburden while in the profile located further east, the fault reaches into the pre-Zechstein (Fig. 4.7b). This area marks the transition zone between basement-involved faulting at the basin margin and thin-skinned faulting decoupled by the Zechstein. In the southwestern part, faults of the Werre Fault Zone (WFZ) are purely thin-skinned as they only pierce the Mesozoic overburden (Fig. 4.7). The Buntsandstein and Muschelkalk units gradually increase towards the southward-directed basin center without local thickness variations, and thus, no signs of active faulting.

Both profiles image significant local thickness variations within the Keuper units. The Keuper II unit in the hangingwall of the Falster Fault has increased thickness, which suggests initial syndepositional faulting (Fig. 4.7a and b). The northeastern border fault of the WFZ is a SW-dipping slightly listric fault forming a rollover structure during deposition of the Keuper II indicated by the increased thickness in the hangingwall (Fig. 4.7b). The overlying Keuper I unit is thin at the basin margin (northeast of the Agricola Fault System) and southwest of the WFZ (Fig. 4.7a and b). In between the WFZ and Agricola Fault System, the thickness of the Keuper I unit is approximately doubled, which suggests increased subsidence in this area (Fig. 4.7a and b). Increased thickness of the Keuper I unit in the hangingwall of the Falster Fault suggests ongoing normal faulting (Fig. 4.7b). The Keuper I unit within the WFZ shows increased thickness compared to southwest of the Werre Fault, however, the unit shows an almost horizontal position (Fig. 4.7b). The fault dip gets steeper and thus, faulting evolved in rather vertical direction. The Jurassic unit has maximum thickness in the southwestern part and thins towards the basin margin, where it pinches out within the Agricola Fault System (Fig. 4.7a and b).

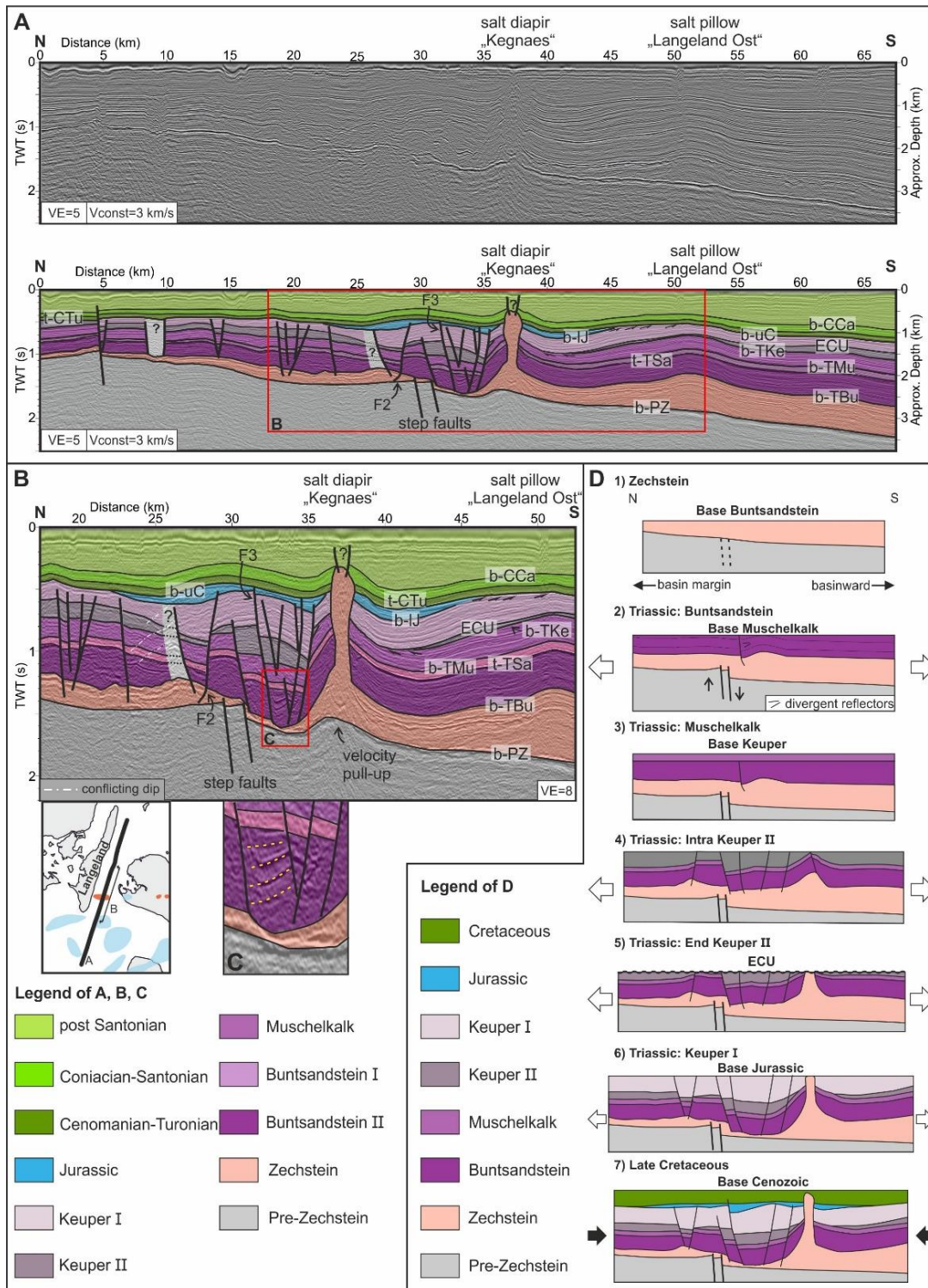


Figure 4.6: Profile crossing the northern basin margin (see Fig. 4.3). A: Uninterpreted and interpreted section in two-way travelttime. An approximated depth is shown at the right axis of the profile to give an idea of the true depth conditions. Depth was calculated using a constant velocity of 3 km/s. Stratigraphy in the light grey areas marked with “?” (ca. profile km 58 and 25) unknown due to highly disturbed reflection pattern. Exact extend of the roof and cover of the diapir unsure. Salt structures are marked on top of the section. Reflectors labeled as in Fig. 4.2. B: Zoom as shown in A (with higher vertical exaggeration). Note the erosional termination of the Keuper II unit at the flanks of the diapir. C: Zoomed in section of B showing divergent reflections within the Buntsandstein north of the Kegnaes Diapir. D: Conceptual sketch visualizing proposed evolution of the Kegnaes Diapir driven by extension and erosional unroofing during the Triassic and subsequent squeezing during the Late Cretaceous. VE: Vertical exaggeration.

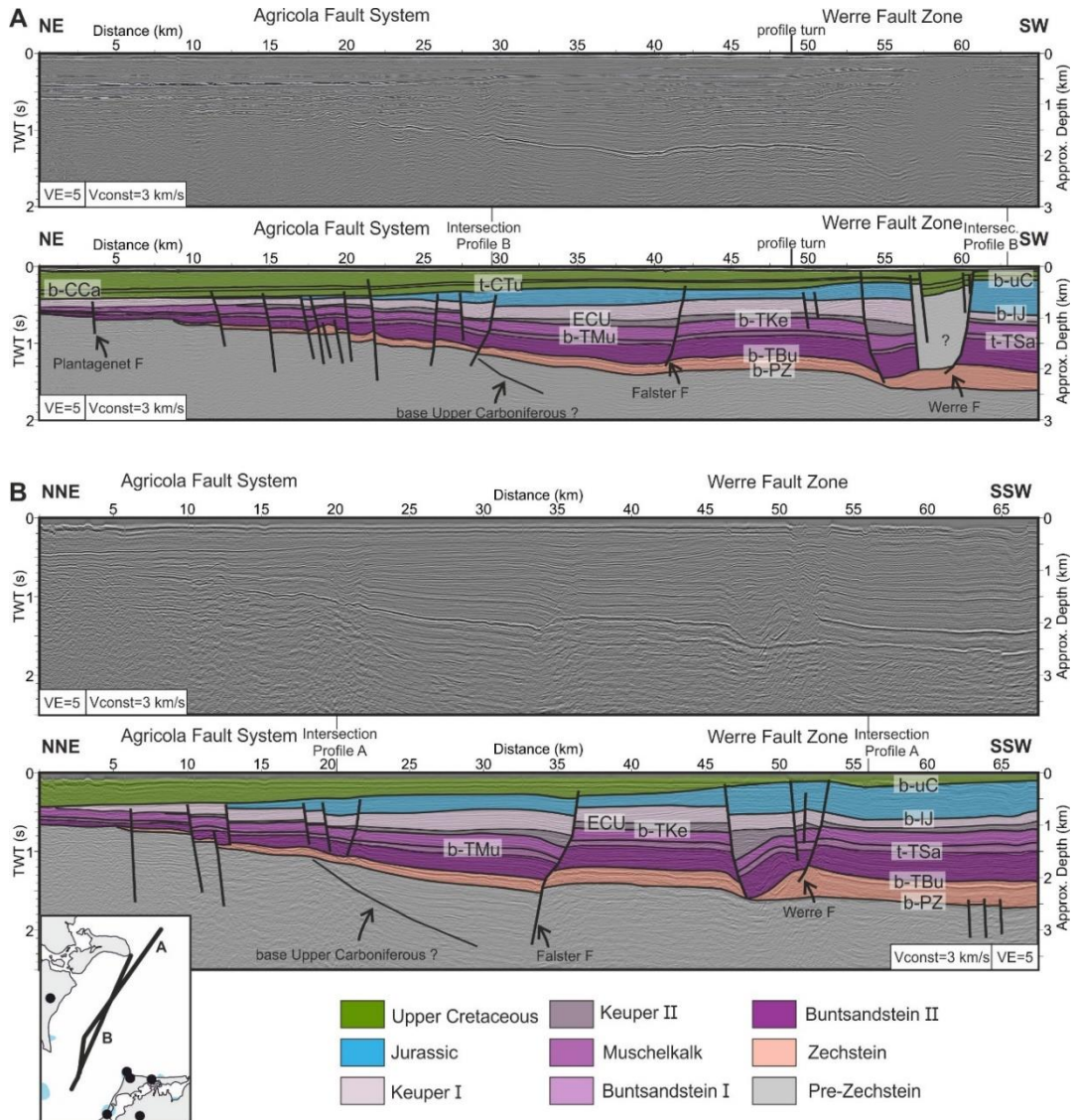


Figure 4.7: Profile A (BGR16-221) and profile B imaging the northeastern basin margin. See Fig. 4.3 for location. Fault systems are marked at the top of the sections. An approximated depth is shown at the right axis of the profile to give an idea of the true depth conditions. Depth was calculated using a constant velocity of 3 km/s, which represents an average velocity of the profile. Note the profile turn and thus different profile orientation of A and B and resulting different appearance of structures, especially of the Werre Fault Zone. VE: vertical exaggeration. F: fault. Reflectors labeled as in Fig. 4.2.

4.4.4. Mapping

4.4.4.1. Zechstein

In the northern part of the study area, the base Zechstein shallows from 2900 ms TWT, representing the central part of the basin, towards its pinch-out at the northeastern basin margin at ca. 500 ms TWT (Fig. 4.8a). West of Rügen Island, the NE-SW trend is locally interrupted by an approx. 20 km wide depression (Fig. 4.8a). Across the basin margin, multiple faults pierce the base Zechstein (Fig. 4.8a, faults marked with AFS, PF, WF, PaF, AVF and faults near the islands of Langeland and Als). Further faults with partly small offsets are visible northwest of the Grimmen High and northwest of Fehmarn Island. In the western Bay of Kiel, a prominent fault showing a large offset of the base Zechstein (as imaged by Fig. 4.5a) strikes N-S, parallel to the salt structures Schönberg-Kieler Bucht (Fig. 4.8a). Therefore, this fault marks the eastern border of

the Eastholstein Trough. Thickness of the Zechstein unit correlates well with the known locations of salt structures (Fig. 4.8b). Mapping in this study reveals a new small salt pillow, here named “Als Ost” (Fig. 4.8b and Fig. 4.5).

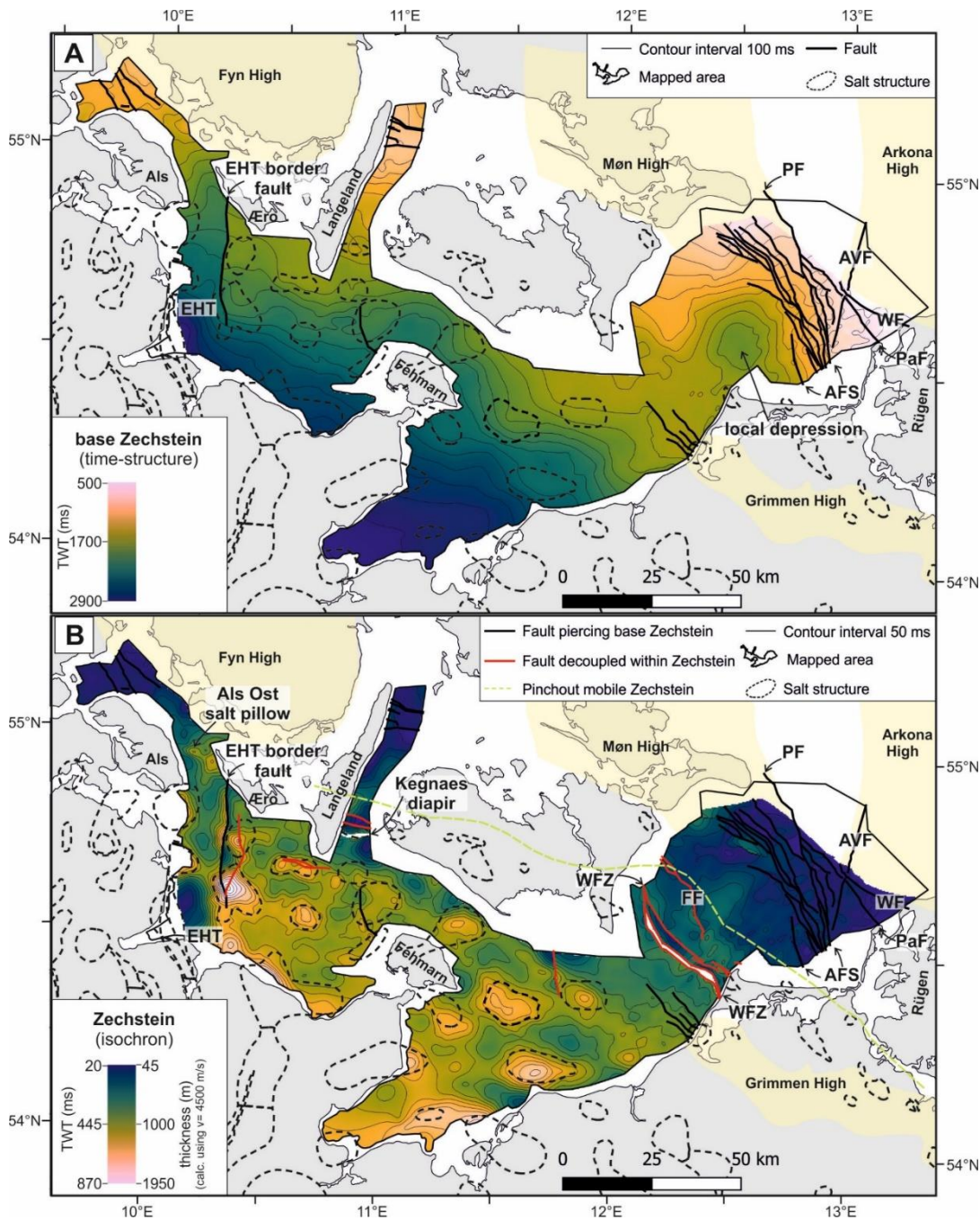


Figure 4.8: Zechstein. A: base Zechstein time-structure map in TWT. B: Zechstein isochron map in TWT. AFS: Agricola Fault System; AVF: Agricola-Svedala Fault; EHT: Eastholstein Trough; FF: Falster Fault; PaF: Parchim Fault; PF: Plantagenet Fault; WF: Wiek Fault; WFZ: Werre Fault Zone.

4.4.4.2. *Buntsandstein and Muschelkalk*

The base Buntsandstein and base Muschelkalk time-structure maps show the general N-S to NE-SW trend from the shallow margin towards the deeper basin locally modified by the presence of Zechstein salt structures (Figs. 4.9a and 4.10a). Thickness of the Buntsandstein and Muschelkalk units gradually increase towards the basin center due to the higher degree of subsidence away from the basin margins (Figs. 4.9b and 4.10b). Thickness variations are small (ca. 50 ms TWT) and do not correlate with the salt structures suggesting that the salt did not move and thus, the Buntsandstein and Muschelkalk units are prekinematic deposits. Between the Werre Fault Zone and Agricola Fault System, the isochron map of the Buntsandstein unit reveals a zone of locally increased thickness standing out from the general thickening trend towards the south, which indicates locally increased subsidence (Fig. 4.9b). In the Muschelkalk, this zone of increased thickness is not visible (Fig. 4.10b). A correlation of further visible thickness variations within the Buntsandstein and Muschelkalk with other tectonic structures cannot be observed from our maps.

4.4.4.3. *Keuper*

The base Keuper time-structure map shows a similar pattern as the base Muschelkalk (Fig. 4.11a). The isochron map of the Keuper II unit reveals the general thickening trend towards the south (Fig. 4.11b). At the northeastern basin margin, south of the island of Æro and south of the Kegnaes Diapir, the Keuper II unit is eroded (Fig. 4.11a and b). Further modifications to the general thickness trend are visible between the Werre Fault Zone and Agricola Fault System, where the thickness of the Keuper II is locally more than doubled (Fig. 4.11b, PD: Prerow Depression). This indicates increased subsidence in this area. The graben within the Werre Fault Zone shows increased infill with Keuper II sediments indicating syndepositional faulting (Fig. 4.11b). Furthermore, the Keuper II isochron map shows local thickness variations across salt structures such as the thinned crest of the Fehmarn salt pillow and the development of the northern peripheral sink of the Kegnaes Diapir, which is also intensely faulted (Fig. 4.11b). In the Eastholstein Trough, the Keuper II shows increased thickness indicating the onset of salt movement.

The ECU time-structure map shows the erosional truncation of the base Keuper at the northeastern basin margin and south of the Kegnaes Diapir in the northwestern part of the study area (compare Fig. 4.12a and Fig. 4.11a). In many parts of the study area, the Keuper I is affected by erosion related to the Mid Jurassic Doming. Thus, when interpreting thickness variations of the Keuper I, one needs to consider that in areas where the Jurassic is missing, the top of the Keuper I unit is eroded too and the present thickness represent the thickness preserved from erosion (Fig. 4.12b, white line and Fig. 4.13). Between the Werre Fault Zone and Agricola Fault System, thickness of the Keuper I is increased suggesting ongoing locally increased subsidence (Fig. 4.12b). Compared to the Keuper II unit, the zone of increased thickness widened and the local depocenter shifted northwest (compare area marked with PD in Fig. 4.12b and 4.11b). Northwest of the Grimmen High, the Keuper I is thinned and the thickness trend shows a local E-W direction (Fig. 4.12b). Northeast of the salt pillow “Trollegrund Nord” in the Bay of Mecklenburg, the Keuper I is locally increased, which could resemble a minor peripheral sink caused by salt movement (Fig. 4.12b). North of the Kegnaes

Diapir, thickening of the Keuper I accompanied by faulting indicates ongoing salt movement. In the Bay of Kiel, the top of the Keuper I is eroded which hampers a direct interpretation of thickness variations. However, in the northernmost Eastholstein Trough, the Keuper I is fully preserved and increased thickness indicates ongoing salt movement and deepening of the rim-synclines in the outer Glückstadt Graben (Fig. 4.12b).

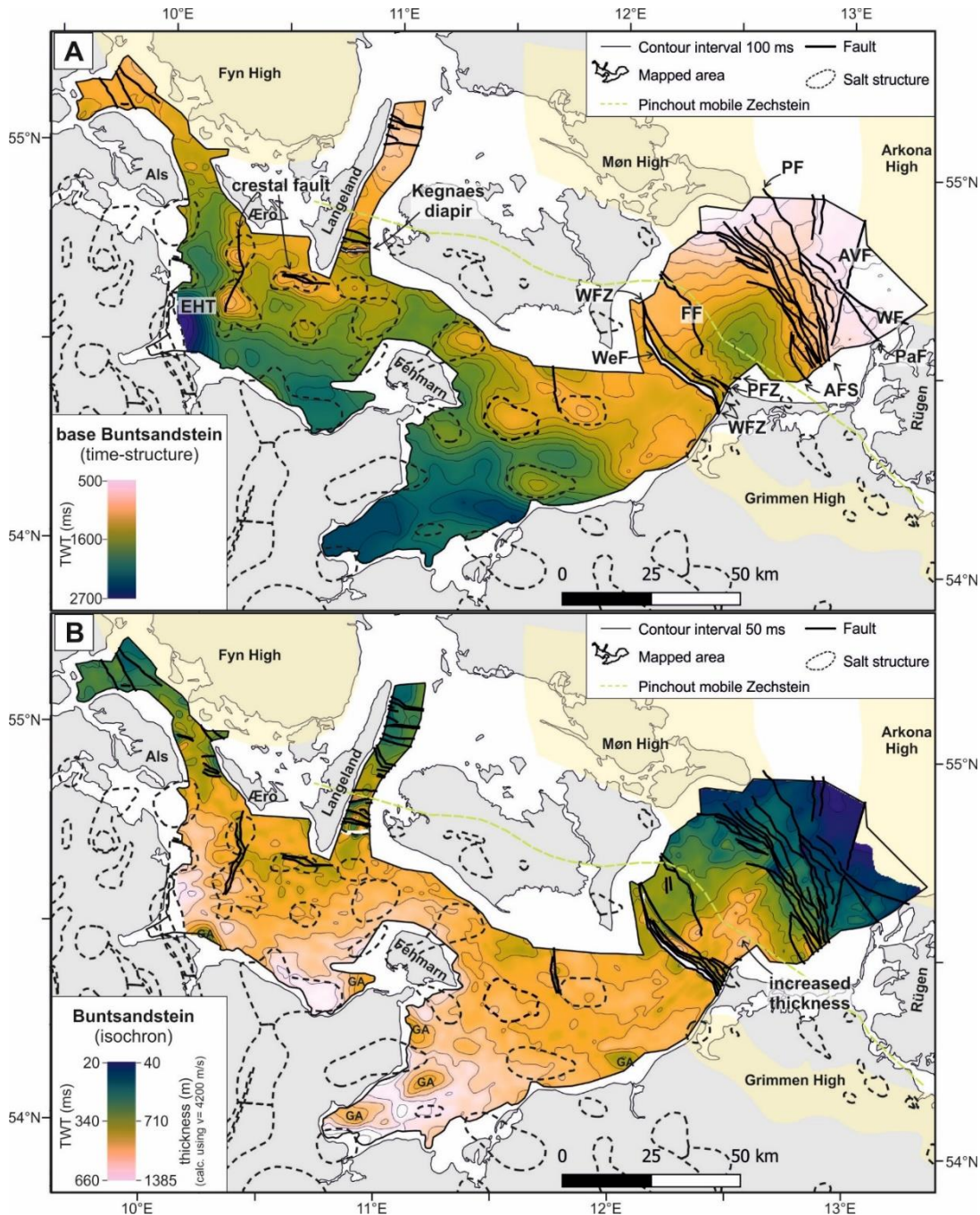


Figure 4.9: Buntsandstein. A: base Buntsandstein (top Zechstein) time-structure map in TWT. B: Buntsandstein isochron map in TWT. AFS: Agricola Fault System; AVF: Agricola-Svedala Fault; EHT: Eastholstein Trough; FF: Falster Fault; PaF: Parchim Fault; PF: Plantagenet Fault; PFZ: Prerow Fault Zone; WF: Wiek Fault; WeF: Werre Fault; WFZ: Werre Fault Zone. GA: Gridding artefact caused by either lack of seismic data in the area or velocity artefacts by e.g. shallow gas.

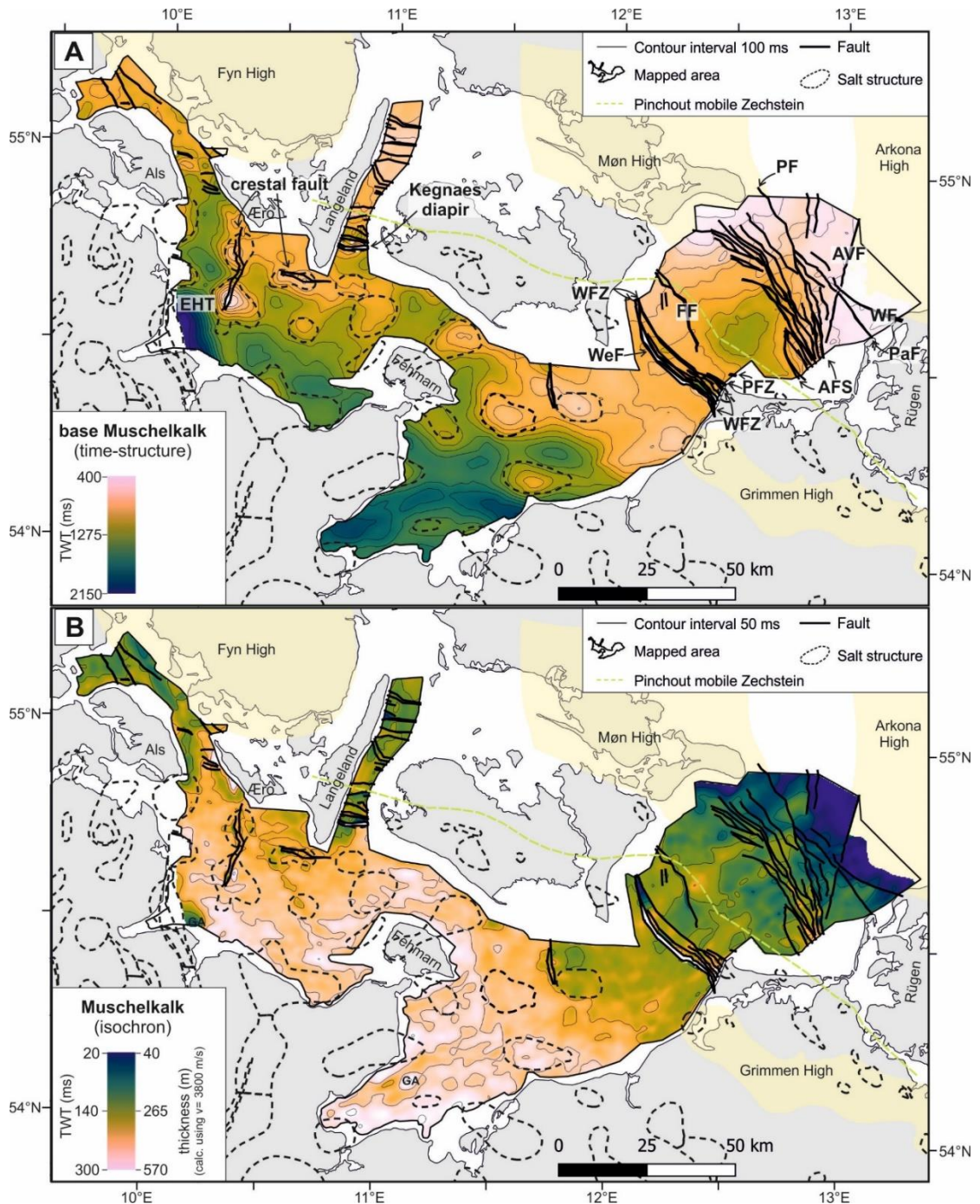


Figure 4.10: Muschelkalk. A: base Muschelkalk time-structure map in TWT. B: Muschelkalk isochron map in TWT. AFS: Agricola Fault System; AVF: Agricola-Svedala Fault; EHT: Eastholstein Trough; FF: Falster Fault; PaF: Parchim Fault; PF: Plantagenet Fault; PFZ: Prerow Fault Zone; WF: Wiek Fault; WeF: Werre Fault; WFZ: Werre Fault Zone. GA: Gridding artefact caused by lack of seismic data in the area or velocity distortions due to e.g. shallow gas.

4.4.4.4. Jurassic

The base Jurassic time-structure map shows the strongly disrupted character of the unit (Fig. 4.13a). Due to the Mid Jurassic erosion event, the mapped Jurassic unit represents only the preserved remnants. Maximum thickness is visible between the Werre Fault Zone and Agricola Fault System in the area of the Prerow Depression, where also the Keuper deposits show increased thickness (Fig. 4.13b). Compared to the Keuper I unit, this zone of increased thickness further widened and includes the area southwest of the

Werre Fault Zone. In the Bay of Mecklenburg, the preserved Jurassic unit is thin and completely eroded above the crest of salt structures (Fig. 4.13b). In the Bay of Kiel, almost the entire Jurassic unit is missing. Across the study area, the Jurassic unit is thin or reduced above the crest of salt structures while thicker Jurassic remnants are located above rim-synclines (Fig. 4.13b).

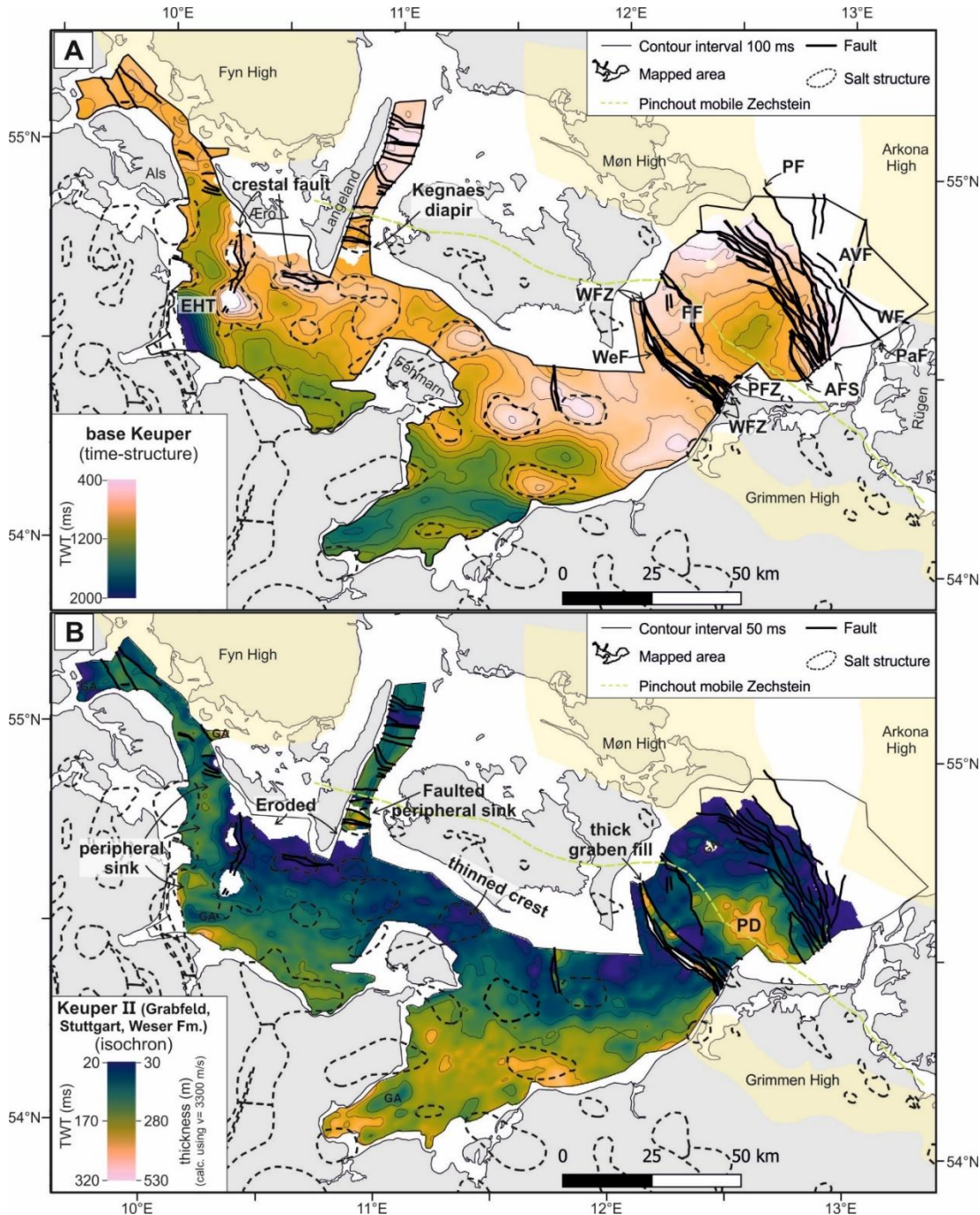


Figure 4.11: Keuper II (Grabfeld, Stuttgart and Weser formations). A: base Keuper time-structure map in TWT. B: Keuper II isochron map in TWT. Note the absence of Keuper II deposits adjacent to the islands of Æro and Langeland and northwest of Rügen due to erosion causing the Early Cimmerian Unconformity (ECU). AFS: Agricola Fault System; AVF: Agricola-Svedala Fault; PD: Perrow Depression; EHT: Eastholstein Trough; FF: Falster Fault; PaF: Parchim Fault; PF: Plantagenet Fault; PFZ: Perrow Fault Zone; WF: Wiek Fault; WeF: Werre Fault; WFZ: Werre Fault Zone. GA: Gridding artefact caused by lack of seismic data in the area or velocity distortions due to e.g. shallow gas.

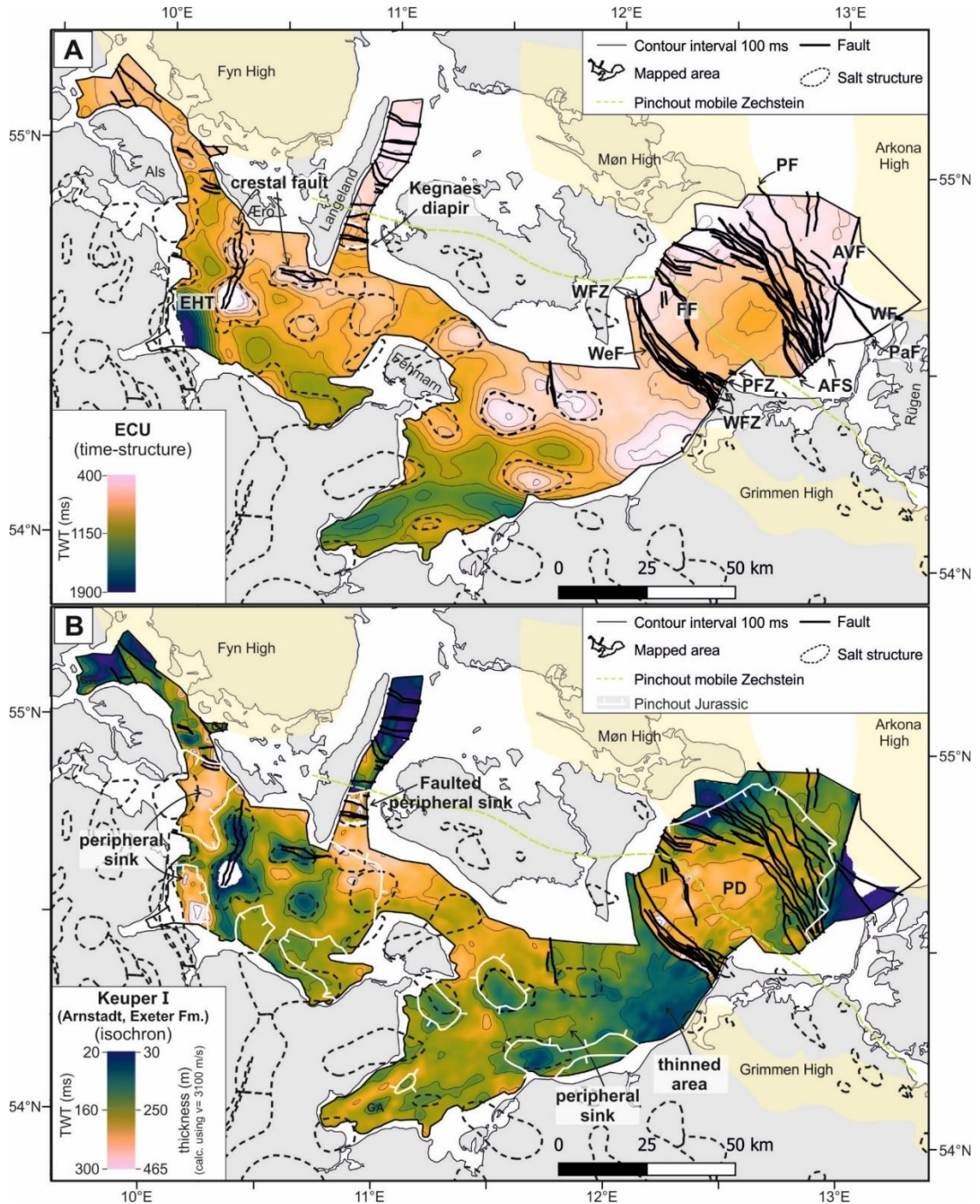


Figure 4.12: Keuper I (Arnstadt and Exeter formations). A: Early Cimmerian Unconformity (ECU) time-structure map in TWT. B: Keuper I isochron map in TWT. White line shows area of preserved Jurassic deposits, hence, where the Keuper I was spared from Mid Jurassic erosion. AFS: Agricola Fault System; AVF: Agricola-Svedala Fault; PD: Prerow Depression; EHT: Eastholstein Trough; FF: Falster Fault; PaF: Parchim Fault; PF: Plantagenet Fault; PFZ: Prerow Fault Zone; WF: Wiek Fault; WeF: Werre Fault; WFZ: Werre Fault Zone. GA: Gridding artefact caused by lack of seismic data in the area or velocity distortions due to e.g. shallow gas.

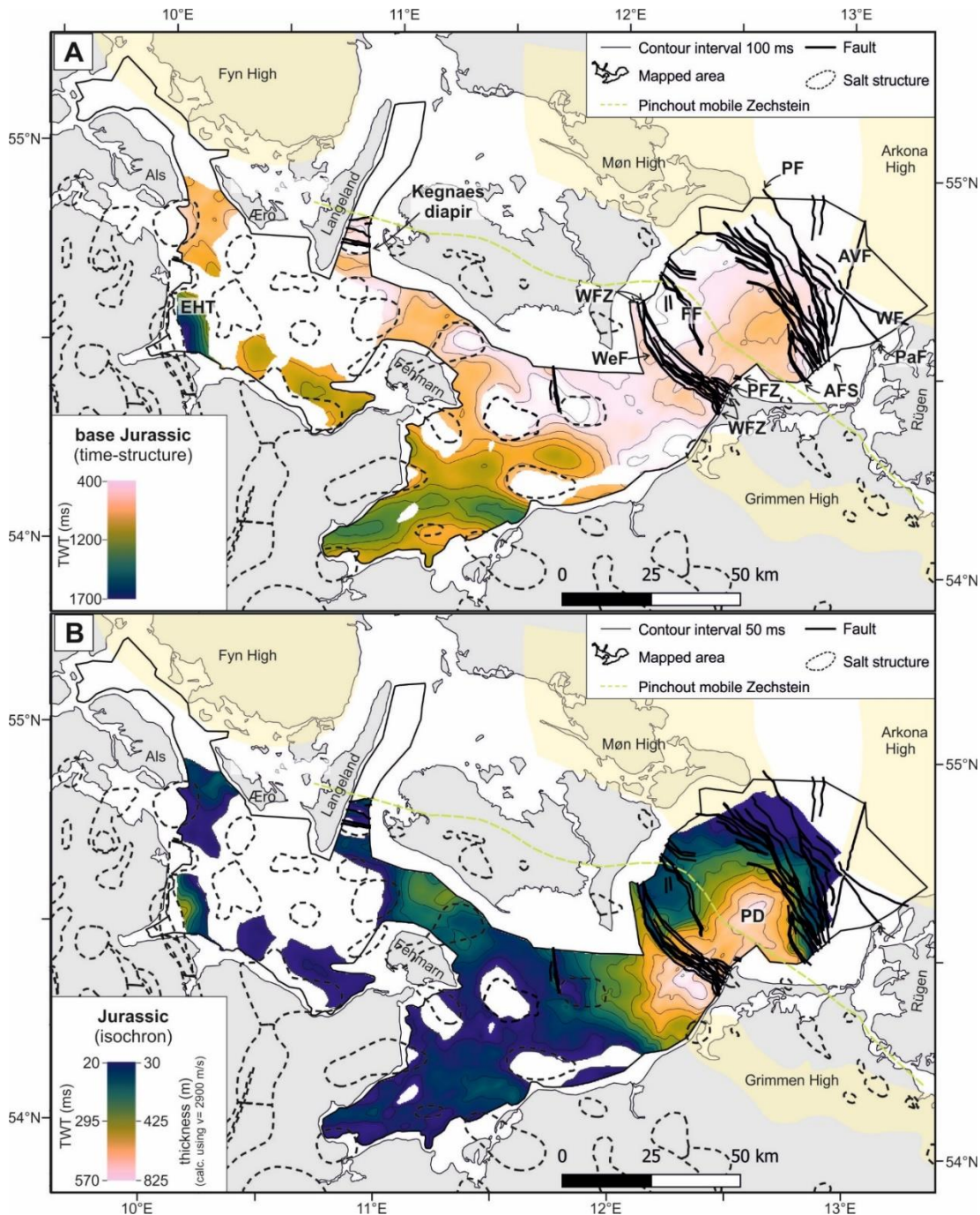


Figure 4.13: Jurassic. A: base Jurassic time-structure map in TWT. B: Jurassic isochron map in TWT. The entire Jurassic unit was affected by strong Mid Jurassic erosion and thus, mapped thickness only represent preserved remnants. AFS: Agricola Fault System; AVF: Agricola-Svedala Fault; PD: Prerow Depression; EHT: Eastholstein Trough; FF: Falster Fault; PaF: Parchim Fault; PF: Plantagenet Fault; PFZ: Prerow Fault Zone; WF: Wiek Fault; WeF: Werre Fault; WFZ: Werre Fault Zone. GA: Gridding artefact caused by lack of seismic data in the area or velocity distortions due to e.g. shallow gas.

4.5. Interpretation and Discussion

The south to southwest dip of the base Zechstein, pinch-out of the Zechstein unit at the northeastern basin margin and location of salt structures within the study area (Figs. 4.5 - 4.8) are in agreement with the overall known basin configuration (Peryt et al.,

2010). Our results revealed a new small salt structure east of the island of Als, which we accordingly named “Als Ost” (Figs. 4.5 and 4.8).

The trend of increasing thickness of the Buntsandstein and Muschelkalk towards the south-directed basin center without signs of salt movement (Figs. 4.9 and 4.10) is in accordance with previous studies and likewise explained by thermal subsidence from late Permian to Middle Triassic times (Baldschuhn et al., 2001; Kossow & Krawczyk, 2002; Hansen et al., 2005; Zöllner et al., 2008; Hübscher et al., 2010). Thereby, subsidence was highest in the basin center leading to increased sedimentary infill with Buntsandstein and Muschelkalk deposits (Scheck & Bayer, 1999; Van Wees et al., 2000). Local modifications of this trend could result from differential compaction, water level fluctuations and sedimentation processes (Figs. 4.9 and 4.10) (Betram & Milton, 1989). The Buntsandstein was mainly deposited in fluvial to lacustrine environments whereas in the Muschelkalk the deposition of clastics and carbonates in shallow marine conditions dominated (Bachmann & Kozur, 2004). Sequence stratigraphic studies showed climate controlled cyclic sedimentation for the Buntsandstein and eustatic and climatic control on the Muschelkalk deposition (e.g. Geluk & Röhlings, 1997; Franz et al., 2015). Besides imaging uncertainties, as discussed in chapter 4.3.4, locally different depositional conditions could have contributed to the development of the imaged local zones of increased or decreased thickness (some tens of meters), e.g. for the Buntsandstein in the central Bay of Mecklenburg or for the Muschelkalk northwest of Fehmarn (Figs. 4.9 and 4.10).

Mapping of the Keuper in this study shows the absence of the Keuper II unit northwest of the island of Rügen due to erosion related to the ECU (Figs. 4.11, 4.12). This is in accordance to previous studies (Beutler & Schüler, 1978; Bachmann et al., 2010). Adding to the existing maps (e.g. subcrop map of the ECU in Bachmann et al., 2010), we observe erosion of the entire lower and middle Keuper unit underlying the ECU south of the island of Aero, west of Langeland and south of the Kegnaes Diapir (Fig. 4.11). Hence, the area affected by Late Triassic erosion seems to stretch across the entire southern margin of the Ringkøbing-Fyn, Møn and Arkona highs, which fits to the observations of Clausen and Pedersen (1999) based on onshore seismic profiles and well data.

This study provides an update to the published fault pattern for the Baltic sector of the NGB and differentiates between subsalt and suprasalt faults (Figs. 4.8-4.13). For the offshore area west of Rügen Island, the fault traces of the fault systems of the Western Pomeranian Fault System (Wiek Fault, Parchim Fault, Plantagenet Fault, Agricola Fault System, Prerow Fault Zone, Were Fault Zone) are generally in agreement with published maps of the area (Schlüter et al., 1997; Hübscher et al., 2010; Al Hseinat & Hübscher, 2017; Deutschmann et al., 2018). However, for some faults, we interpreted slightly different location and strike of the faults. This study provides an update of the strike and internal character of the Were Fault Zone (Figs. 4.8 - 4.13). The Were Fault Zone is characterized by the NE dipping main Were Fault and several antithetic faults. In the southeast, the main Were Fault forms a NE dipping rollover like structure (Deutschmann et al., 2018; Ahlrichs et al., 2020), whereas in the northwest, the

rollover structure dips southwest along the northeasternmost fault of the Werre Fault Zone as shown in the profile in Fig. 4.7b. Northwest of the Grimmen High, we identified subsalt faults with partly small offsets at the base Zechstein. These faults likely form the offshore prolongation of faults visible in the TUNB model onshore Mecklenburg-Western Pomerania (TUNB Working Group, 2021). In the northern Bay of Mecklenburg, suprasalt faults mark the southern prolongation of NW-SE striking faults in Denmark (Figs. 4.9 - 4.13) (Vejbaek, 1997). Northwest of Fehmarn Island, our maps show a subsalt fault (Fig. 4.8), which coincides with a fault mapped by Vejbaek (1997) and which was imaged on a seismic profile published by Ahlrichs et al. (2021a) (see their Fig. 5). Furthermore, our fault analysis shows a prominent basement fault in the western Bay of Kiel, which we interpret as the eastern border fault of the Eastholstein Trough (Fig. 4.5 and 4.8). The fault trace coincides with maps of Vejbaek (1997) and was imaged by Ahlrichs et al. (2021a) (their Fig. 5). The salt structures “Kieler Bucht” and “Schönberg” strike parallel to the fault and are located directly adjacent to it. Salt structures, which are underlain by basement faults are common in many parts of the Glückstadt Graben (e.g. Baldschuhn et al., 2001; Maystrenko et al., 2005b). Hence, the Baltic part of the eastern Glückstadt Graben represents another example of salt structure growth controlled by basement detached extension originating from an underlying basement fault (e.g. Jackson & Hudec, 2017).

4.5.1. Timing of salt movement

In the literature, a triggering of salt movement in the Baltic sector of the North German Basin driven by extension during the Late Triassic is well established (Clausen & Pedersen, 1999; Hansen et al., 2005; Hansen et al., 2007; Zöllner et al., 2008; Hübscher et al., 2010; Al Hseinat et al., 2016). Using a single seismic profile located in the Bay of Mecklenburg, Ahlrichs et al. (2020) established a refined stratigraphic subdivision of the Triassic, which revealed initial salt movement during deposition of the Keuper II unit (Grabfeld, Stuttgart, Weser formations). This study provides regional maps of the Buntsandstein, Muschelkalk, Keuper and Jurassic units with the refined stratigraphic subdivision established by Ahlrichs et al. (2020) to analyze the spatial character of salt movement in the Baltic sector of the North German Basin.

4.5.1.1. Eastholstein Trough

The Buntsandstein and Muschelkalk units do not show local thickness variations and thus, were deposited prior to the development of the salt structures (Figs. 4.9 and 4.10). This prekinematic phase during the early and middle Triassic in the eastern Glückstadt Graben is in agreement with previous onshore and offshore studies (Hansen et al., 2005; Maystrenko et al., 2005b; Al Hseinat et al., 2016; Warsitzka et al., 2016). Local thickness variations of the Keuper II unit, comprising the Grabfeld, Stuttgart and Weser formations, indicate initial salt movement in the Eastholstein Trough (Fig.

4.11). This is in agreement with previous studies covering the Glückstadt Graben and northwest Germany, where discrete pulses of extension and salt movement were observed in the early Late Triassic during deposition of the Grabfeld and Weser formations (Frisch & Kockel, 1999; Kockel, 2002; Maystrenko et al., 2005b; Al Hseinat et al., 2016). Salt movement continued during deposition of the Keuper I unit (Arnstadt and Exeter formations) in the Eastholstein Trough (Fig. 4.12), even though extension abated (Frisch & Kockel, 1999). We explain the ongoing salt withdrawal and corresponding salt structure growth by differential loading induced by the foregone extensionally triggered salt flow. Jurassic sediments were strongly affected by erosion related to the Mid Jurassic Doming event. Thus, the present day thickness represents the thickness of the remnants preserved from erosion and cannot be used directly to infer active salt flow. Preserved Jurassic deposits have increased thickness within the Eastholstein Trough (Fig. 4.13). However, this only evidences salt movement prior to erosion (without prior salt movement, Jurassic and Keuper deposits would be horizontally deposited without local thickness variations). Whether the increased thickness of Jurassic deposits in rim-synclines is solely an effect of salt movement during the Late Triassic or by Late Triassic and Jurassic salt movement cannot be distinguished from the sedimentary record. Maystrenko et al. (2005b) interpreted a Jurassic pulse of salt movement, which temporally correlated with extension in the Lower Saxony Basin. Sedimentation in the Glückstadt Graben during the Late Triassic was relatively high (Bachmann et al., 2008), so assuming that sedimentation during deposition of the Keuper in the Eastholstein Trough exceeded or matched the accommodation space created by deepening of the rim-synclines, we can expect that the peripheral sinks of the Keuper unit were completely synkinematically filled (Fig. 4.14a). Jurassic deposition without salt movement would then yield horizontally layered strata affected by later erosion. Then we would expect that the present-day remnants show no major local thickness variations (Fig. 4.14a). Therefore, the preserved Jurassic depositional pattern indicates ongoing salt movement in the early Jurassic prior to erosion (Fig. 4.14b).

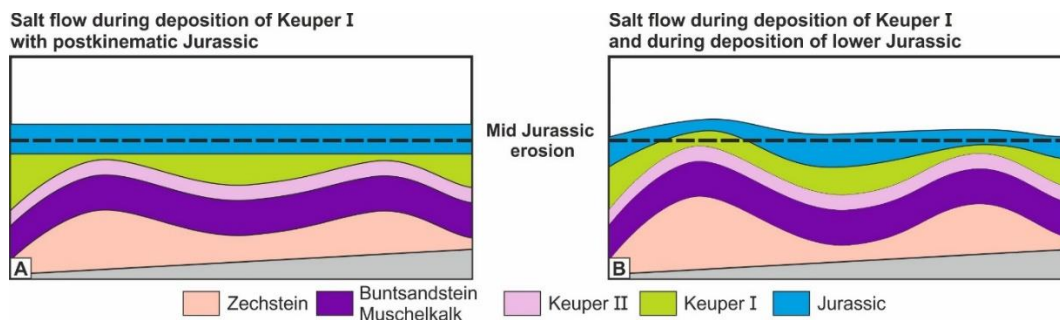


Figure 4.14: Conceptual model assuming high sedimentation rate and syndepositional salt flow during deposition of the Keuper I followed by postkinematic deposition of the Lower Jurassic (A) and with ongoing salt movement in the early Jurassic (B). Model is based on the assumption that a high sedimentation rate during deposition of the Keuper I exceeded salt rise and thus, the rim-synclines are completely filled with Keuper sediments. Black dashed line represents erosional surface due to the Mid Jurassic North Sea Doming event.

4.5.1.2. Eastholstein-Mecklenburg Block

Thickness variations of the Buntsandstein and Muschelkalk within the Eastholstein-Mecklenburg Block (EHMB) do not correlate with the salt structures indicating their prekinematic deposition, which is in agreement with previous studies (Hansen et al., 2007; Zöllner et al., 2008; Hübscher et al., 2010; Ahlrichs et al., 2020). Within the EHMB, local thickness variations of the Keuper II unit hardly correlate with the salt structures (Fig. 4.11). The crest of the “Fehmarn” salt pillow is slightly thinned, which could indicate the onset of minor salt movement. Overall, the Keuper II thickness within the EHMB shows the general thickening trend towards the south. During this time, salt movement seems to be restricted to the Eastholstein Trough, Kegnaes Diapir and Werre Fault Zone, whereas the salt structures of the EHMB remained quiet. In much parts of the Bay of Kiel and above the crests of most salt structures, the top of the Keuper I unit is eroded due to the North Sea Doming event. Thus, thickness variations of the Keuper I unit cannot be directly attributed to salt movement where the overlying Jurassic is completely missing (white line in Fig. 4.12). Jurassic deposits are preserved in large parts of the Bay of Mecklenburg and are only absent above the crest of salt structures. Northeast of the salt pillow “Trollegrund Nord”, increased thickness of the Keuper I unit and slightly divergent reflector suggests the beginning of salt movement and development of a small peripheral sink (Fig. 4.12) (Ahlrichs et al., 2020). The Jurassic in the EHMB is strongly affected by erosion and thicker remnants are preserved in rim-synclines of salt structures (Fig. 4.13). In the absence of salt movement, we would expect Jurassic and Keuper I deposits to be horizontally layered without local thickness variations (Fig. 4.14a). Therefore, the pattern of erosion above the crest of salt structures and increased thickness of preserved remnants for the Keuper I (mostly Bay of Kiel) and Jurassic units, evidences salt movement prior to erosion (Fig. 4.14). Based on the only minor indications for salt movement during deposition of the Keuper I in the Bay of Mecklenburg, we suppose that early Jurassic salt movement dominated in the EHMB. Hence, the onset of salt movement in the EHMB was considerably later than in the surrounding areas (Glückstadt Graben and northeastern basin margin). Therefore, the EHMB acted as a more stable transition zone between the Glückstadt Graben and Tornquist controlled Western Pomeranian Fault System west of Rügen Island.

4.5.1.3. Kegnaes Diapir

The here proposed development of the Kegnaes Diapir is sketched in Fig. 4.6d. Our seismic profile suggests first tectonic activity and salt movement already during deposition of the Buntsandstein. Above the northern rim-syncline, the Buntsandstein shows divergent reflectors suggesting initial suprasalt faulting and salt movement (Fig. 4.6c). This contradicts the within the study area generally accepted concept of thermal subsidence in relatively quiet tectonic conditions, where apart from the central Glückstadt Graben, the salt did not move before the Late Triassic (e.g. Brink et al., 1992; Maystrenko et al., 2005b; Hansen et al., 2007; Hübscher et al., 2010; Warsitzka et al.,

2016). A visible increase in thickness of the Lower Triassic above the northern rim-syncline of the Kegnaes Diapir shown by Bialas et al. (1990) further supports our observations of salt movement during the Buntsandstein. Additionally, the reduced thickness of the Buntsandstein above the hangingwall of the basement faults suggests active tectonics during this time (Fig. 4.6c). Faulting along the two basement step faults during deposition of the Buntsandstein could have triggered salt withdrawal from the northern rim-syncline and suprasalt faulting (Fig. 4.6d – no. 2). Uplift of the footwall by a flexural cantilever model could explain the reduced thickness of the Buntsandstein (Fig. 4.6d – no. 2) (Kusznir & Ziegler, 1992). The location of the basement step faults north of the Kegnaes Diapir coincides with two NW-SE striking top pre-Zechstein faults visible in fault maps of Vejbaek (1997), which formed during Late Carboniferous – early Permian transtension (Fig. 4.1) (Thybo, 1997). Pre-Quaternary maps of Denmark show WNW-ESE striking faults crossing the Lolland Island (Hakansson & Pedersen, 1992). These faults appear roughly parallel to the basin margin. During deposition of the Buntsandstein, the central parts of the basin experienced higher subsidence while the basin margins, where the Kegnaes Diapir is located, were less subsided. Stress induced by this differential subsidence could explain a reactivation of the Late Carboniferous – early Permian faults at the basin margin during the early Triassic. The velocity pull-up directly below the diapir masks the base Zechstein in this area and thus, a basement fault directly below the diapir as interpreted by Bialas et al. (1990) cannot be confirmed by our profile (Fig. 4.6). The Muschelkalk deposits show a relatively constant thickness, which suggests that the tectonic activity abated and salt movement ceased (Fig. 4.6b and d – no. 3). During deposition of the Keuper II unit, salt movement restarted indicated by the thick accumulation of Keuper II sediments north of the diapir (Fig. 4.6b). This time marks the major phase of salt structure growth during the pillow stage of the Kegnaes salt structure, which occurred under approx. E-W regional extension (Maystrenko et al., 2005b). Thereby, extension likely thinned the overburden of the Kegnaes salt structure (Fig. 5.6d – no. 4).

At the flanks of the present diapir, the Keuper II terminates in a toplap against the ECU reflector suggesting that erosion related to the ECU further affected the roof of the Kegnaes salt structure (Fig. 4.6b and d - no. 5). Thus, we interpret the ECU as the unroofing unconformity, which allowed piercing of the overburden and the transition to diapiric growth. The appearance of the Triassic successions south of the Kegnaes Diapir is very similar to the DSW diapir located in the Inez sub-basin within the Norwegian-Danish Basin (Sørensen, 1998), supporting a similar development of the two structures. Salt movement continued during deposition of the Keuper I unit with passive diapirism and faulting within the overburden of the northern rim-syncline (Fig. 4.6d – no. 6). Preserved Jurassic deposits are restricted to the overburden above the rim-synclines north and south of the diapir (Fig. 4.6). Following the same argumentation for the Jurassic as described in chapter 4.5.1.1, we interpret the preservation of Jurassic deposits in the rim-synclines of the Kegnaes Diapir as a sign of ongoing salt movement during the early Jurassic at least prior to Mid Jurassic erosion (Fig. 4.14). The Cenomanian to Santonian units do not show signs of salt movement, which is in accordance to findings from other salt structures in the study area (Ahlrichs et al., 2021a). The narrow waist of the Kegnaes Diapir suggests that the diapir was mildly

squeezed (e.g. Callot et al., 2012). This likely occurred during Late Cretaceous inversion and is known from many other salt structures in the NGB (e.g. Kockel, 2003).

Based on the here proposed structural evolution of the Kegnaes Diapir, the development of salt diapirs at the northern basin margin was only possible due to the reduced overburden thickness and significant Late Triassic erosion. The diapiric breakthrough by erosional unroofing explains the isolated location of the Kegnaes Diapir and possibly of the other three diapirs onshore Lolland, while the absence of major Late Triassic erosion and increased overburden thickness of the salt structures located within the Bays of Kiel and Mecklenburg did not allow diapirism. Such erosional initiation of diapirism is known from other parts of the Southern Permian Basin, such as the southern North Sea (Stewart & Coward, 1995).

4.5.2. Faulting at the northeastern basin margin

Between the Werre Fault Zone and Agricola Fault Zone, mapping of the Zechstein unit shows a local depression of the base Zechstein (Fig. 4.8a), whose location coincides with a zone of increased thickness of the Buntsandstein, Keuper and Jurassic successions (Figs. 4.8, 4.9, 4.11, 4.12 and 4.13). Noticeably, this zone of increased thickness is not visible in the Muschelkalk (Fig. 4.10). The presence of this zone of increased thickness is well known in the literature (Buntsandstein: Scheck & Bayer, 1999; Keuper and Jurassic: Hansen et al., 2007; Hübscher et al., 2010; Deutschmann et al., 2018, the latter named this zone “Prerow Depression” (PD)). Our maps with refined stratigraphic subdivision show that the onset of faulting in the Werre Fault Zone began in the Late Triassic during deposition of the Keuper II unit (Grabfeld, Stuttgart, Weser Fm.) (Fig. 4.11). Faulting in the Agricola Fault System began contemporaneously (Ahlrichs et al., 2020). In between the Werre Fault Zone and Agricola Fault System, the PD forms a narrow NW-SE elongated zone, which is approx. parallel to the basin margin and Agricola Fault System (Fig. 4.11). This indicates increased subsidence of the PD forming a local depocenter in the Late Triassic bound by the Agricola Fault System in the northeast and by the Werre Fault Zone in the southwest (Fig. 4.11) (Deutschmann et al., 2018; Ahlrichs et al., 2020). The onset of faulting was coeval with faulting in other regions of the Western Pomeranian Fault System, where initial faulting occurred during deposition of the Grabfeld Formation (Krauss & Mayer, 2004; Beutler et al., 2012), and with E-W extension in the Glückstadt Graben (Figs. 4.7 and 4.11) (Maystrenko et al., 2005b). Late Triassic faulting within the Western Pomeranian Fault System is attributed to the reactivation of Middle Devonian-Early Carboniferous faults by NW-SE dextral strike slip and NE-SW transtensional movements within the Trans-European Suture Zone (Erlström et al., 1997; Krauss & Mayer, 2004; Seidel et al., 2018). Active faulting in the Werre Fault Zone and Agricola Fault System persisted during deposition of the Keuper I unit (Fig. 4.12) (Ahlrichs et al., 2020). In this unit, the PD became wider and included the entire area between the Werre Fault Zone and Agricola Fault System, which suggests ongoing subsidence (Fig. 4.12). Faults of the Werre Fault Zone and Agricola Fault System remained active in the Jurassic (Hübscher

et al., 2010; Ahlrichs et al., 2020). The Jurassic deposits show a different pattern with a NE-SW elongated zone of increased thickness, which further broadened and additionally included the area southwest of the Werre Fault Zone (Fig. 4.13). This indicates that the area continued to subside.

A possible explanation for the development of the PD would be rotational block faulting along deep-seated Paleozoic faults, which were reactivated in the Triassic and early Jurassic. These deep-seated faults have listric character and are detached near the Paleozoic basement (Krawczyk et al., 2002). During fault reactivation, the subsiding hangingwalls possibly rotated creating locally increased subsidence at the basin margin (Ahlrichs et al., 2020). However, the depositional pattern of the Keuper II unit shown in this study contradicts this explanation. Although, the elongated zone of increased thickness of the Keuper II is parallel to the basin margin, the local depocenter is located in the center between the Werre Fault Zone and Agricola Fault System and not directly adjacent to the basin marginal faults of the Agricola Fault System, where we would expect the maximum subsidence of the hangingwalls (Fig. 4.11). The depositional pattern of the Keuper units fits better to the development of a local transtensional sub-basin, bordered by the Agricola Fault System and Werre Fault Zone. The transtensional basin started as a narrow zone during deposition of the Keuper II unit (Fig. 4.11) and subsequently became wider during ongoing transtensional faulting in latest Triassic and early Jurassic times (Fig. 4.12 and 4.13). Interestingly, the location of the Keuper II depocenter within the PD correlates with the pinch-out of mobile Zechstein units (Fig. 4.11). This could indicate that extensional stress localized here as it could no longer be transferred within the detachment horizon, similar to the model suggested by Krawczyk et al. (2002). The PD is part of a NW-SE oriented transtensional shear zone centered around Rügen Island (Deutschmann et al., 2018; Seidel et al., 2018). During the Triassic – Early Cretaceous, this area was affected by NW-SE dextral transtensional movements, which led to the development of a series of NW-SE to NNW-SSE striking fault systems within the Mesozoic succession, known as the Western Pomeranian Fault System (WPFS) (Krauss & Mayer, 2004). In the southeastern part of the WPFS, numerous en echelon faults formed in between the major fault zones. The Agricola Fault System and Werre Fault Zone mark the northwestern prolongation of the WPFS (Krauss & Mayer, 2004). Contrary to the southeastern part, en echelon faults are absent and it seems that shearing was restricted to the faults of the bordering fault systems, while the area in between subsided without being further faulted (Figs. 4.11 – 4.13). This could be related to the northwestward widening of the Tornquist Fan and thus, wider distribution of shear stress in the northwestern part of the WPFS than in the southeast (e.g. Thybo, 1997; Seidel et al., 2018). A connection of the PD system to deeper Paleozoic structures is evident by the reactivation of the deep-rooted northern bordering faults of the Agricola Fault System. The southwestern border has a different character, as the Werre Fault Zone is a thin-skinned fault system decoupled by the Zechstein. An influence from deep-rooted structures seems likely but needs further investigations by improved subsalt imaging in the area. Furthermore, the visible local depression of the base Zechstein below the PD suggests a connection to underlying Paleozoic structures (Fig. 4.8). Whether the locally increased thickness of the Buntsandstein indicates an earlier

fault reactivation or early minor salt movement at the basin margin remains unclear (Fig. 4.9).

4.6. Conclusions

This study presents high-resolution 2D seismic profiles together with regional time-structure and isochron maps of the Baltic sector of the North German Basin in order to analyze the Triassic to Jurassic structural evolution of the region. Stratigraphic interpretation incorporates well information from research and hydrocarbon wells in the study area and was linked to previous studies. Presented time-structure and isochron maps of the Zechstein, Buntsandstein, Muschelkalk, Keuper II (Grabfeld, Stuttgart, Weser Formations), Keuper I (Arnstadt, Exeter Formations) and Jurassic are created from a dense network of high-resolution 2D seismic data. Mapping of the Zechstein unit revealed a previously unknown small salt structure east of Als Island, which we named “Als Ost”. The fault pattern of the study area is updated including a differentiation between subsalt and suprasalt faults. The refined stratigraphic subdivision of the Keuper allowed a more precise analysis of episodes of increased tectonic activity in the pre-inversion phase of the North German Basin. The main conclusions are:

- We explain the development of salt diapirs at the northern basin margin based on the development of the Kegnaes Diapir by growth of a salt pillow, which reached the diapiric breakthrough by erosional unroofing during the Late Triassic. Thereby, the Kegnaes Diapir could only pierce the overburden because of its location close to the basin margin, and thus reduced overburden thickness when compared to other salt structures closer to the basin center, and Late Triassic erosion affecting the northern basin margin.
- At the northern basin margin, we observed first indications for salt movement and faulting at the Kegnaes Diapir already during deposition of the Buntsandstein. This is in contrast to common observations from other salt structures in the study area, where the Buntsandstein and Muschelkalk were deposited prior to salt movement and salt structure growth did not start before the Late Triassic. Accordingly, the concept of relatively quiet tectonic conditions characterized by thermal subsidence during the Early and Middle Triassic would have to be expanded.
- Tectonic activity strongly increased in the Late Triassic during deposition of the Keuper II unit (Grabfeld, Stuttgart, Weser Formations). Tectonic activity includes the onset of salt movement in the northeastern Glückstadt Graben, major salt movement at the Kegnaes Diapir (pillow stage), faulting at the northeastern basin margin (Werre Fault Zone, Agricola Fault System) and corresponding development of the Prerow Depression. The onset of tectonic activity occurred under regional approx. E-W directed extension.
- During deposition of the Keuper I (Arnstadt and Exeter Formations) and Lower Jurassic units, salt movement continued in the northeastern Glückstadt Graben and at the Kegnaes Diapir, which reached the diapir stage by erosional

unroofing. The Early Cimmerian Unconformity marks the unroofing unconformity of the Kegnaes Diapir. Faulting at the Werre Fault Zone and Agricola Fault System persisted and the local depocenter in between (Prerow Depression) became wider.

- In the Triassic, the Eastholstein-Mecklenburg Block formed a more stable area at the transition between the Glückstadt Graben and the fault systems of the northeastern basin margin. Major faulting is absent and salt movement started only in the latest Triassic with its dominant phase presumably in the early Jurassic.
- We interpreted the thick accumulation of Keuper and Jurassic deposits west of Rügen (Prerow Depression) as a transtensional sub-basin, bordered by the Agricola Fault System and the Werre Fault Zone. The sub-basin forms the northwestern prolongation of the Western Pomeranian Fault System and is connected to deeper Paleozoic structures. In this area, Late Triassic extension induced transtensional movements by a reactivation of deep-seated Paleozoic faults at the northeastern basin margin. This caused increased subsidence of the Prerow Depression and corresponding accumulation of Keuper and Jurassic deposits.

Acknowledgements

We kindly acknowledge ExxonMobil Production Deutschland GmbH for providing the industry seismic profiles and for the permission to publish the interpreted seismic profiles. We thank Emerson for providing licenses of their software under the Paradigm University Research Program. This work is part of the *StrucFlow* project and is a research and development study connected to the TUNB project by the Federal Institute of Geosciences and Natural Resources (BGR) and the geological surveys of the northern German federal states. The used scientific colourmap *batlow* prevents visual distortion and exclusion of readers with colour vision deficiencies (Crameri et al., 2020).

Gefördert durch die Deutsche Forschungsgemeinschaft (DFG) - 396852626/funded by the Deutsche Forschungsgemeinschaft (DFG, German Research Foundation) - 396852626

5. Impact of Late Cretaceous inversion and Cenozoic extension on salt structure growth in the Baltic sector of the North German Basin

Abstract

The Late Cretaceous to Cenozoic is known for its multiple inversion events, which affected Central Europe's intracontinental sedimentary basins. Based on a 2D seismic profile network imaging the basin fill without gaps from the base Zechstein to the seafloor, we investigate the nature and impact of these inversion events on Zechstein salt structures in the Baltic sector of the North German Basin. These insights improve the understanding of salt structure evolution in the region and are of interest for any type of subsurface usage. We link stratigraphic interpretation to previous studies and nearby wells and present key seismic depth sections and thickness maps with a new stratigraphic subdivision for the Upper Cretaceous and Cenozoic covering the eastern Glückstadt Graben and the Bays of Kiel and Mecklenburg. Time-depth conversion is based on velocity information derived from refraction traveltime tomography. Our results show that minor salt movement in the eastern Glückstadt Graben and in the Bay of Mecklenburg started contemporaneous with Late Cretaceous inversion in the Coniacian-Santonian. Minor salt movement continued until the end of the Late Cretaceous. Overlying upper Paleocene and lower Eocene deposits show constant thickness without indications for salt movement suggesting a phase of tectonic quiescence from the late Paleocene to middle Eocene. In the late Eocene to Oligocene, major salt movement recommenced in the eastern Glückstadt Graben. In the Bays of Kiel and Mecklenburg, late Neogene uplift removed much of the Eocene-Miocene succession. Preserved deposits indicate major post-middle Eocene salt movement, which likely occurred coeval with the revived activity in the Glückstadt Graben. Cenozoic salt structure growth critically exceeded salt flow during Late Cretaceous inversion. Cenozoic salt movement could have been triggered by Alpine/Pyrenean-controlled thin-skinned compression, but is more likely controlled by thin-skinned extension, possibly related to the beginning development of the European Cenozoic Rift System.

5.1. Introduction

The inversion of the Permian intracontinental sedimentary basins in Central Europe and its controlling processes have been studied for about 100 years. (e.g. Lamplugh, 1919; Schuh, 1922a; b; c; Voigt, 1962; Ziegler, 1987; Kockel, 2003; Kley & Voigt, 2008; Doornenbal & Stevenson, 2010; Kley, 2018). Intraplate compressional stress, often transmitted over large distance, can invert former extensional sedimentary

basins by compressional reactivation of their fault systems and uplift and folding of the basin fill and basin floor (Ziegler et al., 1995; Brun & Nalpas, 1996; Krzywiec, 2006). The term “basin inversion” refers to a change from subsidence to uplift in a basin controlled by a fault system due to a change in the tectonic regime from extension to shortening (Cooper & Williams, 1989). A mobile salt layer present at the basin floor may decouple the suprasalt sedimentary overburden from subsalt basement deformation, which influences the structural style of both extensional and compressional deformation within the overburden (e.g. Letouzey et al., 1995; Withjack & Callaway, 2000). During basin inversion, preexisting salt structures are preferentially reactivated as halite is weaker than the other laterally adjacent sedimentary rocks. Thereby, even shortening exerted during the earliest stages of basin inversion can remobilize the salt by squeezing the salt structures and arching their roofs (Mohr et al., 2005; Rowan & Vendeville, 2006; Callot et al., 2012; Jackson & Hudec, 2017).

Multiphase uplift and inversion pulses affected the North German Basin (NGB) and other sub-basins of the large intracontinental Southern Permian Basin (Fig. 5.1). After a long-lasting tectonic period of thermal subsidence and extensional deformation since the Carboniferous, shortening and inversion followed from Late Cretaceous times onwards (e.g. Ziegler et al., 1995; Maystrenko et al., 2008). Past publications often considered four major distinct inversion events throughout the history of the Southern Permian Basin. These uplift and inversion events are commonly associated to compressional intraplate stress transmitted within the European foreland during Africa-Iberia-Europe convergence and subsequent Alpine and Pyrenean orogenies (Ziegler et al., 1995; Vejbaek & Andersen, 2002; de Jager, 2003; Kockel, 2003; Krzywiec, 2006; Kley & Voigt, 2008). The first event in the Late Cretaceous (Subhercynian, between 90 and 70 Ma) is widely accepted and has been investigated in most parts of the Southern Permian Basin (e.g. Ziegler et al., 1995; Kley, 2018). Compressional stress during this event induced significant shortening of the basement and caused basin-scale uplift, erosion, large reverse movements along basin-bounding faults and thin-skinned folding of Mesozoic strata detached along the salt layers (Ziegler et al., 1995; de Jager, 2003; Kockel, 2003; Kley & Voigt, 2008; Kley, 2018). The second event occurred in the late Paleocene (Laramide, around 60 Ma) and acted strongest in most Dutch basins. This event is characterized by a widespread unconformity associated to large-scale domal uplift in Central Europe (Ziegler et al., 1995; de Jager, 2003; Deckers & van der Voet, 2018). However, recent studies doubt that far-field effects originating from Africa-Iberia-Adria-Europe convergence caused the unconformity. Instead, these studies suggested sea level fluctuations (Kockel, 2003) or thinning of the mantle lithosphere and dynamic topography driven by mantle plumes as a possible cause of the unconformity (Kley, 2018; von Eynatten et al., 2021). Following inversion pulses in the late Eocene to Oligocene (Pyrenean, 40-30 Ma) and late Oligocene to Miocene (Savian, 30-20 Ma) are documented for the southern North Sea and west of it (Ziegler et al., 1995; Kley, 2018). However, lacking timing constraints hamper a precise separation of the two events in many areas (Kley, 2018).

The terms to distinguish Late Cretaceous to Cenozoic inversion events (“Subhercynian”, “Laramide”, “Pyrenean”, “Savian”) are named after regions, whose context to inversion in Central Europe is partly misleading (e.g. Laramie mountains in North

America, the river Save in Slovenia). However, these inversion events can also be temporally distinguished (e.g. de Jager, 2003; Doornenbal & Stevenson, 2010). Therefore, we refer to the individual inversion events (“Subhercynian”, “Laramide”, “Pyrenean”, “Savian”) discussed in the following based upon the geological time when they occurred (Late Cretaceous, late Paleocene, late Eocene- Oligocene, late Oligocene - Miocene).

The dating of basin inversion is challenging where corresponding uplift and following erosion partly removed the sedimentary record obliterating parts of its inversion history. According to Warsitzka et al. (2019), regions affected by mild inversion and thin-skinned shortening can be identified by the analysis of salt structures and the reactivation of salt flow. Krzywiec (2006) analyzed peripheral salt structures in the Mid Polish Trough (MPT) and showed that peripheral salt structures respond readily to regional shortening by revived growth even during the early stages of basin inversion. In contrast to many other areas in the North German Basin (NGB), the Baltic sector of the NGB contains a relatively complete Cretaceous and Cenozoic sedimentary record. Our study area covers the peripheral region of the NGB and contains numerous salt structures, which formed prior to inversion (Fig. 5.1) (e.g. Hansen et al., 2007; Hübscher et al., 2010). Thus, the Baltic sector of the NGB is an ideal site to identify active phases of Late Cretaceous to Cenozoic inversion and analyze their impact on the sedimentary record.

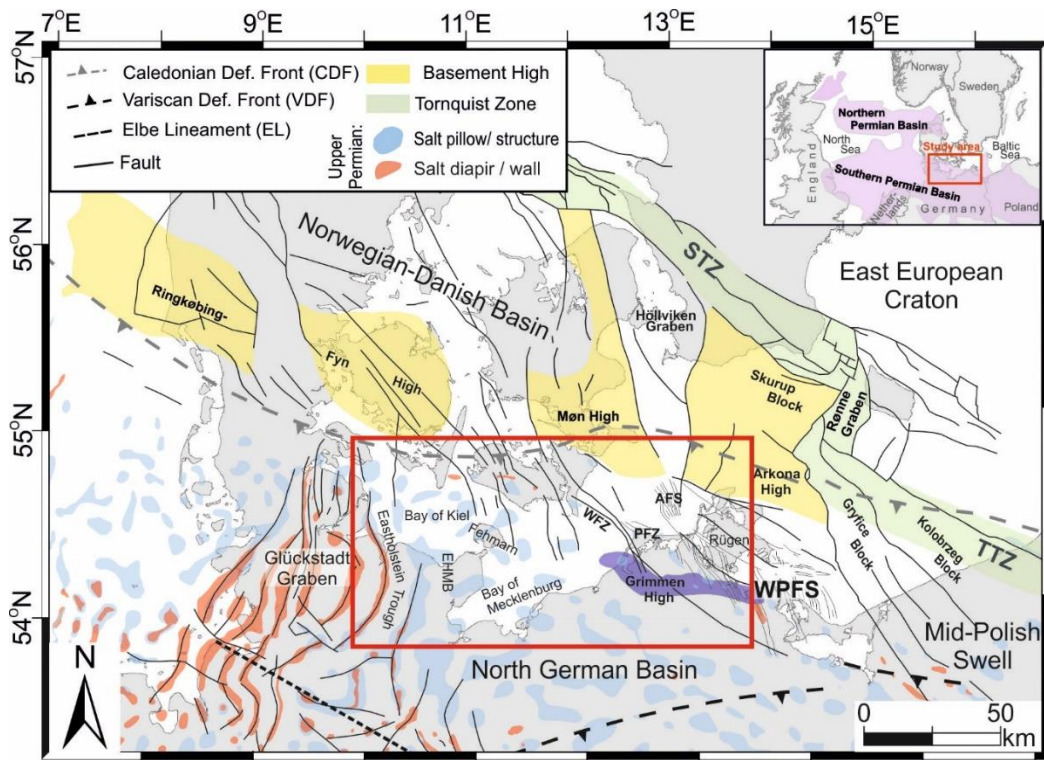


Figure 5.1: Structural elements of the northern North German Basin (modified after Ahlrichs et al., 2020). Inset shows approximate outline of the northern and southern Permian Basin. Red box marks the study area. Salt structures after Vejbaek, 1997; Dadlez & Marek, 1998; Reinhold et al., 2008; Warsitzka et al. (2019). AFS: Agricola Fault System; EHMB: Eastholstein-Mecklenburg Block; PFZ: Prerow Fault Zone; STZ: Sorgenfrei-Tornquist Zone; TTZ: Teisseyre-Tornquist Zone; WFZ: Werre Fault Zone; WPFS: Western Pomeranian Fault System.

Previous studies analyzed salt structure evolution in the Baltic sector of the NGB as a function of the regional tectonic framework by means of seismic imaging and regional mapping (Kossov & Krawczyk, 2002; Hansen et al., 2005; Hansen et al., 2007; Zöllner et al., 2008; Hübscher et al., 2010; Al Hseinat & Hübscher, 2014; Al Hseinat et al., 2016; Al Hseinat & Hübscher, 2017). These authors identified four major post-Permian tectonic phases affecting salt structure evolution: (1) Late Triassic – Early Jurassic extension triggered salt movement. (2) A phase of uplift and erosion related to the North Sea Doming event followed from Middle Jurassic to Early Cretaceous times. (3) Sedimentation resumed towards the end of the Early Cretaceous and the study area experienced a phase of relative tectonic quiescence without salt movement in the Late Cretaceous. (4) At the Late Cretaceous to Cenozoic transition, shortening induced by the onset of Africa-Iberia-Europe convergence lead to basin inversion and reactivated salt flow. However, these studies lack a detailed stratigraphic subdivision to date the onset of basin inversion and to identify individual inversion events. In a local study analyzing a crestal graben above a salt wall of the eastern Glückstadt Graben, Huster et al. (2020) used a refined Cenozoic stratigraphy to identify Paleogene and Neogene fault reactivation, which the authors associated with compressional stress induced by the Alpine and Pyrenean orogenies. In the most recent study, Ahlrichs et al. (2020) used a regional seismic transect from the “BalTec” expedition (Hübscher et al., 2016). The acquisition parameters of the “BalTec” survey allowed to overcome problems of shallow water, low vertical resolution, stretch mute effects caused by large source to receiver distances and sparse well data. As a result, the authors presented a high-resolution gapless seismic image from the base of the Zechstein salt to the seafloor and derived a detailed seismostratigraphic concept for the northeastern NGB margin, which allowed specification of the onset of Late Cretaceous inversion to the Coniacian-Santonian.

In this study, we integrate the “BalTec” database with other 2D seismic surveys from the study area to refine the seismostratigraphy of the Upper Cretaceous and Cenozoic. We present a key two-way traveltime seismic section from the Eastholstein Trough and three key seismic depth sections with an unprecedented a level of vertical resolution for the study area. We focus on mapping of the Upper Cretaceous and Cenozoic reflectors to investigate salt movement during Late Cretaceous to Cenozoic basin inversion. By using refraction traveltime tomography for constraining the time-depth conversion, this results in thickness maps of Upper Cretaceous and Cenozoic units with an unprecedented detailed stratigraphic subdivision for the study area (Cenomanian-Turonian, Coniacian-Santonian, Campanian, Maastrichtian-Danian, upper Paleocene, Eocene-Miocene). The aim of this study is to identify and date phases of salt movement and explain their association with Late Cretaceous to Cenozoic tectonic events along the northern margin of the NGB. Based on our refined stratigraphic subdivision of the Upper Cretaceous and Cenozoic, we differentiate between individual episodes of increased tectonic activity during the Late Cretaceous to Cenozoic, which is novel for the Baltic sector of the NGB. Thereby, the results of this study contribute to a better understanding of the evolution of salt structures in relation to regional tectonics in the NGB, which is of great interest for the usage of the deeper subsurface (e.g. for CO₂ storage (CCS), geothermal energy or nuclear waste repository). Besides,

our findings contribute to a prospective offshore extension of the recently published 3D geological overview model (TUNB Working Group, 2021) that has been developed according to increasing demands on subsurface use in Germany.

5.2. Geological Setting

The study area comprises the Baltic Sea sector of the North German Basin (NGB) from the Bay of Kiel in the west to the Bay of Mecklenburg and Rügen Island in the east (Fig. 5.1). The western Bay of Kiel covers the Eastholstein Trough marking the eastern part of the NNE-SSW trending Mesozoic-Cenozoic Glückstadt Graben, which formed a NGB depocenter with up to 11 km of post-Permian sediment thickness (Maystrenko et al., 2005b). In contrast, the central to eastern Bay of Kiel and the Bay of Mecklenburg cover the Eastholstein Mecklenburg Block, the peripheral region between Glückstadt Graben and the northeastern basin margin towards Rügen Island. Here, the post-Permian sediment thickness is decreased to 2 – 4 km and affected by the Western Pomeranian Fault System (Bachmann et al., 2010). An approximately E-W running set of basement highs (sensu Peacock & Banks, 2020), the Rinkøbing-Fyn High, Møn High and Arkona High, mark the northern basin margin. The Grimmen High is located at the northeastern basin margin and forms a WNW striking uplifted zone where the Cretaceous cover is absent or strongly reduced. On a regional scale, the basin floor in the study area dips gently towards the south.

5.2.1. Late Permian to Early Cretaceous evolution

Basin formation began in the Late Paleozoic with extensive volcanism, faulting, lithospheric thinning and subsequent thermal subsidence (Ziegler, 1990b; Maystrenko et al., 2008). In late Permian times, repeated restricted seawater influx under arid conditions led to the deposition of the Zechstein layered evaporite sequence. In the study area, the Zechstein succession consists of seven cyclothems with varying amounts of clay, carbonates, anhydrite, halite and potash sequences (Strohmenger et al., 1996; Peryt et al., 2010). While the Werra (Z1) cyclothem contains mostly less mobile anhydrites and carbonates, mobile halite components are frequent in the Stassfurt (Z2), Leine (Z3), Aller (Z4) and Ohre (Z5) cyclothems. The Friesland (Z6) and Fulda (Z7) cyclothems consist of mostly lacustrine and continental sediments and are only present in the southern part of the study area (e.g. Best, 1989; Peryt et al., 2010). Throughout the complex, multiphase basin evolution, the presence of the thick Zechstein evaporite sequence led to the formation of numerous salt structures including salt pillows, salt diapirs and salt walls (Fig. 5.1).

Thermal subsidence lasted until the Middle Triassic in the study area. During Early to Middle Triassic times, the Buntsandstein and Muschelkalk successions were deposited. These units consist of interlayered mudstones and carbonates (Fig. 5.2) (Van Wees et al., 2000; Kossow & Krawczyk, 2002). In Early to Middle Triassic times, thermal subsidence was locally interrupted by extension, which formed a narrow graben in the central Glückstadt Graben (Brink et al., 1992). In the Late Triassic, E-W directed extension widened the Glückstadt Graben and triggered intensive salt movement in the study area (Hansen et al., 2005; Maystrenko et al., 2005b; Hansen et al.,

2007; Hübscher et al., 2010). In the Bay of Mecklenburg, salt movement began contemporaneously to the formation of the NW-SE trending Western Pomeranian Fault System and was associated with dextral transtensional strike slip movements at the Tornquist Zone (Ahlrichs et al., 2020). From Middle Jurassic to Albian times, uplift induced by the central North Sea Doming event interrupted sedimentation in the study area and eroded much of the Jurassic and partly Upper Triassic deposits (Fig. 5.2) (Underhill & Partington, 1993; Hansen et al., 2007; Hübscher et al., 2010; Schnabel et al., 2021). Rising sea levels in the Lower Cretaceous led to resumed sedimentation in the Albian.

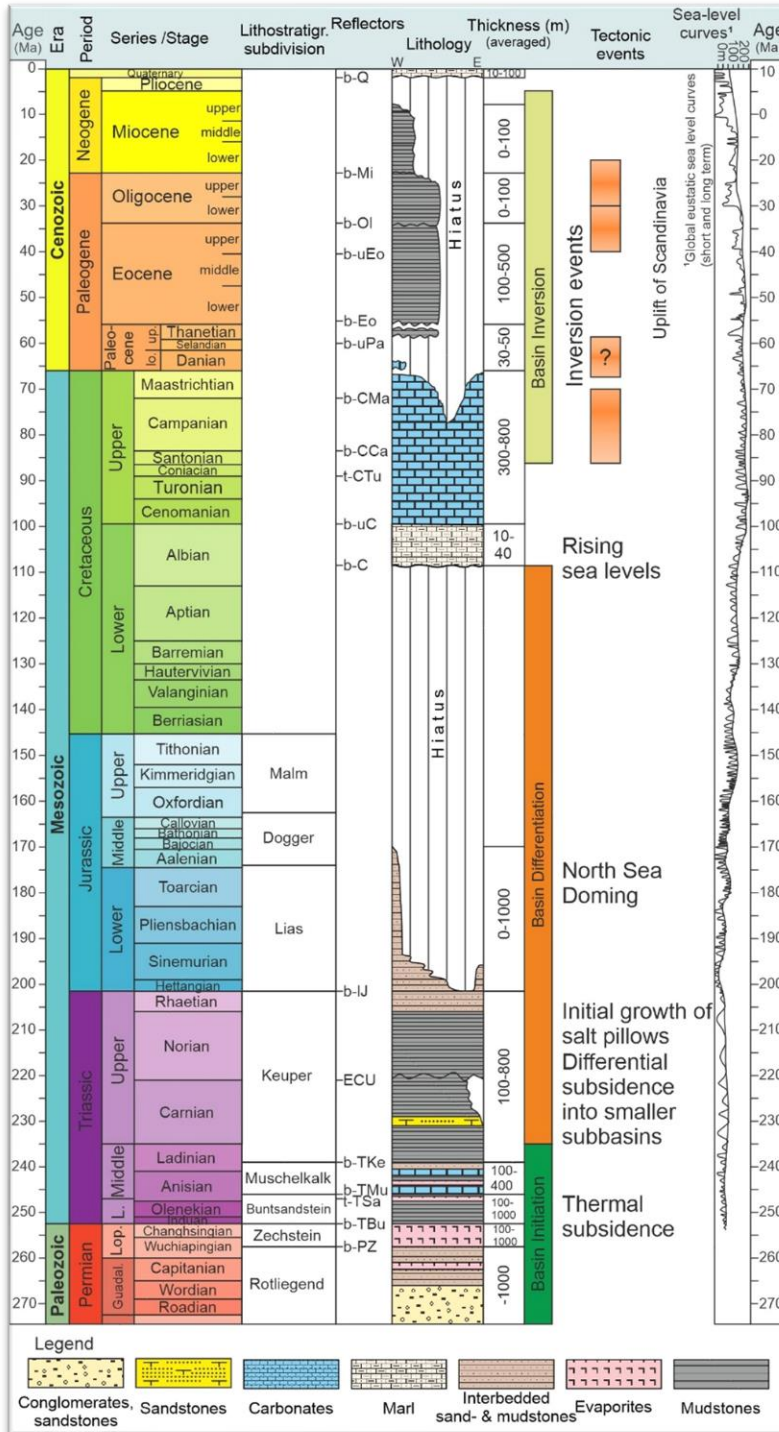


Figure 5.2: Lithostratigraphic chart showing the interpreted key seismic reflectors, dominant lithology and average thickness. Reflectors modified after Ahlrichs et al. (2020). The right columns illustrate important tectonic events of the North German Basin evolution (Kossow & Krawczyk, 2002; Bachmann et al., 2008; Kley, 2018) and the global long and short term eustatic sea level curves (Haq et al., 1987; Haq, 2014, 2017, 2018). b-Q: base Quaternary Unconformity; b-Mi: base Miocene; b-Ol: base Oligocene; b-uEo: base upper Eocene; b-Eo: base Eocene; b-uPa: base upper Paleocene; b-CMa: base Upper Cretaceous Maastrichtian; b-CCa: base Upper Cretaceous Campanian; t-CTu: top Upper Cretaceous Turonian; b-uC: base Upper Cretaceous; b-C: base Cretaceous; b-IJ: base Lower Jurassic; ECU: Early Cimmerian Unconformity; b-TKe: base Triassic Keuper; b-TMu: base Triassic Muschelkalk; t-TSa: top Triassic Salinarröt; b-TBu: base Triassic Buntsandstein; b-PZ: base Permian Zechstein.

5.2.2. Late Cretaceous to recent evolution

After the resumed sedimentation in the Albian, a relatively quiet tectonic phase with long lasting deposition of horizontally layered chalk units in shallow to deep marine conditions persisted from the Cenomanian until the Turonian (Kossow & Krawczyk, 2002; Vejbaek et al., 2010). In the late Turonian to Santonian, major plate reorganization and the onset of the Africa-Iberia-Europe convergence transmitted compressional stress into the European foreland (Kley & Voigt, 2008). Resulting horizontal shortening led to uplift and erosion and renewed salt movement at the northern NGB margin (Kossow & Krawczyk, 2002; Hansen et al., 2007; Hübscher et al., 2010). The uplift of the Grimmen High started in the Coniacian to Santonian and reached its peak in the Campanian-Maastrichtian (Kossow & Krawczyk, 2002; Ahlrichs et al., 2020). This was coeval with salt movement in the Bay of Mecklenburg and fault reactivation at the Werre Fault Zone and within the Western Pomeranian Fault System (Al Hseinat & Hübscher, 2017; Deutschmann et al., 2018; Seidel et al., 2018; Ahlrichs et al., 2020). At the Grimmen High, corresponding erosion removed almost the entire Cretaceous succession while only upper Maastrichtian deposits are missing in most other parts of the study area (Hoth et al., 1993; Katzung, 2004; Ahlrichs et al., 2020). Compressional stress caused only mild inversion of the Glückstadt Graben indicated by slight uplift of diapir roofs and minor salt movement in the marginal parts of the graben (Maystrenko et al., 2005b, 2006). Inversion-generated topographic highs along the Tornquist Zone influenced depositional patterns in the Chalk Sea through contour currents (Hübscher et al., 2019; and references therein).

Paleogene conditions remained shallow to deep marine with Scandinavia serving as a sediment source since its uplift in Paleocene to Oligocene times (Nielsen et al., 2002; Japsen et al., 2007). In the study area, Paleogene successions were deposited relatively far from the paleo coastline (Hinsch, 1986; Japsen et al., 2007). Paleocene deposits in the study area comprise Danian chalk and upper Paleocene (Thanetian) claystones (Fig. 5.2) (Hinsch, 1986; Katzung, 2004). Due to a large-scale domal uplift in the late Paleocene (Ziegler et al., 1995), Selandian sedimentary units are missing and Danian chalk is only preserved in the Eastholstein Trough in the western Bay of Kiel and in the northwestern, Danish part of the study area. Upper Paleocene claystones overlie the corresponding widespread unconformity and are largely preserved west of the Grimmen High (Vinken & International Geological Correlation Programme, 1988).

A phase of relative tectonic quiescence followed in the early to middle Eocene (Hinsch, 1986; Katzung, 2004). In late Eocene times, almost E-W directed extension restarted salt movement in the Glückstadt Graben with thickest sediment accumulation and salt withdrawal in the marginal parts (Maystrenko et al., 2005b). In the Eastholstein Trough in the western Bay of Kiel, salt flow was reactivated in the late Eocene to Oligocene; this was accompanied by faulting above the outer salt wall (Al Hseinat et al., 2016). Huster et al. (2020) noticed that this Eocene phase of salt tectonics started contemporaneous to resumed approx. N-S directed late Eocene to early Miocene intraplate compression related to the Alpine and Pyrenean orogenies (Kley, 2018).

Shallow marine conditions prevailed in the Oligocene to earliest Miocene with ongoing salt movement in the eastern Glückstadt Graben and onshore eastern Germany

(Hinsch, 1986; Katzung, 2004). In Miocene times, the principal horizontal stress regime in the study area changed to NW-SE extension (Kley et al., 2008; Al Hseinat & Hübscher, 2017). This change is associated with reactivation along preexisting structural elements as e.g. the Ringkøbing-Fyn High, and related to intraplate stress transmitted into the European foreland by the Alpine Orogeny (Rasmussen, 2009). At this time, the North Sea Basin was reshaped and the hinterland uplifted, which resulted in regional uplift of the Ringkøbing-Fyn High and adjacent areas by ca. 600 m (Rasmussen, 2009; Japsen et al., 2015). Corresponding erosion removed much of the Miocene, Oligocene and partly upper Eocene deposits in the study area. More complete stratigraphic sequences are only preserved in peripheral sinks adjacent to salt structures in the Glückstadt Graben and onshore Germany (Hinsch, 1986, 1987; Katzung, 2004). Pliocene sediments were not deposited (Hinsch, 1987; Katzung, 2004; Japsen et al., 2015). Quaternary glacial erosion removed further Neogene and Paleogene sedimentary units (e.g. Sirocko et al., 2008).

5.3. Database and Methods

5.3.1. Seismic database

In this study, we use a 2D high-resolution seismic reflection dataset with a total profile length of more than 10.000 km acquired during several surveys in the past decades (Fig. 5.3). The dataset consist of seismic profiles acquired between 1998 and 2004 by the Universities of Aarhus and Hamburg as part of the BaltSeis and NeoBaltic projects (Hübscher et al., 2004). Additional seismic data was acquired during multiple student field exercise cruises of the University of Hamburg between 2005 and 2019 (Hansen et al., 2005; Hansen et al., 2007; Hübscher et al., 2010; Al Hseinat & Hübscher, 2014; Al Hseinat et al., 2016; Kammann et al., 2016; Al Hseinat & Hübscher, 2017; Huster et al., 2020). Furthermore, we use reprocessed seismic profiles of the Petrobaltic database (Rempel, 1992; Schlüter et al., 1997), profiles of the PQ2 cruise of the DEKORP-BASIN'96 campaign (DEKORP-BASIN Research Group, 1999) and lines of the GSI76B survey (kindly provided by ExxonMobil Production Deutschland GmbH, 1976). These individual and more local surveys were connected using the “BalTec” 2D seismic dataset collected during the MSM52 cruise by the University of Hamburg in cooperation with the Federal Institute for Geosciences and Natural Resources (BGR), University of Greifswald, Polish Academy of Sciences, Uppsala University and the German Research Centre for Geosciences Potsdam (BGR & UHH, 2016; Hübscher et al., 2016). The “BalTec” dataset consists of a network of high-resolution multichannel seismic data (dominant frequency of 80 Hz, vertical resolution of ca. 5-30 m) from the western Bay of Kiel up to Bornholm Island (Fig. 5.3a). Acquisition parameters and seismic data processing, including elaborate multiple attenuation and denoising, allowed continuous imaging from the Zechstein salt base up to the seafloor (see Ahlrichs et al., 2020 for a detailed description).

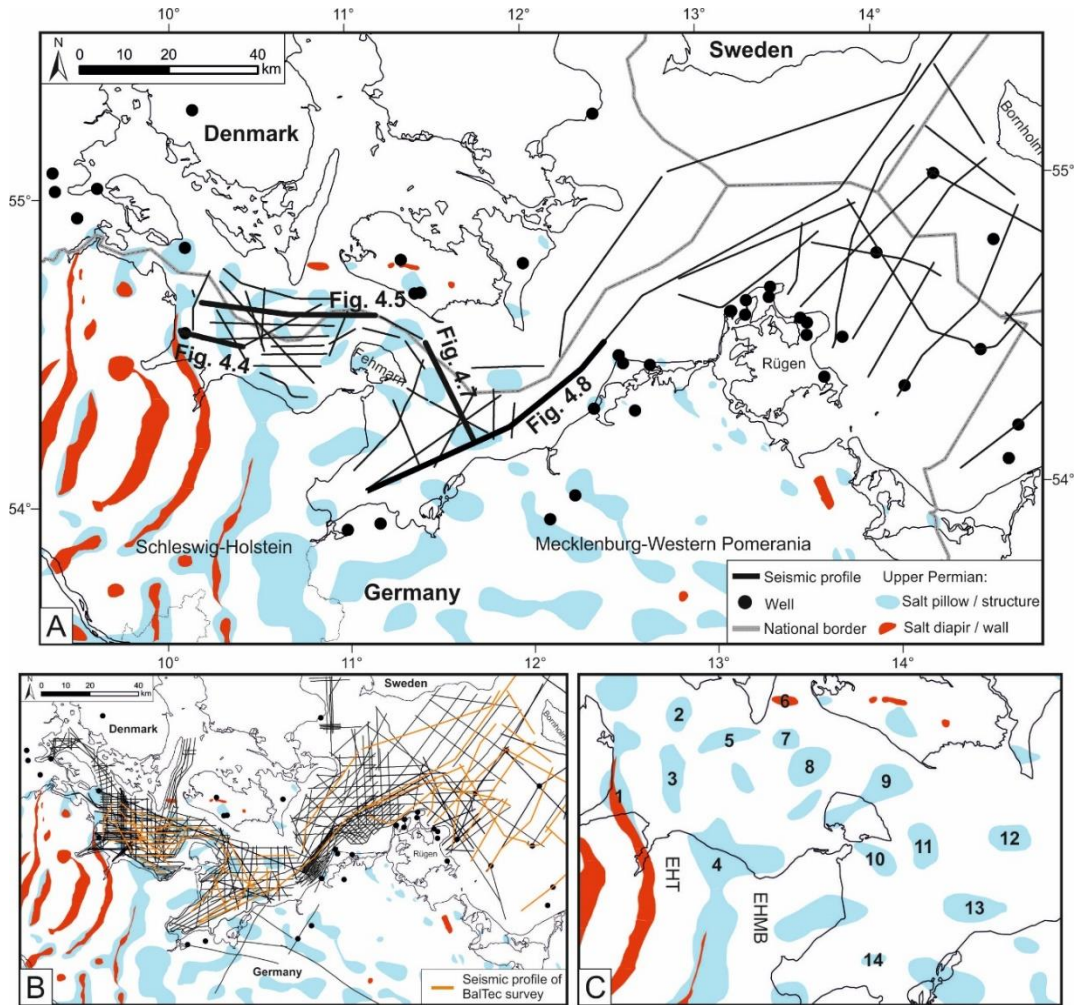


Figure 5.3: Maps showing the location of seismic profiles and wells used in this study. A: Seismic profiles from the BalTec survey and location of shown profiles in this study. B: Complete database with all available seismic profiles and wells used for mapping. Orange lines: seismic profiles of the BalTec survey. C: Names of salt structures in the Bays of Kiel and Mecklenburg. 1: Waabs; 2: Schleimünde; 3: Kieler Bucht; 4: Plön; 5: Langeland; 6: Kegnaes Diapir; 7: Langeland Ost; 8: Vinsgrav; 9: Fehmarn; 10: Fehmarnsund Ost; 11: Staberhuk Ost; 12: Neobaltic; 13: Trollegrund Nord; 14: Boltenhagen Nord. Salt structures after Vejbaek, 1997; Dadlez & Marek, 1998; Reinhold et al., 2008; Hübscher et al., 2010; Warsitzka et al. (2019). EHT: Eastholstein Trough (between salt structures 1 and 2-3-14); EHMB: Eastholstein Mecklenburg Block (east of salt structures 2-3-14).

5.3.2. Stratigraphy

Stratigraphic interpretation of seismic units in this study follows the extended stratigraphic framework described in detail in Ahlrichs et al. (2020). Seismic data was calibrated with well information of nearby deep research and hydrocarbon exploration wells (Fig. 5.3) (Nielsen & Japsen, 1991; Hoth et al., 1993; Schlüter et al., 1997). We linked the stratigraphic interpretation to previous studies in the area, both onshore and offshore (Baldschuhn et al., 2001; Lykke-Andersen & Surlyk, 2004; Hansen et al., 2005; Hansen et al., 2007; Zöllner et al., 2008; Hübscher et al., 2010; Deutschmann et al., 2018; Huster et al., 2020). To further refine the seismo-stratigraphy, especially for the Cenozoic, we tied seismic profiles to undisclosed industry well data in the western Bay of Kiel (Fig. 5.4). We interpreted 17 seismic horizons namely *base Quaternary Unconformity*, *base Miocene*, *base Oligocene*, *base upper Eocene*, *base Eocene*, *base upper Paleocene*, *base Maastrichtian*, *base Campanian*, *top Turonian*, *base*

Cretaceous, base lower Jurassic, Early Cimmerian Unconformity, base Keuper, base Muschelkalk, top Salinarröt, base Buntsandstein, base Zechstein (Fig. 5.2). However, we could only trace the horizons base Miocene, base Oligocene and base upper Eocene within the Eastholstein Trough (Fig. 5.1). The Albian unit is too thin to be resolved throughout the study area so that the base Upper Cretaceous and base Cretaceous reflectors cannot be differentiated.

5.3.3. Depth imaging and refraction traveltime tomography

We focused our velocity analysis on three key profiles: one crossing the Bay of Kiel in E-W direction and two lines crossing the Bay of Mecklenburg in NW-SE and NE-SW direction, respectively (Figs. 5.5, 5.7 and 5.8, see Fig. 5.3 for location). For these profiles, we derived a spatially variant velocity field by migration velocity analysis (MVA). In the MVA procedure, common offset gathers are prestack depth migrated (Stork, 1992). In a top-down approach, the overlying velocity field of a selected horizon is stepwise adjusted until reflections in the common offset gathers are flat (see Schnabel et al., 2021). The derived velocity fields were used for prestack depth migration, which resulted in gapless depth images overcoming imaging artifacts like velocity pull-ups below salt structures (Figs. 5.5 to 5.9).

For the three key seismic depth sections, we derived velocity information using refracted first arrival P-waves (recorded by 2700 m long streamer cable) by performing a traveltime tomography (Figs. 5.5, 5.7 and 5.8). The tomography uses the PStomo_eq algorithm developed and described by Tryggvason (1998). The forward problem is solved by finding a first order finite difference solution to the Eikonal equation resulting in a first arrival traveltime field (Podvin & Lecomte, 1991). The ray paths are found by back tracing the rays from the receivers to the source (Hole, 1992). The inversion uses the iterative LSQR conjugated gradient algorithm (Paige & Saunders, 1982) to minimize the objective function (Eq. 13 in Tryggvason, 1998). Frahm et al. (2020) proved the applicability of this method to the “BalTec” data.

We analyzed the derived velocity field to identify lateral velocity variations within the seismo-stratigraphic units. Beyond the expected velocity increase with depth, the tomography shows no significant lateral velocity variations for the Upper Cretaceous, Paleogene and Neogene successions (Figs. 5.5, 5.7 and 5.8). Table 5.1 summarizes the results from published velocity information together with the velocity range and averaged interval velocities of individual units based on the results of the refraction tomography of all three profiles.

Interval velocity information from published literature and of the refraction tomography in this study							
Method	velocity values in (m/s)						
	Linear velocity relationship [†] k: gradient in (1/s); v ₀ : starting velocity in (m/s)		MVA	MVA	Refraction Tomography		
	Jaritz et al. (1991)	Schlüter et al. (1997)	van Dalfsen et al. (2006)	Hansen et al. (2007)	Schnabel et al. (2021)	This study	Conversion interval velocity
Miocene-Eocene	v ₀ : 1550-1800 k: 0.7		v ₀ : 1700-1875 k: 0.288	2000	1765-2580	1600-2420 ø: 1920	1900
late Paleocene						1790-2600 ø: 2170	2200
Danian-Maastrichtian						1985-2890 ø: 2345	2400
Campanian						2160-3510 ø: 2565	2600
Santonian-Coniacian	v ₀ : 1800-2450 k: 1.0	v ₀ : 1800-3200 k: 1.2-0.9	v ₀ : 1700-2900 k: 0.882	2400	2255-3195	2410-3710 ø: 2925	2900
Turonian-Cenomanian						2740-3465 ø: 3000	3000
Zechstein	4500	4100-5100	4050-5550	4800	4200-4900		4500 [‡]

Table 5.1: Interval velocity information from published literature (Jaritz et al., 1991; Schlüter et al., 1997; van Dalfsen et al., 2006; Hansen et al., 2007; Schnabel et al., 2021) and results of the refraction traveltime tomography and used velocity for conversion of the isochron maps. [†]: These studies use a linear velocity relationship $V_z = V_0 + kZ$. V_z : Velocity at depth Z ; V_0 : starting velocity; k : velocity gradient; ø: average. Velocity values in m/s. [‡]: Zechstein conversion interval velocity is based on the average of published velocities.

5.3.4. Mapping

We mapped Upper Cretaceous and Cenozoic units to identify episodes of salt movement and their possible relationship to Late Cretaceous to Cenozoic tectonic inversion events. To correlate Late Cretaceous and Cenozoic thickness variations with salt structures, we also mapped the Zechstein succession. Base and top of the Zechstein unit are only imaged by the BalTec, Petrobaltic, DEKORP-BASIN'96 and GSI76B surveys and thus only these profiles contributed to the Zechstein mapping procedure. For mapping of the Upper Cretaceous (Cenomanian – Maastrichtian) and Cenozoic (Paleocene – Miocene) units, we used all available seismic profiles in the dataset (Fig. 5.3b). Using the available horizon picks for each horizon, we created two-way travelttime-structure maps by minimum curvature spline interpolation with a grid cell size of 300x300 m. For the Quaternary, we used the base Quaternary Unconformity time-structure map from Al Hseinat and Hübscher (2017). We created isochron maps (vertical thickness in two-way time) for the Zechstein, Cenomanian-Turonian, Coniacian-Santonian, Campanian, Maastrichtian-Danian, upper Paleocene, Eocene-Miocene units (provided in the supporting information, Ahlrichs et al., 2021b). We converted the isochron maps to isochore maps in meters by using constant interval velocities derived from averaging the results of the refraction travelttime tomography (table 5.1). We chose this constant velocity conversion as a first approach because the tomography requires long streamer cables to record refracted waves and, thus, this was only possible for the BalTec data. Accordingly, velocity information is sparsely distributed and creating a sophisticated area-covering laterally variable velocity model is a challenging task of future work.

We interpreted thickness maps, seismic profiles and flattened sections to identify local and regional thickness variations. Besides vertical tectonic movements, differential compaction, water level and sedimentation processes influence the sediment thickness (e.g. Betram & Milton, 1989). For our study area, we assume that sediment thickness variations reflect differential sedimentation and erosion caused by vertical tectonic movements such as uplift/subsidence, faulting and salt movement. Based on the geological conditions during Cretaceous and Paleogene deposition (sedimentation in rather stable shallow to deep marine conditions after large-scale erosion caused by Mid-Jurassic North Sea Doming, see chapter 5.2.), we expect mainly horizontally layered deposition modified by post-depositional vertical tectonic movements and less dominant effects of differential compaction and sea level fluctuations. However, we cannot fully exclude effects of differential compaction and sea level fluctuations, especially for the Neogene since falling sea levels and uplift in early Miocene times likely changed the depositional environment in the study area (Hinsch, 1986, 1987; Rasmussen, 2009).

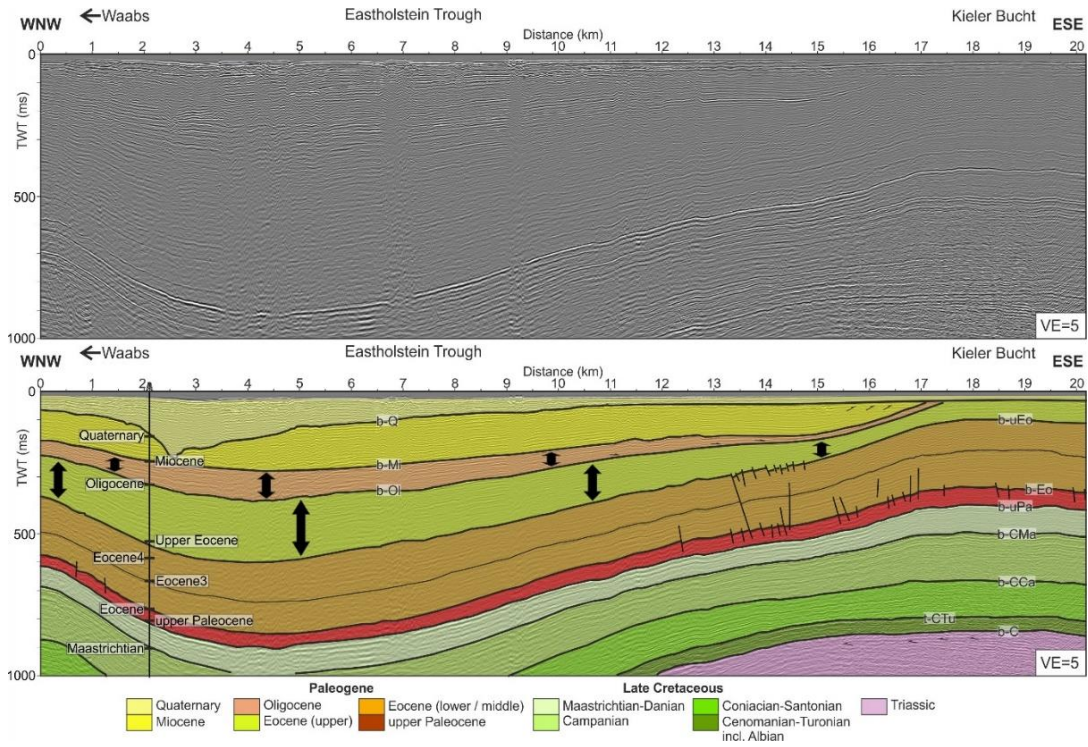


Figure 5.4: Profile AL526-20, covering the Eastholstein Trough in the western Bay of Kiel: Time migrated section with well tie to undisclosed industry well data. Well markers converted to time by check shot data. Note the black arrows pointing out the divergent upper Eocene and Oligocene units with increasing thickness towards the Eastholstein Trough. Note the Quaternary incision at profile distance 2.5 km. For profile location, see Fig. 5.3a. VE: vertical exaggeration. Reflectors (see also Fig. 5.2): b-Q: base Quaternary Unconformity; b-Mi: base Miocene; b-Ol: base Oligocene; b-uEo: base upper Eocene; b-Eo: base Eocene; b-uPa: base upper Paleocene; b-CMa: base Upper Cretaceous Maastrichtian; b-CCa: base Upper Cretaceous Campanian; t-CTu: top Upper Cretaceous Turonian; b-uC: base Upper Cretaceous; b-C: base Cretaceous.

5.4. Observations

Based on key seismic profiles and thickness maps of the Zechstein, Upper Cretaceous and Cenozoic successions, we analyze local thickness variations in the Upper Cretaceous – Cenozoic overburden to identify phases of salt movement during inversion phases. In the following sections, we interpret increased thickness of a unit in the overburden above the rim-syncline of a salt structure (peripheral sink, sensu Jackson & Hudec, 2017) and thinning of the overburden towards the crest of a salt structure, possibly affected by the development of crestal faults as evidence for syndepositional salt movement and salt structure growth. Accordingly, we interpret relatively uniform thickness across salt structures as an indication for no salt movement during this time. For location and names of discussed salt structures, see Fig. 5.3c.

5.4.1. Key seismic profiles

Crestal faulting during Late Cretaceous and late Eocene salt movement in the eastern Glückstadt Graben:

At the eastern Glückstadt Graben in the western Bay of Kiel, faults form a prominent crestal graben above the salt pillow “Kieler Bucht” at the transition from the Eastholstein Trough to the Eastholstein-Mecklenburg Block (Fig. 5.5). The eastern bounding

fault pierces the overburden from within the upper Zechstein up to the Quaternary successions. The profile shows further smaller salt pillows towards the east. The Buntsandstein and Muschelkalk units have uniform thickness throughout the profile. The Keuper unit thins and reflectors converge towards the pillow crests indicating the initiation of salt pillow formation. Jurassic deposits are only preserved in the eastern part of the profile above rim-synclines of salt structures. The Cenomanian-Turonian unit has a quite constant thickness characterized by concordant reflections, which indicates a phase of salt tectonic quiescence (Fig. 5.6). The flattened section at base Campanian shows minor thickness variations in the Coniacian-Santonian and Campanian at the flanks of the salt pillow “Kieler Bucht” (Fig. 5.6b). Thickness of the Maastrichtian-Danian unit slightly increases towards the Eastholstein Trough. The overlying upper Paleocene is concordant and with only ca. 50 m thickness quite thin. Apart from the crestal zone of the salt pillow “Kieler Bucht”, the upper Paleocene has uniform thickness, which suggests ceased salt movement (Fig. 5.6c). Above the crestal zone, the unit is missing, which we explain by post-depositional erosion. The Eocene-Miocene unit, bound at the top by the erosional base Quaternary Unconformity, shows increased thickness at the flanks of the salt pillow “Kieler Bucht”, especially within the western peripheral sink (Eastholstein Trough, Fig. 5.6c). Within the crestal graben, thicker Eocene-Miocene deposits are preserved indicating revived growth of the salt pillow “Kieler Bucht” and reactivation of the crestal faults at least during the Eocene-Miocene.

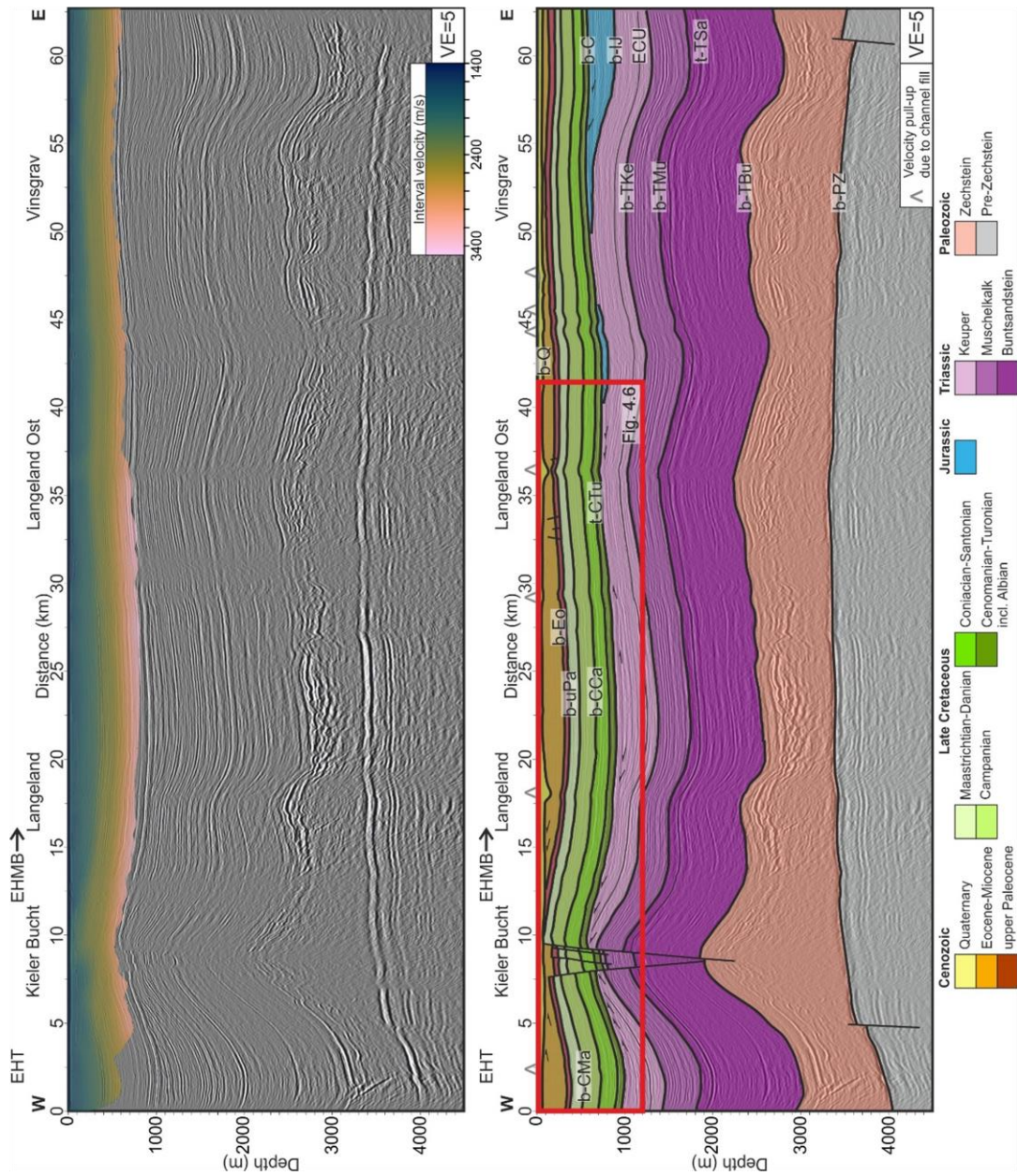


Figure 5.5: Profile BGR 16-232, located in the Bay of Kiel: Uninterpreted prestack depth migrated section showing velocity results from the traveltome tomography (top) and interpreted section (bottom). For location, see Fig. 5.3a. Salt structures are marked on top of the section. Note the small velocity pull-ups due to high-velocity channel infill near the seafloor (marked with grey “^”) symbols along the distance axis. See Frahm et al., 2020 for further details). VE: vertical exaggeration. EHT: Eastholstein Trough; EHMB: Eastholstein-Mecklenburg Block. Reflectors (see also Fig. 5.2): b-Q: base Quaternary Unconformity; b-Eo: base Eocene; b-uPa: base upper Paleocene; b-CMa: base Upper Cretaceous Maastrichtian; b-CCa: base Upper Cretaceous Campanian; t-CTu: top Upper Cretaceous Turonian; b-C: base Cretaceous; b-IJ: base Lower Jurassic; ECU: Early Cimmerian Unconformity; b-TKe: base Triassic Keuper; b-TMu: base Triassic Muschelkalk; t-TSa: top Triassic Salinarrot; b-TBu: base Triassic Buntsandstein; b-PZ: base Permian Zechstein.

Late Eocene – Oligocene salt movement in the Eastholstein Trough:

The central part of the Eastholstein Trough, in the western Bay of Kiel, contains a relatively complete succession of Paleogene and Neogene sedimentary units (Fig. 5.4). Upper Paleocene and lower Eocene units show rather uniform thickness characterized by concordant reflections, which indicates a phase of relatively tectonic quiescence without salt movement. The upper Paleocene and lower Eocene units contain numerous small-scale faults, which remind of polygonal faults. Upper Eocene and Oligocene units are divergent towards the center of the Eastholstein Trough, which indicates recommencing salt movement in the late Eocene (Fig. 5.4, compare black arrows). Towards the east, thickness of the upper Eocene unit decreases while Oligocene and Miocene units are truncated by the base Quaternary Unconformity.

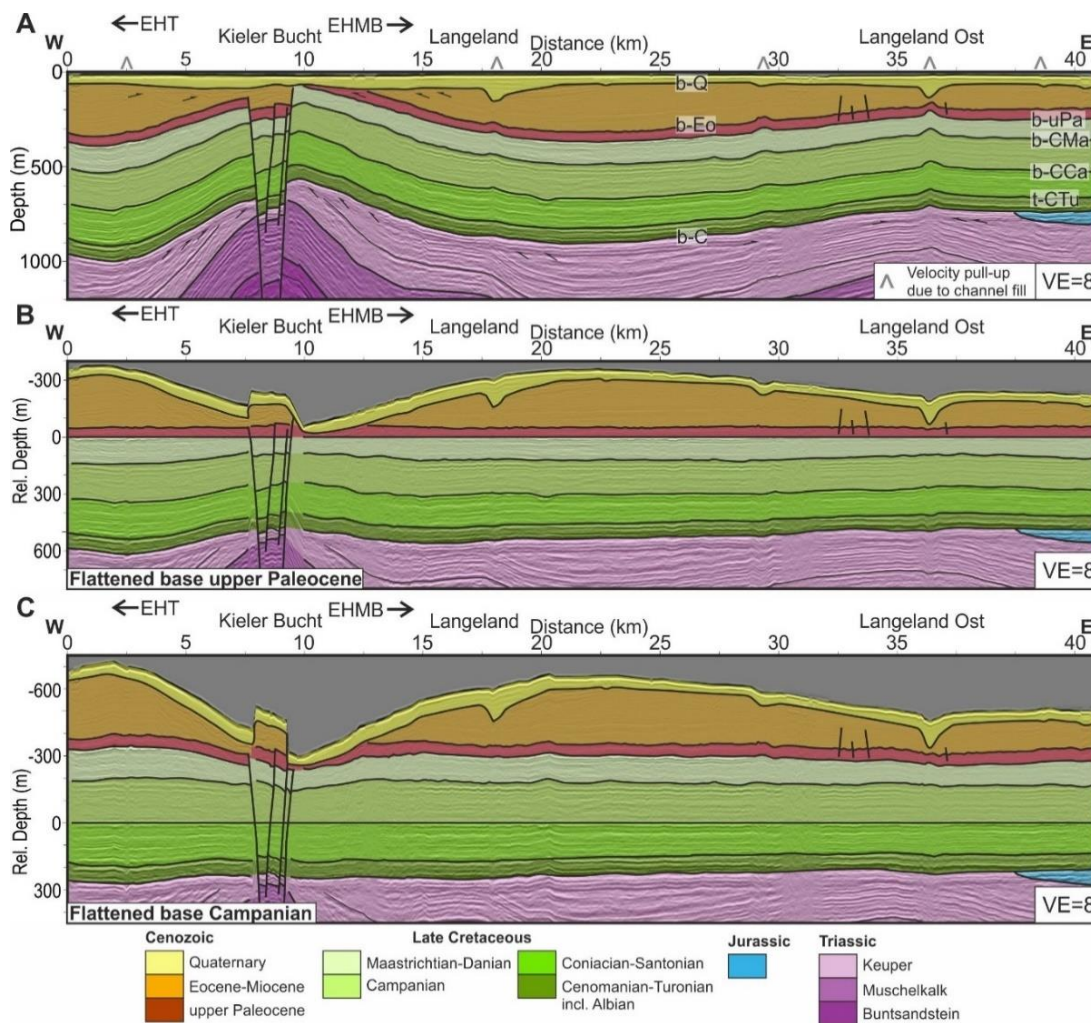


Figure 5.6: Zoom of profile BGR16-232 (Fig. 5.5), located in the bay of Kiel. Note the increased vertical exaggeration. B and C show flattened section at base Campanian and base late Paleocene respectively. Note the small velocity pull-ups due to high-velocity channel infill near the seafloor (marked with grey “^” symbols along the distance axis). See Frahm et al., 2020 for further details). EHT: Eastholstein Trough; EHMB: Eastholstein-Mecklenburg Block. VE: vertical exaggeration. Reflectors labeled as in Figs. 5.2 and 5.5.

Late Cretaceous and Eocene-Miocene salt movement in the Bay of Mecklenburg:

Fig. 5.7 shows a NW-SE profile in the Bay of Mecklenburg imaging the salt pillow “Staberhuk Ost” and adjacent rim-synclines. Multiple faults with partly small offsets characterize the base Zechstein. The Buntsandstein and Muschelkalk units show uniform thickness throughout the profile, whereas convergence and crestal erosion of Keuper strata denote the initiation of salt pillow development. The Jurassic unit is only preserved above the rim-synclines. The Cenomanian-Turonian unit shows gradually increasing thickness from the NW to SE reflecting a thickness increase towards the basin center as the profile is not exactly parallel to the basin margin. Local thickness variations within the Cenomanian-Turonian around the salt pillow as well as crestal faults are not visible. Thus, we interpret this as a phase of salt tectonic quiescence. Minor local thickness variations (50 to 60 m) in the Coniacian-Santonian and Campanian between the pillow crest and above the adjacent rim-synclines indicate the development of small peripheral sinks and revived salt movement (Fig. 5.7). Minor salt pillow growth continued in the Maastrichtian-Danian represented by increased thickness of the unit above the rim-synclines and thinning and erosion towards the crest of the salt pillow “Staberhuk Ost”. The upper Paleocene unit shows uniform thickness suggesting ceased salt movement during this time. Preserved Eocene-Miocene deposits above the rim-synclines show concordant internal reflections, which are truncated by the base Quaternary Unconformity above the pillow crest. Assuming a locally constant amount of Neogene and Quaternary erosion, increased thickness of the Eocene-Miocene unit above the rim-synclines indicates salt withdrawal from the rim-synclines during the Cenozoic, where the observed remnants of the Eocene-Miocene unit are prekinematic.

Late Cretaceous and Eocene-Miocene salt movement in the Bay of Mecklenburg at the transition to the Grimmen High:

The SW-NE profile shown in Fig. 5.8 crosses two salt pillows in the Bay of Mecklenburg. Multiple faults offset the base Zechstein in the northeastern part of the profile. The thickness of the Buntsandstein and Muschelkalk increases gradually towards the southwest, in the direction of the basin center. The Keuper unit shows local thickness variations around the salt pillows, especially in the upper part, indicating the initiation of salt movement and pillow growth, which is in accordance to the observations from Fig. 5.7. In the SW part of the profile, preserved Jurassic strata have slightly increased thickness while the unit terminates in a toplap towards the crest of the salt pillow “Trollegrund Nord”. Towards the Grimmen High, the Jurassic unit shows increased thickness. The Cenomanian-Turonian unit has uniform thickness and relatively concordant layering (Fig. 5.9). Coniacian-Santonian units thin and reflectors converge towards the Grimmen High, whereas thinning becomes more prominent in the Campanian and Maastrichtian-Danian (Fig. 5.9b). Above the crest of the salt pillows, the Coniacian-Santonian and more prominent the Campanian and Maastrichtian-Danian units show reduced thickness compared to the flanking peripheral sinks, which evidences salt pillow rise by salt withdrawal from the rim-synclines. At the salt pillow “Trollegrund Nord”, numerous crestal faults with relatively small throw dissect the Upper Cretaceous units. They likely developed in response to the rising salt. The upper

Paleocene unit shows relatively uniform thickness. Numerous small-scale faults pierce this unit (Fig. 5.9c). Thickness of the Eocene to Miocene unit is increased in peripheral sinks while reduced thickness is visible towards the salt structures. However, the Eocene-Miocene unit lacks internal diverging reflectors (Fig. 5.8c).

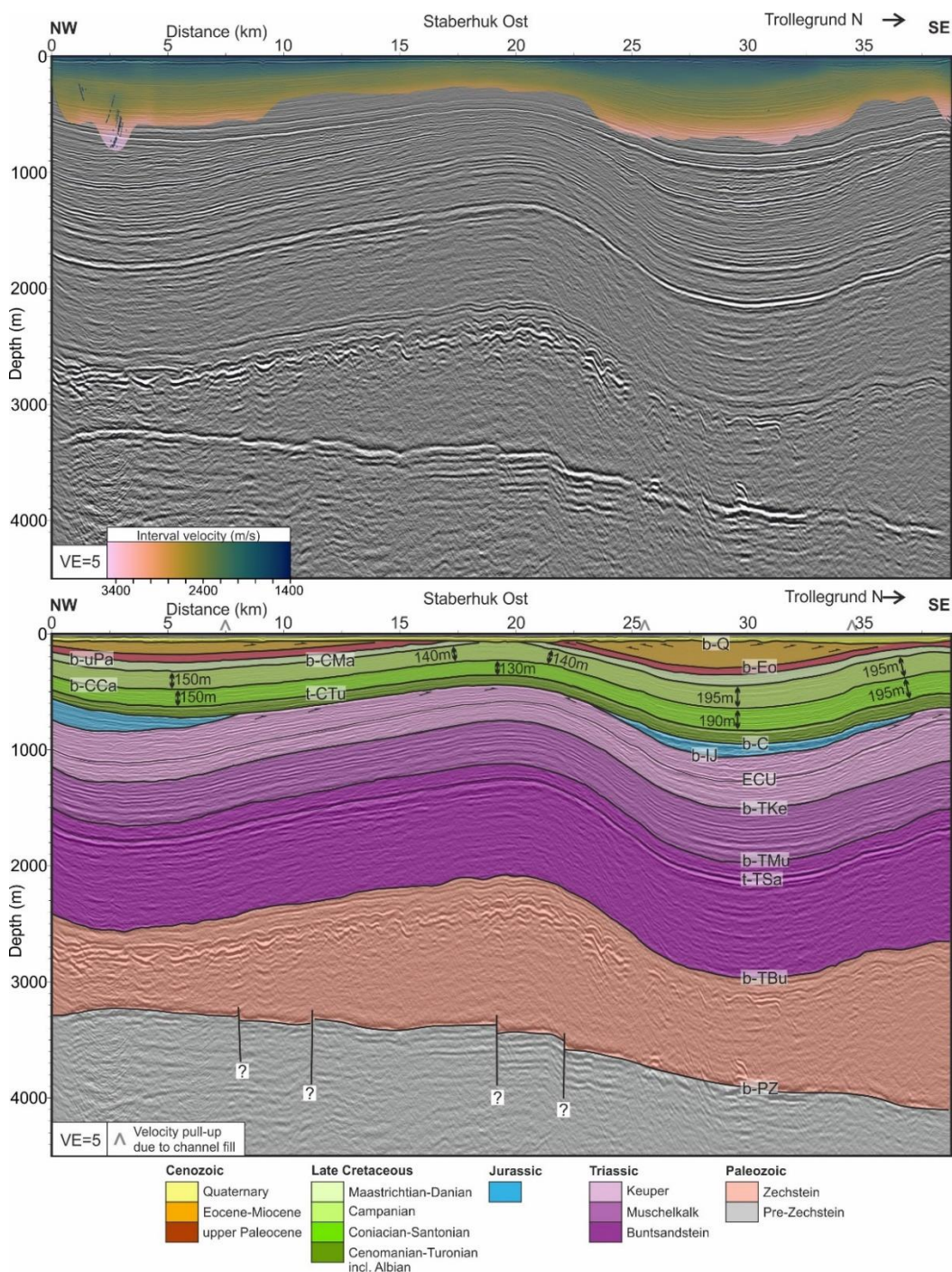


Figure 5.7: Profile BGR16-230, located in the Bay of Mecklenburg: Uninterpreted prestack depth migrated section showing velocity results from the traveltime tomography (top) and interpreted section (bottom). For location, see Fig. 5.3a. Salt structures are marked on top of the section. Values within Coniacian-Santonian and Campanian units denote approximate thickness at the black arrow location. Faults at the base Zechstein with question mark are uncertain as the small offsets could also be velocity artefacts. Note the small velocity pull-ups due to high-velocity channel infill near the seafloor (marked with grey “^” symbols along the distance axis). See Frahm et al., 2020 for further details). VE: vertical exaggeration. Reflectors labeled as in Figs. 5.2 and 5.5.

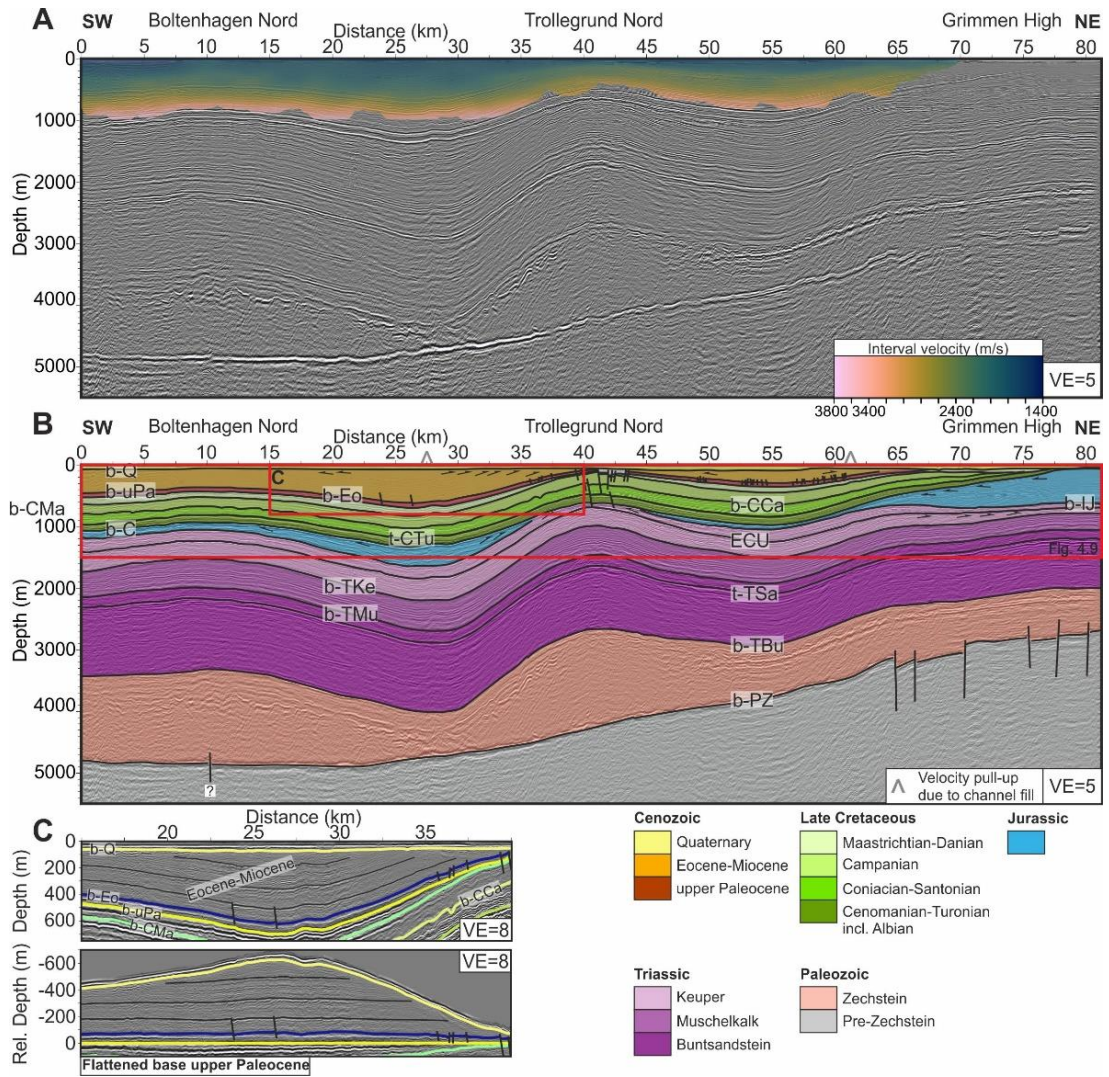


Figure 5.8: Profile BGR16-254, located in the Bay of Mecklenburg: A: Uninterpreted prestack depth migrated section showing velocity results from the traveltome tomography. B: Interpreted section. For location, see Fig. 5.3a. Salt structures are marked on top of the section. Fault at the base Zechstein with question mark is uncertain as the small offset could also be velocity artefacts. C: Zoomed in section of Eocene-Miocene unit. Note the concordant internal layering of the Eocene-Miocene unit and missing of diverging strata. Note the small velocity pull-ups due to high-velocity channel infill near the seafloor (marked with grey “^” symbols along the distance axis. See Frahm et al., 2020 for further details). VE: vertical exaggeration. Reflectors labeled as in Figs. 5.2 and 5.5.

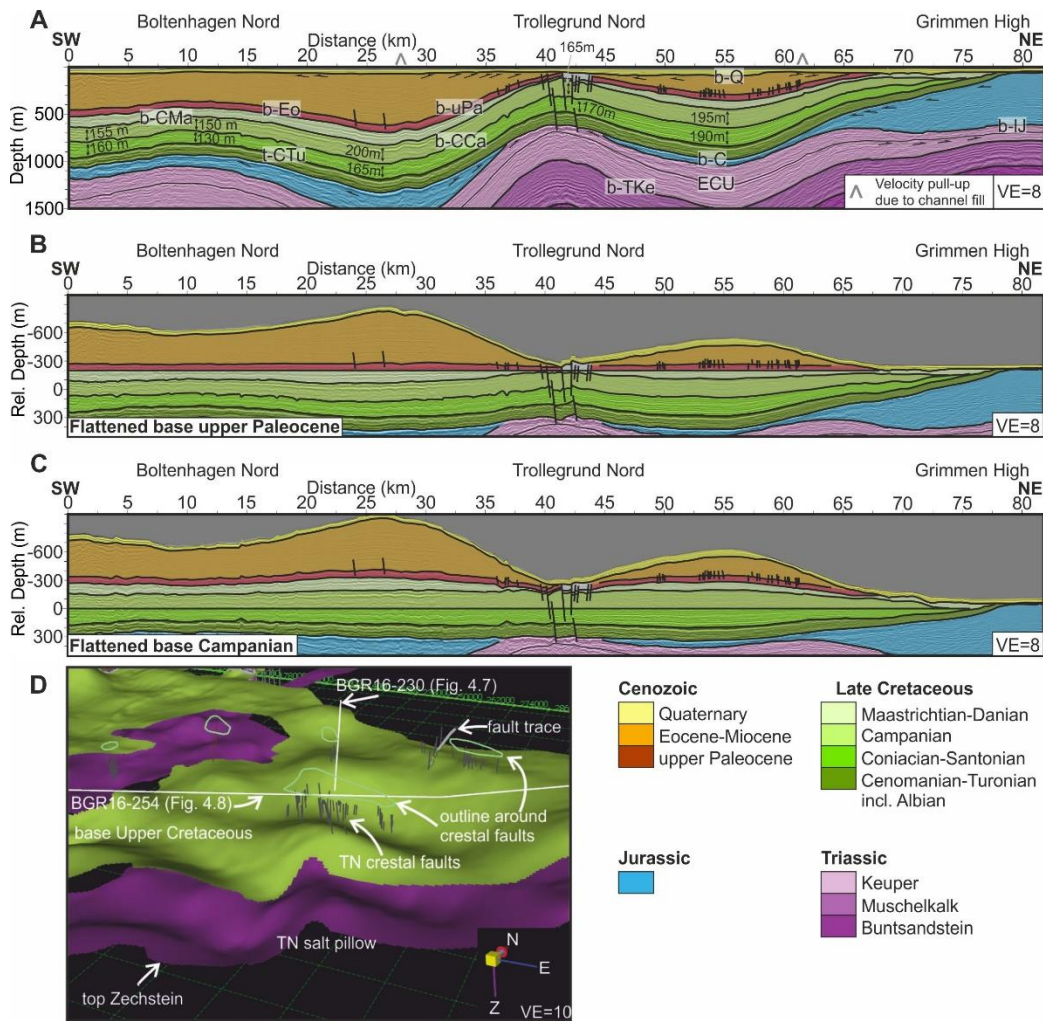


Figure 5.9: Zoom of profile BGR16-254 (Fig. 5.8), located in the Bay of Mecklenburg. See Fig. 5.3 for location. Note the increased vertical exaggeration. B and C show flattened section at base Campanian and base upper Paleocene respectively. D: 3D view from the southeast on the Trollegrund Nord (TN) salt pillow in the Bay of Mecklenburg in order to visualize small crestal faults above the pillow. Grey lines mark crestal faults piercing the Upper Cretaceous units. Mint-green line above the faults outlines the location of the crestal fault picks and is displayed accordingly in map view in Figs. 5.11 and 5.12. Note the small velocity pull-ups due to high-velocity channel infill near the seafloor (marked with grey “^” symbols along the distance axis). See Frahm et al., 2020 for further details). VE: vertical exaggeration.

5.4.2. Thickness maps

5.4.2.1. Zechstein

Due to the basin configuration, Zechstein thickness shows a general trend of increasing thickness from the basin margin in the north towards the south (Fig. 5.10). Areas of locally increased thickness coincide well with the published locations of Zechstein salt structures (Vejbaek, 1997; Reinhold et al., 2008; Hübscher et al., 2010; Warsitzka et al., 2019). However, for three structures in the Bay of Kiel and one in the Bay of Mecklenburg, our new mapping reveals a slightly different location and shape. The better coverage of the subsurface by the new BalTec data imaging the deeper subsurface leads to a more circular outline of the salt structures “Kieler Bucht”, “Langeland”, “Langeland Süd” and “Staberhuk Ost” (compare dashed yellow and adjacent dashed black lines in Fig. 5.10). We did not modify the shape for salt structures that were not

well covered by seismic profiles, as only a subset of the database imaged top and base Zechstein (inset of Fig. 5.10, e.g. salt pillow “Neobaltic”), or where the thickness map does not show a distinctively different shape. Northeast of the Werre Fault Zone, a zone of increased Zechstein thickness trending parallel to the fault is visible (Prerow anticline in Fig. 5.10).

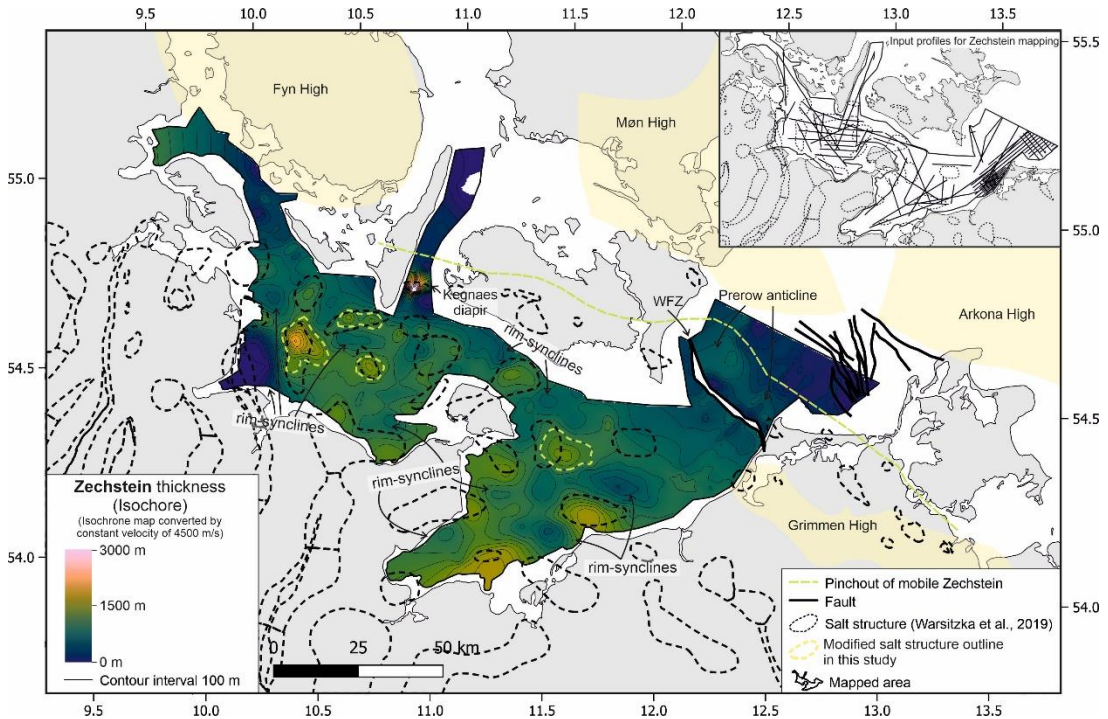


Figure 5.10: Zechstein isochore map (isochrone map converted using a constant interval velocity of 4500 m/s. Yellow dashed lines mark modified outline of salt structures based on mapped thickness in this study. Pinchout of mobile Zechstein after Katzung (2004); Pharaoh et al. (2010). Inset shows input profiles for Zechstein mapping (top and base Zechstein are only imaged by subset of the database). WFZ: Werre Fault Zone.

5.4.2.2. Upper Cretaceous

The Cenomanian-Turonian isochore map (Fig. 5.11a) shows relatively uniform thickness throughout the study area. While the mean thickness of the unit is approx. 80 m within the Bay of Kiel, mean thickness in the Bay of Mecklenburg is with approx. 100 m slightly higher. Thickness variations do not correlate with the location of salt structures. The variations are small and occur across large distances.

The mean thickness of the Coniacian-Santonian unit is approx. 150 m, both in the Bay of Kiel and Bay of Mecklenburg (Fig. 5.11b). The NE-SW trend of increasing thickness resembles the basin configuration. Minor local thickness variations are observed in the Eastholstein Trough, whereas no local thickness variations are observed in the eastern Bay of Kiel. In the Bay of Mecklenburg, we observe minor local thickness variations around salt structures. From the Bay of Mecklenburg towards the Grimmen High, the Coniacian-Santonian unit thins out (Fig. 5.11b). We interpret the thinning as a result of syndepositional uplift of the Grimmen High in response to the onset of basin inversion.

The Campanian has a mean thickness of approx. 180 m in the Bay of Kiel and 160 m in the Bay of Mecklenburg (Fig. 5.11c). Increased thickness of the Campanian unit

within the Eastholstein Trough and south of the salt pillow “Kieler Bucht” indicate the development of peripheral sinks and revived salt movement in the Glückstadt Graben. However, thickness variations are only in the range of several tens of meters, thus, representing only minor salt movement. The eastern Bay of Kiel shows the typical NNE-SSW trend of increased thickness reflecting the basin configuration. Above the crests of salt pillows in the Bay of Mecklenburg, thickness of the Campanian is reduced. Adjacent areas of slightly increased thickness suggest the development of minor peripheral sinks, which indicates at least minor salt movement (Fig. 5.11c). Thinning towards the Grimmen High is evident from both the southwest and northeast. An approx. 25 km wide zone of eroded Campanian forms the northwestern flank of the Grimmen High, which suggest ongoing uplift of the Grimmen High during the Campanian.

The Maastrichtian-Danian unit has a mean thickness of 105 m in the Bay of Kiel and approx. 70 m in the Bay of Mecklenburg (Fig. 5.11d). Danian chalk is only preserved in the Eastholstein Trough in the western Bay of Kiel and in the northwestern study area (note blue dashed line in Fig. 5.11d). Thus, the mapped thickness represents mainly Maastrichtian deposits in most parts of the study area. The isochore map shows local thickness variations in the Eastholstein Trough and adjacent areas with slightly increased thickness adjacent to the salt structures. These areas coincide with increased thickness visible in the Campanian. In the eastern Bay of Kiel, the depositional trend seems to have changed from previously NNE-SSW increasing thickness as e.g. visible for the Campanian to NW-SE in the Maastrichtian-Danian. However, the thickness variations are minor over a large distance. Note the NNE-SSW striking contour line west of Fehmarn. In the Bay of Mecklenburg, areas of locally increased thickness adjacent to salt structures coincide with those in the Campanian. The Maastrichtian-Danian unit is thinned or partly eroded above salt pillow crests, which indicates ongoing salt movement accompanied by the development of peripheral sinks.

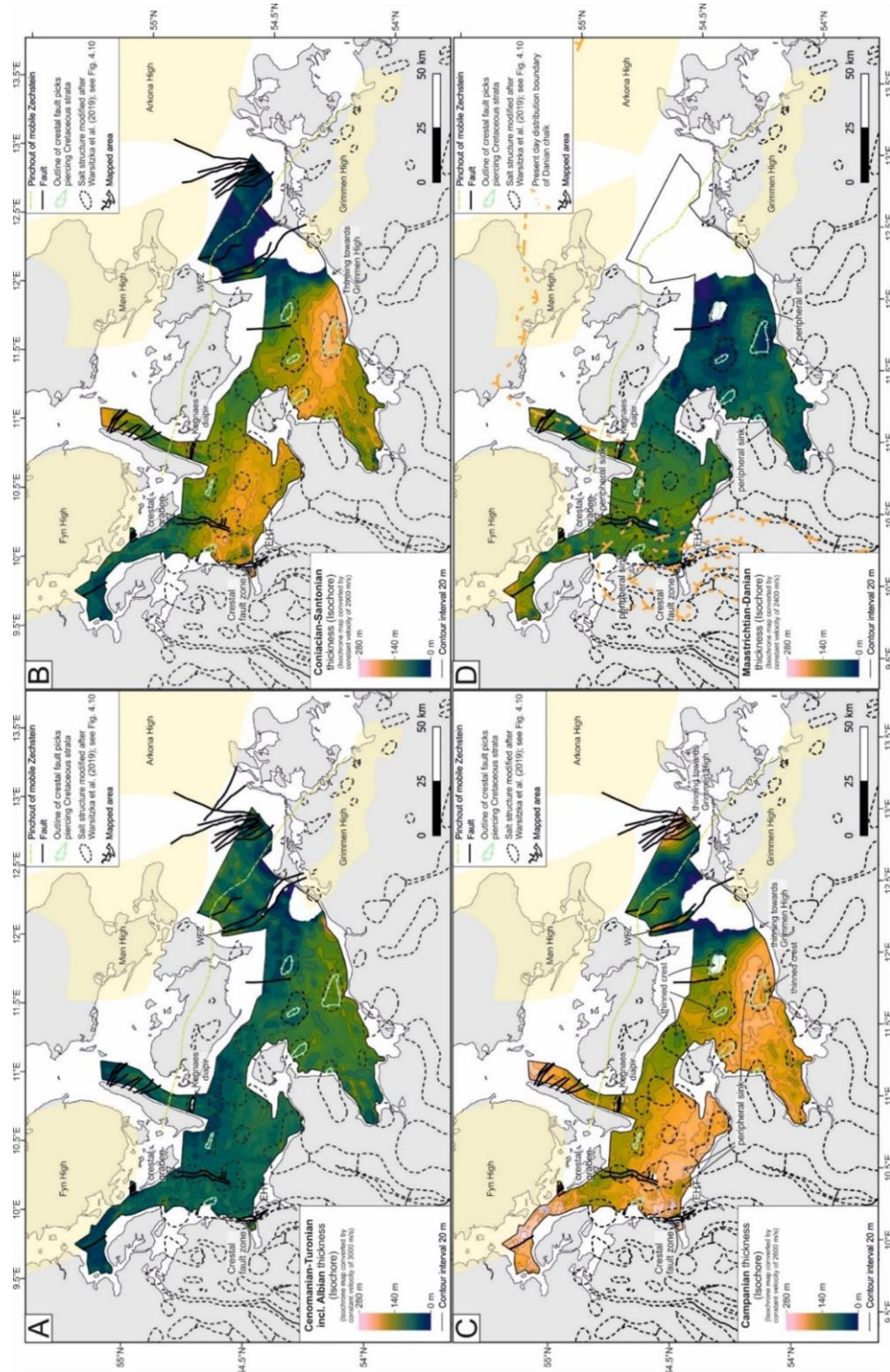


Figure 5.11: Isochore maps of the Upper Cretaceous (isochrone maps converted using a constant interval velocity). A: Cenomanian-Turonian, B: Coniacian-Santonian, C: Campanian, D: Maastrichtian-Danian). Present-day distribution boundary of Danian chalk simplified after Vinken & International Geological Correlation Programme, 1988. Pinchout of mobile Zechstein after Katzung (2004); Pharaoh et al. (2010). EHT: Eastholstein Trough; WFZ: Werre Fault Zone.

5.4.2.3. *Cenozoic*

The upper Paleocene unit is relatively thin and uniform in thickness throughout the study area (Fig. 5.12a). The mean thickness is approx. 70 m. The NW-SE thickness trend of the Maastrichtian-Danian unit prevails in the upper Paleocene. Above many salt pillows, the upper Paleocene thickness is reduced due to crestral erosion. Where the top Paleocene is preserved, the unit shows relatively constant thickness. Deepening of peripheral sinks is not visible. Thus, the crestral erosion must have been post-depositional and salt movement ceased during the late Paleocene.

The Eocene-Miocene unit shows comparable large thicknesses (Fig. 5.12b, note the higher contour interval of 50 m). Within the Eastholstein Trough, more than 700 m of Eocene to Miocene deposits accumulated, whereas thickness of the unit ranges between 0 m and 100 – 200 m above the adjacent salt structures. In the northeastern Bay of Kiel, thickness variations are small and do not clearly correlate with the salt structures “Langeland Ost” and “Vinsgrav”. In the southeastern Bay of Kiel and within the Bay of Mecklenburg, we observe increased thickness adjacent to salt structure, while the unit shows reduced thickness above the crests. Though, overall thickness within the peripheral sinks is smaller than in the Eastholstein Trough. Throughout the study area, local thickness variations clearly correlate with the salt structures and indicate salt withdrawal from rim-synclines due to revived salt movement during the Eocene to Miocene in the Eastholstein Trough, southern Bay of Kiel and Bay of Mecklenburg.

5.4.3. *Faults*

Multiple faults cut the Upper Cretaceous and Cenozoic units (Figs. 5.11 and 5.12). At the western boundary of the Eastholstein Trough, a crestral graben formed above the salt wall “Waabs”. At the eastern border of the Eastholstein Trough, two prominent N-S striking faults cut the Upper Cretaceous and Cenozoic units and form a crestral graben above the salt structures “Schleimünde” and “Kieler Bucht” (Fig. 5.11). At least the eastern boundary fault is detached in the Zechstein (Fig. 5.5). The thickness of the Upper Cretaceous and Paleocene units within the crestral graben is relatively similar to the graben shoulders. The top part of the crestral graben is filled with Eocene-Miocene deposits, which leads to a locally increased thickness within the graben comparing the adjacent area (Figs. 5.5 and 5.12b). This indicates a reactivation of the crestral faults within the Eocene to Miocene.

Above the salt structures “Langeland” (Bay of Kiel), “Staberhuk Ost”, “Neobaltic”, “Fehmarnsund Ost” and “Trollegrund Nord” (all Bay of Mecklenburg), many small faults pierce the Upper Cretaceous and Cenozoic units. We outlined the area where these small-scale crestral faults are visible (Fig. 5.9d and mint line in Figs. 5.11 and 5.12). They are restricted to the crest of salt pillows, which suggests they developed during the growth of the salt structures.

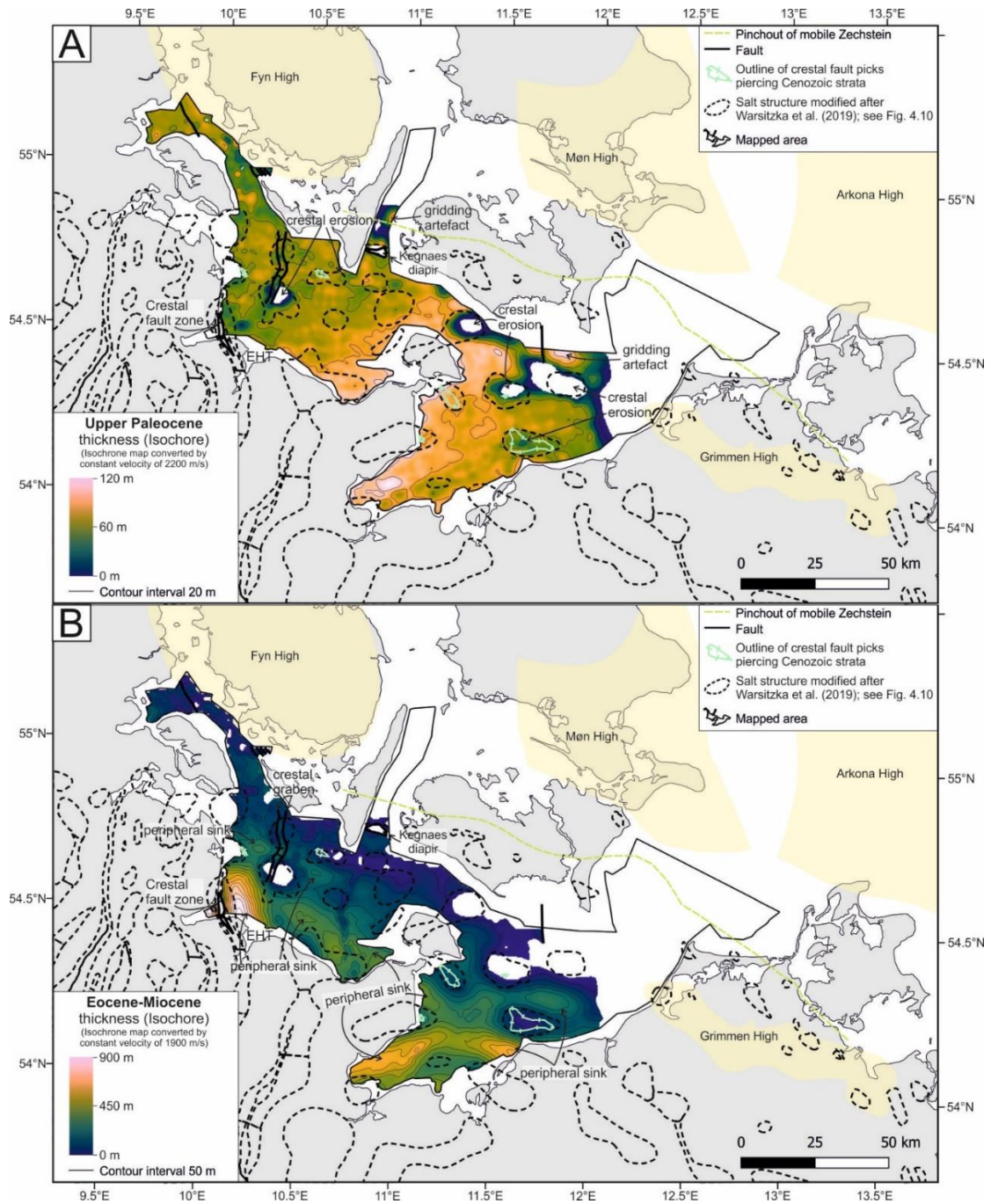


Figure 5.12: Isochore maps of Paleogene and Neogene units (isochrone maps converted using a constant interval velocity). A: upper Paleocene, B: Eocene-Miocene. EHT: Eastholstein Trough. Pinchout of mobile Zechstein after Katzung (2004); Pharaoh et al. (2010).

5.5. Interpretation and Discussion

In this section, we interpret and discuss our observations derived from seismic imaging and mapping of the Zechstein, Upper Cretaceous and Cenozoic units in the context of the structural evolution and tectonic framework of the North German Basin (NGB) and adjacent areas. Special emphasis is put on identification and characterization of basin inversion phases. Common criteria of inversion tectonics include the reactivation of normal faults as reverse faults as well as folding and uplift of sedimentary units. Furthermore, inversion induced compression can reactivate salt movement including squeezing, arching of the roofs and growth of salt structures. This leads to the

development of peripheral sinks and thinned overburden above the crest of the salt structure (e.g. Cooper & Williams, 1989; Letouzey et al., 1995; Jackson & Hudec, 2017). In the following, we interpret and discuss phases of salt movement and their relation to phases of Late Cretaceous to Cenozoic inversion. Thereby, we use the terminology explained in the introduction to refer to the individual inversion events (“Subhercynian”, “Laramide”, “Pyrenean”, “Savian”) based upon the geological time when they occurred (Late Cretaceous, late Paleocene, late Eocene- Oligocene, late Oligocene - Miocene).

We presented thickness (isochore) maps of the Zechstein, Upper Cretaceous and Cenozoic units, which represent isochrone maps converted by a constant interval velocity (table 5.1). As the velocity of sedimentary units in the overburden generally increases with depth due to higher compaction, the converted maps underestimate the thickness of the Upper Cretaceous and Cenozoic units in an area, which experienced higher burial depth, e.g. above the rim-syncline of salt structures. Similarly, for areas which experienced less burial, e.g. above the crest of a salt structure, the thickness is overestimated. Therefore, we can expect that the true local thickness variations around salt structures are slightly more pronounced than shown by Fig. 5.11 and 5.12. Zechstein interval velocity varies by composition based on the relative content of halite. Interval velocity increases in rim-synclines, where halite is depleted and mechanically stronger portions of the Zechstein succession dominate (mostly anhydrite and non-evaporite rocks). In salt structures, where halite accumulated, the Zechstein interval velocity converges to the interval velocity of pure halite (4500 m/s) (Schnabel et al., 2021). Thus, we underestimate Zechstein thickness for areas with major salt depletion (Fig. 5.10).

During the mapping procedure, we analyzed and traced visible faults in the Upper Cretaceous and Cenozoic units (Fig. 5.11 and 5.12). Thereby, the extended seismic dataset allowed a reevaluation of previously published fault traces in the study area (Al Hseinat & Hübscher, 2017).

5.5.1. Late Cretaceous: from tectonic quiescence to inversion

The study area wide relatively uniform thickness and concordant layering of the Cenomanian-Turonian unit resulted from the relatively quiet tectonic conditions persisting until the Coniacian to Santonian. This is in good accordance with the results of previous studies (Baltic sector of the NGB: e.g. Hansen et al., 2007; Hübscher et al., 2010; onshore Mecklenburg-Western Pomerania: e.g. Kossow & Krawczyk, 2002; Glückstadt Graben: e.g. Maystrenko et al., 2006).

At the northeastern basin margin, mapping of the Upper Cretaceous units with a detailed stratigraphic subdivision allowed to date the uplift of the Grimmen High and define its northwestern, offshore, spatial extent (Fig. 5.11). The uplift started in the Coniacian-Santonian and persisted in the Campanian. Thus, the uplift occurred contemporaneous to the onset (90-70 Ma) of the Africa-Iberia-Europe convergence and the corresponding inversion in adjacent sub-basins of the Southern Permian Basin (Ziegler et al., 1995; Kley & Voigt, 2008; Kley, 2018; Harz mountains: Voigt et al.,

2004; Lower Saxony: Kockel, 2003; Netherlands: de Jager, 2003; Poland: Krzywiec, 2006; Denmark: Vejbaek & Andersen, 2002). The direction of shortening during this Late Cretaceous inversion event was rather uniformly in NNE-SSW direction (Kley & Voigt, 2008). The Grimmen High strikes NW-SE, which is almost perpendicular to the direction of shortening, which further supports a causative relation (Kossow & Krawczyk, 2002).

In the Eastholstein Trough and in the Bay of Mecklenburg, minor local thickness variations of the Coniacian-Santonian when comparing the overburden above salt structures and their vicinity suggest revived salt movement coeval with uplift of the Grimmen High and the onset of basin inversion (Figs. 5.6, 5.7, 5.9 and 5.11). Thickness variations become more prominent in the Campanian and Maastrichtian, which suggests increased salt movement. In the eastern Bay of Kiel, local thickness variations of Upper Cretaceous units are smaller suggesting less salt movement in the transition between Glückstadt Graben and the northeastern basin margin.

Because of the observed uniform thickness of the Cenomanian-Turonian, we can exclude that differential loading caused the reactivation of salt movement in the Baltic sector of the NGB. The horizontal layering and tectonic quiescence in the Cenomanian-Turonian requires a tectonic trigger for salt movement in the Coniacian-Santonian. The coeval onset of basin inversion makes a thin-skinned reactivation of salt structures driven by compressional intraplate stress related to the Africa-Iberia-Europe convergence reasonable. Minor basement shortening and corresponding reverse movements at inverted basement faults could be sufficient to induce thin-skinned shortening and minor reactivation of preexisting salt structures. Kossow and Krawczyk (2002) estimated about 1 km of subsalt and 3 km of suprasalt shortening for the area north of the Gardelegen Fault up to the northeastern basin margin with progressively decreasing deformation intensity towards the NE (see Fig. 3 in Kossow & Krawczyk, 2002). The expected minor deformation intensity is in accordance to minor salt movement in the Baltic sector of the NGB. At the northeastern basin margin, uplift of the Grimmen High and fault reactivation of the thin-skinned Werre Fault Zone (Ahlrichs et al., 2020) evidence compressional deformation. Onshore Mecklenburg-Western Pomerania, at the southwestern flank of the Western Pomeranian Fault System (WPFS, Fig. 5.1), a recently published 3D geological overview model shows numerous NW-SE striking faults at the base Zechstein (TUNB Working Group, 2021). These faults are decoupled from the overburden and reach at least partly from the onshore mainland up to the eastern coast of the Bay of Mecklenburg. Faults dissecting the base Zechstein in the northeastern part of Fig. 5.8 might represent the offshore prolongation of these onshore faults. The NW-SE orientation of the base Zechstein faults is favorable for a reactivation during Late Cretaceous shortening and similar to the reactivated faults of the WPFS further north, where mobile Zechstein units are absent (Deutschmann et al., 2018; Seidel et al., 2018). Further visible offsets of the base Zechstein imaged by seismic data in the Bay of Mecklenburg could represent additional basement faults (Figs. 5.7 and 5.8). However, the partly small offsets might also represent velocity artefacts, which needs further investigations to verify this assumption.

In the outer Glückstadt Graben, a thin-skinned compressional reactivation of salt movement due to Late Cretaceous inversion was already interpreted by Maystrenko et al. (2006). These authors observed squeezed salt diapirs with arched roofs. However, indications for Late Cretaceous basement shortening in the Glückstadt Graben are lacking and the link of thin- and thick-skinned deformation needs further investigation (Warsitzka et al., 2016). Our interpretation of minor salt movement caused by thin-skinned compression in the Eastholstein Trough and Bay of Kiel is in agreement with Maystrenko et al. (2006). In contrast to the faults of the WPFS, Late Cretaceous contraction acted almost parallel to the approx. NNE-SSW trending salt structures and underlying basement faults of the Glückstadt Graben (Fig. 5.1), which explains the small intensity of salt flow in the Eastholstein Trough (Fig. 5.11). Thereby, the eastern Bay of Kiel and the area around Fehmarn Island represents a transition zone from the influence of the Glückstadt Graben in the west to higher influence of the basin margin faults of the WPFS in the east.

5.5.2. Late Paleocene: large-scale uplift

The upper Paleocene thickness map shows only small variations with large wavelengths in the study area (Fig. 5.12a). In comparison with the NNE-SSW to NE-SW trend of increasing thickness of the Upper Cretaceous units (Fig. 5.11), the upper Paleocene trend is rather NW-SE with a NE-SW elongated zone of increased thickness around Fehmarn Island. However, thickness variations are small and the mapped area might not display the true regional pattern. Thickness variations do not correlate with salt structures in the Bays of Kiel and Mecklenburg. Missing peripheral sinks and concordant layering (see flattened sections in Figs. 5.6 and 5.9) approve that post-depositional erosion caused the thinned overburden above salt structure crests (Fig. 5.12a). Furthermore, lower and middle Eocene deposits imaged in the Eastholstein Trough are likewise relatively uniform in thickness, which indicates ceased salt movement and relative tectonic quiescence during the late Paleocene to middle Eocene (Fig. 5.4).

There are different views in the literature concerning a late Paleocene inversion phase within the Southern Permian Basin. While some authors considered a fault-controlled uplift (e.g. Nalpas et al., 1995; de Jager, 2003) or proposed a domal uplift mechanism by lithospheric folding (e.g. Nielsen et al., 2005; Deckers & van der Voet, 2018), others questioned the existence of late Paleocene inversion and suggested that sea-level fluctuations caused the unconformity (Kockel, 2003). Recent studies explain the unconformity by large-scale domal uplift caused by thinning of the mantle lithosphere and dynamic topography driven by mantle plumes (Kley, 2018; von Eynatten et al., 2021). For the study area, well information and paleogeographic maps prove a stratigraphic gap between Danian chalk and preserved upper Paleocene claystones (Thanetian) (Vinken & International Geological Correlation Programme, 1988; Hoth et al., 1993). Assuming that fault-controlled uplift caused the stratigraphic gap, we would expect local thickness variations and thin-skinned compressional reactivation of salt movement similar to the Late Cretaceous inversion event. However, the structural style of deformation of the Paleocene is quite different to the Late Cretaceous inversion. The lack of salt movement and the regional unconformity overlain by upper

Paleocene deposits of relatively uniform thickness are in better accordance with a large-scale domal uplift. The structural style in the Paleocene is similar to the Mid Jurassic North Sea Doming event, where large-scale uplift and erosion in the Jurassic was followed by a period of relative tectonic quiescence in the Albian to Turonian (Hansen et al., 2007; Hübscher et al., 2010). The temporal correlation of the stratigraphic gap in the study area (ca. 66 - 59 Ma) with the late Paleocene domal uplift in other parts of the Southern Permian Basin suggests a causative relation (Central Europe, 75 - 55 Ma: von Eynatten et al., 2021; southern North Sea, 62 - ca. 59 Ma: Deckers & van der Voet, 2018; British Isles, 65 - 55 Ma: Holford et al., 2009). Thereby, the Baltic sector of the NGB could mark the northeastern prolongation of the domal uplift in central Germany (von Eynatten et al., 2021).

5.5.3. Cenozoic salt movement

Diverging upper Eocene strata and development of a large peripheral sink in the Eastholstein Trough evidence the reactivation of salt movement and renewed activity in the outer Glückstadt Graben (Figs. 5.4 and 5.12). Salt movement persisted during the late Eocene to Miocene indicated by the development of peripheral sinks and crestal faulting above the salt structures “Schleimünde” and “Kieler Bucht” with increased infill of the crestal graben with Eocene-Miocene deposits. This is in accordance to previous studies investigating the eastern Glückstadt Graben (onshore: Baldschuhn et al., 2001; Maystrenko et al., 2005a; offshore: Hansen et al., 2005; Al Hseinat et al., 2016; Huster et al., 2020).

Outside of the Eastholstein Trough, we observe eroded or thinned Eocene-Miocene strata above salt structure crests, whereas the unit shows increased thickness above rim-synclines (Fig. 5.12b). These local thickness variations clearly correlate with the salt structures in the Bays of Kiel and Mecklenburg. This suggests salt withdrawal from rim-synclines and subsidence of the overlying overburden, while corresponding growth of salt structures subjects the crestal overburden to a higher degree of erosion. However, the preserved Eocene-Miocene unit lacks divergent strata, even above rim-synclines, that would directly date the salt movement (Figs. 5.7, 5.8 and 5.9). Neogene uplift and erosion and subsequent Quaternary glacial erosion (Sirocko et al., 2008; Rasmussen, 2009) removed much of the Eocene-Miocene deposits in the Baltic sector of the NGB. Well information and pre-Quaternary maps of the study area and adjacent onshore regions indicate that preserved sedimentary units are mostly of early to middle Eocene and partly late Eocene, Oligocene and early Miocene age (wells onshore Mecklenburg Western Pomerania: Hoth et al., 1991; Pre-Quaternary maps of Schleswig Holstein and Mecklenburg - Western Pomerania: Hinsch, 1991; Schulze, 1995). The latter occur mostly above rim-synclines of salt structures. Therefore, we can assume that outside of the Eastholstein Trough, our mapped Eocene-Miocene unit comprises mostly lower to middle Eocene deposits. Based on a conceptual model (Fig. 5.13), we propose that the reactivation of salt movement took place in post-middle Eocene times due to the following considerations:

The Albian and Upper Cretaceous units were deposited above a major erosional unconformity (Fig. 5.2). During deposition, relative tectonic quiescence persisted with

uniform thickness distribution and horizontal layering. During Late Cretaceous inversion, minor salt movement led to minor local thickness variations. Thus, we can still consider layering as approx. horizontal at the Late Cretaceous-Danian to late Paleocene transition, especially as large-scale late Paleocene erosion presumably re-flattened the paleo-relief (Fig. 5.13a). Assuming no salt movement occurred during the Cenozoic, we would expect horizontally layered sedimentary units deposited in Eocene to early Miocene shallow to deep marine conditions. Neogene and Quaternary erosion removed sedimentary units but a more or less horizontal layering would remain (Fig. 5.13b). However, seismic images show that the Eocene-Miocene unit is folded across the salt structures (Figs. 5.5, 5.7 and 5.8), which requires a post-middle Eocene phase of salt movement that overprinted prior horizontal layering of upper Paleocene to middle Eocene deposits (Fig. 5.13c). Neogene and Quaternary erosion then removed synkinematic divergent strata (Fig. 5.8c), leaving behind mostly the prekinematic lower to middle Eocene (Fig. 5.13c). We cannot fully exclude that the reactivation of salt movement in the Cenozoic was during the Neogene. However, the observed renewed salt movement in the eastern Glückstadt Graben during the late Eocene to Oligocene makes a coeval reactivation of the salt structures of the Eastholstein Mecklenburg Block likely. Local thickness variations of the Eocene-Miocene units exceed those of Upper Cretaceous units by far (Figs. 5.4, 5.11 and 5.12b). Hence, after the initial growth of salt structures in the Triassic and Jurassic, the second major phase of salt movement and growth of salt structures was likely in the late Eocene to early Miocene.

Late Cretaceous - Danian to late Paleocene transition:

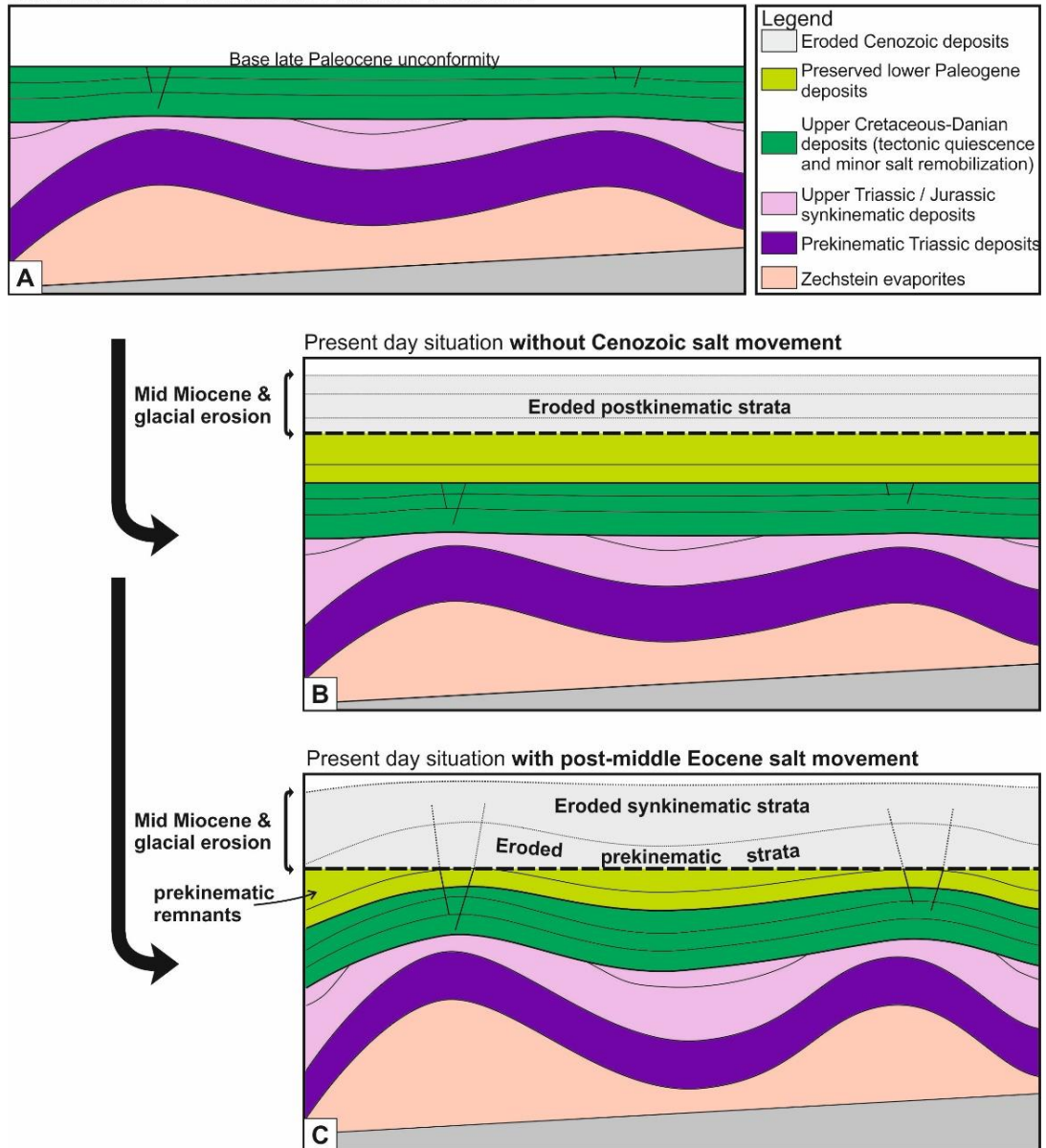


Figure 5.13: Conceptual model visualizing the necessity of a Cenozoic phase of salt movement. A: Initial situation at Late Cretaceous-Danian to late Paleocene transition. B: Present-day situation without Cenozoic salt movement. Note that only postkinematic strata is eroded. C: Present-day situation with post-middle Eocene salt movement. Note the eroded prekinematic strata, prekinematic remnants and the eroded synkinematic (divergent) strata.

5.5.4. Cause of Cenozoic reactivation of salt movement

The uniform thickness of the upper Paleocene unit suggests a phase of salt tectonic quiescence that ended in the late Eocene. In the following, we discuss potential trigger mechanism for the late Eocene salt remobilization.

The late Eocene to Oligocene reactivation of salt movement was contemporaneous to recommencing northward movement of Iberia and increasing rates of Africa-Iberia-Adria-Europe convergence associated to the Pyrenean and Alpine orogenies (e.g. Handy et al., 2010). This resulted in approx. N-S directed shortening in the European foreland and a further phase of inversion in the Southern Permian Basin (e.g. Kley, 2018). The direction of compression is similar to the Late Cretaceous inversion event

and almost parallel to the NNE-SSW striking Glückstadt Graben. As discussed before, this makes the structures unfavorable for compressional reactivation. At the northeastern basin margin, shortening during the late Eocene-Oligocene inversion event acted oblique to the NW-SE striking faults of the WPFS (Fig. 5.1) and further SW located base Zechstein faults (shown in a 3D geological overview model, see TUNB Working Group, 2021). Here, we cannot exclude a contribution to salt movement driven by compression. However, salt movement in post-middle Eocene times exceeded the salt flow during the Late Cretaceous. It is therefore questionable why similar directed compressional stress would result in a quite different response of the salt structures in the study area, especially in the Glückstadt Graben (minor Late Cretaceous vs. major late Eocene movement), in particular as shortening during the Late Cretaceous event was stronger than during the Paleogene (e.g. Vejbaek et al., 2010).

Coeval with the late Eocene-Oligocene revived activity in the Glückstadt Graben, Central Europe experienced rifting and the development of the European Cenozoic Rift System (ECRIS, Fig. 5.14) (Dèzes et al., 2004). Development of the northern part of the ECRIS, namely the Upper Rhine Graben, the Roer Graben and the Hessian grabens, began during the late Eocene (Dèzes et al., 2004). The authors attributed opening of the rifts to transtensional reactivation of older crustal discontinuities controlled by orthogonal N to NE directed compressional stress originating in the Alpine and Pyrenean collision zones. However, missing strike-slip deformation of upper Eocene-Oligocene deposits, as well as poorly constrained dating of compressional deformation, in the Upper Rhine Graben and the Massif Central grabens led Michon and Merle (2005) to question an Alpine control. They interpreted the late Eocene-Oligocene development in terms of passive rifting due to E-W to ESE-WNW extension (Fig. 5.14).

The Glückstadt Graben is located approx. 500 km north of the Upper Rhine Graben (Fig. 5.14). In contrast to the Rhine Rift System, it is floored by thick Zechstein salt. Maystrenko et al. (2005a) noted that the rapid subsidence in the Glückstadt Graben during the Paleogene to Neogene coincided with subsidence of the North Sea and was likely related to E-W extension. An E-W extensional event acted almost perpendicular to the graben axis, thus making a reactivation favorable. This is in agreement with a higher degree of salt movement compared to the Late Cretaceous and the observed reactivation of the N-S striking crestal graben in the western Bay of Kiel (Fig. 5.12b). Moreover, the development of a N-S striking normal fault, which pierces from the basement into the Paleogene successions, proves E-W extension (Scheck-Wenderoth et al., 2008). This fault is located at the eastern border of the Eastholstein Trough, below the onshore part of the salt structure “Plön” (Figs. 5.1 and 5.3). In the Bay of Kiel, a thick-skinned fault like this is not visible and thin-skinned faulting predominates. The coeval activity of the ECRIS and similar favorable orientation makes an extensional trigger for Cenozoic salt movement in the southwestern Baltic sector of the NGB plausible and suggests a causative relationship to the development of the ECRIS (Fig. 5.14). At the northeastern basin margin, an extensional reactivation of the approx. NNW-SSE striking basement faults, south to southeast of the Bay of Mecklenburg, could also induce a reactivation of salt movement by thin-skinned extension. However, whether these faults were reactivated during the Cenozoic is unclear. To validate this, further research, including improved images of the subsalt, is needed.

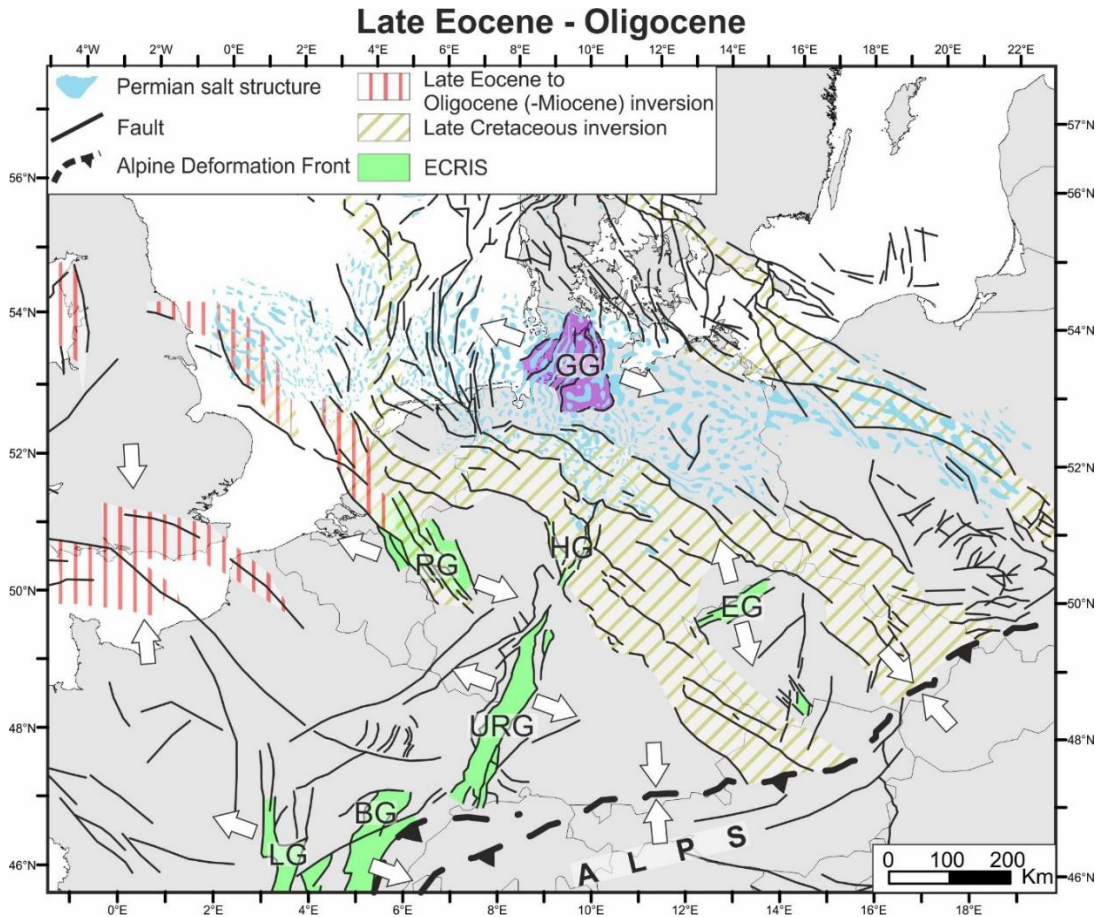


Figure 5.14: Regional sketch map showing late Eocene to Oligocene stage of structural evolution of the European Cenozoic Rift System (ECRIS) in relation to the Glückstadt Graben and salt structures in the study area. Arrows indicate kinematics. Areas affected by Late Cretaceous and late Eocene to Oligocene (Miocene) inversion are also shown. Compiled after Michon et al., 2003; Dèzes et al., 2004; Mazur et al., 2005; Kley et al., 2008; Kley, 2018. Fault pattern simplified and without claim to completeness. BG: Bresse Graben; EG: Eger Graben; HG: Hessian grabens; LG: Limagne Graben; GG: Glückstadt Graben; Roer Graben; URG: Upper Rhine Graben.

5.6. Conclusions

We analyzed the Late Cretaceous and Paleogene evolution in the Baltic sector of the North German Basin margin using a dense network of high-resolution 2D seismic data. Stratigraphic interpretation was linked to previous studies and nearby wells. We presented key prestack depth migrated seismic profiles and thickness maps of the Zechstein, Upper Cretaceous and Cenozoic units with refined stratigraphic subdivisions that are novel for the study area. We used a refraction traveltime tomography to estimate an averaged interval velocity for key Upper Cretaceous and Cenozoic units, which we used to constrain constant velocities for time-depth conversion. The Zechstein thickness map allowed redefining the geometry of four salt structures in the Bays of Kiel and Mecklenburg. The refined stratigraphic subdivision allows differentiating between episodes of increased tectonic activity during the Late Cretaceous and Cenozoic. The main conclusions are:

- Late Cretaceous basin inversion in the Baltic sector of the North German Basin started coevally with neighboring sub-basins in the Coniacian-Santonian with increased activity in the Campanian. Shortening induced by Africa-Iberia-

Europe convergence caused uplift of the Grimmen High and contemporaneous minor movement of Zechstein salt in the outer Glückstadt Graben and Bay of Mecklenburg. However, salt movement leading to growth of salt structures and the development of peripheral sinks was relatively small compared to later Cenozoic movements.

- Upper Paleocene thickness variations are minor and have large wavelengths in the study area. Salt movement ceased during the Paleocene without further growth until the middle Eocene. The regional unconformity at the base of the upper Paleocene unit is in accordance with a large-scale domal uplift in the late Paleocene. The structural style is similar to the Jurassic/early Cretaceous, where large-scale erosion due to the North Sea doming event was followed by a phase of tectonic quiescence.
- Upper Eocene and Neogene successions in the eastern Glückstadt Graben proof salt movement by increased sediment accumulation and diverging reflectors within peripheral sinks. The reactivation of salt movement began in the late Eocene and lasted to early Miocene times.
- Outside the Glückstadt Graben, eroded Paleogene deposits hamper direct evidence for late Eocene salt movement in the Bays of Kiel and Mecklenburg. However, thickness variations of preserved strata and missing synkinematic strata indicate significant salt movement in post-middle Eocene times. We propose that this phase of intensified salt movement was coeval and causally related to the salt flow in the eastern Glückstadt Graben during the late Eocene to Oligocene. However, we cannot fully exclude a phase of Neogene salt movement. Salt structure growth during the Cenozoic exceeded growth during Late Cretaceous inversion and represents the phase of major growth since the Late Triassic to Jurassic initial salt structure growth.
- Cenozoic salt movement in the study area is coeval with renewed compressional stress in Central Europe induced by the Pyrenean and Alpine orogenies. Thin-skinned compressional salt movement induced by a reactivation of basement faults at the northeastern basin margin could explain the reactivation of salt movement in the Cenozoic in the Bay of Mecklenburg. For the Glückstadt Graben, a compressional reactivation seems unlikely. The different structural style of minor Late Cretaceous and major Cenozoic movement suggests that compression is not the best explanation for the reactivation of salt flow during the Cenozoic, especially for the Glückstadt Graben. An E-W directed extensional event possibly related to the development of the European Cenozoic Rift System is more suitable as a driver of Cenozoic salt movement in the southwestern Baltic sector of the North German Basin. Whether salt movement at the northeastern basin margin might also be induced by an extensional reactivation of basement fault at the basin margin needs further analysis.

Acknowledgements

We would like to thank the reviewers Piotr Krzywiec, Clara Rodriguez and Torsten Hundebøl Hansen for their helpful and detailed comments. Further, we are thankful to Michael Schnabel for his helpful remarks on the manuscript. We thank Emerson for providing licenses of their software under the Paradigm University Research Program.

The scientific colormap *batlow* is used in this study to prevent visual distortion of the data and exclusion of readers with color-vision deficiencies (Cramer et al., 2020). This work is a research and development study connected to the TUNB project by the Federal Institute of Geosciences and Natural Resources (BGR) and the geological surveys of the northern German federal states.

Data availability: Seismic profiles, isochore maps (in TWT and meters) shown in this study and time-structure maps used to create the isochore maps are available in the supplementary material of this article (see Ahlrichs et al., 2021b). Further seismic data used for mapping, are available from the authors and the Federal Institute for Geosciences and Natural Resources (BGR) upon reasonable request. The authors thank ExxonMobil Production Deutschland GmbH for providing the seismic profiles of the GSI76B survey.

Author contributions: Conceptualization of this work was done by NA, CH and VN. NA is the corresponding author and carried out the seismic processing, seismic interpretation and mapping in this study. NA created the figures and was the primary writer of the manuscript. Structural interpretation and the discussion of the results in the context of the regional framework was done by NA, VN, CH and ES. AW applied the refraction traveltimes tomography, extracted the velocity information and mainly wrote the paragraph describing the tomography method in section 3.3. JK provided further input in the discussion of the results and their association with inversion events in Central Europe. All authors contributed to editing of the manuscript.

Funding: Gefördert durch die Deutsche Forschungsgemeinschaft (DFG) - 396852626/funded by the Deutsche Forschungsgemeinschaft (DFG, German Research Foundation) - 396852626.

Conflicts of interest: The authors declare that they have no conflict of interest.

6. Discussion and Conclusions

This thesis represents a comprehensive evaluation of the structural and salt tectonic evolution of the Baltic sector of the North German Basin from Permian to recent times using a regional dense network of 2D high-resolution reflection seismic profiles in combination with onshore and offshore wells. The presented results improve the understanding of regional tectonics and its impact on salt structure evolution in the northern North German Basin over the course of late Permian deposition of the Zechstein salt, Triassic initial salt movement until Late Cretaceous and Cenozoic reactivation of salt flow.

In the scope of this thesis, the Mesozoic – Cenozoic stratigraphic framework of the study area was refined to a stratigraphic subdivision beyond the level of geological series. Using the 2D high-resolution seismic profiles of the BalTec data, previous more local seismic surveys could be connected and incorporated into a regional dense network of multichannel seismic data covering the area from the western Bay of Kiel up to northeast of Rügen Island. As a starting point, stratigraphic correlation of key seismic horizons with nearby onshore well data was established using a 170 km SW-NE regional seismic transect extending from the Bay of Mecklenburg to northeast of Rügen Island (Chapter 3). Subsequently, identified post-Permian horizons were traced across the entire study area and further well-control was added which resulted in a for the study area unprecedented seismo-stratigraphic subdivision of Triassic to Cenozoic units (Triassic – Jurassic: Chapter 4, Late Cretaceous – Cenozoic: Chapter 5.). The derived regional maps of post-Permian units visualize the depth structure and thickness of the Zechstein to Cenozoic subsurface. Thereby, fault analysis differentiated between subsalt and suprasalt faults and yielded an update of basement faults and of the suprasalt faults of Mesozoic – Cenozoic fault systems in the study area. Mapping of the Zechstein unit revealed a novel salt structure in the Little Belt and provided an update of the shape and location of salt structures in the bays of Kiel and Mecklenburg.

Collectively, the articles in the framework of this thesis provide a comprehensive reassessment of salt tectonics in the Baltic sector of the North German Basin. The results specified the temporal episodes of salt movement and their spatial differences across the study area and allowed a conclusive interpretation of the underlying driving mechanisms. In most parts of the study area, no indications for salt movement during the Early and Middle Triassic could be observed. However, at the Kegnaes Diapir, located at the northern basin margin, seismic interpretation revealed indications for salt movement and faulting in Early Triassic times during deposition of the Buntsandstein. This is in contrast to common interpretations of relatively quiet tectonic conditions and the absence of salt movement during Early to Middle Triassic thermal subsidence suggesting that this concept of quiet tectonic conditions characterized by thermal subsidence would have to be at least expanded for the northern basin margin. In the Late Triassic, major salt movement began at the northeastern Glückstadt Graben during deposition of the Grabfeld, Stuttgart and Weser formations (Ladinian – Carnian times) under regional E-W extension. At the northeastern basin margin, thin-skinned faulting was observed coeval with the onset of salt movement. Thin-skinned faulting is associated with transtensional movements within the Trans-European Suture Zone and

corresponding reactivation of deep-seated Paleozoic faults. Transtensional faulting caused increased subsidence at the northeastern basin margin which formed a local sub-basin characterized by increased accumulation of Keuper and Jurassic deposits. In between the Glückstadt Graben and the Tornquist Zone controlled fault systems of the northeastern basin margin, the salt structures located within the Eastholstein-Mecklenburg Block do not show indications for salt movement earlier than the latest Triassic – Early Jurassic. Accordingly, this area marks a more stable transition zone which likely experienced less extension. Basement faults are absent underneath the salt structures of the Eastholstein-Mecklenburg Block. Due to the temporal correlation of initial salt movement and regional E-W extension, thin-skinned extension is interpreted as the trigger mechanism for the Triassic initial development of salt structures. The Mid Jurassic North Sea Doming event subjected the study area to erosion causing a widespread hiatus. When sedimentation resumed in the Albian, the study area experienced a phase of relative tectonic quiescence without salt movement until the Turonian.

Seismic imaging in this thesis allowed specifying the onset of Late Cretaceous inversion to the Coniacian - Santonian. Late Cretaceous inversion in the study area is expressed by uplift of the Grimmen High, reactivation of normal as reverse faults at the northeastern basin margin and the reactivation of minor salt flow in the northeastern Glückstadt Graben and Bay of Mecklenburg. However, salt movement lasted only until the end of the Late Cretaceous. Thin-skinned shortening most likely caused the reactivation of salt flow during the Late Cretaceous. Based on a detailed discussion, a significant contribution to salt structure growth by gravity gliding induced by basin margin tilt seems unlikely. A minor contribution to salt accumulation by slow downdip creeping and updip depletion could be possible.

Further postulated Cenozoic inversion events temporally correlate with increased tectonic activity in the Baltic sector of the North German Basin. In the Paleocene, regional and relatively uniform erosion of upper Paleocene units without indications for fault reactivation and salt movement suggest that the study area experienced large-scale domal uplift rather than inversion. Overlying upper Paleocene and lower to middle Eocene deposits evidence a renewed phase of relative tectonic quiescence lacking salt movement. In the late Eocene to Oligocene, major reactivation of salt movement occurred at the northeastern Glückstadt Graben and regional mapping indicated contemporaneous reactivation of salt flow within the Eastholstein-Mecklenburg Block. This Cenozoic phase of salt structure growth critically exceeded growth during Late Cretaceous inversion. The different structural style of minor Late Cretaceous and major Cenozoic salt movement in the northeastern Glückstadt Graben contradicts a compressional control of Cenozoic salt flow even though it temporally correlates with inversion events which are associated to rebuilding N-S directed compressional stress in Central Europe induced by the Pyrenean and Alpine orogenies. For the Baltic sector of the North German Basin, late Eocene to Oligocene extension is a better explanation for major reactivation of salt flow in the Glückstadt Graben and this extensional event is possibly related to the contemporaneous development of the European Cenozoic Rift System.

Overall, this thesis shows that salt structure evolution in the Baltic sector of the North German Basin is strongly controlled by regional tectonics. Periods characterized by increased salt movement correlate with phases of extension or shortening. These periods of active salt movement in the Late Triassic –Early Jurassic and Cenozoic (beginning in late Eocene) were triggered by extension while Late Cretaceous salt movement started with the onset of regional shortening. In between, phases of relative tectonic quiescence lacking salt movement have been documented. These periods without salt movement were each preceded by regional erosion events (e.g. erosion due to Middle Jurassic North Sea Doming and Paleocene large-scale domal uplift), which seemed to have balanced the differential load driving salt movement.

7. Outlook

While the results of this thesis provide a comprehensive evaluation of the structural evolution of the Baltic sector of the North German Basin from Permian to recent times, there are still open questions and further research topics regarding the structural evolution of the area. Some aspects of future research are briefly highlighted below.

This thesis provided an analysis of the fault pattern in the Baltic sector of the North German Basin and revealed repeated reactivation of faults during the Mesozoic and Cenozoic basin history. In seismic data analyzed in this work, many faults could be traced up to the base Quaternary. However, whether these faults reach into the Quaternary deposits and were active during the Quaternary glaciations could not be shown due to the limited resolution of the shallow strata in most seismic profiles. Future research could strive for an improved imaging of the Quaternary unit and its internal geometry. Incorporating high-resolution seismic data and sediment echosounder data would allow imaging the seafloor and uppermost sedimentary layers. This could help to identify shallow faults within the Quaternary deposits. In combination with the dense seismic database in the Baltic sector of the North German Basin, these shallow Quaternary faults can be interpreted within the Mesozoic – Cenozoic structural framework to investigate the impact of glaciation on fault reactivation and a possible impact on underlying salt structures.

Another aspect of future research is the reassessment of Pre-Permian tectonics using the BalTec data. The large offsets of this dataset (active cable length of 2700 m) allow improved subsalt imaging by e.g. inverse Q filtering, prestack depth migration or multiparameter stacking (CRS). Based on these improved images, the basement geometry and the presence of basement faults can be investigated to better understand the influence of preexisting basement structures on the Mesozoic – Cenozoic development of salt structures and fault systems.

Future research could further integrate the findings of this thesis into the tectonic framework of Central Europe. Open questions remain especially regarding the Cenozoic tectonic evolution of Central Europe. While Paleogene and Neogene inversion and uplift are reported e.g. for the Dutch basins, the Channel region and the Danish North Sea (e.g. de Jager, 2003; Rasmussen, 2009; Kley, 2018), other adjacent areas like the NGB have undergone simultaneous extension (e.g. the Glückstadt Graben as reported in this study or the grabens of the European Cenozoic Rift System, e.g. Michon et al., 2003; Dèzes et al., 2004; Scheck-Wenderoth et al., 2008; Ahlrichs et al., 2021a). These events of extension or shortening are commonly associated with far-field stress originating from the Alpine Orogeny, which is transferred within the European foreland. Additionally, parts of Central Europe experienced large-scale domal uplift related to mantle processes such as dynamic topography during the Paleocene and Neogene (e.g. von Eynatten et al., 2021; Green et al., 2022). The exact timing and spatial extent of these domal uplift events remain partly unclear and require further regional mapping efforts. Future research, which aims to better understand the underlying mechanisms of extension, shortening and domal uplift during the Cenozoic would need to incorporate the different local to regional observations into a European-wide tectonic framework to establish a consensus tectonic model of the Cenozoic

structural evolution of Central Europe. Combining geological data used in sedimentary basin analysis with global mantle circulation models would help to better understand the impact of mantle processes on the stress transferred within the crust of Central Europe.

Acknowledgements

I am very grateful to all the support and assistance I have received while working on this thesis.

First of all, I would like to thank my supervisor Prof. Dr. Christian Hübscher for setting me up on this project, his continuous support and guidance throughout the project, the confidence in my work and the administrative help on all University of Hamburg related issues. Thank you Christian for the numerous inspiring and insightful discussions, the friendly and supportive contact and your enthusiasm when discussing new research.

Further, I would like to thank Dr. Vera Noack for her supervision on the part of the Federal Institute for Geosciences and Natural Resources (BGR). I am grateful for your great support, guidance, tireless proofreading and help dealing with administrative issues at the BGR. Your door was always open for me, which I really appreciated.

I would further like to thank Dr. Michael Schnabel for his support during the project, especially the help on all seismic processing related topics. Thank you for sharing some of your processing tricks with me and your constructive and lucid remarks when reviewing my work.

I am very grateful to Dr. Elisabeth Seidel for plenty of fruitful discussions, support and great help during this project. Further I like to thank Elisabeth Seidel, Jonas Preine and Henrik Grob for proofreading the manuscript of this dissertation.

I like to thank Tobias Häcker (Univ. of Hamburg) for reprocessing seismic profiles located in the Bay of Mecklenburg and the Bay of Kiel.

I thank Emerson for providing licenses of their software under the Paradigm University Research Program.

Last, but not least, I am incredibly grateful to my wife Anna for her endless support, love and patience.

Gefördert durch die Deutsche Forschungsgemeinschaft (DFG) - 396852626/funded by the Deutsche Forschungsgemeinschaft (DFG, German Research Foundation) – 396852626.

References

- Ahlrichs, N., Hübscher, C., Noack, V., Schnabel, M., Damm, V., & Krawczyk, C. M. (2020). Structural Evolution at the Northeast North German Basin Margin: From Initial Triassic Salt Movement to Late Cretaceous-Cenozoic Remobilization. *Tectonics*, 39(7), 1-26. <https://doi.org/10.1029/2019TC005927>
- Ahlrichs, N., Noack, V., Hübscher, C., Seidel, E., Warwel, A., & Kley, J. (2021a). Impact of Late Cretaceous inversion and Cenozoic extension on salt structure growth in the Baltic sector of the North German Basin. *Basin Research*, 34(1), 220-250. <https://doi.org/10.1111/bre.12617>
- Ahlrichs, N., Noack, V., Hübscher, C., Seidel, E., Warwel, A., & Kley, J. (2021b). *Prestack depth migrated, multichannel seismic data, thickness maps and time-structure maps of the Baltic Sea sector of the North German Basin* PANGAEA. <https://doi.org/10.1594/PANGAEA.932928>
- Ahlrichs, N., Noack, V., Seidel, E., & Hübscher, C. (2022). Triassic-Jurassic salt movement in the Baltic sector of the North German Basin and its relation to post-Permian regional tectonics. *Submitted to Basin Research*.
- Al Hseinat, M. (2016). *A seismic reflection study of the Late Cretaceous to recent structural evolution of the North German Basin and the transition zone to the Baltic Shield (Southwest Baltic Sea)* [Dissertation, University of Hamburg]. Hamburg.
- Al Hseinat, M., & Hübscher, C. (2014). Ice-load induced tectonics controlled tunnel valley evolution – instances from the southwestern Baltic Sea. *Quaternary Science Reviews*, 97, 121-135. <https://doi.org/10.1016/j.quascirev.2014.05.011>
- Al Hseinat, M., & Hübscher, C. (2017). Late Cretaceous to recent tectonic evolution of the North German Basin and the transition zone to the Baltic Shield/southwest Baltic Sea. *Tectonophysics*, 708, 28-55. <https://doi.org/10.1016/j.tecto.2017.04.021>
- Al Hseinat, M., Hübscher, C., Lang, J., Lüdmann, T., Ott, I., & Polom, U. (2016). Triassic to recent tectonic evolution of a crestal collapse graben above a salt-cored anticline in the Glückstadt Graben/North German Basin. *Tectonophysics*, 680, 50-66. <https://doi.org/10.1016/j.tecto.2016.05.008>
- Allen, P. A., & Allen, J. R. (2005). *Basin Analysis - Principles and Applications* (second ed. ed.). Blackwell Publishing Ltd.
- Arndt, G., Stollenwerk, M., & Zenker, F. (1996). *Ergebnisbericht: Reprocessing von digitaleismischen Daten aus der südlichen Ostsee (Petrobaltic)* [unpublished report].
- BABEL Working Group. (1991). Deep seismic survey images crustal structure of Tornquist Zone beneath southern Baltic Sea. *Geophysical Research Letters*, 18(6), 1091-1094.
- BABEL Working Group. (1993). Deep Seismic Reflection/Refraction Interpretation of Crustal Structure Along Babel Profiles A and B In the Southern Baltic Sea. *Geophysical Journal International*, 112(3), 325-343. <https://doi.org/10.1111/j.1365-246X.1993.tb01173.x>
- Bachmann, G. H., Geluk, M., Warrington, G., Becker-Roman, A., Beutler, G., Hagdorn, H., Hounslow, M., Nitsch, E., Röhling, H.-G., Simon, T., & Szulc, A. (2010). Triassic. In H. Doornenbal & A. G. Stevenson (Eds.), *Petroleum Geological Atlas of the Southern Permian Basin Area* (pp. 149-173). EAGE Publications.

- Bachmann, G. H., & Kozur, H. W. (2004). The Germanic Triassic: correlations with the international chronostratigraphic scale, numerical ages and Milankovitch cyclicity. *Hallesches Jahrbuch für Geowissenschaften*, 26, 17-62.
- Bachmann, G. H., Voigt, T., Bayer, U., von Eynatten, H., Legler, B., & Littke, R. (2008). Depositional history and sedimentary cycles in the Central European Basin System. In R. Littke, U. Bayer, D. Gajewski, & S. Nelskamp (Eds.), *Dynamics of complex intracontinental basins, the Central European Basin System* (pp. 17-34). Springer Verlag. <https://doi.org/10.1007/978-3-540-85085-4>
- Baldschuhn, R., Binot, F., Fleig, S., & Kockel, F. (2001). Geotektonischer Atlas von Nordwest-Deutschland und dem deutschen Nordsee Sektor [Bilingual digital atlas of the geotectonic structure of Northwestern Germany and the German North Sea sector]. *Geologisches Jahrbuch*, A(153), 1-88.
- Baltic Sea Hydrographic Commission. (2013). *Baltic Sea Bathymetry Database*. Retrieved 15.02.2022 from <http://data.bshc.pro/>
- Benek, R., Kramer, W., McCann, T., Scheck, M., Negendank, J., Korich, D., Huebscher, H.-D., & Bayer, U. (1996). Permo-Carboniferous magmatism of the Northeast German Basin. *Tectonophysics*, 266, 379-404.
- Berthelsen, A. (1992). Tectonic evolution of Europe. From Precambrian to Variscan Europe. In M. D. Blum (Ed.), *A continent revealed: The European Geotraverse* (pp. 153-164). Cambridge University Press.
- Berthelsen, A. (1998). The Tornquist Zone northwest of the Carpathians: An intraplate pseudosuture. *GFF*, 120, 223-230. <https://doi.org/10.1080/11035899801202223>
- Best, G. (1989). Die Grenze Zechstein/Buntsandstein in Nordwest-Deutschland nach Bohrlochmessungen [The Boundary Zechstein/Buntsandstein in Northwest Germany according to Wireline Logs]. *Zeitschrift der Deutschen Geologischen Gesellschaft*, 140(1), 73-85. <https://doi.org/10.1127/zdgg/140/1989/73>
- Best, G. (1996). Floßtektonik in Norddeutschland: Erste Ergebnisse reflexionsseismischer Untersuchungen an der Salzstruktur "Oberes Allertal". *German Journal of Geology*, 147(4), 455-464.
- Betram, G. T., & Milton, N. J. (1989). Reconstructing basin evolution from sedimentary thickness; the importance of palaeobathymetric control, with reference to the North Sea. *Basin Research*, 1, 247-257. <https://doi.org/10.1111/j.1365-2117.1988.tb00020.x>
- Beutler, G., Dietrich, D., Dockter, J., Ernst, R., Etzold, A., Farrenschon, J., & et al. (2005). Stratigraphie von Deutschland IV – Keuper. *Courier Forschungsinstitut Senckenberg, Germany*, 253, 1-296.
- Beutler, G., Junker, R., Niedieck, S., & Rößler, D. (2012). Tektonische Diskordanzen und tektonische Zyklen im Mesozoikum Nordostdeutschlands. [Tectonic unconformities and tectonic cycles of the Mesozoic in Northeastern Germany.]. *Zeitschrift der Deutschen Gesellschaft für Geowissenschaften*, 163(4), 447-468. <http://dx.doi.org/10.1127/1860-1804/2012/0163-0447>
- Beutler, G., & Schüler, F. (1978). Die altkimmerischen Bewegungen im Norden der DDR und ihre regionale Bedeutung. *Zeitschrift für Geologische Wissenschaften*, 6, 403-420.
- Bialas, J., Flueh, E. R., & Jokat, W. (1990). Seismic investigations of the Ringkøbing-Fyn High on Langeland, Denmark. *Tectonophysics*, 176(1-2), 25-41. [https://doi.org/10.1016/0040-1951\(90\)90257-9](https://doi.org/10.1016/0040-1951(90)90257-9)

- Blanc, E. J. P., Allen, M. B., Inger, S., & Hassani, H. (2003). Structural styles in the Zagros Simple Folded Zone, Iran. *Journal of the Geological Society*, *160*, 401-412. <https://doi.org/10.1144/0016-764902-110>
- Bond, C. E. (2015). Uncertainty in structural interpretation: Lessons to be learnt. *Journal of Structural Geology*, *74*, 185-200. <http://dx.doi.org/10.1016/j.jsg.2015.03.003>
- Brink, H., Dürschner, H., & Trappe, H. (1992). Some aspects of the late and post-Variscan development of the Northwestern German Basin. *Tectonophysics*, *207*(1), 65-95. [https://doi.org/10.1016/0040-1951\(92\)90472-I](https://doi.org/10.1016/0040-1951(92)90472-I)
- Brink, H., Franke, D., Hoffmann, N., Horst, W., & Oncken, O. (1990). Structure and evolution of the North German Basin. In R. Freeman, P. Giese, & S. Müller (Eds.), *The European Geotraverse: Integrative studies* (pp. 195-212). European Science Foundation.
- Brun, J.-P., & Fort, X. (2011). Salt tectonics at passive margins: Geology versus models. *Marine and Petroleum Geology*, *28*(6), 1123-1145. <https://doi.org/10.1016/j.marpetgeo.2011.03.004>
- Brun, J.-P., & Fort, X. (2012). Salt tectonics at passive margins: Geology versus models – Reply. *Marine and Petroleum Geology*, *37*(1), 195-208. [10.1016/j.marpetgeo.2012.04.008](https://doi.org/10.1016/j.marpetgeo.2012.04.008)
- Brun, J.-P., & Nalpas, T. (1996). Graben inversion in nature and experiments. *Tectonics*, *15*(3), 677-687. <https://doi.org/10.1029/95tc03853>
- Bundesanstalt für Geowissenschaften und Rohstoffe, & University of Hamburg. (2016). *BalTec* Federal Institute for Geosciences and Natural Resources. https://www.geo-seas.eu/search/welcome.php?query=1651&query_code={AE327628-EB83-4FDE-B5BB-FA5D547E957D}
- Callot, J.-P., Trocmé, V., Letouzey, J., Albouy, E., Jahani, S., & Sherkati, S. (2012). Pre-existing salt structures and the folding of the Zagros Mountains. *Geological Society, London, Special Publications*, *363*(1), 545-561. [10.1144/sp363.27](https://doi.org/10.1144/sp363.27)
- Cartwright, J. (1990). The structural evolution of the Ringkøbing-Fyn High. In D. J. Blundell & A. D. Gibbs (Eds.), *Tectonic evolution of North Sea rifts* (pp. 200-2106). Oxford University Press.
- Clausen, O., & Pedersen, P. (1999). Late Triassic structural evolution of the southern margin of the Ringkøbing-Fyn High, Denmark. *Marine and Petroleum Geology*, *16*(7), 653-665. [https://doi.org/10.1016/S0264-8172\(99\)00026-4](https://doi.org/10.1016/S0264-8172(99)00026-4)
- Cobbold, P. R., & Szatmari, P. (1991). Radial gravitational gliding on passive margins. *Tectonophysics*, *188*(3-4), 249-289. [https://doi.org/10.1016/0040-1951\(91\)90459-6](https://doi.org/10.1016/0040-1951(91)90459-6)
- Coleman, A. J., Jackson, C. A. L., & Duffy, O. B. (2017). Balancing sub- and supra-salt strain in salt-influenced rifts: Implications for extension estimates. *Journal of Structural Geology*, *102*, 208-225. <https://doi.org/10.1016/j.jsg.2017.08.006>
- Cooper, M. A., & Williams, G. D. (1989). *Inversion Tectonics* (Vol. 44). Geological Society. <https://doi.org/10.1144/GSL.SP.1989.044.01.25>
- Coward, M. P. (1983). Thrust tectonics, thin skinned or thick skinned, and the continuation of thrusts to deep in the crust. *Journal of Structural Geology*, *5*(2), 113-123. [https://doi.org/10.1016/0191-8141\(83\)90037-8](https://doi.org/10.1016/0191-8141(83)90037-8)
- Cramer, F., Shephard, G. E., & Heron, P. J. (2020). The misuse of colour in science communication. *Nature Communications*, *11*, 1-10. <https://doi.org/10.1038/s41467-020-19160-7>

- Dadlez, R., & Marek, S. (1998). Major faults, salt- and non-salt anticlines. In R. Dadlez, S. Marek, & J. Pokorski (Eds.), *Paleogeographic atlas of Epicontinental Permian and Mesozoic in Poland (1:2500000)*. Polish Geological Institute.
- Davis, D., & Engelder, T. (1985). The role of salt in fold-and-thrust belts. *Tectonophysics*, *119*(1), 67 - 88. [https://doi.org/10.1016/0040-1951\(85\)90033-2](https://doi.org/10.1016/0040-1951(85)90033-2)
- de Jager, J. (2003). Inverted basins in the Netherlands, similarities and differences. *Netherlands Journal of Geosciences - Geologie en Mijnbouw*, *82*(3), 339-349. <https://doi.org/10.1017/S0016774600020175>
- Deckers, J., & van der Voet, E. (2018). A review on the structural styles of deformation during Late Cretaceous and Paleocene tectonic phases in the southern North Sea area. *Journal of Geodynamics*, *115*, 1-9. <https://doi.org/10.1016/j.jog.2018.01.005>
- DEKORP-BASIN Research Group. (1999). Deep crustal structure of the Northeast German basin: New DEKORP-BASIN '96 deep-profiling results. *Geology*, *27*(1), 55-58. [https://doi.org/10.1130/0091-7613\(1999\)027<0055:Dcsotn>2.3.Co;2](https://doi.org/10.1130/0091-7613(1999)027<0055:Dcsotn>2.3.Co;2)
- Deutschmann, A., Meschede, M., & Obst, K. (2018). Fault system evolution in the Baltic Sea area west of Rügen, NE Germany. *Geological Society, London, Special Publications*, *469*(1), 83-98. <https://doi.org/10.1144/sp469.24>
- Dèzes, P., Schmid, S. M., & Ziegler, P. A. (2004). Evolution of the European Cenozoic Rift System: interaction of the Alpine and Pyrenean orogens with their foreland lithosphere. *Tectonophysics*, *389*, 1-33. <https://doi.org/10.1016/j.tecto.2004.06.011>
- Doornenbal, J. C., & Stevenson, A. G. (2010). *Petroleum Geological Atlas of the Southern Permian Basin Area*. EAGE Publications.
- Drummon, B. J., Hobbs, R. W., & Goleby, B. R. (2004). The effects of out-of-plane seismic energy on reflections in crustal-scale 2D seismic sections. *Tectonophysics*, *388*(1-4), 213-224. <https://doi.org/10.1016/j.tecto.2004.07.040>
- Duval, B., Cramez, C., & Jackson, M. P. A. (1992). Raft tectonics in the Kwanza Basin, Angola. *Marine and Petroleum Geology*, *9*(4), 389 - 404. [https://doi.org/10.1016/0264-8172\(92\)90050-O](https://doi.org/10.1016/0264-8172(92)90050-O)
- Erlström, M., Thomas, S., Deeks, N., & Sivhed, U. (1997). Structure and tectonic evolution of the Tornquist Zone and adjacent sedimentary basins in Scania and the southern Baltic Sea area. *Tectonophysics*, *271*(3), 191 - 215. [https://doi.org/10.1016/S0040-1951\(96\)00247-8](https://doi.org/10.1016/S0040-1951(96)00247-8)
- EUGENO-S Working Group. (1988). Crustal structure and tectonic evolution of the transition between the Baltic Shield and the North German Caledonides (the EUGENO-S Project). *Tectonophysics*, *150*, 253-348. [https://doi.org/10.1016/0040-1951\(88\)90073-X](https://doi.org/10.1016/0040-1951(88)90073-X)
- ExxonMobil Production Deutschland GmbH. (1976). *GS176B* [Seismic reflection, deep]. <https://corporate.exxonmobil.de/>
- Frahm, L., Hübscher, C., Warwel, A., Preine, J., & Huster, H. (2020). Misinterpretation of velocity pull-ups caused by high-velocity infill of tunnel valleys in the southern Baltic Sea. *Near Surface Geophysics*, *18*(6), 643-657. <https://doi.org/10.1002/nsg.12122>
- Franz, M., Kaiser, S. I., Fischer, J., Heunisch, C., Kustatscher, E., Luppold, F. W., Berner, U., & Röhling, H. G. (2015). Eustatic and climatic control on the Upper

- Muschelkalk Sea (late Anisian/Ladinian) in the Central European Basin. *Global and Planetary Change*, 135, 1-27. <https://doi.org/10.1016/j.gloplacha.2015.09.014>
- Frisch, U., & Kockel, F. (1999). Quantification of Early Cimmerian movements in NW-Germany. *Zentralblatt für Geologie und Paläontologie, Teil 1, 1-2*, 571-600.
- Gast, R., Pasternak, M., Piske, J., & Rasch, H.-J. (1998). Rotliegend in northeastern Germany: Regional overview, stratigraphy, facies and diagenesis. *Geologisches Jahrbuch der BGR, A(149)*, 59-79.
- Geißler, M., Breitzkreuz, C., & Kiersnowski, H. (2008). Late Paleozoic volcanism in the central part of the Southern Permian Basin (NE Germany, W Poland): facies distribution and volcano-topographic hiatus. *International Journal of Earth Sciences*, 97(5), 973-989. <https://doi.org/10.1007/s00531-007-0288-6>
- Geluk, M. C., & Röhling, H.-G. (1997). High-resolution sequence stratigraphy of the Lower Triassic 'Buntsandstein' in the Netherlands and northwestern Germany. *Geologie en Mijnbouw*, 76, 227-246. <https://doi.org/10.1023/A:1003062521373>
- GeoERA Working Group. (2022). *3D geomodelling for Europe (3DGEO-EU)*. Retrieved 23.03.2022 from <https://geoera.eu/projects/3dgeo-eu/>
- Gill, J., C. (2017). Geology and the Sustainable Development Goals. *Episodes - Journal of International Geoscience*, 40(1), 70-76. <https://doi.org/10.18814/epiiugs/2017/v40i1/017010>
- Graversen, O. (2006). The Jurassic-Cretaceous North Sea rift dome and associated basin evolution. *AAPG Search and Discovery*, #30040.
- Green, P. F., Japsen, P., Bonow, J. M., Chalmers, J. A., Duddy, I. R., & Kukkonen, I. T. (2022). The post-Caledonian thermo-tectonic evolution of Fennoscandia. *Gondwana Research*, 107, 201-234. <https://doi.org/10.1016/j.gr.2022.03.007>
- Guterch, A., Grad, M., Materzok, R., & Perchuc, E. (1986). Deep structure of the Earth's crust in the contact zone of the Palaeozoic and Precambrian Platforms in Poland (Tornquist-Teisseyre Zone). *Tectonophysics*, 128(3-4), 251-279. [https://doi.org/10.1016/0040-1951\(86\)90296-9](https://doi.org/10.1016/0040-1951(86)90296-9)
- Guterch, A., Wybraniec, S., Grad, M., Chadwick, A., Krawczyk, C., Ziegler, P. A., Thybo, H., & De Vos, W. (2010). Crustal structure and structural framework. In H. Doornenbal & A. Stevenson (Eds.), *Petroleum Geological Atlas of the Southern Permian Basin Area* (pp. 11-23). EAGE Publications.
- Hakansson, E., & Pedersen, S. A. S. (1992). *Map of Bedrock Geology of Denmark*. Copenhagen, Varv and Geological Survey of Denmark and Greenland.
- Handy, M. R., Schmid, S. M., Bousquet, R., Kissling, E., & Bernoulli, D. (2010). Reconciling plate-tectonic reconstructions of Alpine Tethys with the geological-geophysical record of spreading and subduction in the Alps. *Earth-Science Reviews*, 102, 121-158. <https://doi.org/10.1016/j.earscirev.2010.06.002>
- Hansen, M. B., Lykke-Andersen, H., Dehghani, A., Gajewski, D., Hübscher, C., Olesen, M., & Reicherter, K. (2005). The Mesozoic–Cenozoic structural framework of the Bay of Kiel area, western Baltic Sea. *International Journal of Earth Sciences*, 94(5-6), 1070-1082. <https://doi.org/10.1007/s00531-005-0001-6>
- Hansen, M. B., Scheck-Wenderoth, M., Hübscher, C., Lykke-Andersen, H., Dehghani, A., Hell, B., & Gajewski, D. (2007). Basin evolution of the northern part of the

- Northeast German Basin — Insights from a 3D structural model. *Tectonophysics*, 437(1-4), 1-16. <https://doi.org/10.1016/j.tecto.2007.01.010>
- Haq, B. U. (2014). Cretaceous eustasy revisited. *Global and Planetary Change*, 113, 44-58. <https://doi.org/10.1016/j.gloplacha.2013.12.007>
- Haq, B. U. (2017). Jurassic Sea-Level Variations: A reappraisal. *GSA Today*, 28(1), 4-10. <https://doi.org/10.1130/GSATG359A.1>
- Haq, B. U. (2018). Triassic eustatic variations reexamined. *GSA Today*, 28(12), 4-9. <https://doi.org/10.1130/GSATG381A.1>
- Haq, B. U., Hardenbol, J., & Vail, P. R. (1987). Chronology of Fluctuating Sea Levels. *Science*, 235(4793), 1156-1167. <https://doi.org/10.1126/science.235.4793.1156>
- Hinsch, W. (1986). Lithology, Stratigraphy and Paleogeography of the Paleogene in Schleswig-Holstein. *Beiträge zur regionalen Geologie der Erde*, 18, 10-21.
- Hinsch, W. (1987). Lithology, Stratigraphy and Paleogeography of the Neogene in Schleswig-Holstein. *Beiträge zur regionalen Geologie der Erde*, 18, 22-38.
- Hinsch, W. (1991). *Karte des präquartären Untergrunds von Schleswig-Holstein*. Kiel, Geologisches Landesamt Schlewzig-Holstein.
- Hole, J. A. (1992). Nonlinear high-resolution three-dimensional seismic travel time tomography. *Journal of Geophysical Research: Solid Earth*, 97(B5), 6553-6562. <https://doi.org/10.1029/92JB00235>
- Holford, S. P., Green, P. F., Duddy, I. R., Turner, J. P., Hillis, R. R., & Stoker, M. S. (2009). Regional intraplate exhumation episodes related to plate-boundary deformation. *GSA Bulletin*, 121(11/12), 1611-1628. <https://doi.org/10.1130/B26481.1>
- Hoth, K., Rusbült, J., Zagora, K., Beer, H., & Hartmann, O. (1993). Die tiefen Bohrungen im Zentralabschnitt der Mitteleuropäischen Senke - Dokumentation für den Zeitabschnitt 1962-1990. *Verlag der Gesellschaft für Geologische Wissenschaften*, 2(7), 1-145.
- Hübscher, C., Ahlrichs, N., Allum, G., Behrens, T., Bülow, J., Krawczyk, C., Damm, V., Demir, Ü., Engels, M., Frahm, L., Grzyb, J., Hahn, B., Heyde, I., Juhlin, C., Knevels, K., Lange, G., Lydersen, I., Malinowski, M., Noack, V., . . . Stakemann, J. (2016). *MSM52 BalTec Cruise Report*.
- Hübscher, C., & Gohl, K. (2014). Reflection/Refraction Seismology. In *Encyclopedia of Marine Geosciences* (pp. 1-15). https://doi.org/10.1007/978-94-007-6644-0_128-1
- Hübscher, C., Hansen, M. B., Triñanes, S. P., Lykke-Andersen, H., & Gajewski, D. (2010). Structure and evolution of the Northeastern German Basin and its transition onto the Baltic Shield. *Marine and Petroleum Geology*, 27(4), 923-938. <https://doi.org/10.1016/j.marpetgeo.2009.10.017>
- Hübscher, C., Hseinat, M. a. A., Schneider, M., Betzler, C., & Eberli, G. (2019). Evolution of contourite systems in the late Cretaceous Chalk Sea along the Tornquist Zone. *Sedimentology*, 66(4), 1341-1360. <https://doi.org/10.1111/sed.12564>
- Hübscher, C., Lykke-Andersen, H., Hansen, M., & Reicherter, K. (2004). Investigating the structural evolution of the western Baltic. *Eos*, 85(12), 115-115. <https://doi.org/10.1029/2004EO120006>
- Hudec, M. R., & Jackson, M. P. A. (2007). Terra infirma: Understanding salt tectonics. *Earth-Science Reviews*, 82(1-2), 1-28. <https://doi.org/10.1016/j.earscirev.2007.01.001>

- Huster, H., Hübscher, C., & Seidel, E. (2020). Impact of Late Cretaceous to Neogene plate tectonics and Quaternary ice loads on supra-salt deposits at Eastern Glückstadt Graben, North German Basin. *International Journal of Earth Sciences*, 109, 1029-1050. <https://doi.org/10.1007/s00531-020-01850-8>
- Jackson, M. P. A., & Hudec, M. R. (2005). Stratigraphic record of translation down ramps in a passive-margin salt detachment. *Journal of Structural Geology*, 27(5), 889-911. <https://doi.org/10.1016/j.jsg.2005.01.010>
- Jackson, M. P. A., & Hudec, M. R. (2017). *Salt Tectonics - Principles and Practice*. Cambridge University Press. <https://doi.org/10.1017/9781139003988>
- Jackson, M. P. A., Vendeville, B., & Schultz-Ela, D. D. (1994). Structural dynamics of salt systems. *Annual Review of Earth and Planetary Sciences*, 22(1), 93-117. <https://doi.org/10.1146/annurev.earth.22.050194.000521>
- Janik, T., Wojcik, D., Ponikowska, M., Mazur, S., Skrzynik, T., Malinowski, M., & Hübscher, C. (2022). Crustal structure across the Teisseyre-Tornquist Zone offshore Poland based on a new refraction/wide-angle reflection profile and potential field modelling. *Tectonophysics*. <https://doi.org/10.1016/j.tecto.2022.229271>
- Japsen, P., Green, P. F., Bonow, J. M., & Erlström, M. (2015). Episodic burial and exhumation of the southern Baltic Shield: Epeirogenic uplifts during and after break-up of Pangaea. *Gondwana Research*, 35, 357-377. <https://doi.org/10.1016/j.gr.2015.06.005>
- Japsen, P., Green, P. F., Nielsen, L. H., Rasmussen, E. S., & Bidstrup, T. (2007). Mesozoic-Cenozoic exhumation events in the eastern North Sea Basin: a multi-disciplinary study based on palaeothermal, palaeoburial, stratigraphic and seismic data. *Basin Research*, 19, 451-490. <https://doi.org/10.1111/j.1365-2117.2007.00329.x>
- Jaritz, W. (1973). Zur Entstehung der Salzstrukturen Nordwestdeutschlands. *Geologisches Jahrbuch*, A(10), 1-77.
- Jaritz, W. (1987). The origin and development of salt structures in Northwest Germany. In I. O'Brien & J. Lerche (Eds.), *Dynamical geology of salt and related structures* (pp. 479-493). Academic Press.
- Jaritz, W., Best, G., Hildebrand, G., & Jürgens, U. (1991). Regionale Analyse der seismischen Geschwindigkeiten in Nordwestdeutschland [Regional Analysis of the Seismic Velocities in NW Germany]. *Geologisches Jahrbuch. Reihe E, Geophysik*, 45, 23-57.
- Kaiser, R. (2001). *Fazies und Sequenzstratigraphie: Das Staßfurtkarbonat (Ca₂) am nördlichen Beckenrand des südlichen Zechsteinbeckens (NE-Deutschland)* [Doctoral dissertation, University of Cologne.]. Cologne.
- Kammann, J., Hübscher, C., Boldreel, L. O., & Nielsen, L. (2016). High-resolution shear-wave seismics across the Carlsberg Fault zone south of Copenhagen - Implications for linking Mesozoic and late Pleistocene structures. *Tectonophysics*, 682, 56-64. <https://doi.org/10.1016/j.tecto.2016.05.043>
- Katzung, G. (2004). *Geologie von Mecklenburg-Vorpommern [Regional Geology of the State of Mecklenburg-Western Pomerania, NE Germany]* (Vol. 1). E. Schweizerbart'sche Verlagsbuchhandlung.
- Kley, J. (2018). Timing and spatial patterns of Cretaceous and Cenozoic inversion in the Southern Permian Basin. *Geological Society, London, Special Publications*, 469(1), 19-31. <https://doi.org/10.1144/sp469.12>
- Kley, J., Franzke, H.-J., Jähne, F., Krawczyk, C., Lohr, T., Reicherter, K., Scheck-Wenderoth, M., Sippel, J., Tanner, D., van Gent, H., & Group, t. S. S. G.

- (2008). Strain and Stress. In R. Littke, U. Bayer, D. Gajewski, & S. Nelskamp (Eds.), *Dynamics of complex intracontinental basin system, the Central European Basin System* (pp. 97-124). Springer Verlag. <https://doi.org/10.1007/978-3-540-85085-4>
- Kley, J., & Voigt, T. (2008). Late Cretaceous intraplate thrusting in central Europe: Effect of Africa-Iberia-Europe convergence, not Alpine collision. *Geology*, 36(11). <https://doi.org/10.1130/g24930a.1>
- Kockel, F. (1999). Die Bildung von Salzstrukturen in Norddeutschland - neue Einsichten und offene Fragen. *Mitteilungen der Deutschen Geophysikalischen Gesellschaft*, 3, 38-47.
- Kockel, F. (2002). Rifting processes in NW-Germany and the German North Sea Sector. *Netherlands Journal of Geosciences - Geologie en Mijnbouw*, 81(2), 149-158. <https://doi.org/10.1017/S0016774600022381>
- Kockel, F. (2003). Inversion structures in Central Europe - Expressions and reasons, an open discussion. *Netherlands Journal of Geosciences - Geologie en Mijnbouw*, 82(4), 367-382. <https://doi.org/10.1017/S0016774600020187>
- Kossow, D., Krawczyk, C., McCann, T., Strecker, M., & Negendank, J. F. W. (2000). Style and evolution of salt pillows and related structures in the northern part of the Northeast German Basin. *International Journal of Earth Sciences*, 89(3), 652-664. <https://doi.org/10.1007/s005310000116>
- Kossow, D., & Krawczyk, C. M. (2002). Structure and quantification of processes controlling the evolution of the inverted NE-German Basin. *Marine and Petroleum Geology*, 19(5), 601-618. [https://doi.org/10.1016/S0264-8172\(02\)00032-6](https://doi.org/10.1016/S0264-8172(02)00032-6)
- Krauss, M., & Mayer, P. (2004). The Vorpommern Fault System and its Regional Structural Relationships to the Trans-European Fault. *Zeitschrift für Geologische Wissenschaften*, 32, 227-246.
- Krawczyk, C., Eilts, F., Lassen, A., & Thybo, H. (2002). Seismic evidence of Caledonian deformed crust and uppermost mantle structures in the northern part of the Trans-European Suture Zone, SW Baltic Sea. *Tectonophysics*, 360(1-4), 215-244. [https://doi.org/10.1016/S0040-1951\(02\)00355-4](https://doi.org/10.1016/S0040-1951(02)00355-4)
- Krawczyk, C., McCann, T., Cocks, L. R. M., England, R., McBride, J., & Wybraniec, S. (2008). Caledonian Tectonics. In T. McCann (Ed.), *The Geology of Central Europe* (Vol. 1, pp. 2-115). The Geological Society.
- Krawczyk, C., Rabbel, W., Willert, S., Hese, F., Götze, H.-J., Gajewski, D., & SPP-Geophysics Group. (2008). Crustal structures and properties in the Central European Basin System from geophysical evidence. In R. Littke, U. Bayer, D. Gajewski, & S. Nelskamp (Eds.), *Dynamics of complex intracontinental basins, the Central European Basin System* (pp. 67-95). Springer-Verlag. <https://doi.org/10.1007/978-3-540-85085-4>
- Krawczyk, C., Stiller, M., & Group, D.-B. R. (1999). Reflection seismic constraints on Paleozoic crustal structure and Moho beneath the NE German Basin. *Tectonophysics*, 314, 241-253. [https://doi.org/10.1016/S0040-1951\(99\)00246-2](https://doi.org/10.1016/S0040-1951(99)00246-2)
- Krzywiec, P. (2006). Structural inversion of the Pomeranian and Kuiavian segments of the Mid-Polish Trough - lateral variations in timing and structural style. *Geological Quarterly*, 50(1), 151-168. <https://doi.org/10.1127/zdgg/2016/0068>
- Krzywiec, P. (2012). Mesozoic and Cenozoic evolution of salt structures within the Polish basin: An overview. In G. I. Alsop, S. G. Archer, A. J. Hartley, N. T.

- Grant, & R. Hodgkinson (Eds.), *Salt Tectonics, Sediments and Prospectivity, Special Publications* (pp. 381-394). The Geological Society. <https://doi.org/10.1144/SP363.17>
- Krzywiec, P., Kiersnowski, H., & Peryt, T. (2019). Fault-controlled Permian sedimentation in the central Polish Basin (Bydgoszcz-Szubin area) - Insights from well and seismic data. *Zeitschrift der Deutschen Gesellschaft für Geowissenschaften*, 170(3-4), 255-272. <https://doi.org/10.1127/zdgg/2019/0198>
- Krzywiec, P., Peryt, T., Kiersnowski, H., Pomianowski, P., Czapowski, G., & Kwolek, K. (2017). Permo-Triassic evaporites of the Polish Basin and their bearing on the tectonic evolution and hydrocarbon system, an overview. In J. Soto, J. Flinch, & G. Tari (Eds.), *Permo-Triassic salt provinces of Europe, North Africa and the Central Atlantic: Tectonics and hydrocarbon potential* (pp. 243-261). Elsevier. <https://doi.org/10.1016/B978-0-12-809417-4.00012-4>
- Kukla, P. A., Urai, J. L., & Mohr, M. (2008). Dynamics of salt structures. In R. Littke, U. Bayer, D. Gajewski, & S. Nelskamp (Eds.), *Dynamics of complex intracontinental basins, the Central European Basin System* (pp. 249-276). Springer-Verlag. <https://doi.org/10.1007/978-3-540-85085-4>
- Kukla, P. A., Urai, J. L., Raith, A., Shiyuan, L., Barabasch, J., & Strozyk, F. (2019). *The European Zechstein Salt Giant - Trusheim and Beyond* 37th Annual GCSSEPM Foundation Perkins-Rosen Research Conference, Houston, USA.
- Kusznir, N. J., & Ziegler, P. A. (1992). The mechanics of continental extension and sedimentary basin formation: A simple shear/pure-shear flexural cantilever model. *Tectonophysics*, 215(1-2), 117-131. [https://doi.org/10.1016/0040-1951\(92\)90077-J](https://doi.org/10.1016/0040-1951(92)90077-J)
- Lamplugh, G. W. (1919). Structure of the Weald and analogues tracts. *Quarterly Journal Geological Society London*, 75(LXXIII-XCV (Anniversary Address of the President)).
- Lehné, R. J., & Sirocko, F. (2010). Recent vertical crustal movements and resulting surface deformation within the North German Basin (Schleswig-Holstein) derived by GIS-based analysis of repeated precise leveling data [GIS-basierte Auswertung von Nivellementdaten zur Beschreibung und Quantifizierung rezenter vertikaler Krustenbewegungen und daraus resultierender Oberflächen deformationen im Bereich des Norddeutschen Beckens (Schleswig-Holstein)]. *Zeitschrift der Deutschen Gesellschaft für Geowissenschaften*, 161(2), 175-188. <https://doi.org/10.1127/1860-1804/2010/0161-0175>
- Letouzey, J., Colletta, B., Vially, R., & Chermette, J. C. (1995). Evolution of salt-related structures in compressional settings. In M. P. A. Jackson, D. G. Roberts, & S. Snelson (Eds.), *Salt tectonics: a global perspective* (pp. 41-60). AAPG. <https://doi.org/10.1306/M65604C3>
- Lykke-Andersen, H., & Surlyk, F. (2004). The Cretaceous-Paleogene boundary at Stevns Klint, Denmark: inversion tectonics or sea-floor topography? *Journal of the Geological Society*, 161, 343-352. <https://doi.org/10.1144/0016-764903-021>
- Maystrenko, Y., Bayer, U., Brink, H.-J., & Littke, R. (2008). The Central European Basin System - an Overview. In R. Littke, U. Bayer, D. Gajewski, & S. Nelskamp (Eds.), *Dynamics of complex intracontinental basins, the Central European Basin System* (pp. 17-34). Springer Verlag. <https://doi.org/10.1007/978-3-540-85085-4>

- Maystrenko, Y., Bayer, U., & Scheck-Wenderoth, M. (2005a). The Glueckstadt Graben, a sedimentary record between the North and Baltic Sea in north Central Europe. *Tectonophysics*, 397(1-2), 113-126. <https://doi.org/10.1016/j.tecto.2004.10.004>
- Maystrenko, Y., Bayer, U., & Scheck-Wenderoth, M. (2005b). Structure and evolution of the Glueckstadt Graben due to salt movements. *International Journal of Earth Sciences*, 94(5-6), 799-814. <https://doi.org/10.1007/s00531-005-0003-4>
- Maystrenko, Y., Bayer, U., & Scheck-Wenderoth, M. (2006). 3D reconstruction of salt movements within the deepest post-Permian structure of the Central European Basin System - the Glueckstadt Graben. *Netherlands Journal of Geosciences - Geologie en Mijnbouw*, 85(3), 181-196. <https://doi.org/10.1017/S0016774600021466>
- Maystrenko, Y. P., Bayer, U., & Scheck-Wenderoth, M. (2013). Salt as a 3D element in structural modeling — Example from the Central European Basin System. *Tectonophysics*, 591, 62-82. <https://doi.org/10.1016/j.tecto.2012.06.030>
- Maystrenko, Y. P., & Scheck-Wenderoth, M. (2013). 3D lithosphere-scale density model of the Central European Basin System and adjacent areas. *Tectonophysics*, 601, 53-77. <https://doi.org/10.1016/j.tecto.2013.04.023>
- Mazur, S., Aleksandrowki, P., Gagala, L., Krzywiec, P., Zaba, J., Gaidzik, K., & Sikora, R. (2020). Late Paleozoic strike-slip tectonics versus oroclinal bending at the SW outskirts of Baltica: Case of the Variscan belt's eastern end in Poland. *International Journal of Earth Sciences*, 109(4), 1133-1160. <https://doi.org/10.1007/s00531-019-01814-7>
- Mazur, S., Krzywiec, P., Malinowski, M., Lewandowski, M., Aleksandrowki, P., & Mikolajczak, M. (2018). On the nature of the Teisseyre-Tornquist Zone. *Geology, Geophysics & Environment*, 44(1), 17-30. <https://doi.org/10.7494/geol.2018.44.1.17>
- Mazur, S., Mikolajczak, M., Krzywiec, P., Malinowski, M., Buffenmyer, V., & Lewandowski, M. (2015). Is the Teisseyre-Tornquist Zone an ancient plate boundary of Baltica? *Tectonics*, 34(12), 2465-2477. <https://doi.org/10.1002/2015tc003934>
- Mazur, S., Scheck-Wenderoth, M., & Krzywiec, P. (2005). Different modes of the Late Cretaceous–Early Tertiary inversion in the North German and Polish basins. *International Journal of Earth Sciences*, 94(5-6), 782-798. <https://doi.org/10.1007/s00531-005-0016-z>
- Meinhold, R., & Reinhardt, H.-G. (1967). Halokinese im Nordostdeutschen Tiefland. *Berichte der Deutschen Gesellschaft für Geologische Wissenschaften*, 12, 329-353.
- Michelsen, O. (1978). Stratigraphy and distribution of Jurassic deposits of the Norwegian-Danish Basin. *Danmarks Geologiske Underøgelse, Serie B(2)*, 1-28.
- Michon, L., & Merle, O. (2005). Discussion on "Evolution of the European Cenozoic Rift System: interaction of the Alpine and Pyrenean orogens with their foreland lithosphere" by P. Dèzes, S.M. Schmid and P.A. Ziegler, *Tectonophysics* 389 (2004) 1-33. *Tectonophysics*, 401(3-4), 251-256. <https://doi.org/10.1016/j.tecto.2005.01.006>
- Michon, L., Van Bahlen, R. T., Merle, O., & Pagnier, H. (2003). The Cenozoic evolution of the Roer Valley Rift System integrated at a European scale. *Tectonophysics*, 367, 101-126. [https://doi.org/10.1016/S0040-1951\(03\)00132-X](https://doi.org/10.1016/S0040-1951(03)00132-X)

- Mohr, M., Kukla, P. A., Urai, J. L., & Bresser, G. (2005). Multiphase salt tectonic evolution in NW Germany: seismic interpretation and retro-deformation. *International Journal of Earth Sciences*, 94(5-6), 917-940. <https://doi.org/10.1007/s00531-005-0039-5>
- Nalpas, T., Le Douran, S., Brun, J.-P., Unternehr, P., & Richert, J.-P. (1995). Inversion of the Broad Fourteens Basin (offshore Netherlands), a small-scale model investigation. *Sedimentary Geology*, 95(3-4), 237-250. [https://doi.org/10.1016/0037-0738\(94\)00113-9](https://doi.org/10.1016/0037-0738(94)00113-9)
- Nielsen, L. H., & Japsen, P. (1991). Deep wells in Denmark - 1935-1990. *Danmarks Geologiske Undersøgelse, Serie A*(31), 1-179.
- Nielsen, S. B., Paulsen, G. E., Hansen, D. L., Gemmer, L., Clausen, O. R., Jacobsen, B. H., Balling, N., Huuse, M., & Gallacher, K. (2002). Paleocene initiation of Cenozoic uplift in Norway. In A. G. Doré, J. Cartwright, M. S. Stoker, J. P. Turner, & N. White (Eds.), *Exhumation of the North Atlantic Margin: Timing, Mechanisms and Implication for Petroleum Exploration* (Vol. 196, pp. 45-65). The Geological Society. <https://doi.org/10.1144/GSL.SP.2002.196.01.04>
- Nielsen, S. B., Thomsen, E., Hansen, D. L., & Clausen, O. (2005). Plate-wide stress relaxation explains European palaeocene basin inversions. *Nature*, 435, 195-198. <https://doi.org/10.1038/nature03599>
- Noack, V., Schnabel, M., Damm, V., & Hübscher, C. (2018). *Velocity model building for depth conversion and interpretation of multichannel seismic data in the Mecklenburg Bay of the southern Baltic Sea* DKMK/ÖGEW Frühjahrstagung, Celle, Germany.
- Nöldecke, W., & Schwab, G. (1976). Zur tektonischen Entwicklung des Tafeldeckgebirges der Norddeutsch-Polnischen Senke unter besonderer Berücksichtigung des Nordteils der DDR. *Zeitschrift für Angewandte Geologie*, 23, 369-379.
- Paige, C. C., & Saunders, M. A. (1982). LSQR: An algorithm for sparse linear equations and sparse least squares. *ACM Transactions on Mathematical Software (TOMS)*, 8(1), 43-71. <https://doi.org/10.1145/355984.355989>
- Peacock, D. C. P., & Banks, G. J. (2020). Basement highs: Definitions, characterisation and origins. *Basin Research*, 32, 1685-1710. <https://doi.org/10.1111/bre.12448>
- Peryt, T. M., Geluk, M., Mathiesen, A., Paul, J., & Smith, K. (2010). Zechstein. In J. C. Doornenbal & A. G. Stevenson (Eds.), *Petroleum Geological Atlas of the Southern Permian Basin Area* (pp. 123-147). EAGE Publications.
- Pharaoh, T. (1999). Palaeozoic terranes and their lithospheric boundaries within the Trans-European Suture Zone (TESZ): A review. *Tectonophysics*, 314, 17-41. [https://doi.org/10.1016/S0040-1951\(99\)00235-8](https://doi.org/10.1016/S0040-1951(99)00235-8)
- Pharaoh, T., Dusar, M., Geluk, M., Kockel, F., Krawczyk, C., Krzywiec, P., Scheck-Wenderoth, M., Thybo, H., Vejbaek, O. V., & van Wees, J.-D. (2010). Tectonic evolution. In H. Doornenbal & A. G. Stevenson (Eds.), *Petroleum Geological Atlas of the Southern Permian Basin Area* (pp. 25-57). EAGE Publications.
- Pichel, L., Huuse, M., Redfern, J., & Finch, E. (2019). The influence of base-salt relief, rift topography and regional events on salt tectonics offshore Morocco. *Marine and Petroleum Geology*, 103, 87-113. <https://doi.org/10.1016/j.marpetgeo.2019.02.007>
- Podvin, P., & Lecomte, I. (1991). Finite difference computation of traveltimes in very contrasted velocity models: a massively parallel approach and its associated

- tools. *Geophysical Journal International*, 105(1), 271-284. <https://doi.org/10.1111/j.1365-246X.1991.tb03461.x>
- Prather, B. E., Booth, J. R., Steffens, G. S., & Craig, P. A. (1998). Classification, lithologic calibration and stratigraphic succession of seismic facies of intraslope basins, deep-water Gulf of Mexico. *AAPG Bulletin*, 52, 701-728. <https://doi.org/10.1306/1D9BC5D9-172D-11D7-8645000102C1865D>
- Rasmussen, E. S. (2009). Neogene inversion of the Central Graben and Ringkøbing-Fyn High, Denmark. *Tectonophysics*, 465, 84-97. <https://doi.org/10.1016/j.tecto.2008.10.025>
- Reiche, S., Hübscher, C., & Beitz, M. (2014). Fault-controlled evaporate deformation in the Levant Basin, Eastern Mediterranean. *Marine Geology*, 354, 53-68. <https://doi.org/10.1016/j.margeo.2014.05.002>
- Reinhardt, H.-G. (1993). Structure of Northeast Germany: Regional depth and thickness maps of Permian to Tertiary intervals compiled from seismic reflection data. In A. M. Spencer (Ed.), *Generation, accumulation and production of Europe's hydrocarbons III* (pp. 155-165). Springer-Verlag.
- Reinhold, K., Krull, P., Kockel, F., & Rätz, J. (2008). *Salzstrukturen Norddeutschlands: Geologische Karte*. Hannover, Bundesanstalt für Geowissenschaften und Rohstoffe.
- Rempel, H. (1992). Erdölgeologische bewertung der Arbeiten der Gemeinsamen Organisation 'Petrobaltic' im deutschen Schelfbereich [Evaluation of the petroleum geological work of the consortium Petrobaltic in the German shelf area]. *Geologisches Jahrbuch*, D99, 3-32.
- Richard, P., Mocquet, B., & Cobbold, P. R. (1991). Experiments on simultaneous faulting and folding above a basement wrench fault. *Tectonophysics*, 188, 133-141. [https://doi.org/10.1016/0040-1951\(91\)90319-N](https://doi.org/10.1016/0040-1951(91)90319-N)
- Rowan, M., Peel, F., & Vendeville, B. (2004). Gravity-driven fold belts on passive margins. *American Association of Petroleum Geologists Memoir*, 82, 157-182.
- Rowan, M., & Vendeville, B. (2006). Foldbelts with early salt withdrawal and diapirism: Physical model and examples from the northern Gulf of Mexico and the Flinders Ranges, Australia. *Marine and Petroleum Geology*, 23, 871-891. <http://doi.org/10.1016/j.marpetgeo.2006.08.003>
- Rowan, M. G., Peel, F. J., Vendeville, B. C., & Gaullier, V. (2012). Salt tectonics at passive margins: Geology versus models – Discussion. *Marine and Petroleum Geology*, 37(1), 184-194. <https://doi.org/10.1016/j.marpetgeo.2012.04.007>
- Rühberg, N. (1976). Probleme der Zechsteinsalzbewegung. *Zeitschrift für Angewandte Geologie*, 22, 413-420.
- Sangree, J. B., & Widmier, J. M. (1979). Interpretation of depositional facies from seismic data. *Geophysics*, 44(2), 131-160. <https://doi.org/10.1190/1.1440957>
- Scheck-Wenderoth, M., & Lamarche, J. (2005). Crustal memory and basin evolution in the Central European Basin System—new insights from a 3D structural model. *Tectonophysics*, 397(1-2), 143-165. <https://doi.org/10.1016/j.tecto.2004.10.007>
- Scheck-Wenderoth, M., Maystrenko, Y., Hübscher, C., Hansen, M., & Mazur, S. (2008). Dynamics of salt basins. In R. Littke, U. Bayer, D. Gajewski, & S. Nelskamp (Eds.), *Dynamics of complex intracontinental basins, the Central European Basin System* (pp. 307-322). Springer Verlag. <https://doi.org/10.1007/978-3-540-85085-4>
- Scheck, M., Barrio-Alvers, L., Bayer, U., & Götze, H.-J. (1999). Density structure of the Northeast German basin: 3D modelling along the DEKORP line BASIN96.

- Physics and Chemistry of the Earth, Part A: Solid Earth and Geodesy*, 24(3), 221 - 230. [https://doi.org/10.1016/S1464-1895\(99\)00022-8](https://doi.org/10.1016/S1464-1895(99)00022-8)
- Scheck, M., & Bayer, U. (1999). Evolution of the Northeast German Basin - inferences from a 3D structural model and subsidence analysis. *Tectonophysics*, 313, 145-169. [https://doi.org/10.1016/S0040-1951\(99\)00194-8](https://doi.org/10.1016/S0040-1951(99)00194-8)
- Scheck, M., Bayer, U., & Lewerenz, B. (2003). Salt movements in the Northeast German Basin and its relation to major post-Permian tectonic phases—results from 3D structural modelling, backstripping and reflection seismic data. *Tectonophysics*, 361(3-4), 277-299. [https://doi.org/10.1016/s0040-1951\(02\)00650-9](https://doi.org/10.1016/s0040-1951(02)00650-9)
- Scheidt, W., Schmidt, A., Zenker, F., & Arndt, G. (1995). *Bericht über das Reprocessing 2D-seismischer Daten aus der südlichen Ostsee* [unpublished report].
- Schlüter, D., Jürgens, D., Best, G., Binot, F., & Stamme, H. (1997). *Analyse geologischer und geophysikalischer Daten aus der südlichen Ostsee - Strukturatlas südliche Ostsee (SASO)*.
- Schnabel, M., Noack, V., Ahlrichs, N., & Hübscher, C. (2021). A comprehensive model of seismic velocities for the Bay of Mecklenburg (Baltic Sea) at the North German Basin margin - implications for basin development. *Geo-Marine Letters*.
- Schröder, B. (1982). Entwicklung des Sedimentbeckens und Stratigraphie der klassischen Germanischen Trias. *Geologische Rundschau*, 71(3), 783-794. <https://doi.org/10.1007/BF01821103>
- Schuh, F. (1922a). Beitrag zur Tektonik unserer Salzstöcke. *Kali*, 16(1), 1-10.
- Schuh, F. (1922b). Die saxonische Gebirgsbildung. I. Teil. *Kali*, 16(8-9), 145-152.
- Schuh, F. (1922c). Die saxonische Gebirgsbildung. II. Teil. *Kali*, 16(15-16).
- Schulze, K. (1995). *Übersichtskarte Präquartär*. Güstrow, Landesamt für Umwelt, Naturschutz und Geologie Mecklenburg-Vorpommern (LUNG).
- Seidel, E. (2019). *The Tectonic Evolution of the German offshore area, as part of the Trans-European Suture zone (North and East of Rügen Island)* [Dissertation, University of Greifswald]. Greifswald.
- Seidel, E., Meschede, M., & Obst, K. (2018). The Wiek Fault System east of Rügen Island: origin, tectonic phases and its relationship to the Trans-European Suture Zone. *Geological Society, London, Special Publications*, 469(1), 59-82. <https://doi.org/10.1144/sp469.10>
- Sirocko, F., Reicherter, K., Lehné, R., Hübscher, C., Winsemann, J., & Stackebrandt, W. (2008). Glaciation, salt and the present landscape. In R. Littke, U. Bayer, D. Gajewski, & S. Nelskamp (Eds.), *Dynamics of complex intracontinental basins, the Central European Basin System* (pp. 233-245). Springer Verlag. <https://doi.org/10.1007/978-3-540-85085-4>
- Sørensen, K. (1986). Rim syncline volume estimation and salt diapirism. *Nature*, 319(2), 23-27. <https://doi.org/10.1038/319023a0>
- Sørensen, K. (1998). The salt pillow to diapir transition; evidence from unroofing unconformities in the Norwegian-Danish Basin. *Petroleum Geoscience*, 4, 193-202. <https://doi.org/10.1144/petgeo.4.3.193>
- STD 2016 (German Stratigraphic Commission, ed.; editing, coordination and layout: Menning, M., & Hendrich, A. (2016). Stratigraphic Table of Germany 2016. In. Potsdam: German Research Centre for Geosciences.

- Stewart, S. A. (1996). Influence of detachment layer thickness on style of thin-skinned shortening. *Journal of Structural Geology*, 18(10), 1271-1274. [https://doi.org/10.1016/S0191-8141\(96\)00052-1](https://doi.org/10.1016/S0191-8141(96)00052-1)
- Stewart, S. A. (2007). Salt tectonics in the North Sea Basin: a structural style template for seismic interpreters. *Geological Society, London, Special Publications*, 272(1), 361-396. <https://doi.org/10.1144/gsl.Sp.2007.272.01.19>
- Stewart, S. A., & Coward, M. P. (1995). Synthesis of salt tectonics in the southern North Sea, UK. *Marine and Petroleum Geology*, 12(5), 457-475. [https://doi.org/10.1016/0264-8172\(95\)91502-G](https://doi.org/10.1016/0264-8172(95)91502-G)
- Stewart, S. A., & Coward, M. P. (1996). Genetic interpretation and mapping of salt structures. *First Break*, 14(4), 135-141. <https://doi.org/10.3997/1365-2397.1996009>
- Stork, C. (1992). Reflection tomography in the postmigrated domain. *Geophysics*, 57, 680-692. <https://doi.org/10.1190/1.1443282>
- Strohmenger, C., Voigt, E., & Zimdars, J. (1996). Sequence stratigraphy and cyclic development of Basal Zechstein carbonate-evaporite deposits with emphasis on Zechstein 2 off-platform carbonates (Upper Permian, Northeast Germany). *Sedimentary Geology*, 102(1), 33 - 54. [https://doi.org/10.1016/0037-0738\(95\)00058-5](https://doi.org/10.1016/0037-0738(95)00058-5)
- Strozyk, F., Gent, H. V., Urai, J. L., Kukla, P. A., Alsop, G. I., Archer, S. G., Hartley, A. J., Grant, N. T., & Hodgkinson, R. (2012). 3D seismic study of complex intra-salt deformation: An example from the Upper Permian Zechstein 3 stringer, western Dutch offshore. In *Salt Tectonics, Sediments and Prospectivity* (Vol. 363, pp. 0). Geological Society of London. <https://doi.org/10.1144/sp363.23>
- Thieme, B., & Rockenbauch, K. (2001). Triassic rift-raft tectonics in the German Southern North Sea. *Erdöl, Erdgas, Kohle*, 117, 568-573.
- Thore, P., Shtuka, A., Lecour, M., Ait-Ettajer, T., & Cognot, R. (2002). Structural uncertainties: Determination, management and applications. *Geophysics*, 67(3), 840-852. <https://doi.org/10.1190/1.1484528>
- Thybo, H. (1997). Geophysical characteristics of the Tornquist Fan area, northwest Trans-European Suture Zone: indication of late Carboniferous to early Permian dextral transtension. *Geological Magazine*, 134(5), 597-606. <https://doi.org/10.1017/S0016756897007267>
- Trusheim, F. (1960). Mechanism of salt migration in northern Germany. *AAPG Bulletin*, 44(9), 1519-1540. <https://doi.org/10.1306/0BDA61CA-16BD-11D7-8645000102C1865D>
- Tryggvason, A. (1998). *Seismic tomography: Inversion for P- and S-wave velocities* [Doctoral thesis, Uppsala University]. Uppsala, Sweden.
- Tucker, M. E. (1991). Sequence stratigraphy of carbonate-evaporite basins: models and application to the Upper Permian (Zechstein) of northeast England and adjoining North Sea. *Journal of the Geological Society*, 148(6), 1019-1036. <https://doi.org/10.1144/gsjgs.148.6.1019>
- TUNB Working Group. (2021). *TUNB - Potenziale des unterirdischen Speicher- und Wirtschaftsraumes im Norddeutschen Becken*. Bundesanstalt für Geowissenschaften und Rohstoffe. Retrieved 05.03.2021 from <https://gst.bgr.de/>
- Underhill, J. R. (1998). Jurassic. In K. W. Glennie (Ed.), *Petroleum geology of the North Sea: Basic concepts and recent advances* (Vol. 4, pp. 245-293). Blackwell Science.

- Underhill, J. R., & Partington, M. A. (1993). Jurassic thermal doming and deflation in the North Sea: implications of the sequence stratigraphic evidence. *Geological Society, London, Petroleum Geology Conference series*, 4(1), 337-345. <https://doi.org/10.1144/0040337>
- van Dalfsen, W., Doornenbal, J. C., Dortland, S., & Gunnink, J. L. (2006). A comprehensive seismic velocity model for the Netherlands based on lithostratigraphic layers. *Netherlands Journal of Geosciences - Geologie en Mijnbouw*, 85(4), 277-292. <https://doi.org/10.1017/S0016774600023076>
- van Gent, H., Urai, J. L., & Keijzer, M. (2010). The internal geometry of salt structures—A first look using 3D seismic data from the Zechstein of the Netherlands. *Structural Geology*, 1-20. <https://doi.org/10.1016/j.tecto.2008.09.038>
- Van Wees, J.-D., Stephenson, R., Ziegler, P. A., Bayer, U., McCann, T., Dadlez, R., Gaupp, R., Narkiewicz, M., Bitzer, F., & Scheck, M. (2000). On the origin of the Southern Permian Basin, Central Europe. *Marine and Petroleum Geology*, 17(1), 43 - 59. [https://doi.org/10.1016/S0264-8172\(99\)00052-5](https://doi.org/10.1016/S0264-8172(99)00052-5)
- Vejbaek, O. V. (1997). Dybe strukturer i danske sedimentære bassiner. *Geologisk Tidsskrift*, 4, 1-31.
- Vejbaek, O. V., & Andersen, C. (2002). Post mid-Cretaceous inversion tectonics in the Danish Central Graben - regionally synchronous tectonic events? *Bulletin of the Geological Society of Denmark*, 49(2), 129-144.
- Vejbaek, O. V., Andersen, C., Dussar, M., Herngreen, W., Krabbe, H., Leszczynski, K., Lott, G. K., Mutterlose, J., & van der Molen, A. S. (2010). Cretaceous. In J. C. Doornenbal & A. G. Stevenson (Eds.), *Petroleum Geological Atlas of the Southern Permian Basin Area* (pp. 195-209). EAGE Publications.
- Vejbaek, O. V., & Britze, P. (1994). *Top pre-Zechstein, Geological Map of Denmark*. Copenhagen, Denmark, Geological Survey of Denmark.
- Vendeville, B., & Jackson, M. P. A. (1992). The rise of diapirs during thin-skinned extension. *Marine and Petroleum Geology*, 9(4), 331 - 354. [https://doi.org/10.1016/0264-8172\(92\)90047-1](https://doi.org/10.1016/0264-8172(92)90047-1)
- Vendeville, B., & Nilsen, K. T. (1995). *Episodic growth of salt diapirs driven by horizontal shortening* Salt, sediment and hydrocarbons, Houston, U.S.A.
- Verschuur, D. J. (2006). *Seismic multiple removal techniques—Past, present and future*. EAGE Publications.
- Vinken, R., & International Geological Correlation Programme. (1988). *The Northwest European Tertiary Basin: Results of the International Geological Correlation programme project no. 124*. Bundesanstalt für Geowissenschaften und Rohstoffe.
- Voigt, E. (1962). Über Randtröge vor Schollenrändern und ihre Bedeutung im Gebiet der Mitteleuropäischen Senke und angrenzender Gebiete. *Zeitschrift der Deutschen Geologischen Gesellschaft*, 114, 378-414.
- Voigt, T., von Eynatten, H., & Franzke, H.-J. (2004). Late Cretaceous unconformities in the Subhercynian Cretaceous Basin (Germany). *Acta Geologica Polonica*, 54(4), 673-694.
- von Eynatten, H., Kley, J., Dunkl, I., Hoffmann, V.-E., & Simon, A. (2021). Late Cretaceous to Paleogene exhumation in Central Europe - localized inversion vs. large-scale domal uplift. *Solid Earth*, 12(4), 935-958. <https://doi.org/10.5194/se-12-935-2021>
- Warren, J. (2008). Salt as sediment in the Central European Basin System as seen from a deep time perspective. In R. Littke, U. Bayer, D. Gajewski, & S. Nelskamp

- (Eds.), *Dynamics of complex intracontinental basins, the Central European Basin System* (pp. 249-276). Springer-Verlag. <https://doi.org/10.1007/978-3-540-85085-4>
- Warren, J. K. (2010). Evaporites through time: Tectonic, climatic and eustatic controls in marine and nonmarine deposits. *Earth-Science Reviews*, 98(3-4), 217-268. <https://doi.org/10.1016/j.earscirev.2009.11.004>
- Warsitzka, M., Jähne-Klingberg, F., Kley, J., & Kukowski, N. (2019). The timing of salt structure growth in the Southern Permian Basin (Central Europe) and implications for basin dynamics. *Basin Research*, 31(2), 337-360. <https://doi.org/10.1111/bre.12323>
- Warsitzka, M., Kley, J., Jähne-Klingberg, F., & Kukowski, N. (2016). Dynamics of prolonged salt movement in the Glückstadt Graben (NW Germany) driven by tectonic and sedimentary processes. *International Journal of Earth Sciences*, 106(1), 131-155. <https://doi.org/10.1007/s00531-016-1306-3>
- Withjack, M. O., & Callaway, S. (2000). Active Normal Faulting Beneath a Salt Layer: An Experimental Study of Deformation Patterns in the Cover Sequence. *AAPG Bulletin*, 84(5), 627-651. <https://doi.org/10.1306/C9EBCE73-1735-11D7-8645000102C1865D>
- Yilmaz, Ö. (2001). *Seismic Data Analysis: Processing, Inversion and Interpretation of Seismic Data* (Vol. 1). Society of Exploration Geophysicists. <http://dx.doi.org/10.1190/1.9781560801580>
- Zagora, I., & Zagora, K. (1997). An Upper Permian (Ca1) Reef in the German part of the Baltic Sea. *Freiberger Forschungshefte, C 466*(4), 19-31.
- Ziegler, P. A. (1987). Late Cretaceous and Cenozoic intra-plate compressional deformations in the Alpine foreland. *Tectonophysics*, 137, 389-420. [https://doi.org/10.1016/0040-1951\(87\)90330-1](https://doi.org/10.1016/0040-1951(87)90330-1)
- Ziegler, P. A. (1990a). *Geological Atlas of Western and Central Europe* (Vol. 2nd). Shell Internationale Petroleum Maatschappij B. V.
- Ziegler, P. A. (1990b). Tectonic and paleogeographic development of the North Sea Rift System. In D. Blundell & A. D. Gibbs (Eds.), *Tectonic Evolution of North Sea Rifts* (pp. 1-36). Oxford University Press.
- Ziegler, P. A., Cloetingh, S., & van Wees, J.-D. (1995). Dynamics of intra-plate compressional deformation: the Alpine foreland and other examples. *Tectonophysics*, 252, 7-59. [https://doi.org/10.1016/0040-1951\(95\)00102-6](https://doi.org/10.1016/0040-1951(95)00102-6)
- Zöllner, H., Reicherter, K., & Schikowsky, P. (2008). High-resolution seismic analysis of the coastal Mecklenburg Bay (North German Basin): the pre-Alpine evolution. *International Journal of Earth Sciences*, 97(5), 1013-1027. <https://doi.org/10.1007/s00531-007-0277-9>

Eidesstattliche Versicherung | Declaration on Oath

Hiermit erkläre ich an Eides statt, dass ich die vorliegende Dissertationsschrift selbst verfasst und keine anderen als die angegebenen Quellen und Hilfsmittel benutzt habe.

|

I hereby declare upon oath that I have written the present dissertation independently and have not used further resources and aids than those stated.

A handwritten signature in black ink, appearing to read 'Ahlneke', with a long horizontal stroke extending to the right.

Hamburg, den 01 Juni. 2022 | Hamburg, 1st June 2022

Unterschrift | Signature